To the Graduate Council:

I am submitting herewith a thesis written by Scott Mitchell Wood entitled "Internal Forces in a Reinforced Concrete Box Culvert." I have examined the final copy of this thesis for form and content and recommend that it be accepted in partial fulfillment of the requirements for the degree of Master of Science, with a major in Civil Engineering.

Richard M. Bennett

Dr. Richard M. Bennett, Major Professor

We have read this thesis
And recommend its acceptance

Eric C. Drumm

Dr. Eric C. Drumm

Edwin G. Burdette

Dr. Edwin G. Burdette

Accepted for the Council:

Associate Vice Chancellor and
Dean of the Graduate School

Internal Forces in a Reinforced Concrete Box Culvert.

A Thesis
Presented for the
Master of Science
Degree
The University of Tennessee, Knoxville

Scott Mitchell Wood
May 2000

ACKNOWLEDGEMENTS

I would like to thank the Department of Civil and Environmental Engineering at the University of Tennessee, Knoxville for the valuable knowledge that I received during both as an undergraduate and graduate student. I would especially like to thank my Major Professor, Dr. Richard Bennett, and my other committee members Dr. Eric Drumm and Dr. Edwin Burrdette. I would also like to recognize the Institute of Geotechnology for all the support that they give to so many graduate students.

Abstract

In 1996, a reinforced concrete box culvert with approximately 19 meters of embankment fill was instrumented with strain gages and pressure cells to determine the internal forces applied to the culvert. Strain and pressure readings were taken for a period of 3 years during and after the construction of the embankment. From a knowledge of the culvert's dimensions and material properties, the strain readings were converted to forces and bending moments. These forces were then compared to the allowable criteria from the American Association of State Highway and Transportation Officials (AASHTO) Standard Specifications for Highway Bridges. A computer model of the culvert was performed to compare the results of the strain gages and pressure cells to the unit weight of the embankment fill. The computer model was also used to study the changes in internal forces due to different boundary conditions.

The results showed that axial forces and bending moments are linearly related to the embankment fill height. The box culvert has adequate capacity according to the design equations from AASHTO. Computer modeling of the culvert showed that the effects of different boundary conditions give slightly different moments in the roof and the wall. Load distributions on the roof show very little change in bending moments and shears, but when the load distribution on the wall increases on the bottom, a significant increase in shear forces is seen.

Table of Contents

Page Number

Chapter 1 Introduction

1.1 - Introduction..... 1
1.2 - Background..... 1
1.3 - Description of Culvert..... 2
1.4 - Factors Affecting the Performance of
Cast-in-Place Box Culverts..... 3
1.5 - Design and Installation of Instrumented
Culvert Sections..... 3
1.6 - Monitoring Earth Pressures and Strains..... 5

Chapter 2 Literature Review

2.1 - Classification of Culverts..... 7
2.2 - Recommended Earth Pressures..... 9
2.3 - Earth Pressures on Buried Box Culverts..... 13

Chapter 3 Instrumentation

3.1 - Measurement of Strain in Reinforced
Concrete Sections..... 17
3.2 - Measuring Strain..... 20
3.3 - Installation of Vibrating Wire Strain Gage..... 20
3.4 - Temperature Correction..... 21
3.5 - Strain Gage Datums..... 26
3.6 -Pressure Cells..... 29

Chapter 4 Internal Forces

4.1 - Conversion of Strain to Forces
4.1.1 - Modulus of Elasticity..... 31
4.1.2 - Modulus of Rupture..... 32
4.1.3 - Axial Force and Bending Moments..... 32
4.1.4 - Back Calculated Pressures
From Culvert Forces..... 33
4.1.5 - Calculation of Shear Forces..... 34
4.2 - Forces Results..... 35
4.2.1 - Axial Forces
4.2.1a - Wall Axial Forces..... 36
4.2.1b - Roof Axial Forces..... 40

Table of Contents

Page Number

4.2.2 - Bending Moments
4.2.2a - Wall Bending Moments..... 41
4.2.2b - Roof Bending Moments..... 45
4.3 - Pressures..... 48
4.3.1 - Roof Pressures..... 48
4.3.2 - Wall Pressures..... 53
4.4 - Pressure Differences in the Sections A and B..... 57
4.5 - Shears
4.5.1 - Wall Shears..... 58
4.5.2 - Roof Shears..... 59

Chapter 5 Computer Modeling of Buried Box Culvert
5.1 - Introduction..... 60
5.2 - Roof Forces
5.2.1 - Effeects of Boundary Conditions..... 60
5.2.1a - Bending Moments..... 62
5.2.1b - Shear Forces..... 62
5.2.2 - Effects of Load Distributions..... 62
5.2.2a - Bending Moments..... 65
5.2.2b - Shear Forces..... 68
5.2.3 - Conclusions on Roof Forces..... 68
5.3 - Wall Forces..... 68
5.3.1 - Bending Moments..... 71
5.3.2 - Shear Forces..... 71
5.3.3 - Conclusions on Wall Forces..... 79
5.4 - Roof Bending Moments with
Varying Fill Height..... 79

Chapter 6 Comparison of Forces to Culvert Capacity
6.1 - Introduction..... 88
6.2 - Comparison of Axial Force and Moment
to Culvert Capacity
6.2.1 - Development of Capacity
Interaction Diagram..... 88
6.2.2 - Comparison of Axial Forces
and Moment to Capacity..... 89

Table of Contents

Page Number

6.3 - Shear Capacity..... 89
6.3.1 - Comparison of Shear Forces and Capacity in the Culvert Wall..... 97
6.3.2 - Comparison of Shear Forces and Capacity in the Culvert Roof..... 101
6.4 Conclusion on Culvert Capacity..... 103

Chapter 7 Conclusion

7.1 - Internal Forces..... 104
7.2 - Capacity..... 104

References..... 106

Appendixes

Appendix A - Greene County Dimensions and Details..... 109

Appendix B - Section A Strain Gage Results..... 112

Appendix C - Section B Strain Gage Results..... 137

Appendix D - Pressure and Shear Force Measurements..... 162

Appendix E - Greene County Culvert Concrete Test Data..... 171

Vita..... 177

List of Tables

Page Number

Chapter 2

2-1 Summary of AASHTO Design Pressures for Buried box Culverts..... 9

2-2 Summary of Design Earth Pressures for Buried Structures..... 13

Chapter 4

4-1 Wall Axial Force vs Fill Height with Equivalent Unit Weight..... 36

4-2 Section B Axial Forces vs. Fill Height at Section B and Section A..... 38

4-3 Roof Axial Forces vs. Fill Height..... 41

4-4 Wall Bending Moments vs. Fill Height..... 42

4-5 Roof Bending Moments vs. Fill Height..... 45

4-6 Soil Modification Factors for Different Average Pressure Measurements..... 52

4-7 Different Load Distribution Cases..... 56

4-8 Wall Pressure per Meter Height of Fill Using Different Load Cases..... 57

4-9 Wall Shear Forces with Various Load Distributions..... 58

4-10 Roof Shear Forces with Different Load Distributions..... 59

List of Figures

Page Number

Chapter 1

1-1 Typical Culvert Instrumentation and Numbering Scheme..... 4

1-2 Schematic of Embankment and Culvert Cross-Section..... 6

Chapter 2

2-1 Various Classes of Culvert Installation..... 8

2-2 Classififcation of Culverts..... 10

2-3 Pressure Distribution with 2.4 m sand Fill..... 15

Chapter 3

3-1 Strain in Concrete and Steel in Cracked Reinforced Concrete Member..... 17

3-2 Creep Coefficient Versus Time after Application of Load..... 19

3-3 Schematic of Strain Gage Installation..... 22

3-4 Reference Gage Reading..... 24

3-5 Reference Gage Reading vs Temperature..... 25

3-6 Corrected Reference Gage Reading..... 27

3-7 Corrected Reference Gage Reading vs Temperature..... 28

3-8 Pressure Cell..... 30

List of Figures

Page Number

Chapter 4

4-1 Conversion of Strain to Stress and Force..... 33

4-2 Beam with Distributed Load..... 34

4-3 Axial Force vs. Fill Height at Section A3..... 37

4-4 Section B1 Axial Force vs. Fill Height from Section A..... 39

4-5 Deflected Shape of Culvert..... 42

4-6 Section A Wall Bending Moments vs. Fill Height..... 43

4-7 Section B Wall Bending Moments vs. Fill Height..... 44

4-8 Section A Roof Bending Moments vs. Fill Height..... 46

4-9 Section B Roof Bending Moments vs. Fill Height..... 47

4-10 Location of Pressure Cells..... 48

4-11 Section A Roof Pressure Cell Readings vs. Fill Height..... 49

4-12 Section B Roof Pressure Cell Readings vs. Fill Height..... 51

4-13 Section A Wall Pressure Cell Readings vs. Fill Height..... 54

4-14 Section B Wall Pressure Cell Readings vs. Fill Height..... 55

4-15 Example Pressure Distributions..... 56

List of Figures

Page Number

Chapter 5

5-1 Boundary Conditions for Roof Forces..... 61

5-2 Bending Moments in Top Slab with Different Support Conditions..... 63

5-3 Shear Forces in Top Slab with Different Support Conditions..... 64

5-4 Approximated Linear Pressure Distribution..... 65

5-5 Load Distributions for Roof Forces..... 66

5-6 Effect of Load Distribution on Culvert Roof Moments.....67

5-7 Effect of Load Distribution on Culvert Roof Shear Forces..... 69

5-8 Load Distributions and Boundary Conditions on Wall Forces..... 70

5-9 Wall Bending Moments with Varying Load Distributions Flexible Support..... 72

5-10 Wall Bending Moments with Varying Load Distributions Rigid Support..... 73

5-11 Wall Bending Moments with Varying Load Distributions Simple Support..... 74

5-12 Wall Shear Forces with Uniform Load and Different Support Conditions..... 75

5-13 Wall Shear Forces with Varying Load Distributions Flexible Support..... 76

List of Figures

Page Number

5-14 Wall Shear Forces with Varying Load Distributions Rigid Support..... 77

5-15 Wall Shear Forces with Varying Load Distributions Simple Support..... 78

5-16 Location of Roof Bending Moments..... 80

5-17 Section A Roof Bending Moments at Side Wall..... 81

5-18 Section A Roof Bending Moments at Center..... 82

5-19 Section A Roof Bending Moments at Middle Wall..... 83

5-20 Section B Roof Bending Moments at Side Wall..... 84

5-21 Section B Roof Bending Moments at Center..... 85

5-22 Section B Roof Bending Moments at Middle Wall..... 86

Chapter 6

6-1 Section A1 - Moment Interaction Diagram..... 90

6-2 Section A2 - Moment Interaction Diagram..... 91

6-3 Section A3 - Moment Interaction Diagram..... 92

6-4 Section A4 - Moment Interaction Diagram..... 93

6-5 Section A5 - Moment Interaction Diagram..... 94

6-6 Section A6 - Moment Interaction Diagram..... 95

6-7 Comparison of AASHTO Shear Strength..... 97

List of Figures

Page Number

6-8 Shear Force vs. Axial Force Case 1 (Uniform Load)..... 98

6-9 Shear Force vs. Axial Force Case 2 (Triangular Load)..... 99

6-10 Shear Force vs. Axial Force Case 3 (High Pressure at Base)..... 100

6-11 Section A Roof Shear Strength..... 102

Appendix A

A - 1 Reinforcement Details..... 110

A - 2 Strain Gage Locations..... 111

Appendix B

B - 1 Strain Readings Section A1..... 113
B - 2 Axial Force and Bending Moment Section A1..... 114
B - 3 Axial Force vs Fill Height Section A1..... 115
B - 4 Bending Force vs Fill Height Section A1..... 116
B - 5 Strain Readings Section A2..... 117
B - 6 Axial Force and Bending Moment Section A2..... 118
B - 7 Axial Force vs Fill Height Section A2..... 119
B - 8 Bending Force vs Fill Height Section A2..... 120
B - 9 Strain Readings Section A3..... 121
B - 10 Axial Force and Bending Moment Section A3..... 122
B - 11 Axial Force vs Fill Height Section A3..... 123
B - 12 Bending Force vs Fill Height Section A3..... 124
B - 13 Strain Readings Section A4..... 125
B - 14 Axial Force and Bending Moment Section A4..... 126
B - 15 Axial Force vs Fill Height Section A4..... 127
B - 16 Bending Force vs Fill Height Section A4..... 128
B - 17 Strain Readings Section A5..... 129
B - 18 Axial Force and Bending Moment Section A5..... 130

List of Figures

		Page Number
B - 19	Axial Force vs Fill Height Section A5	131
B - 20	Bending Force vs Fill Height Section A5	132
B - 21	Strain Readings Section A6	133
B - 22	Axial Force and Bending Moment Section A6	134
B - 23	Axial Force vs Fill Height Section A6	135
B - 24	Bending Force vs Fill Height Section A6	136

Appendix C

C - 1	Strain Readings Section B1	138
C - 2	Axial Force and Bending Moment Section B1	139
C - 3	Axial Force vs Fill Height Section B1	140
C - 4	Bending Force vs Fill Height Section B1	141
C - 5	Strain Readings Section B2	142
C - 6	Axial Force and Bending Moment Section B2	143
C - 7	Axial Force vs Fill Height Section B2	144
C - 8	Bending Force vs Fill Height Section B2	145
C - 9	Strain Readings Section B3	146
C - 10	Axial Force and Bending Moment Section B3	147
C - 11	Axial Force vs Fill Height Section B3	148
C - 12	Bending Force vs Fill Height Section B3	149
C - 13	Strain Readings Section B4	150
C - 14	Axial Force and Bending Moment Section B4	151
C - 15	Axial Force vs Fill Height Section B4	152
C - 16	Bending Force vs Fill Height Section B4	153
C - 17	Strain Readings Section B5	154
C - 18	Axial Force and Bending Moment Section B5	155
C - 19	Axial Force vs Fill Height Section B5	156
C - 20	Bending Force vs Fill Height Section B5	157
C - 21	Strain Readings Section B6	158
C - 22	Axial Force and Bending Moment Section B6	159
C - 23	Axial Force vs Fill Height Section B6	160
C - 24	Bending Force vs Fill Height Section B6	161

List of Figures

Page Number

Appendix D

D - 1 Roof Pressure vs Days Section A..... 163
D - 2 Roof Shear Forces vs Days Section A..... 164
D - 3 Wall Pressure vs Days Section A..... 165
D - 4 Wall Shear Forces vs Days Section A..... 166
D - 5 Roof Pressure vs Days Section B..... 167
D - 6 Roof Shear Forces vs Days Section B..... 168
D - 7 Wall Pressure vs Days Section B..... 169
D - 8 Wall Shear Forces vs Days Section B..... 170

Chapter 1
Introduction

1.1 Introduction

Cast-in-place concrete box culverts are often used to as conduits to carry water from one side of a highway to the other. Although this is a simple role, the loadings applied to these structures are rather complex. These structures must resist large vertical and lateral earth pressures, and are often subjected to significant loadings during construction of the embankment. Due to the soil-structure interaction effects, the state of stress on the culvert depends on the stiffness of both the structure and the backfill material. Although the pressures applied to the structure are quite complex, a simple approach must be used for analysis and design due to the large number of culverts that are being built.

1.2 Background

In late 1995 a reinforced concrete box culvert in Sullivan County, Tennessee with approximately 12 meters of clayey black shale fill failed shortly after being placed in service. The mode of failure was a shear failure at the bottom of the culvert wall. Earth pressures in excess of the design pressure could have contributed to the failure. Uncertainties in the estimation of earth pressures for culverts have resulted in several changes to the American Association of State Highway and Transportation Officials (AASHTO) Specifications during the period 1973 - 1996 (AASHTO 11th to 16th editions).

To investigate the earth pressures acting on box culverts, an instrumentation project was initiated in March 1996. Pressure cells and strain gages were installed on the new replacement culvert constructed in Sullivan County. The new replacement culvert, which was much stiffer then the old culvert, was backfilled with a minimum compactive effort to reduce the applied earth pressures. To confirm the recorded pressures on the Sullivan County culvert and to study the effects of compaction, another culvert was instrumented in Greene County, Tennessee. The culvert in Greene County was constructed according to Tennessee Department of Transportation Standards and has approximately 19 meters of silty clay fill. The Greene County culvert is the culvert discussed in this thesis.

1.3 Description of Culvert

The culvert in Greene County, Tennessee is a cast-in-place double cell culvert made with reinforced concrete. The dimensions of the culvert are 4 meters high, 7 meters wide and 92 meters long. The backfill has a slope of 2 to 1, with a height of 19 meters, and supports a 2-lane highway. To aid in the construction of the culvert, a prestressed panel was used in the roof. The dimensions and amount of reinforcing in the culvert vary slightly along the length to account for the different fill heights. Typical concrete and steel strengths, 20.67 kPa (3 ksi) and 413 kPa (60 ksi) respectively, were used for the materials in the culvert.

1.4 Factors Affecting the Performance of Cast-in-Place Box Culverts

There are several factors that may affect the performance of cast-in-place concrete box culverts. Some of the factors are as follows:

- height of embankment
- orientation of culvert with respect to the alignment of the embankment
- analysis and design procedures for concrete box culvert structures
- lateral earth pressures induced during compaction of the backfill
- loadings due to construction equipment
- foundation support condition (yielding/unyielding foundation)
- expansive minerals in the backfill material
- changes in backfill material over time due to weathering, grain size distribution
- seasonal groundwater table fluctuations

1.5 Design and Installation of Instrumented Culvert Sections

Both strain gages and pressure cells were used to determine the internal forces and pressures in the culvert due to the backfill. Only one cell of the culvert was instrumented since the loading and response may be assumed to be symmetrical about the culvert centerline. The locations of the pressure cells and the strain gages are shown in Figure 1-1.

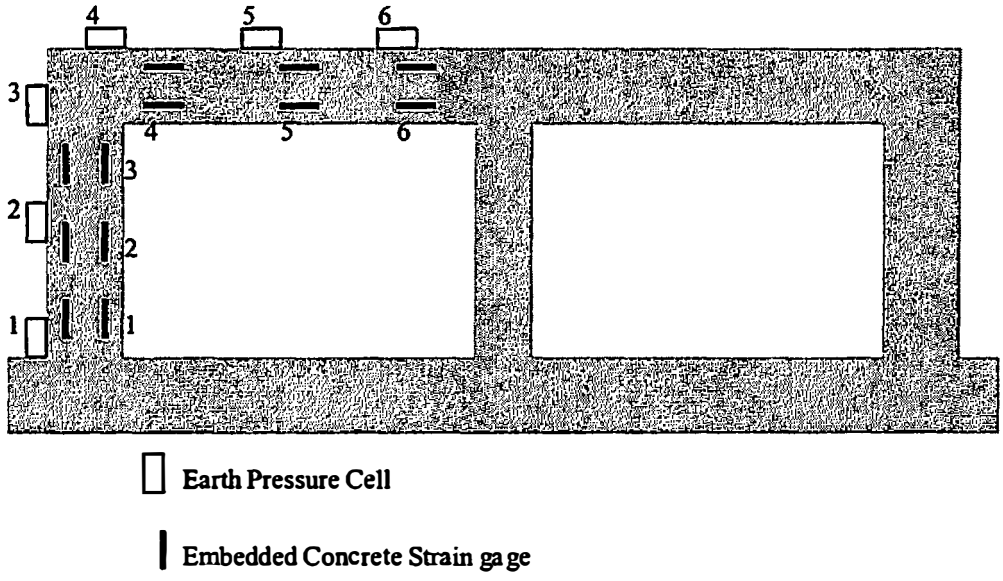


Figure 1-1. Typical Culvert Instrumentation Layout and Numbering Scheme.

Two sections along the length of the culvert were instrumented, Figure 1-2. Section A is located approximately in the center of the culvert length under the full embankment height. Section B is located so that the embankment height is less than the maximum height.

Instruments were installed to measure both the loading and strain response of the culvert. From these strains and pressures and also the material properties, internal forces can be determined. These internal forces include axial force, bending moments and shear forces.

1.6 Monitoring Earth Pressures and Strains

The box culvert was monitored from the time of installation through the end of the research period, thus providing a series of background and service measurements for approximately three years. This period should be sufficient to determine any seasonal changes in embankment water content and temperature effects.

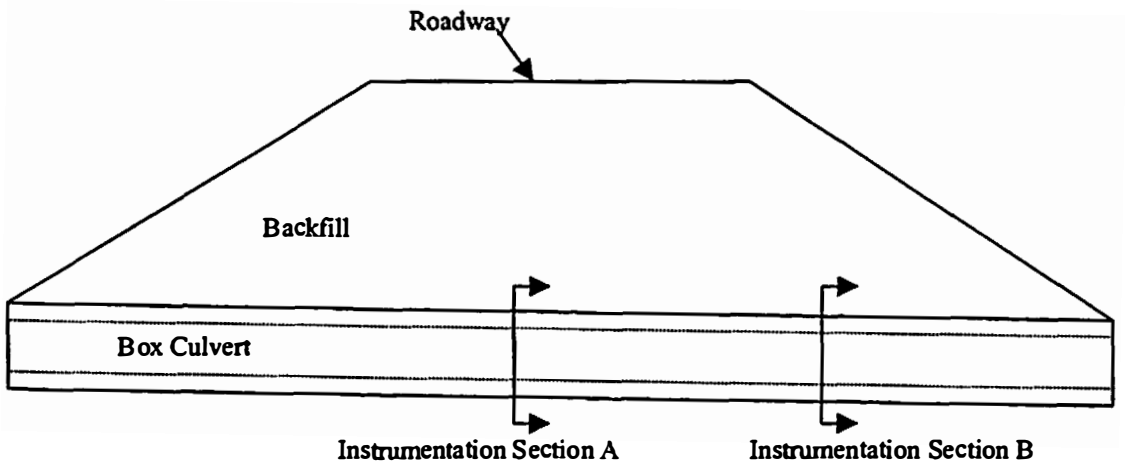


Figure 1-2. Schematic of Embankment and Culvert Cross-Section with Typical Sections A and B

Chapter 2
Literature Review

2.1 Classification of Culverts

Culverts are classified as rigid or flexible depending on their structural stiffness and are further divided by the installation method used. Based on the construction and environmental conditions, culvert installation may be classified as a trench condition or an embankment condition. The embankment condition is further subdivided into positive embankment condition and negative projecting embankment condition (Spangler and Handy, 1982).

A trench condition is defined as an installation in a narrow trench that is dug in undisturbed soil and then covered with earth backfill, as shown in Figure 2-1A. Many utility pipes are installed using the trench method. A positive embankment condition is constructed by placing the culvert on the natural ground and then covering it with an embankment, as shown in Figure 2-1B. Railway and highway culverts are frequently installed with the positive embankment method. A negative projecting embankment is installed in a relatively narrow and shallow trench below the ground surface and then covered with an embankment that is above the natural ground surface, as shown in Figure 2-1C. This is a favorable condition for small highway and railway construction since it produces a smaller vertical load than the positive embankment condition. The negative embankment condition can be even more effective with respect to vertical pressures if the backfill in the trench is filled with a highly compressible material. The imperfect trench condition, also known as induced trench condition, Figure 2-1D, is a

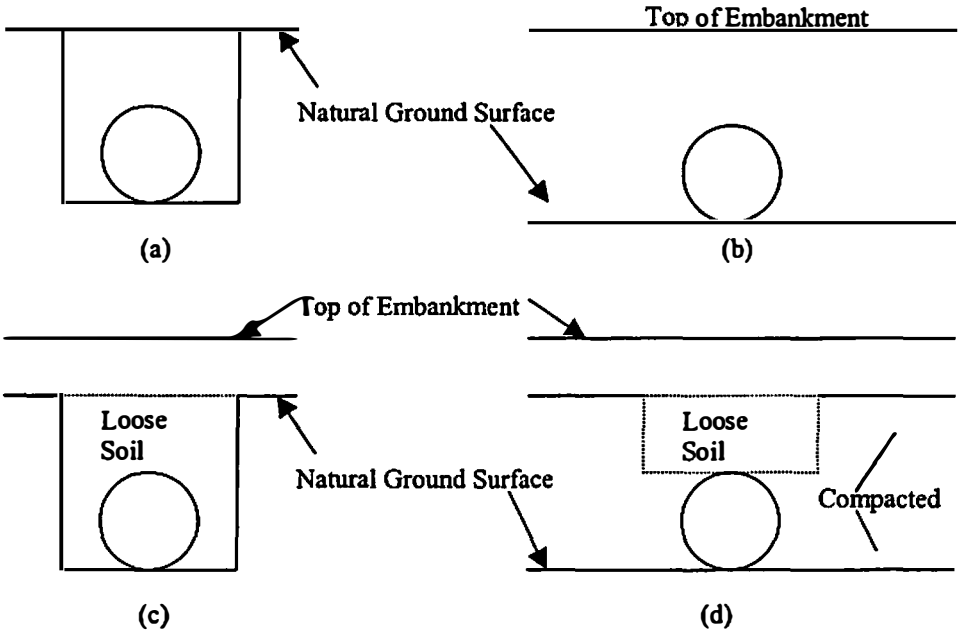


Figure 2-1. Various classes of culvert installation. (a) Trench Condition; (b) Positive projection embankment condition; (c) Negative projection embankment condition; (d) Imperfect trench condition (Spangler, 1982).

special mixed case. The culvert is placed on the natural ground and then an extremely compressible material is placed immediately above the culvert to some height and then covered with normal compacted materials. This installation method can also greatly reduce the vertical pressures on the culvert. These installation methods are used in the AASHTO 1996 design guideline to distinguish soil-structure interaction effects. Figure 2-2 shows a summery of the classification of culverts.

2.2 Recommended Earth Pressures

AASHTO design guidelines state that vertical and horizontal earth pressures may be computed by recognized or appropriately documented tests, or may be assumed by an equivalent fluid weight using the pressures in the design guide. These pressures in the design guide distinguish between rigid and flexible culverts, and reinforced concrete box culverts. These pressures also assume a yielding foundation, whereas an unyielding foundation would require a special analysis. The design pressures make no distinction between a trench and an untrenched installation. Table 2-1 shows a summary of the assumed pressures

Table 2-1. Summary of AASHTO Design Pressures for Buried Box Culverts

	Max. Pressure	Min. Pressure
Equivalent Unit Weight for Vertical Earth Pressure (kN/m^3)	18.8	18.8
Equivalent Unit Weight for Horizontal Earth Pressure (kN/m^3)	9.4	4.7

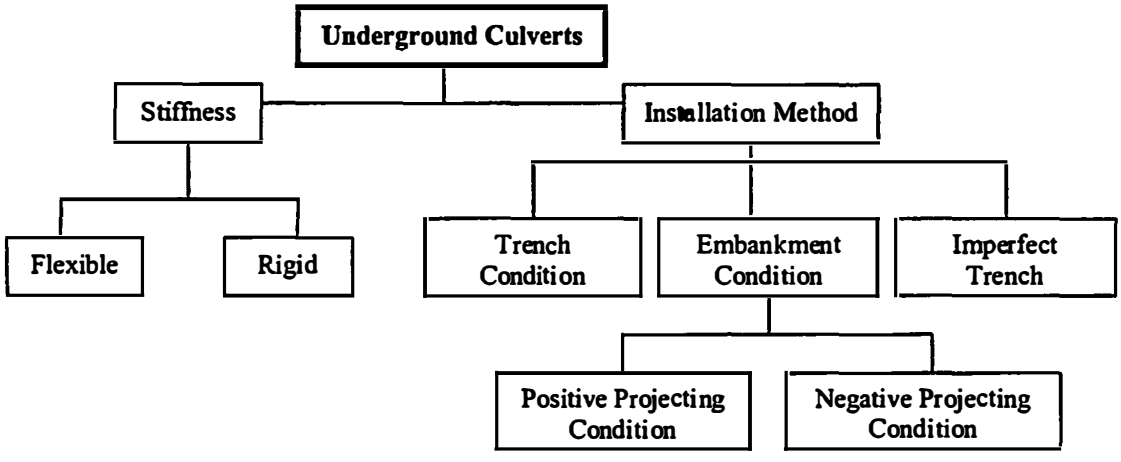


Figure 2-2. Classification of Culverts

AASHTO takes account of soil structure interaction by means of a modification factor applied to the assumed soil pressure. This modification factor is based on the design earth cover, sidefill compaction and bedding characteristics. The total load, W_e, on the box section is:

$$W_e = F_e w B_c H \qquad (2\text{-}1)$$

where F_e is the modification factor that is based on the Marston-Spangler theory of earth loads, B_c is the width of the culvert and H is the backfill height.

The modification factor, F_e, is calculated based on the installation condition. For an embankment condition, F_{e1} is calculated as:

$$F_{e1} = 1 + 0.20\frac{H}{B_c} \qquad (2\text{-}2)$$

F_{e1} need not be greater than 1.15 for installations with compacted fill at the sides of the culvert, and need not be greater than 1.4 for installations with uncompacted fill on the sides of the culvert. For a trench condition, the modification factor is calculated as:

$$F_{e2} = \frac{C_d B_d^2}{H B_c} \qquad (2\text{-}3)$$

where C_d is a load coefficient and B_d is the width of the trench. The maximum value of F_{e2} need not exceed F_{e1}.

For the design of railway culverts (AREA, 1996), the vertical earth pressure is taken as that due to an equivalent fluid pressure with a unit weight of 18.8 kN/m^3 without a factor for soil-structure interaction. The horizontal earth pressures are

calculated by multiplying the vertical pressure by a coefficient. The maximum coefficient is 1.0 and the minimum coefficient is 0.33. This corresponds to lateral pressures of 18.8 kN/m^3 and 6.2 kN/m^2, respectively. Compared to AASHTO pressures, the vertical pressure is smaller since there is no modification factor; however, the lateral pressure is greater than the AASHTO lateral pressure with the modification factor.

The lateral thrust on basement walls and similar vertical structures below grade is given in ASCE "Minimum Design Loads for Buildings and Other Structures: (ASCE 7-95). The load magnitude depends on the soil type and structure stiffness. It suggests a lateral pressure for cohesionless backfill material on a relatively flexible structure of about 5.5 kPa per meter depth, and about 9.43 kPa per meter height for a relatively stiff structure. For silty soil backfill the lateral pressure is 13.4 kPa for flexible structures and 15.7 kPa for rigid structures. These design pressures are for moist conditions at the soil optimum densities above the ground water line.

Table 2-2 shows a summary of the different design earth pressures for underground structures. As can be seen, there is significant difference among the different guidelines with both vertical and horizontal pressures. These wide differences in lateral pressure may reflect the uncertainties of the earth pressures on buried structures.

Table 2-2. Summary of Equivalent Fluid Pressure for the Design Earth Pressures for

Design Guide	Vertical Earth Pressure (kN/m^3)		Lateral Earth Pressure (kN/m^3)	
	Maximum	Minimum	Maximum	Minimum
AASHTO	18.8	18.8	9.4	4.7
AREA	18.8	18.8	18.8	6.2
ASCE 7-95	NA	NA	15.7	5.5

Buried Structures.

2.3 Earth Pressures on Buried Box Culverts

While there has been an extensive amount of research done on flexible metal and circular concrete culverts (Davis and Bacher, 1972; Selig et al. 1982; Duncan and Seed, 1996), there has been limited research done on concrete box culverts. Soil arching effects are greater on circular culverts and also the lateral pressure provides some added support. Typically, metal and circular culverts are also more flexible than concrete box culverts. Therefore, research done on metal and circular culverts is of limited use in the study of concrete box culverts.

Tadros et al, (1989) conducted a full scale test on a functional cast-in-place reinforced concrete culvert in Sarpy County, Nebraska. The culvert was a double-cell box on a 35° skew with a soil fill height of 8.5 feet. Measurement of soil pressures, strains, deflections and settlements were made both during and after construction. Some of the results concluded that AASHTO values were unconservative with respect to the lateral earth pressure. When the study was conducted, AASHTO allowed the use of a vertical soil pressure of 0.7 of 18.8 kN/m^3 (120 pcf) and a lateral soil pressure

of 4.7 kN/m^3 (30 pcf) equivalent fluid pressure. Current AASHTO specifications do not have the reduction factor for the vertical pressure, and have increased the lateral equivalent fluid pressure to a range from 4.7 kN/m^3 (30 pcf) to 9.4 kN/m^3 (60 pcf). The study also mentioned that both the magnitude and distribution of the actual pressures are greatly influenced by the effects of compaction.

In another study done by Tadros, Benak and Gilliland (1998), a computer analysis was performed on two different buried box culverts with average fill heights. The computer software used was *CANDE-1980.* The developers of the computer program compared the results to actual field data from circular and buried box culverts. In the computer modeling study done by Tadros, Benak and Gilliland, they found that the soil pressures can be much greater than AASHTO specifications. *CANDE* pressures were also found to be higher at the more rigid corners and less at the midspan of the top and bottom slabs.

In a study done by Dasgupta and Sengupta (1991) a concrete box culvert was constructed in a sand bed and backfilled to a height of 2.4 meters above the top slab of the culvert. The culvert dimensions were 1200 by 1200 mm with 75 mm thick walls. Deflections, strains and pressures were recorded at different sections in the culvert. Figure 2-3 shows the distribution of pressure from the completed fill on the top and bottom slabs and also the walls of the culvert. The pressure distribution on the top and bottom slabs shows a parabolic distribution where the higher pressure was measured at the more rigid corners. The pressure distribution on the wall was not trapezoidal, as

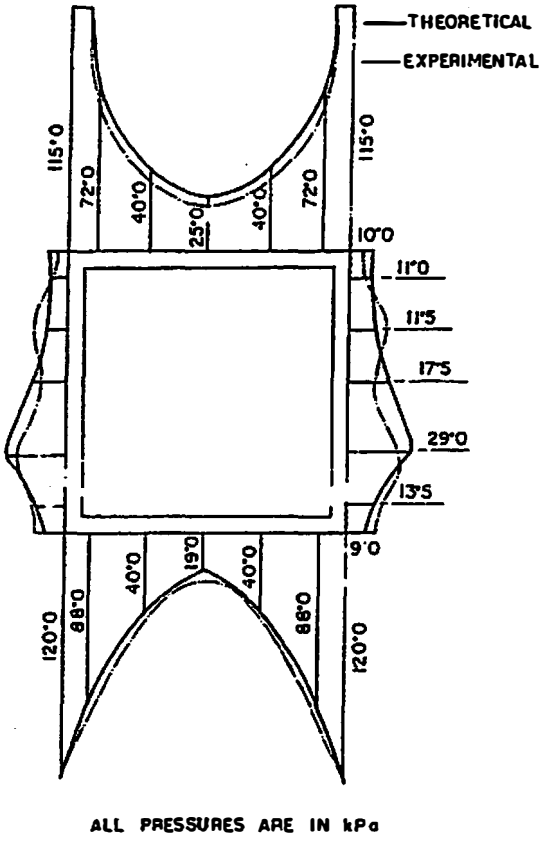


Figure 2-3. Pressure Distribution with a 2.4 meter sand fill. Dasgupta, A. and Sengupta, B. (1991). "Large-Scale Model Test On Square Box Culvert Backfilled With Sand." *Journal of. Geotechenial Engineering. Div.*, ASCE, 117(1), 156-161.

AASHTO assumes, but more of a parabolic distribution with the maximum pressure at about 0.3 times the height of the wall from the base of the culvert.

Chapter 3
Instrumentation

3.1 Measurement of Strain in Reinforced Concrete Sections

Concrete can be assumed to be a homogeneous, isotropic material at the macro level. However, at the micro level, concrete is not homogeneous, consisting of coarse and fine aggregates and hydrated cement. There can be large local variations in strain at the micro level. The strain at the micro level is not the strain of interest in this project, but rather the average strain at the macro level is of importance. To obtain the average strain, the gage length for measuring the strain needs to be several times longer than the largest aggregate size.

After cracking in the concrete, there are strain variations between the cracks in the concrete and steel, as illustrated in Figure 3-1. To obtain an average strain, a gage length must be several times longer than the crack spacing. Thus, gage lengths of up to 1 meter have been used to measure strain in reinforced concrete members.

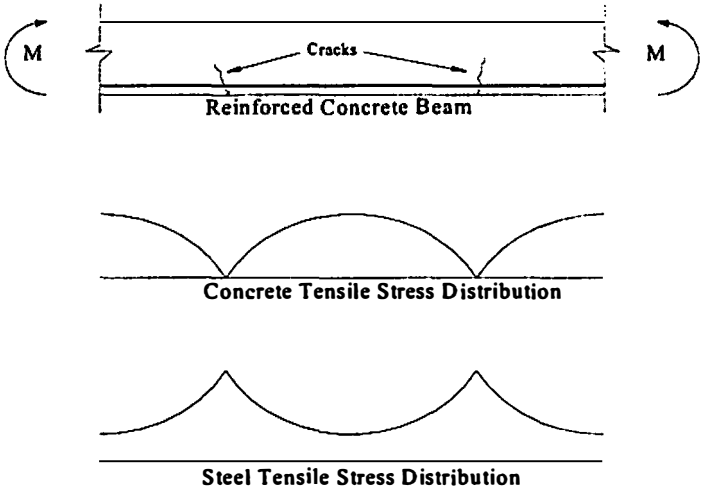


Figure 3-1. Strain in Concrete and Steel in Cracked Reinforced Concrete Member.

In a reinforced concrete box culvert, there are large differences between bending moments across a particular section. For example, the moment at the ends of the culvert roof would be negative, while towards the center, the bending moments would be positive, with the typical box culvert roof being 3-4 meters long. Thus, with such large changes in moments, and strains, a gage length of 1 meter would be too long. The gage length chosen must be small enough to show the large gradients, but it must also be long enough to extend across several cracks.

For the present project, a gage length of 150 mm was chosen for measuring the strain. This gage length is long enough to avoid the strain variations due to the variation at the micro level, and it is also small enough to have nearly a constant strain over the gage length. However, if the concrete were to crack in flexure this gage length would probably not be sufficient to span several cracks. Nonetheless, it was felt that the 150-mm gage length would be best suited for these conflicting requirements.

The strain in the concrete not only comes from the load on the culvert, but also from the creep and shrinkage of the concrete. Both creep and shrinkage are primarily a function of relative humidity, thickness of the concrete member, the fines coefficient and the air content. Because the culvert is buried, the relative humidity will remain high which will decrease the effects of both creep and shrinkage.

Creep strains were estimated for the culvert using ACI 209 (1971). The creep coefficient (C_t) is the ratio of creep strains to the initial elastic strain. The creep coefficient is obtained as:

$$C_t = C_u K_t K_a K_h K_{th} K_s K_f K_e \quad (3\text{-}1)$$

Where C_u is the ultimate creep coefficient, which can range from 1.30 to 4.15, with an average of 2.35. The average value of 2.35 was used herein. K_t is the time under load, and is $t^{0.6}/(10+t^{0.6})$, with t in days. K_a is the age when the structure was loaded. It was assumed that the structure was moist cured, and loaded at 220 days, resulting in K_a=0.66. K_h is the relative humidity coefficient. A relative humidity of 90% was assumed, resulting in K_h=0.67. K_{th} is the minimum thickness of the member coefficient, and is 0.82 for member greater than 25-mm thick. The other coefficients are the slump coefficient (K_s), the fines coefficient (K_f), and the air content coefficient (K_e), which are all assumed to be 1.0. This results in a creep coefficient of 1.16 for the time equal to infinity. The creep coefficient versus time to 100 days is plotted in Figure 3-2.

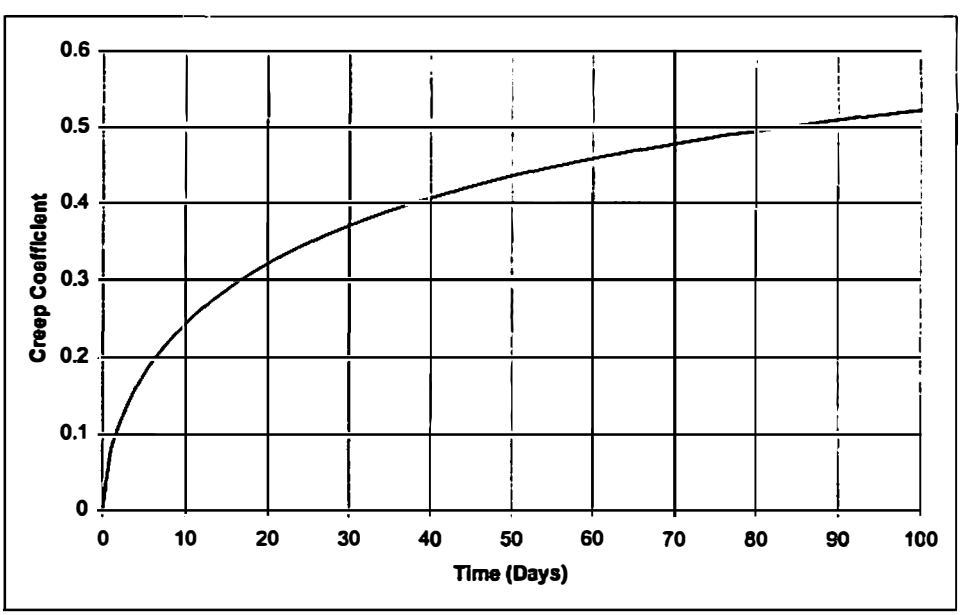


Figure 3-2. Creep coefficient versus time after application of load.

Although creep will affect the strain readings, it is difficult to determine the magnitude of creep. Also as the creep occurs, the concrete culvert will continue to be loaded which will in turn effect the amount of creep. Creep is expected to cause the strain readings to increase, but the amount of the increase is unknown.

3.2 Measuring Strain

Vibrating wire strain gages were used for all strain measurements involving long term internal forces in the culvert. The Goekon Model VCE-4200 vibrating wire strain gage chosen for this project is designed for long term strain measurements in concrete structures. The strain gages were embedded in the concrete and attached to the steel reinforcement. The measured frequency of the gages was automatically converted to strain readings by use of the microprocessor in the Geokon Model GK-403 readout box. The readout box automatically reads strain and the real time temperature, which was used for temperature correction.

3.3 Installation of Vibrating Wire Strain Gages

Before the concrete was poured, the vibrating wire strain gages were installed by tying the gages to the rebar with plastic ties. The gages were separated from the rebar with Styrofoam blocks at the ends of each gage. The Styrofoam blocks served as isolators to prevent possible high frequency oscillation generated by the concrete vibrator during the placement of the concrete. The Styrofoam block also prevented the gages from direct pull damage, which may happen from the movement of the

reinforcing bars during placement of the concrete. It is assumed that there is no relative slip between the concrete and the rebar provided the concrete is not cracked. On the bottom of the culvert roof, a 150-mm thick prestressed pre-cast concrete panel was used, so that reinforcing bars were not available to mount the gage. To compensate for this, "dummy" rebars of the same diameter as the top reinforcing bars were suspended about 25-mm above the concrete panel and used to mount the strain gages. A schematic of a typical gage installation is shown in Figure 3-3.

The gages were mounted to the reinforcing rebar, such that the concrete deformation can be recorded by the strain along the active length of the gage. The gage length of 150 mm is long enough to cross several interfaces between the aggregate and the cement, which are the locations where micro-cracks would likely develop first.

In order to measure the axial forces and bending moments in the culvert, the gages were installed in pairs at each particular location. The position of the gages was recorded so that it was possible to convert the strains into moments and axial forces (Yang 2000).

3.4 Temperature Correction

Although the vibrating wire strain gages have a self-temperature-compensation mechanism, the gages would still likely undergo some temperature induced no-stress readings. In order to provide some correction for temperature effects, a stress-free reference gage was placed in the culvert. The procedure for installing the stress-free gage was placing a vibrating wire gage in a 150-mm dia. cylinder of the same concrete

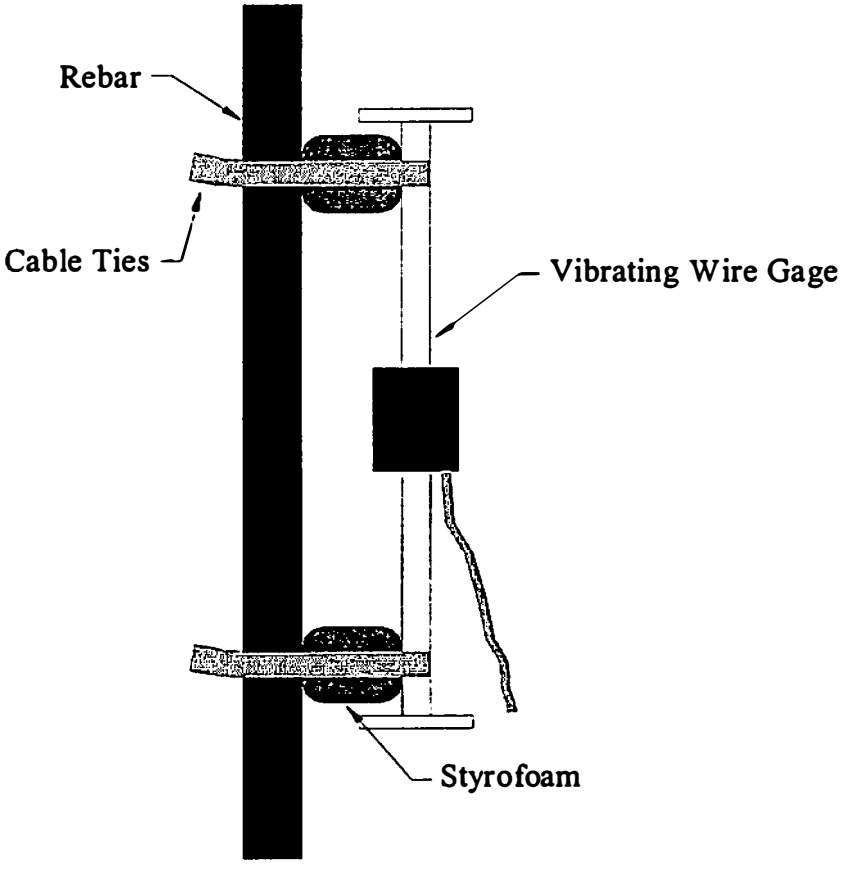


Figure 3-3. Schematic of strain gage installation.

used in the culvert. The cylinder was then placed in the bottom of the culvert wall and isolated from the surrounding concrete by approximately a 30-mm thick layer of Styrofoam so that the gages in the cylinder would not be affected by the external stress by the backfill. The stress-free gage should then experience the same temperature as the gages mounted to the reinforcing steel. The reference gage was monitored throughout the study to find a correlation between temperature and strain readings. Figure 3-4 shows that, over time there is some relationship between temperature and strain readings.

A correlation value was needed in order to correct for temperature changes in all of the strain gages. Figure 3-5 shows a graph of the stress free reference gage readings vs. temperature; a best-fit trend line was generated through the points. From the slope of the best-fit trend line, a correction factor (k) was found to be 1.0026 με/°C. An r^2 value of 0.3627 was proven to be significant by the R.A. Fisher method using the t-distribution with a significance level of 5%(Sachs,1984).

The corrected reading can be found by using the equation:

$$R = R_1 + k\,(T_o - T_1) \qquad (3\text{-}2)$$

where R is the corrected reading, R_1 is the original reading, k is the correction factor, T_o is the average initial temperature and T_1 is the temperature of the gage when the reading was taken.

Before the stress free reference gage readings were corrected, the standard deviation of the reference gage readings was 7.02 με. After the temperature correction

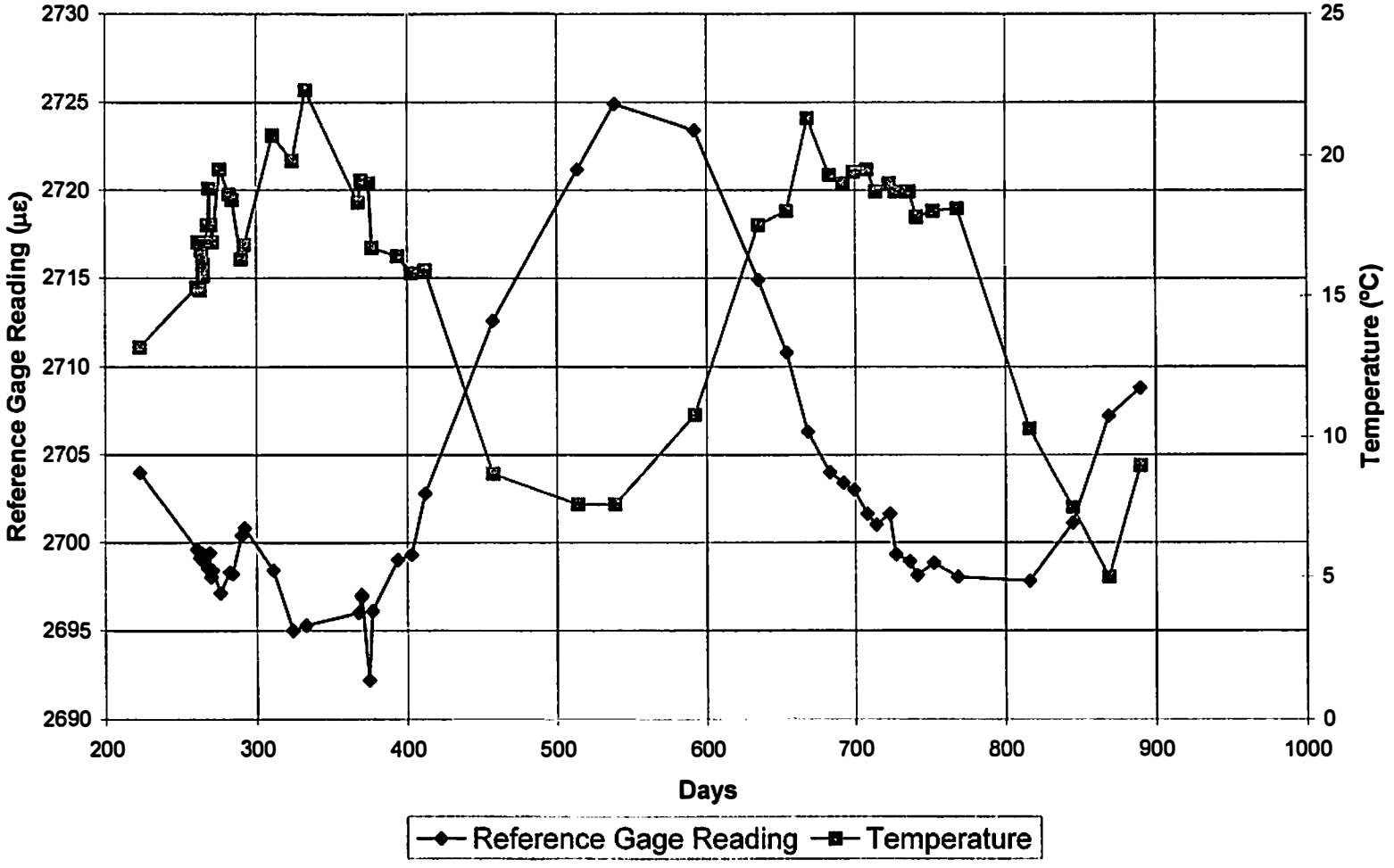


Figure 3-4. Reference Gage Readings

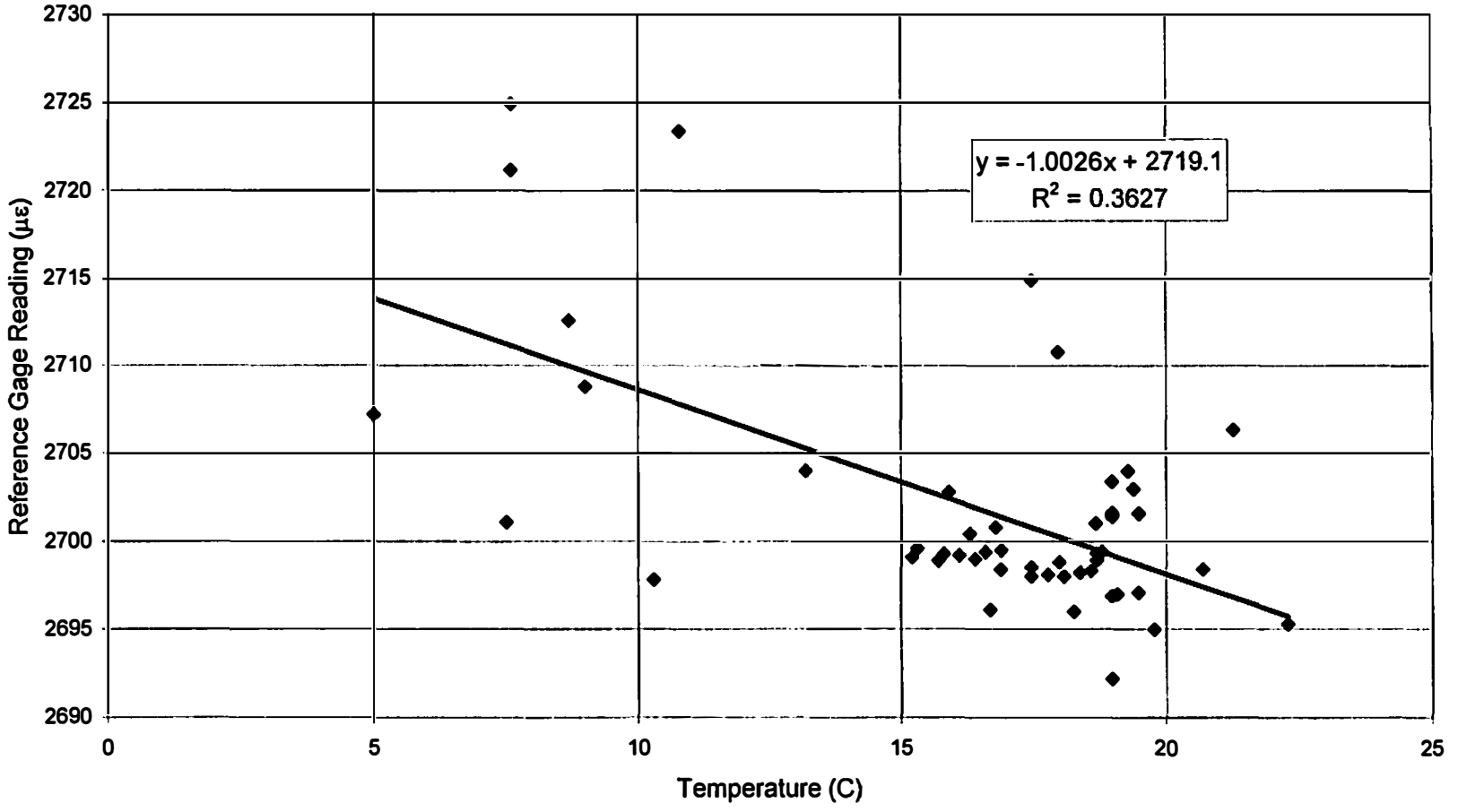


Figure 3-5. Reference Gage Readings vs Temperature

was applied the standard deviation decreased to 5.61 με. A strain of 5.61 με corresponds to a change in concrete stress of approximately 142 kPa (20 psi). This shows the relative stability the stress free reference gage reading, and the long term stability of the vibrating wire strain gages. Figures 3-6 and 3-7 show the stress free gage readings after the temperature correction.

3.5 Strain Gage Datums

Finding the correct datum for each of the strain gages was very important since all other readings would be compared to it in order to find the change in strain. The time period after the concrete was poured and before the backfill was placed was the best time for datum readings. Between 9 and 20 readings were taken from each of the strain gages before the backfill was placed. This many readings from each strain gage allowed for a good average value for a datum.

Before an average was taken for the datum, the readings that were considered outliers were removed. An outlier is a reading that is much higher or lower than the rest of the data set. Several factors such as equipment malfunctions or improper readings of the strain gage could cause these outliers. The statistical test chosen for the detection of outliers was the Maximum Normed Residual (MNR) method (DOD, 1997). By this method, a reading is labeled an outlier if it has an absolute deviation from the sample mean when compared to the sample standard deviation and is too distinct to be due to chance.

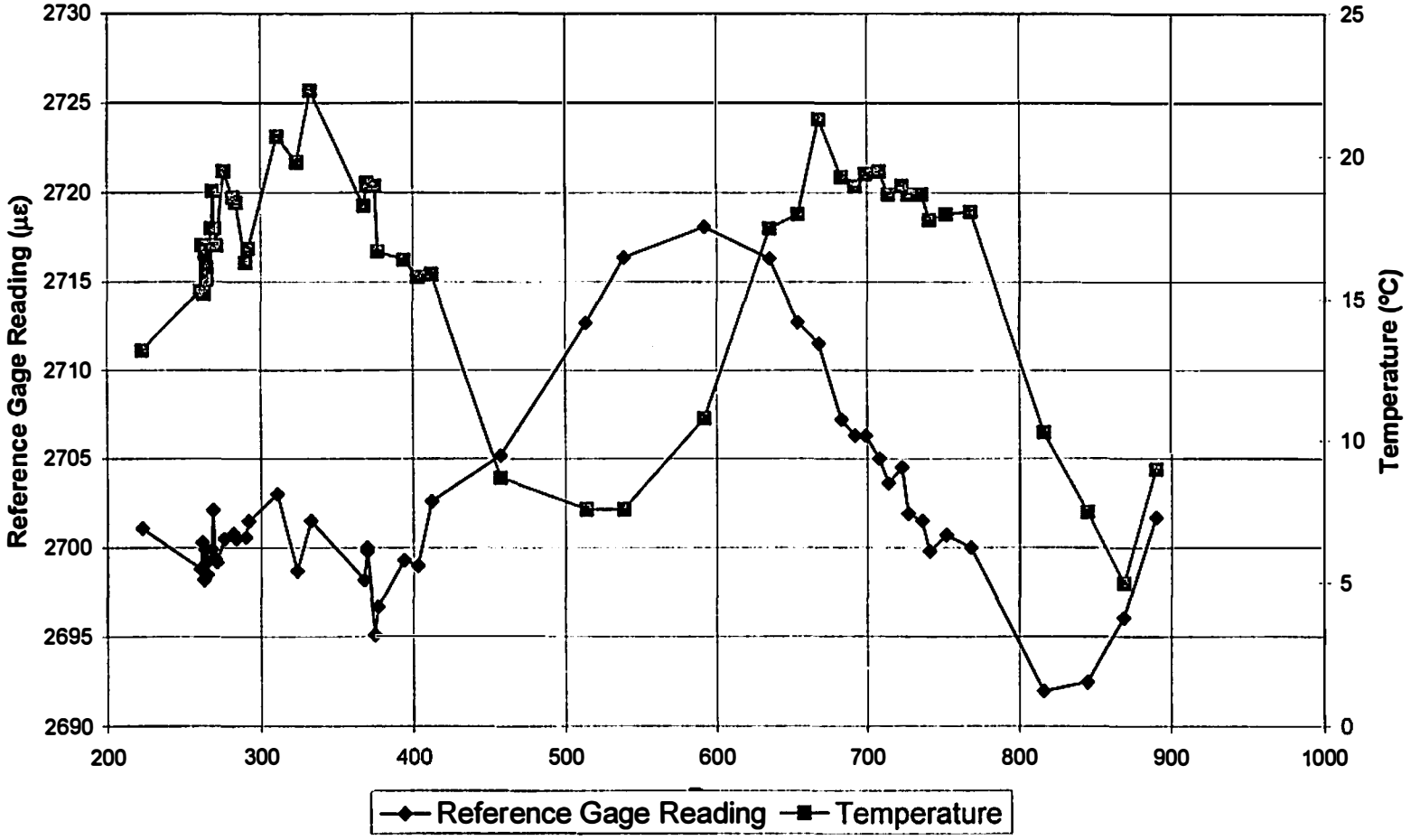


Figure 3-6
Corrected Reference Gage Readings

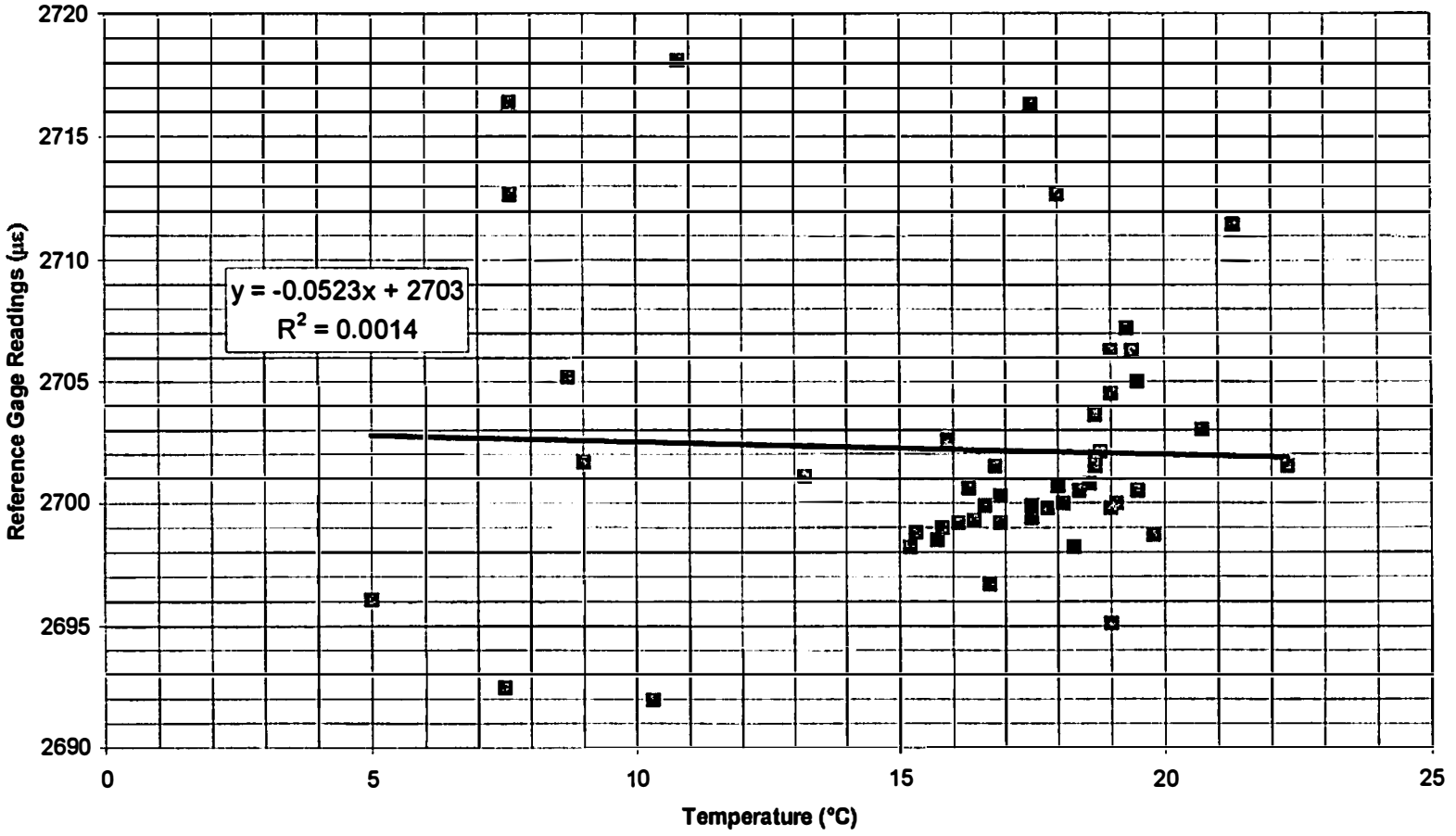


Figure 3-7. Corrected Reference Gage Readings vs Temperature

The MNR statistical test is the maximum absolute deviation from the sample mean, divided by the sample standard deviation:

$$MNR = \max_i \frac{|x_i - \bar{x}|}{s}, i = 1,2,...,n \qquad (3\text{-}3)$$

where x_i is the i^{th} observation, $\bar{x}$ is the sample mean, and s is the sample standard deviation. This equation is then compared to the critical value for the specified sample size n. These critical values are calculated by the following formula:

$$C = \frac{n-1}{\sqrt{n}} \sqrt{\frac{t^2}{n-2+t^2}} \qquad (3\text{-}4)$$

where n is the number of samples, t is the value from the t-distribution with n-2 degrees of freedom. The significance level used for this test was α=0.05. If the MNR value is smaller than the critical value, the value is not an outlier. If the MNR value is larger than the critical value then the data value with the largest $|x_i - \bar{x}|$ is recognized as an outlier. If an outlier is found, that data value is omitted from the set and the test is run again until no outliers are found.

All of the readings taken before the backfill was placed were run through a MNR test. In all of the strain gage locations only four outliers were found and removed, then the average of each data set was used for the datums.

3.6 Pressure Cells

Earth pressure cells were used to measure the contact pressure between the walls and roof of the culvert. The type pressure cells used for this study were the vibrating wire type, Goekon model 4810. Pressure cells are useful to compare the

pressure results from the strain gage measurements. The pressure cells register the stress input into the structure, whereas the strain gages in the concrete give the structural response. Figure 3-8 shows a diagram of the pressure cells used.

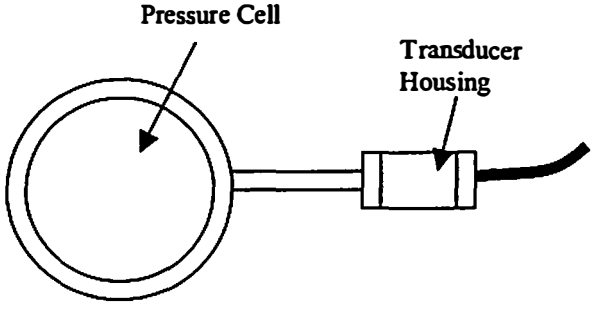


Figure 3-8. Pressure Cell

Chapter 4
Internal Forces

4.1 Conversion of Strain to Forces

4.1.1 Modulus of Elasticity

Strain gage readings are converted to axial force and bending moments at each cross section. It is assumed that plane sections remain plane and the strains are small enough so that the materials are linear elastic. The modulus of elasticity of the concrete is obtained from the equations (Mirza et al, 1979):

$$E_c = 60{,}400 f_{cr}^{1/2} \qquad (4\text{-}1)$$

$$f_{cr} = 0.89 f'_{c35}(1 + 0.08 \log R) \qquad (4\text{-}2)$$

in which E_c is the modulus of elasticity of the concrete in psi, f_{cr} is the corrected strength of the concrete due to speed of loading in psi, f'_{c35} is the 28-day compressive strength of the concrete in psi loaded at the nominal testing speed for cylinder test which is approximately 35 psi/sec, and R is the loading rate ($0.1 \leq R$ psi/sec $\leq 10{,}000$). Equation 4-1 is a mean relationship between compressive strength and modulus, and Equation 4-2 accounts for changes in ultimate compressive strength due to the rate of loading (Mirza et al, 1979).

The average concrete cylinder strength from five cylinders was 33,000 kPa. The rate of loading of the culvert was quite slow, with R being assumed to be 0.1 psi/sec. This results in a corrected strength of the concrete (f_{cr}) of 27,000 kPa (3930 psi). The value for the modulus of elasticity (E_c) was found to be 25,200,000 kPa (3668 ksi).

4.1.2 Modulus of Rupture

To account for changes in concrete stress due to cracking, the extreme fiber tensile strain was compared to the cracking strain of the concrete. The cracking strain was calculated by dividing the modulus of rupture by the modulus of elasticity. The modulus of rupture is obtained from the empirical mean relationship (Mirza et al, 1979):

$$f_r = 6.04\ f_c'^{.538} \qquad (4\text{-}3)$$

where f_r is the modulus of rupture (psi), and f'_c is the compressive strength of the concrete (psi). The equation was obtained from Mirza et al. (1979) to compare the modulus of rupture to the compressive strength of the concrete. Using the above equation, the modulus of rupture of the concrete was found to be 3,870 kPa. When divided by the modulus of elasticity, the cracking strain was calculated as 153 με.

4.1.3 Axial Forces and Bending Moments

Using the strain from the strain gages and the dimensions from the cross-section, a strain distribution was obtained for a particular cross-section. By use of the modulus of elasticity of the concrete and the modulus of elasticity of the steel, the strain was converted to stress, which is then converted to compressive and tensile forces in the concrete and reinforcement, Figure 4-1. The axial force is the sum of the forces, and the bending moment is the sum of the moments taken about the mid-point of the cross-section. Compressive forces were taken as positive. Bending moments were considered positive when the tensile stressses were on the inside of the culvert.

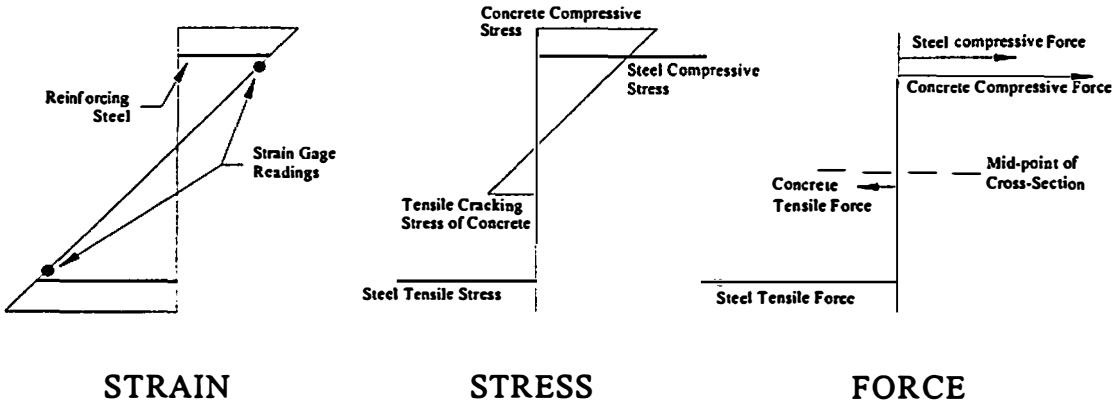


Figure 4-1 Conversion of Strain to Stress and Forces

4.1.4 Back Calculated Pressures from Culvert Forces

Applied pressures acting on the culvert were calculated using the moments from the strain gages. Consider the beam segment in Figure 4-2 with an assumed parabolic load distribution. Since the force on the beam segment is the second derivative of the bending moment, only one unknown can be solved for. Thus, values of k_1, k_2, and k_3 are assumed such that equation 4-5 holds true. The value of the average pressure can then be calculated by the following equation:

$$w = \frac{96}{L^2(-k_1 + 14k_2 - k_3)}\left(M_{cl} - \frac{M_A + M_B}{2}\right) \qquad (4\text{-}4)$$

with: $$\frac{1}{6}k_1 + \frac{2}{3}k_2 + \frac{1}{6}k_3 = 1 \qquad (4\text{-}5)$$

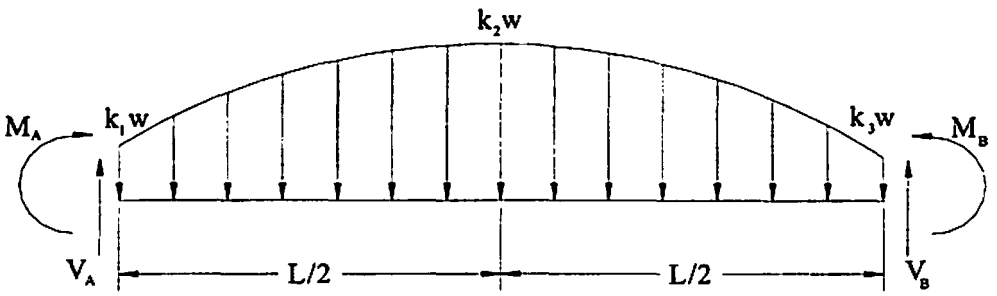


Figure 4-2 Beam with Distributed Load

where w is the average pressure, or the total area under the load diagram divided by the length, and M_A, M_{cl}, and M_B is the moment at the left, center, and right of the beam section.

Using equation 4 -4 different load patterns could be analyzed. For example, a uniform load would have values of $k_1 = k_2 = k_3 = 1$, and a triangular load could be presumed by making $k_1 = 2$, $k_2 = 1$, and $k_3 = 0$.

4.1.5 Calculation of Shear Forces

Shear strength of reinforced concrete comes from many sources, including the tensile strength of concrete, dowel action of the reinforcing bars, aggregate interlock, and the shear transfer in the flexural compression regions. With all these different sources of shear strength, there is virtually no method of measuring the actual shear

force in reinforced concrete. However, internal shear forces can be obtained from the derivative of the bending moment with respect to length along the beam.

Based on the assumption of the same pressure distribution as above and given the moments at A and B, a shear force at each of these section can then be calculated by the following equations:

$$V_A = \frac{M_B - M_A}{L} + \frac{k_1 wL}{6} + \frac{k_2 wL}{3} \qquad (4\text{-}6)$$

$$V_B = \frac{M_A - M_B}{L} + \frac{k_3 wL}{6} + \frac{k_2 wL}{3}$$

where M_A and M_B are the moments at section A and B respectively, L is the length of the beam section and w is the average pressure.

4.2 Force Results

Forces are per meter length of the culvert. For example, an axial force shown as 30 kN/m would mean the 30 kN was applied over a 1 m length.

Force result values are shown by comparing the force with the fill height above the culvert roof. A linear regression was performed between the force and the fill height for each location. The slope of the line gave the change in force per unit increase in backfill height. With this method, the variations between the readings are reduced.

4.2.1 Axial Forces

4.2.1.a Wall Axial Forces

A typical graph of the axial force in a wall section versus the fill height is shown in Figure 4-3. Results of the axial forces in the wall from each section are shown in Table 4-1. Using half of the distance along the roof to the center wall as the tributary width, an equivalent unit weight can be obtained. This equivalent unit weight is then compared to the measured soil unit weight of 18 kN/m^3.

Sections A1 and A2 are essentially the same, while the axial force at section A3, the top of the wall, is about 23% greater. Section B shows variability between each location and also a lower equivalent unit weight than from section A.

Table 4-1. Wall axial forces versus fill height with equivalent unit weight.

Section	Slope (kN/m/m)	r^2	Equivalent Unit Weight (kN/m^3)	Equivalent Unit Weight Divided by Soil Unit Weight
A1	67.4	0.903	38.5	2.14
A2	67.9	0.925	38.7	2.15
A3	83.1	0.982	47.4	2.63
B1	45.0	0.958	25.7	1.43
B2	22.1	0.653	12.6	0.70
B3	9.58	0.495	5.5	0.30

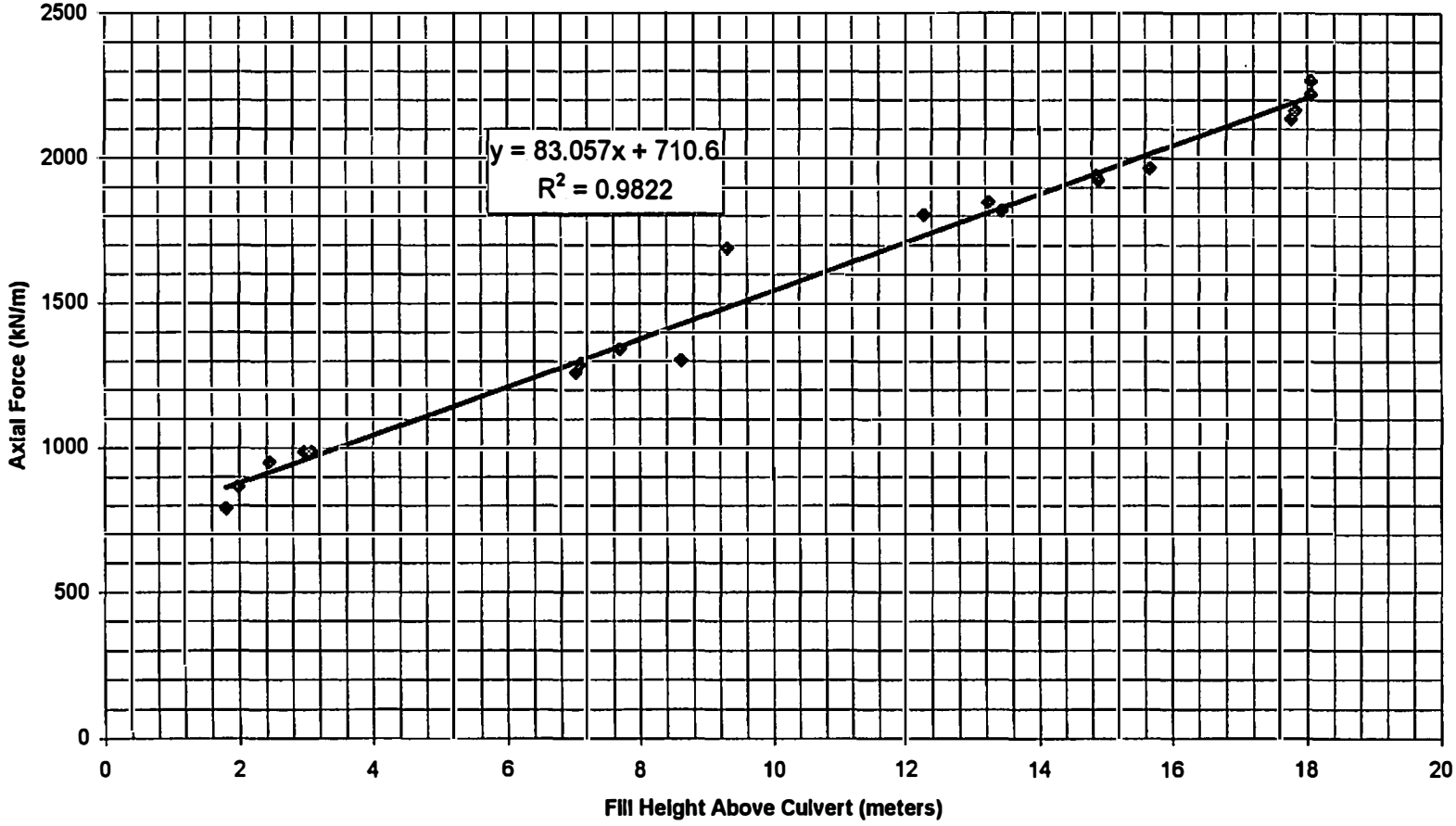


Figure 4-3. Axial Force vs Fill Height at Section A3

The axial force in the wall at section B indicates a continued increase of axial force after the fill at section B was completed. A linear regression line was plotted to find a correlation between the axial force in the wall at B and the fill height at A. A typical graph of this is shown in Figure 4-4. Table 4-2 shows a summary of the results from section B.

The American Association of Highway and Transportation Officials (AASHTO) Standard Specifications for Highway Bridges gives earth pressures for the design of a buried box culvert. AASHTO uses a vertical earth pressure of 18.9 kN/m^3 with a modification factor for soil structure interaction.

Table 4-2. Section B axial forces versus fill height at section B and section A.

Fill from Section B			
Section	Slope (kN/m/m)	r^2	Equivalent Unit Weight Divided by Soil Unit Weight
B1	45.0	0.958	1.43
B2	22.1	0.653	0.70
B3	9.58	0.495	0.30
Fill from Section A			
Section	Slope (kN/m/m)	r^2	Equivalent Unit Weight Divided by Soil Unit Weight
B1	32.3	0.9323	1.02
B2	16.4	0.6869	0.52
B3	1.34	0.01	0.04
Fill from Section A above Section B			
Section	Slope (kN/m/m)	r^2	Equivalent Unit Weight Divided by Soil Unit Weight
B1	23.4	0.9091	0.74
B2	24.4	0.8731	0.77
B3	30.8	0.7383	0.98

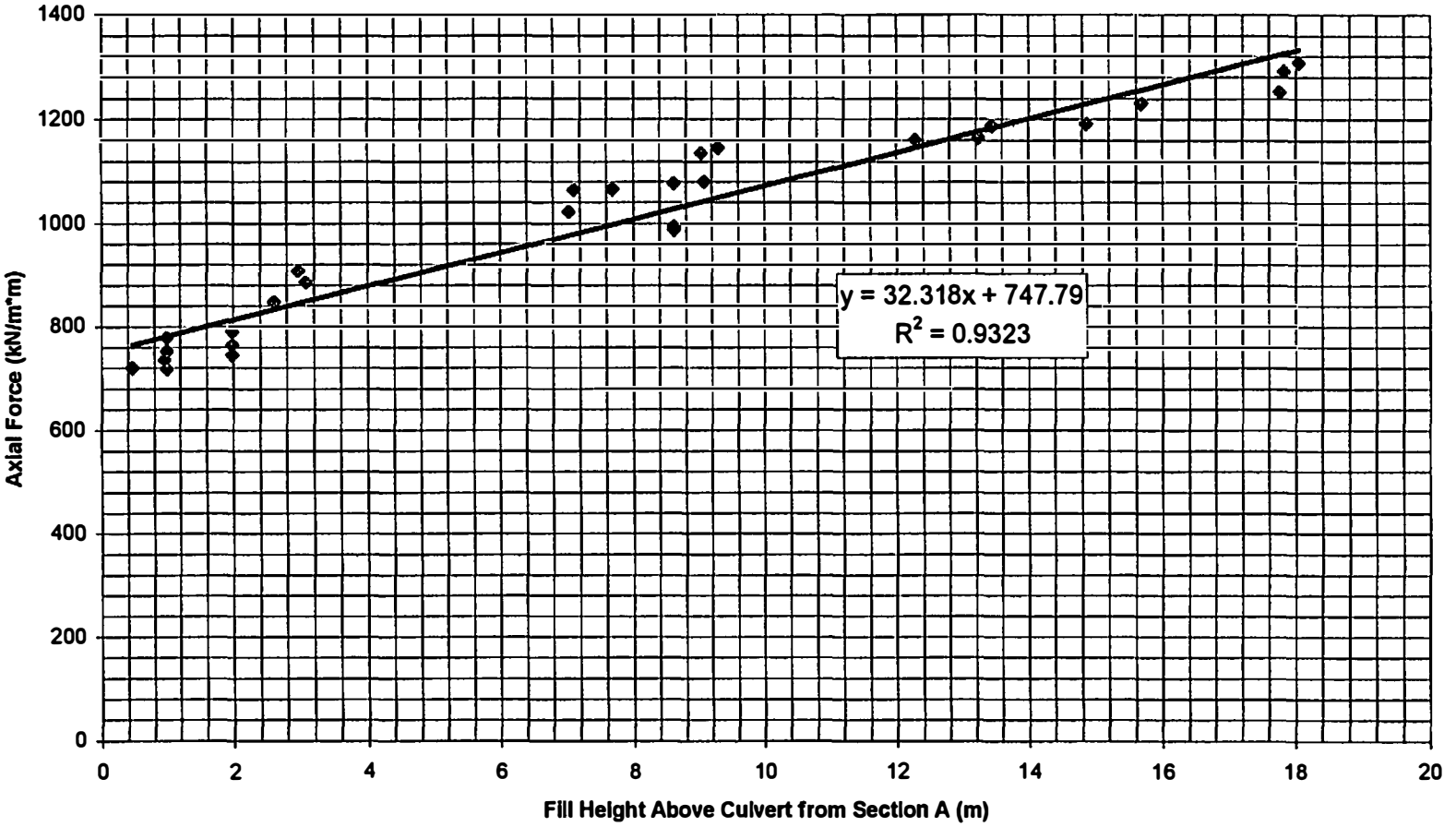


Figure 4-4. Section B1 Axial Force vs Fill height from Section A

The modification factor for this type of embankment culvert is given by the following formula:

$$F_{el} = 1 + 0.20\frac{H}{B_c} \qquad (4\text{-}7)$$

Where F_{el} is the modification factor that is multiplied by the soil pressure and need not be greater than 1.15, H is the fill height, B_c is the width of the culvert. For this project, the width of the culvert is 7 meters so with any fill over 5.26 meters the modification factor is 1.15. This modification factor can then be compared to the equivalent unit weight divided by the soil unit weight as shown in Tables 4-1 and 4-2.

The wall at section A shows a high soil modification factor when compared to AASHTO. At section B1, which is at the bottom of the wall, the soil modification factor is higher than AASHTO but at sections B2 and B3 the value is lower.

4.2.1.b Roof Axial Force

The results of the axial forces versus fill height on the culvert roof are shown in Table 4-3. Axial forces in the culvert roof are more variable with respect to each other. Also, the correlation coefficients are much lower. The axial force in the roof at section B indicates a continued increase of axial force after the fill at section B was completed. A linear regression line was preformed with the axial force at B versus the fill height at A.

Table 4-3. Roof axial forces verses fill height.

Fill Height From Respective Section		
Section	Slope (kN/m/m)	r^2
A4	59.20	0.7375
A5	15.05	0.2405
A6	12.20	0.2951
B4	50.64	0.6343
B5	35.73	0.4544
B6	79.08	0.6935
Fill Height From Section A		
Section	Slope (kN/m/m)	r^2
B4	33.27	0.5078
B5	25.26	0.4168
B6	63.06	0.7635

Using the fill at section A proved no greater correlation than using the fill at section B. Axial forces decreased at section B at all three locations. Using the fill height at section A also lowered the correlation coefficient when compared to using the fill height at section B.

4.2.2 Bending Moments

4.2.2.a Wall Bending Moments

Figure 4-5 qualitatively shows the bending induced in the culvert by both vertical and horizontal loads. Vertical loads will induce primarily negative moments in the wall, while horizontal loads will induce primarily positive moments in the wall.

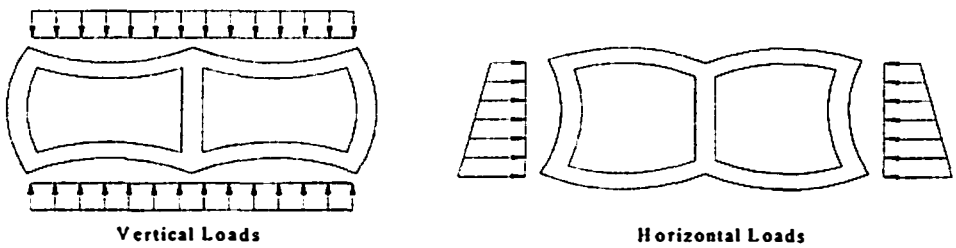


Figure 4-5. Deflected shape of culvert

Figures 4-6 and 4-7 show wall bending moments versus fill height above the roof. On sections A1 and A2 there appears to be two distinct linear regression lines. The two distinct lines show that the culvert forces may behave differently for low fill heights and high fill heights. The change in the moment behavior occurs approximately at a fill height equal to the culvert width. A summary of the applied bending moments for the high fill heights in the culvert wall versus fill height above the roof is shown in Table 4-4.

Table 4-4. Wall bending moments versus fill height.

Section	Slope (kN*m/m/m)	r^2
A1	-19.3	0.985
A2	-8.82	0.9237
A3	-9.29	0.9369
B1	-0.965	0.7852
B2	5.59	0.9288
B3	15.7	0.9631

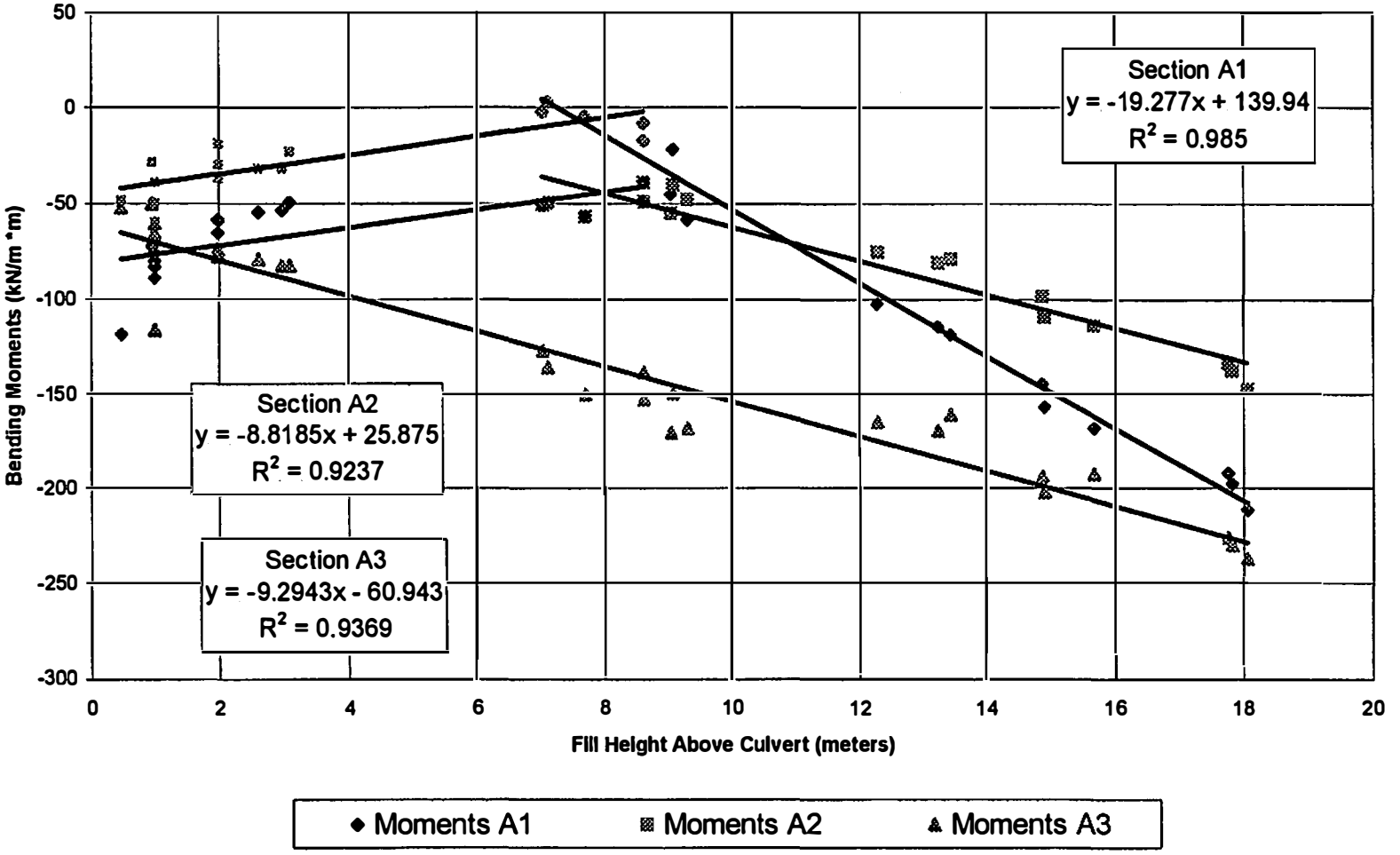


Figure 4-6. Section A Wall Bending Moment vs. Fill Height

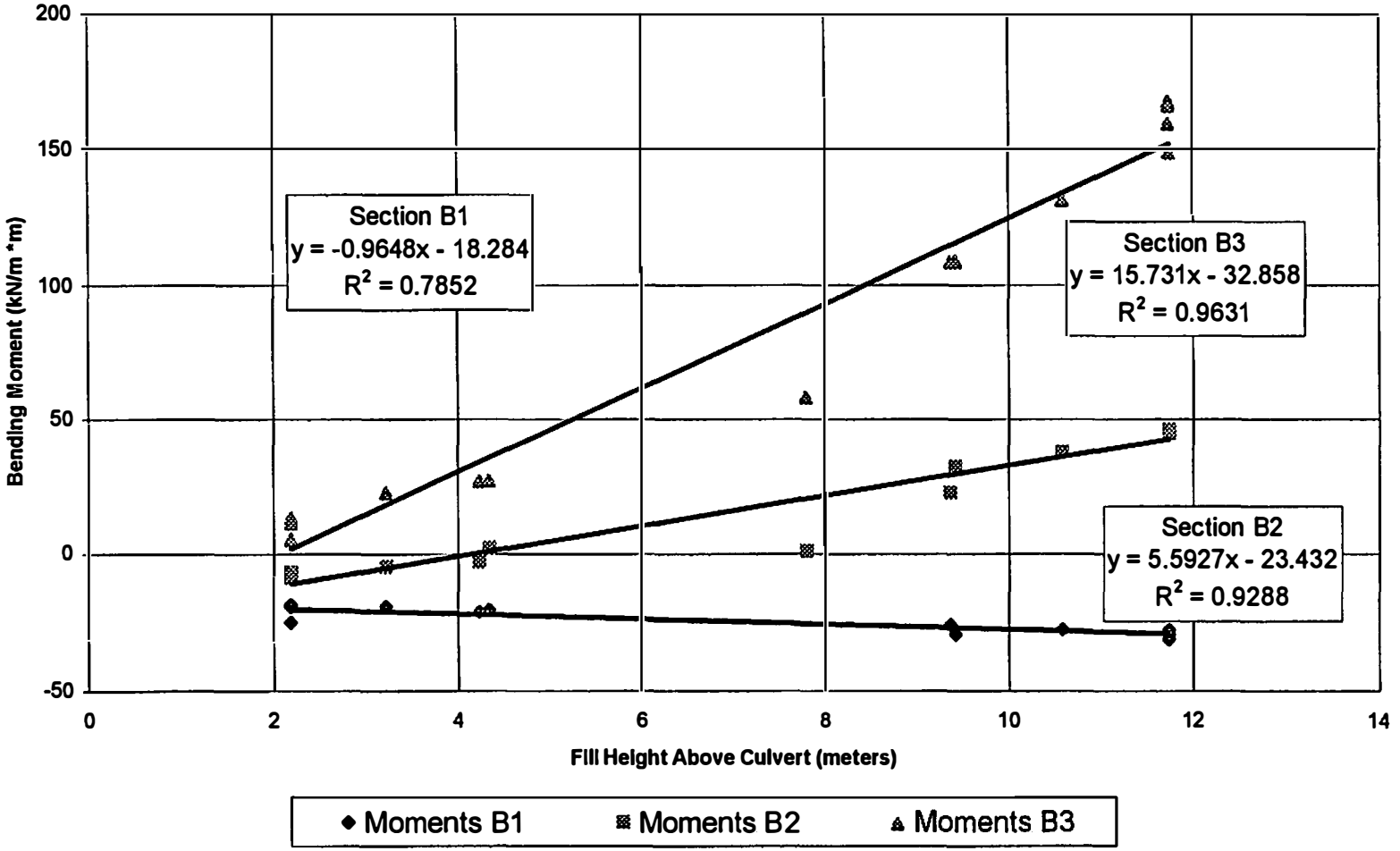


Figure 4-7. Section B Wall Bending Moments vs. Fill Height

The bending moments at section A are all negative, indicating that lateral pressure has little effect and that the vertical pressure controls in the wall bending moments. Section B has a negative bending moment at the bottom of the culvert wall and is positive in the middle and upper part of the wall indicating that the lateral pressure has an influence on the bending moment on the culvert wall.

4.2.2.b Roof Bending Moments

Figures 4-8 and 4-9 show the roof bending moments versus fill height above the culvert roof. A summary of roof bending moments versus fill heights are shown in Table 4-5. Both sections show positive moments close to the center section, while the sections close to the center wall show a negative moment, Figure 4-5. Since the top slab is a continuous member this moment distribution would be qualitatively correct. Also, both sections have close to the same magnitudes across the section, except for near the center wall.

Table 4-5. Roof bending moments verses fill height.

Section	Slope (kN*m/m/m)	r^2
A4	11.6	0.9126
A5	12.1	0.9295
A6	-22.2	0.9046
B4	13.8	0.9038
B5	10.2	0.8357
B6	-6.9	0.7029

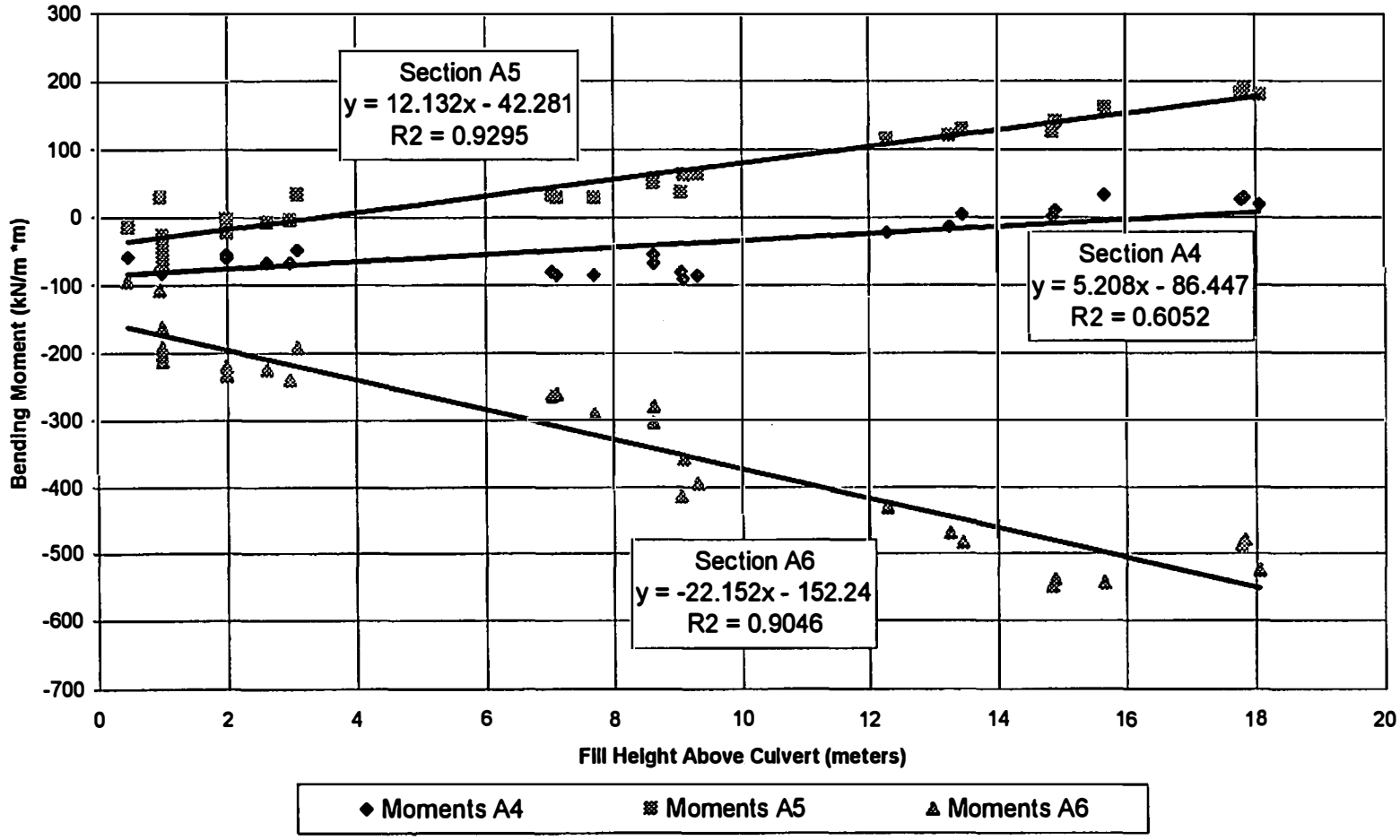


Figure 4-8. Section A Roof Bending Moments vs. Fill Height

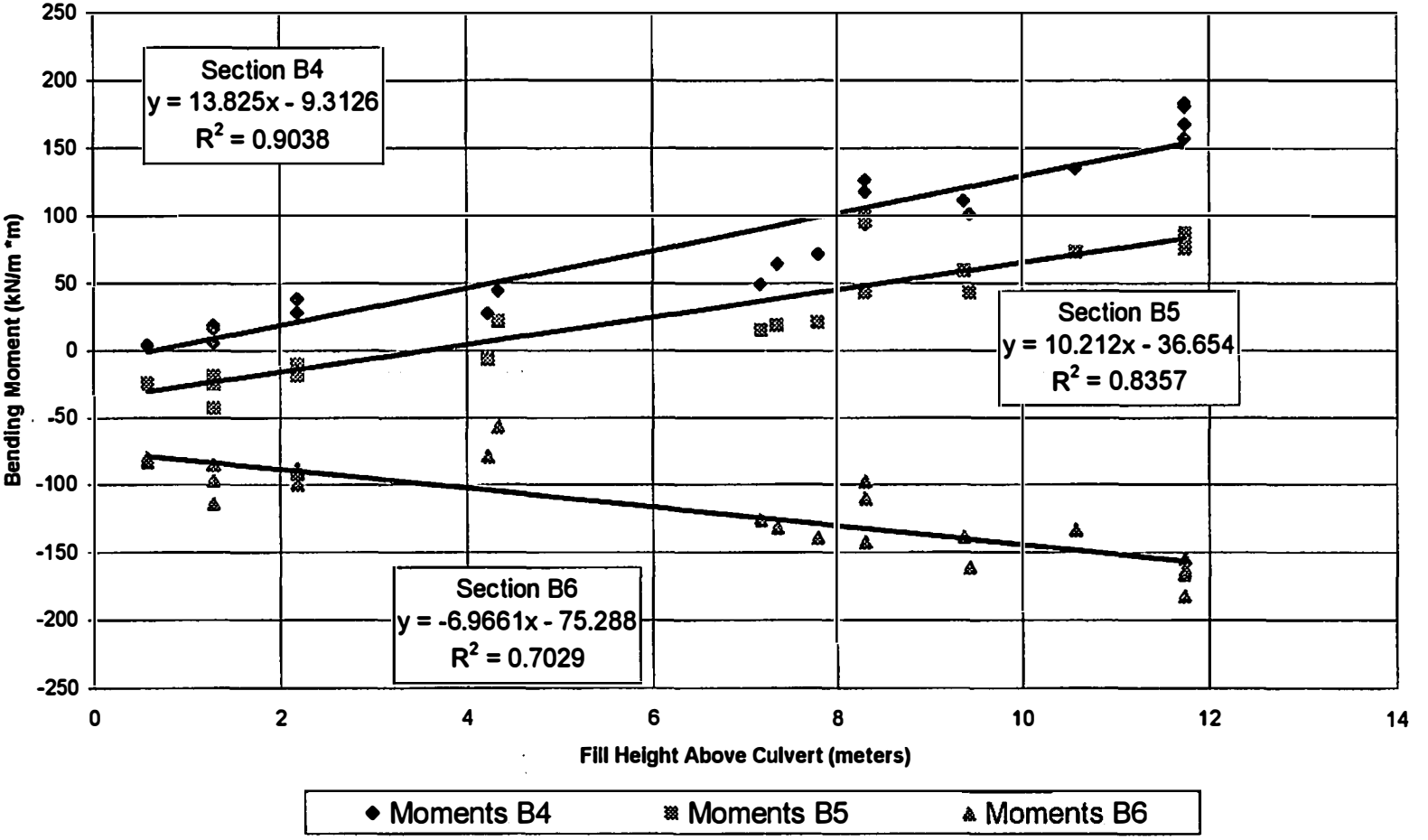


Figure 4-9. Section B Roof Bending Moments vs. Fill Height

4.3 Pressures

Pressure cells were installed at each section on the culvert to measure the actual pressure that was applied to the culvert from the fill. At each section, three pressure cells were attached to the wall and three pressure cells were attached to the roof, Figure 4-10. The average pressure from the three pressure cell readings was then compared to the calculated pressure from the bending moments. Consistent with the assumption that the pressure distribution is parabolic, which was used to back calculate pressure from the bending moments. Simpson's rule was used to calculate an average pressure from the pressure cell readings.

4.3.1 Roof Pressures

Roof pressures versus fill height above the culvert roof at section A are shown in Figure 4-11. The average roof pressure from the pressure cells is 30.9 kPa per meter height of fill. The pressure cell near the end wall is the highest reading while the middle and center are close to the same.

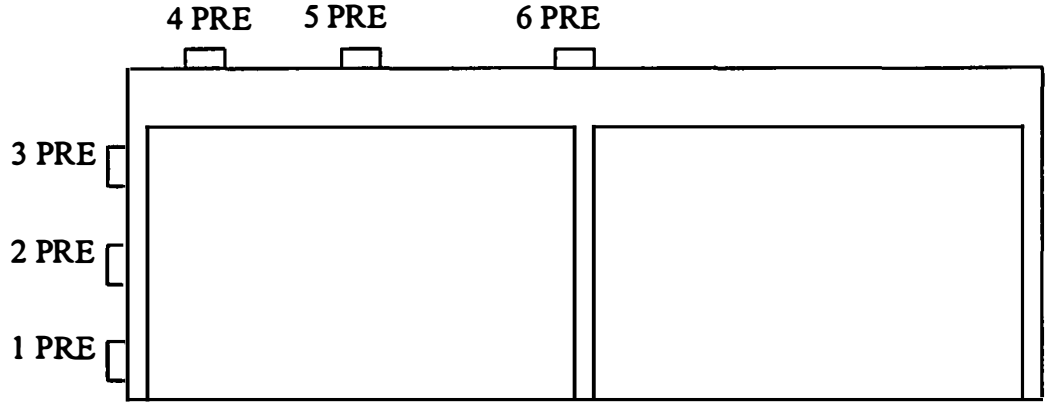


Figure 4-10. Location of the pressure cells

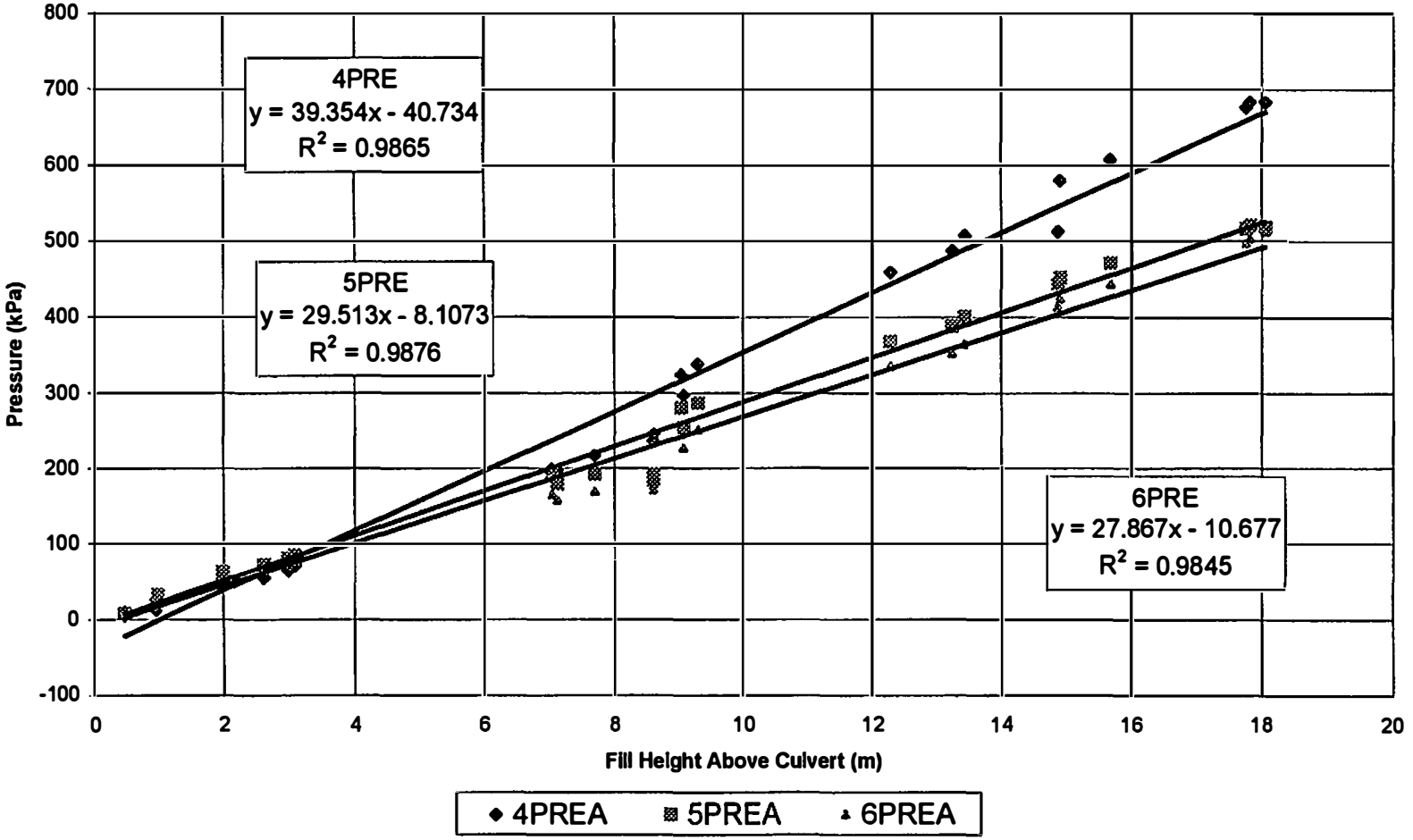


Figure 4-11. Section A Roof Pressure Cell Readings vs Fill Height

Roof pressures at section B are shown in Figure 4-12. The average roof pressure reading is 19.6 kPa per meter height of fill. All three pressure cell readings have a relatively uniform pressure distribution with the pressure cell near the end of the wall having the highest pressure.

To back calculate the pressure from the moments an assumption has to be made for the values of k_1, k_2 and k_3. Two different load cases were examined for the roof. One was an assumed uniform pressure ($k_1 = k_2 = k_3 = 1$). The other pressure distribution was obtained by performing a linear regression between pressure cells to determine the relationship between pressures at different locations. This resulted in $k_1 = 1.18$, $k_2 = 0.97$, and $k_3 = 092$ for section A and $k_1 = 1.24$, $k_2 = 0.94$ and $k_3 = 1.00$ for section B.

Results for the average roof pressures from the pressure cells, the bending moments and the wall axial force are summarized in Table 4-6.

At section A, the three methods of calculating an equivalent unit weight do not vary much from each other. The calculated equivalent unit weight from the axial forces in the wall is the highest followed by the calculated pressure from the bending moment in the roof and then the pressure cell readings. It is also noted that all of the equivalent unit weights divided by the soil unit weight are all higher than AASHTO's soil modification factor (F_{e1}). The equivalent unit weight is nearly twice the soil weight.

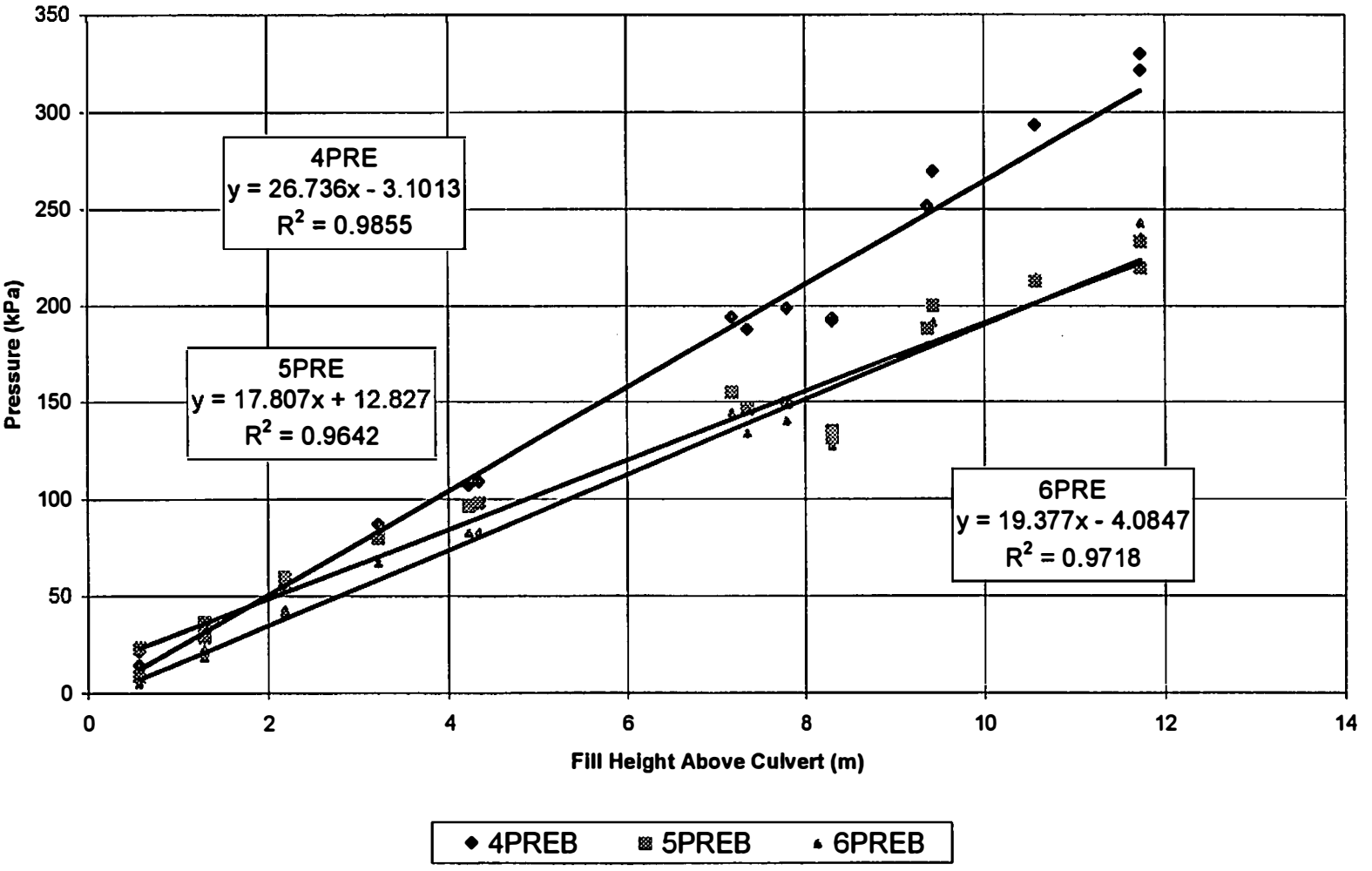


Figure 4-12. Section B Roof Pressure Cell Readings vs Fill Height

Table 4-6. Soil modification factors for different average pressure measurements.

	Section A		Section B	
	Equivalent Unit Weight (kPa/m)	Equivalent Unit Weight Divided by Soil Unit Weight	Equivalent Unit Weight (kPa/m)	Equivalent Unit Weight Divided by Soil Unit Weight
From Pressure Cells	30.9	1.72	19.6	1.09
From Roof Moments				
Assumed Uniform Pressure	34.5	1.92	11.8	0.66
Pressure Dist. as Measured	36.1	2.01	13.06	0.73
From Wall Axial Force				
Section 1	38.5	2.14	25.7	1.43
Section 2	38.7	2.15	12.6	0.70
Section 3	47.4	2.63	5.5	0.31

At section B, the three methods of calculating an equivalent unit weight vary slightly from each other but are still fairly close to one another. The calculated unit weight is highest in the pressure cell readings, and the average of the wall axial force unit weight and the calculated pressure from the bending moments are about the same. The equivalent unit weight is near the soil unit weight.

4.3.2 Wall Pressure

The wall pressures are shown in Figures 4-13 and 4-14. In both sections A and B, the wall has a high pressure at the base compared to the rest of the wall. With this high pressure at the base it is difficult to back calculate the pressure from the moments. The pressure cell at the bottom of the wall at section A failed shortly after installation, thus readings are only available up to about 3 meters of backfill height.

To use equation 4-4 to back calculate the pressure from the moments an assumption has to be made for the values of k_1, k_2 and k_3. Five different load cases were examined, as summarized in Table 4 –7. The first load case assumes a uniform load, the second load case assumes a triangular load and the third, fourth, and fifth case are used to simulate a high base pressure. Some example pressure distributions are shown in Figure 4-15.

A calculated wall pressure could be found by using the strain gage bending moments, but an assumption of the value of k to use in equation 4-4 was difficult to assume with such a pressure distribution. The first five load cases were examined and the calculated average pressures are summarized in Table 4-8.

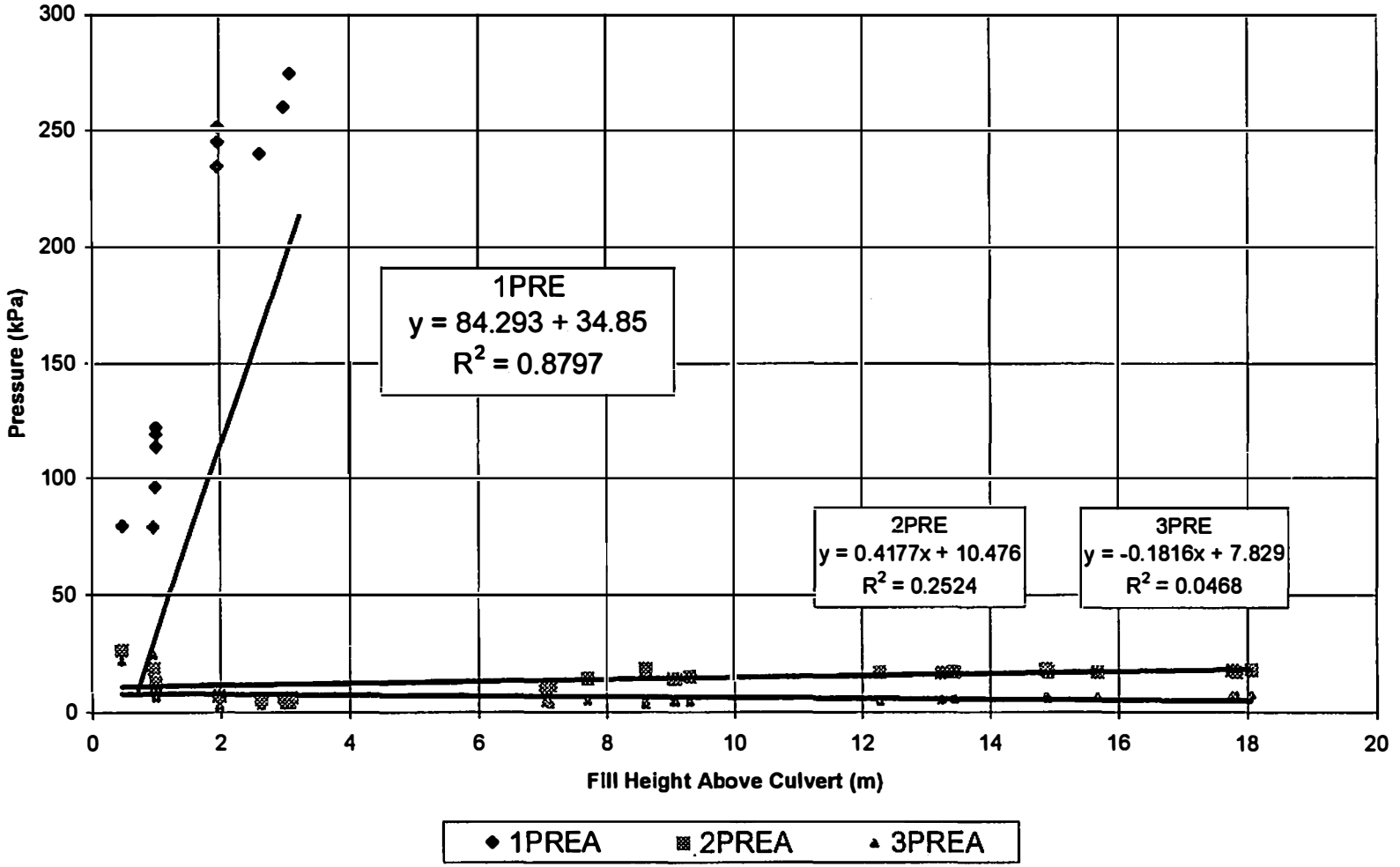


Figure 4-13. Section A Wall Pressure Cell Readings vs Fill Height

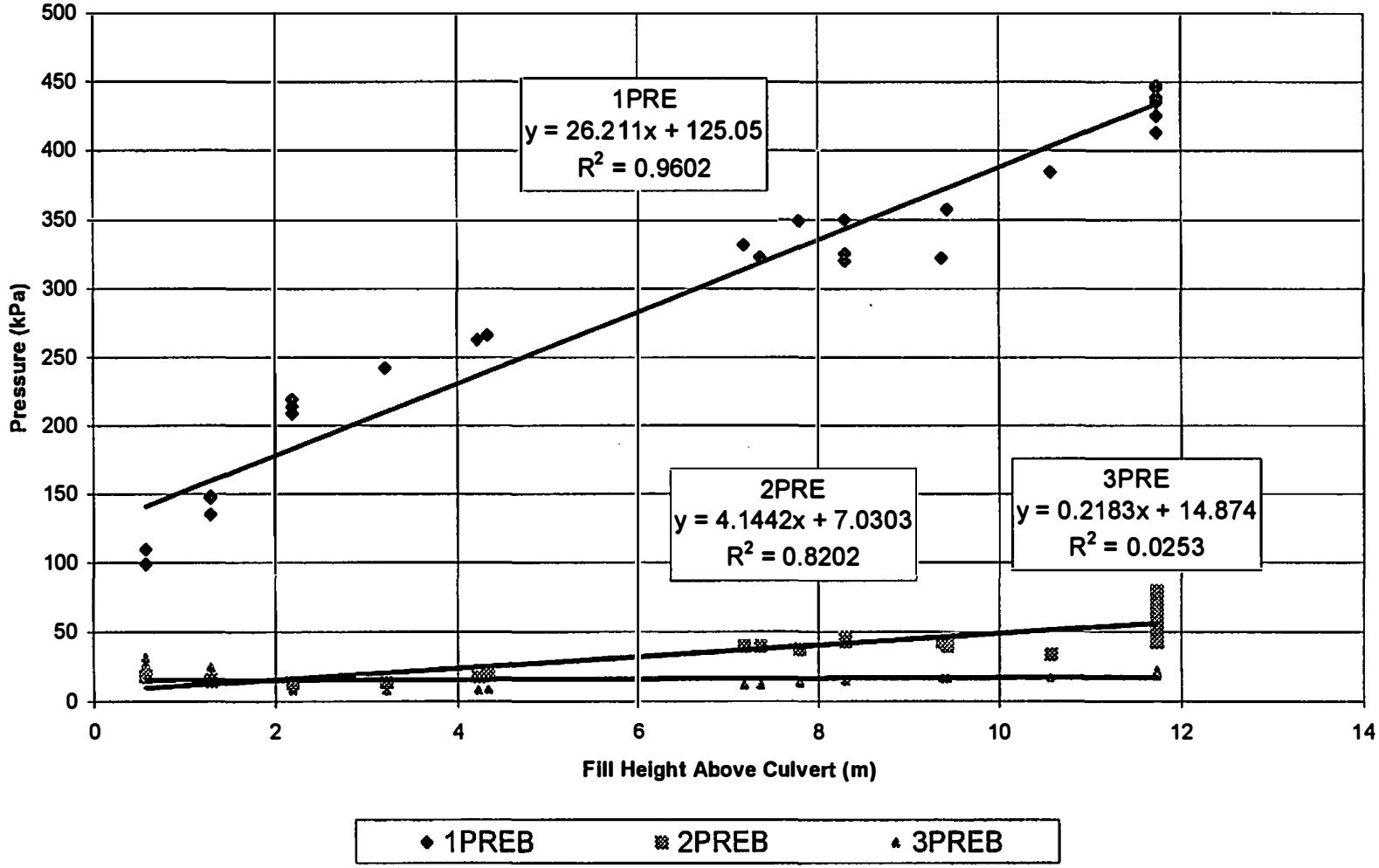


Figure 4-14. Section B Wall Pressure Cell Readings vs Fill Height

Table 4-7. Different load distribution Cases.

Case	k_1	k_2	k_3	
①	1	1	1	(uniform)
②	2	1	0	(triangular)
③	3	0.75	0	(High Pressure at Base)
④	4	0.5	0	
⑤	6	0	0	

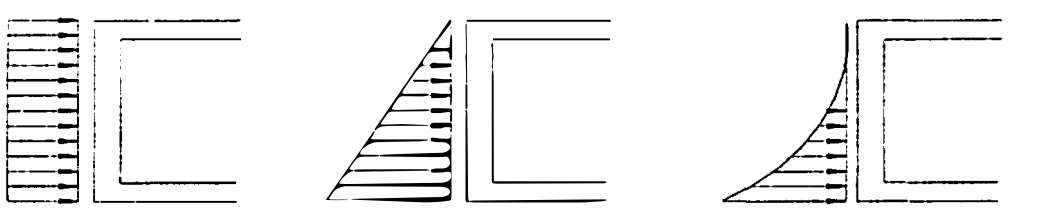


Figure 4-15. Example Pressure Distributions

Table 4-8. Wall pressure per meter height of fill using different load cases.

Pressure Slope (kPa/m)					
Case	①	②	③	④	⑤
Section A Wall	22.01	22.01	35.21	88.04	-44.02
Section B Wall	-6.07	-6.07	-9.71	-24.28	12.14

At section A, the average pressure from the pressure cell readings using Simpson's rule is 14.3 kPa per meter of fill height. Using the calculated pressure with the different load cases gives values that are higher than the pressure cell readings. At section B the average pressure from the pressure cell readings using Simpson's rule is 7.2 kPa per meter height of fill. The calculated pressures from the bending moments are not close to the pressure cell readings except for case six, which is higher than the pressure cells.

4.4 Pressure Differences in the Sections A and B

Section A consistently showed higher pressures than at section B. One possible reason for this may be due to the stiffness of the culvert. A stiffer culvert may attract more of the soil load that is above it, thus the soil does not have any arching effect. The wall at Section A has a height to thickness ratio of 6 while at section B the height to thickness ratio is 6.86. This shows that section A is a stiffer section and thus attracts more of the soil load to it.

The roof at section A has a length to thickness ratio of 3.76 and at section B the length to thickness ratio is 4.15. Again, this shows that section A is a stiffer section and thus attracts more of the soil load.

4.5 Shears

4.5.1 Wall Shears

Wall shears were calculated from equation 4-6 using the five different load combinations from the wall pressure distribution, Table 4-7. As with the pressure distribution, the wall shear was difficult to determine because of the high pressure at the base of the culvert. The results of the shear forces are shown in Table 4-9. V_A is the shear force near the bottom of the wall and V_B is the shear force near the top.

Section A					
Case	①	②	③	④	⑤
V_A (kN/m)	16.39	21.98	39.87	111.43	-67.46
V_B (kN/m)	17.15	11.56	13.79	22.74	0.38
Section B					
Case	①	②	③	④	⑤
V_A (kN/m)	5.54	4.00	-0.94	-20.67	28.66
V_B (kN/m)	-14.79	-13.25	-13.86	-16.33	-10.16

Table 4-9. Wall shear forces with various load distributions.

4.5.2 Roof Shears

The roof shears were calculated using equation 4-6 with the assumed uniform loading and the pressure distribution from the pressure cell readings. Results from each section are shown in Table 4-10. Significantly higher shear forces exist near the center wall than near the outside wall.

Table 4-10. Roof shear forces with different load distributions.

Section A		
Case	Uniform	Measured Pressure Distribution
V_A (kN/m)	25.2	28.5
V_B (kN/m)	50.3	50.1
Section B		
Case	Uniform	Measured Pressure Distribution
V_A (kN/m)	6.08	8.09
V_B (kN/m)	21.9	22.6

Chapter 5
Computer Modeling of Buried Box Culvert

5.1 Introduction

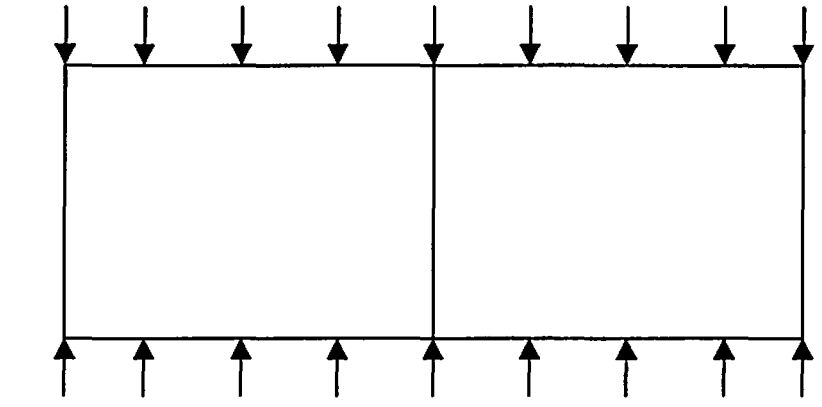
A computer analysis was performed on the buried box culvert at Greene County to study the behavior of the culvert using different unit load distributions and boundary conditions. The analysis was a frame model using Visual Analysis 3.1. Different unit load distributions were applied to both the roof and wall of the culvert model to determine if there were any significant changes in shear forces and bending moments. Different boundary conditions with uniform unit loads were also applied to the model to study the change in forces in the culvert due to support conditions.

An analysis was also performed on the culvert to study changes in the culvert forces by varying the fill height. The forces from the fill height were calculated using AASHTO loads, pressure cell readings and strain gage calculated pressures.

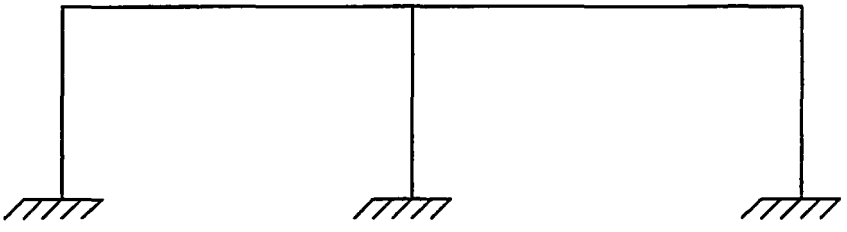
5.2 Roof Forces

5.2.1 Effects of Boundary Conditions

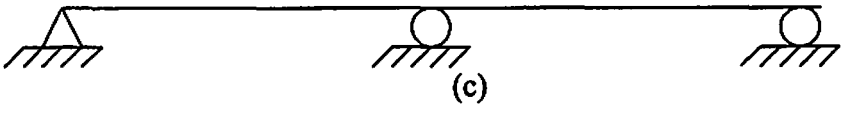
Three different boundary conditions were modeled and are shown in Figure 5-1. The first condition that was analyzed was an assumed flexible support where the pressure was applied equally to both the top and bottom of the culvert. The second condition was a stiff support where the bottom of the culvert was assumed to have fixed supports. On the third boundary condition the roof of the culvert was assumed to be a continuous beam.



(a)



(b)



(c)

Figure 5-1. Boundary Conditions for Roof Forces. (a) Bottom Support Assumed to Provide Uniform Pressure.(b) Bottom Support Assumed to be a Stiff Support.(c) Culvert Roof Assumed to Be a Continuous Beam.

5.2.1a Bending Moments

Figure 5-2 shows the results of the roof bending moments with the three boundary conditions for a uniform distributed load. There is not much difference in the maximum positive moment between the three support conditions with the continuous beam being the lowest and the fixed support being approximately 7% higher. The continuous beam gives the greatest negative moment, which is about 50% higher than the fixed support. The uniform support pressure gives intermediate values which are only about 4% lower than the fixed support for the positive moment and about 25% lower than the continuous support for the negative moment. For all three conditions, the negative moment at the outside wall was much smaller than the negative moment at the middle wall.

5.2.1b Shear Forces

Figure 5-3 show the results of the shear forces with the three different support conditions. The shear forces change only slightly with a change in the support conditions. The percent change between the maximum and minimum shear force is about 16% between the different support conditions.

5.2.2 Effects of Load Distributions

Three load distribution cases were applied to see the effect on bending moments and shear forces. The first load distribution was a uniform load, which is what is assumed by AASHTO. The second and third load distributions were the load

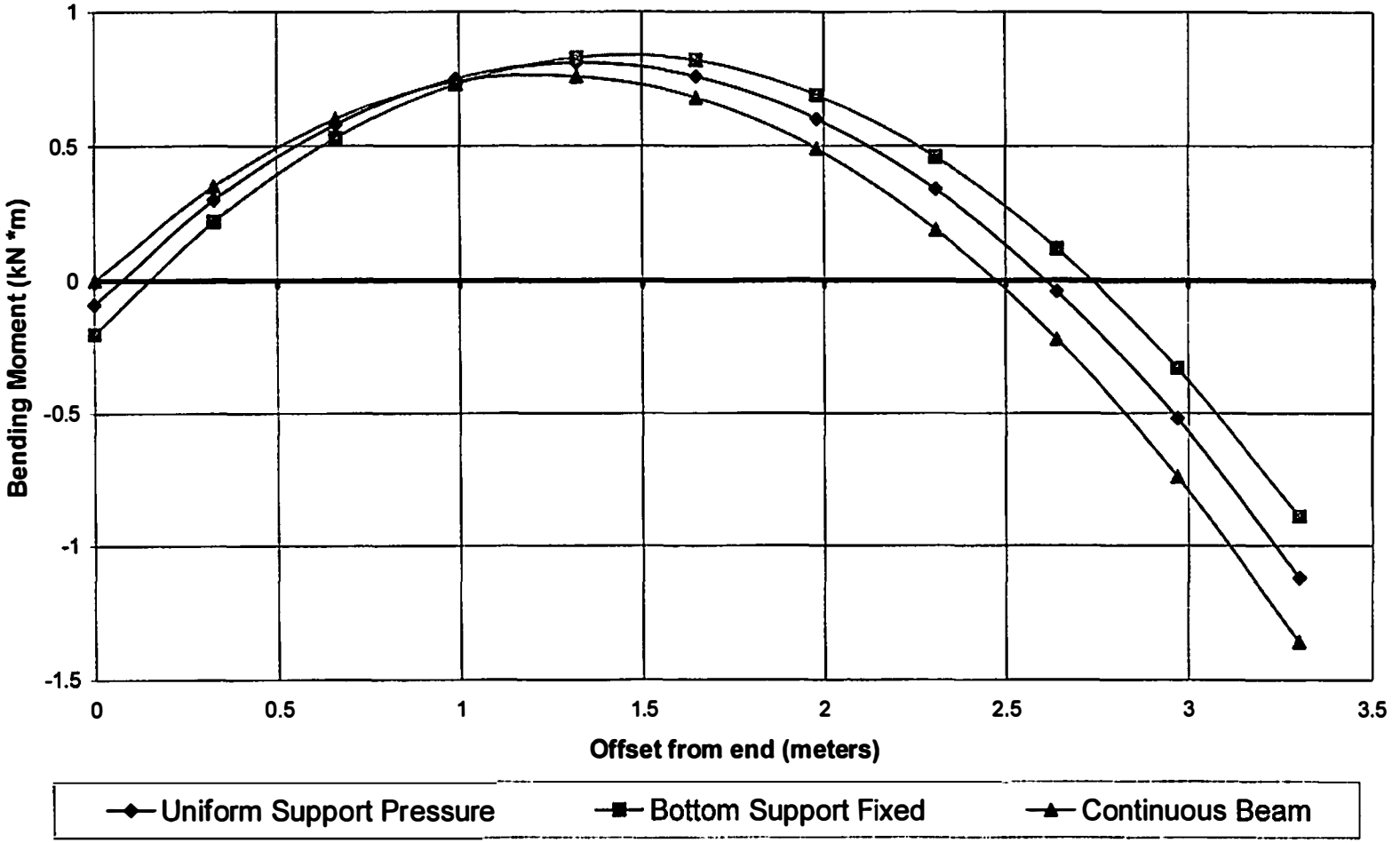


Figure 5-2. Bending Moments in Top Slab with Different Support Conditions

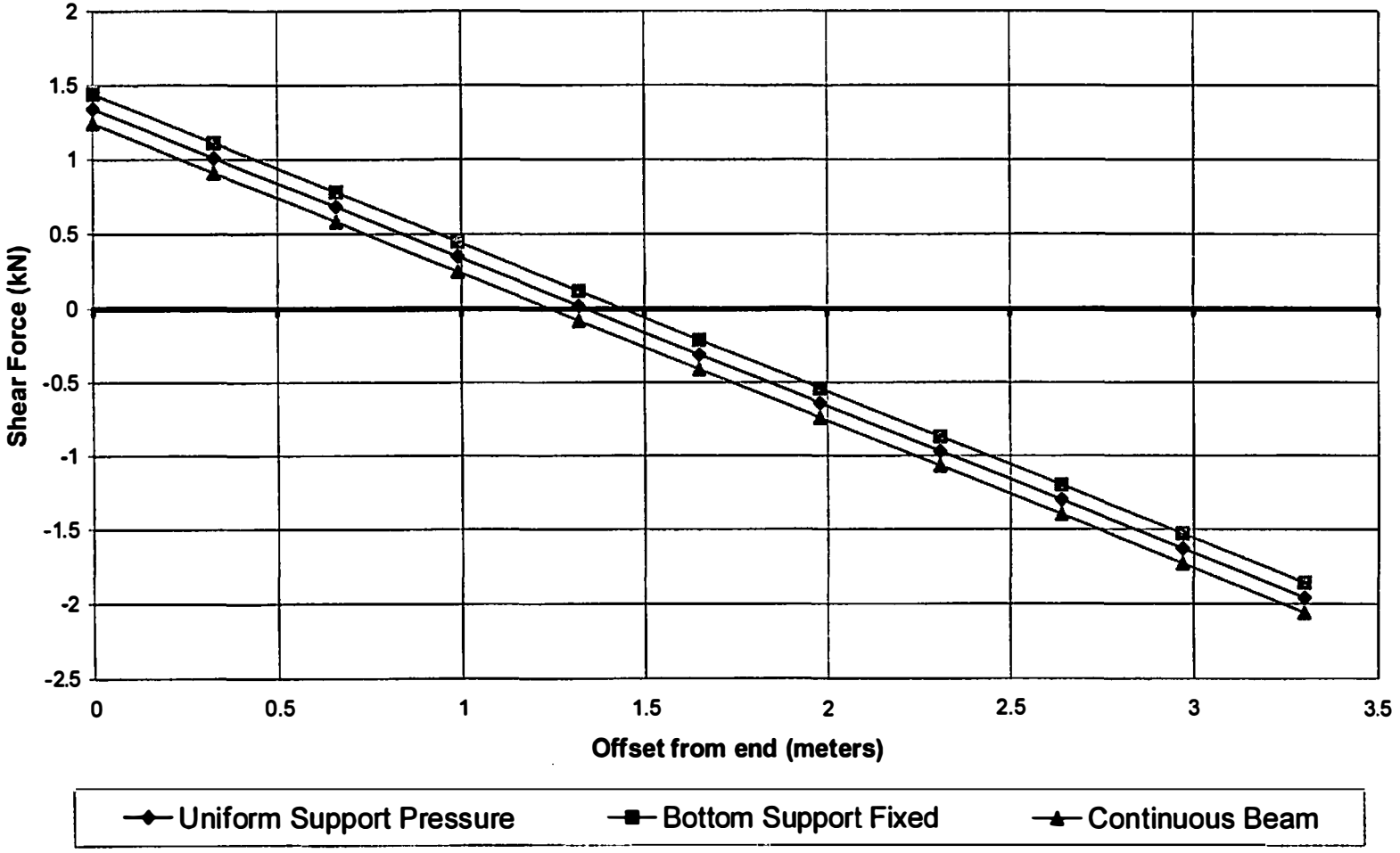


Figure 5-3. Shear Force in Top Slab with Different Support Conditions

distributions measured from the pressure cells that were installed on the culvert at sections A and B. These three load distributions are shown in Figure 5-4. In all these analysis, no load was applied to the culvert wall.

The same average load was used in all cases, that is, the total area under the load diagram was the same in all cases. The measured pressure distribution from the pressure cells was modeled with a parabolic load, but the computer model can only apply linear loads. The parabolic loads were approximated by four line segments, Figure 5-5. Interstices were chosen at quarter points of the span so that the area under the piecewise linear approximation had the same area under the load curve as the parabolic load distribution. The equations used for the interstices are shown in Figure 5-5.

5.2.2a Bending Moments

The effects of the three load distributions are shown in Figure 5-6. The different load distributions cause almost no difference in the bending moments.

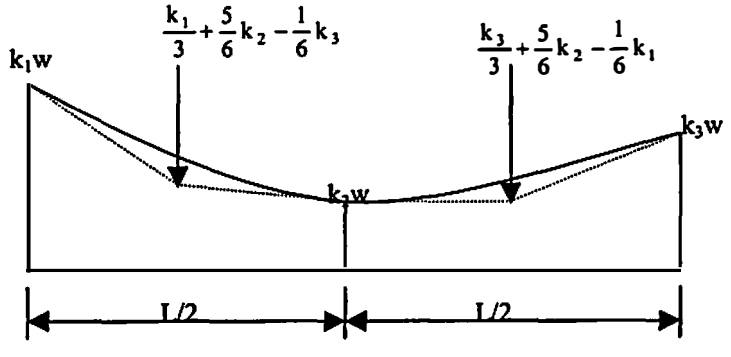
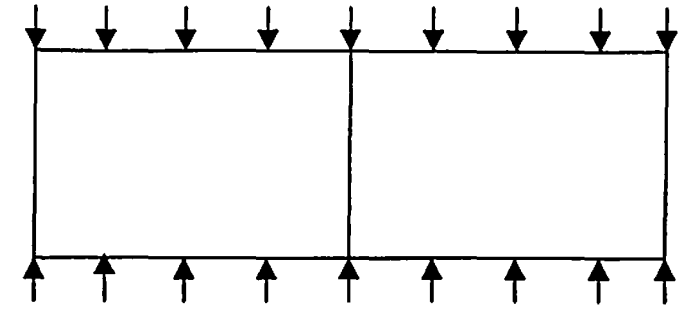
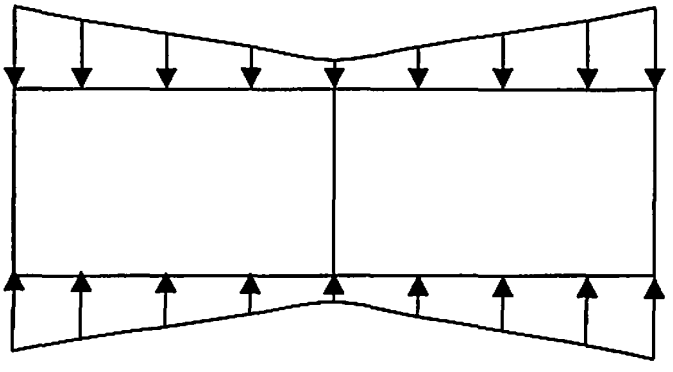


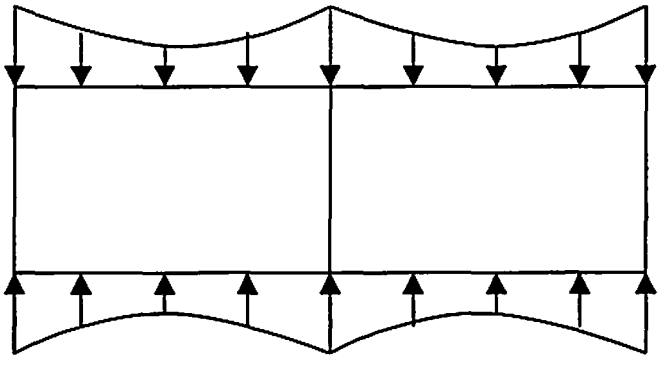
Figure 5-4. Approximated Linear Pressure Distribution.



(a)



(b)



(c)

Figure 5-5. Load Distributions for Roof Forces. (a) Uniform Load Distribution (AASHTO). (b) Pressure Distribution from Pressure Cells at Section A. (c) Pressure Distribution from Pressure Cells at Section B.

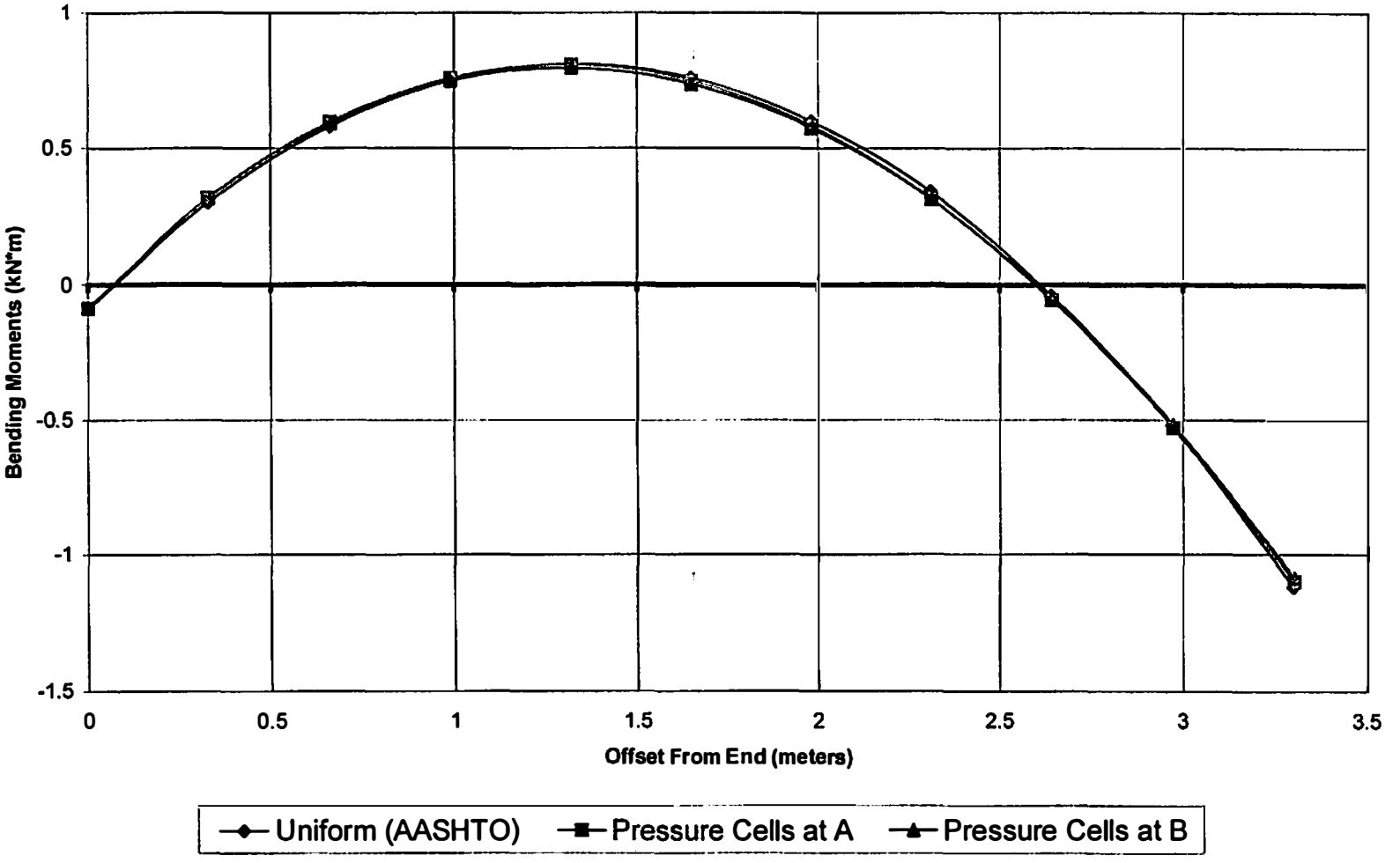


Figure 5-6. Effect of Load Distribution on Culvert Roof Moments

5.2.2b Shear Forces

Figure 5-7 shows the effect on the roof shear forces of the three different load distributions. The different load distributions produce almost no difference in the shear forces.

5.2.3 Conclusions on Roof Forces

The effects of using different support conditions on the culvert roof give a slightly higher positive bending moment using a fixed support and much higher negative moment using a continuous beam. Roof shear forces are not affected much by changing the support condition.

The effect of changing the load distribution on the culvert roof gives almost no change in the bending moment and shear forces. This infers that the AASHTO method of using a uniform pressure on the culvert roof is adequate for obtaining internal culvert forces.

5.3 Wall Forces

Three boundary conditions along with three load distributions are modeled on the exterior culvert wall. The three load distributions and boundary conditions are shown in Figure 5-8. The first load distribution is a uniform load which is close to AASHTO specifications for high embankments. The second load distribution is a triangular load which is close to what AASHTO assumes for low embankments. The third load distribution is a parabolic load with a high pressure at the base, similar to

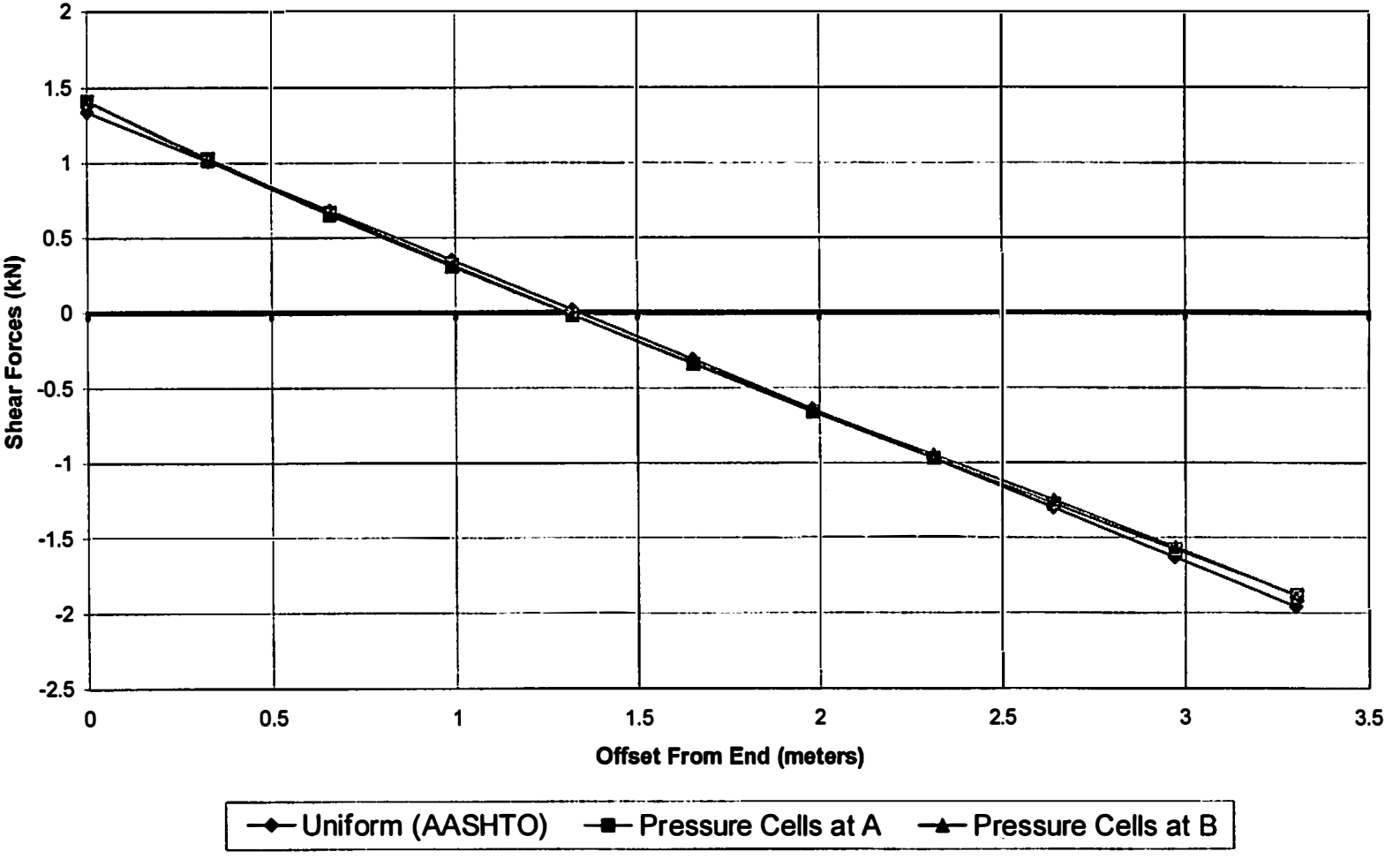


Figure 5-7. Effect of Load Distribution on Culvert Roof Shear Forces

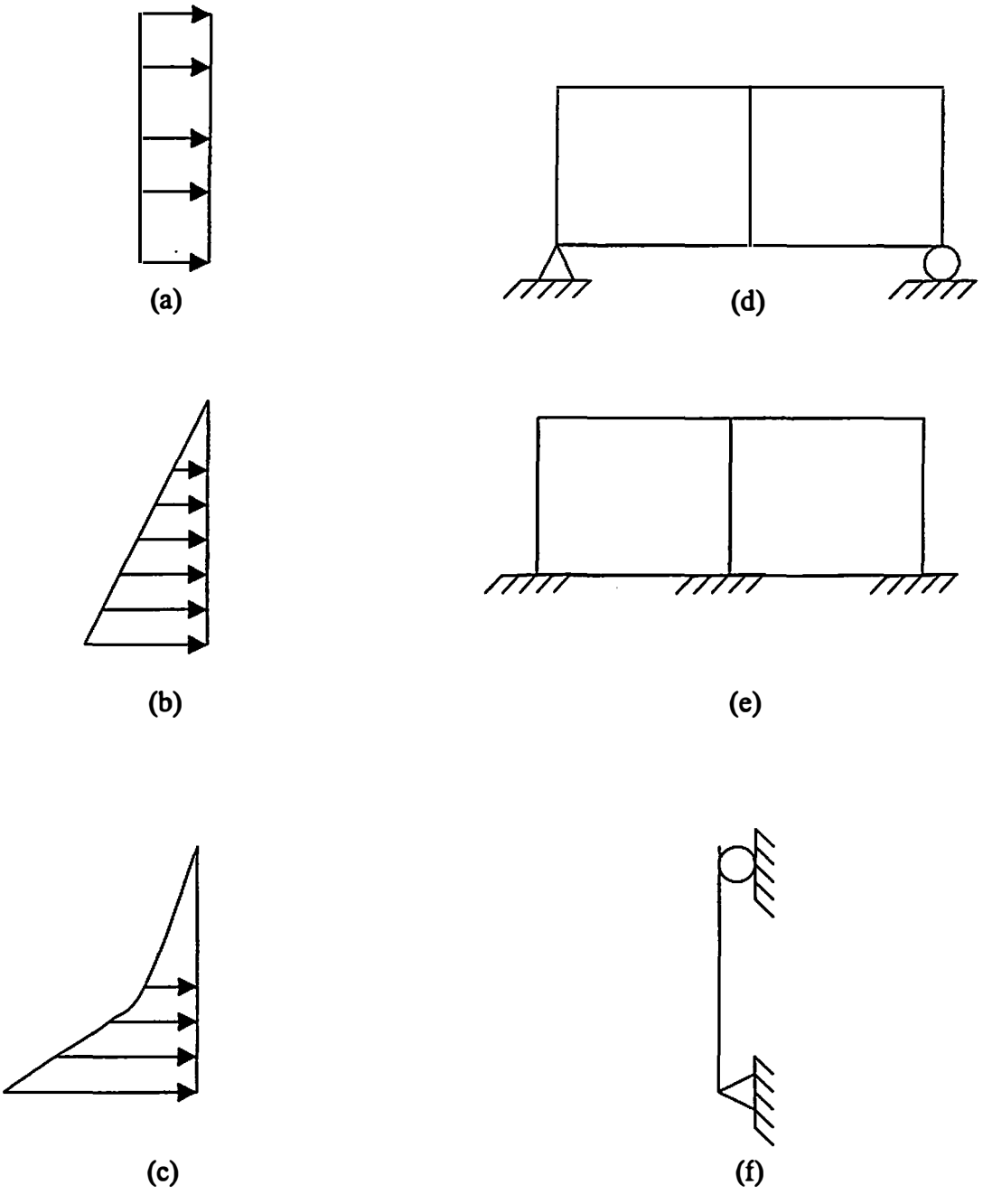


Figure 5-8. Load Distributions and Boundary conditions on wall Forces. (a) Uniform Pressure. (b) Triangular Pressure. (c) Parabolic Pressure. (d) Flexible Support. (e) Rigid Support. (f) Simple Support.

what was measured by the pressure cells. The vertex of the parabola is at the top of the culvert. In all these analysis, no load was applied to either the base or roof of the culvert.

The three boundary conditions are similar to what was assumed in the culvert roof. The three different boundary conditions are a flexible support, a fixed support and a simple beam. An equal lateral load is applied to each side of the culvert.

5.3.1 Bending Moments

Figures 5-9, 5-10 and 5-11 show the effects of different boundary conditions and load distributions on wall bending moments. Varying the load distribution has very little effect on the wall bending moments when using the flexible and rigid support. Using a simple support increased the positive moment in the wall by approximately 270%, and also since a simple support has no continuity, the wall shows no negative moment.

5.3.2 Shear Forces

Figure 5-12 shows the effects of different boundary conditions on wall shear forces for a uniform lateral load. The support conditions did not have a significant affect on the shear force.

Figures 5-13 to 5-15 show the effect of different load distributions on the shear force for the three different support conditions. Using different load distributions has a large effect on the shear at the base of the culvert. Using a uniform pressure, which

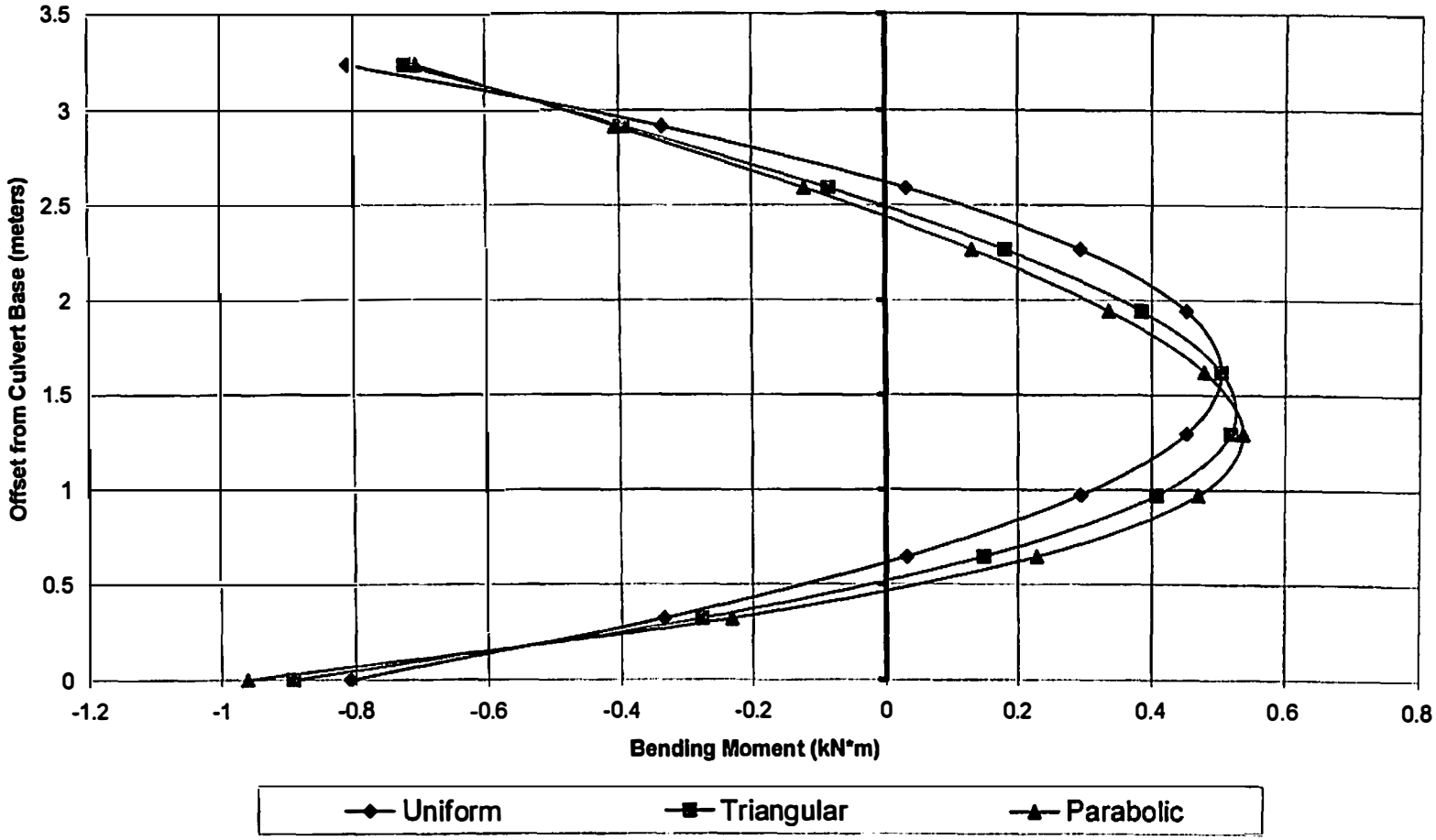


Figure 5-9. Wall Bending Moment with varying Load Distributions Flexible Support

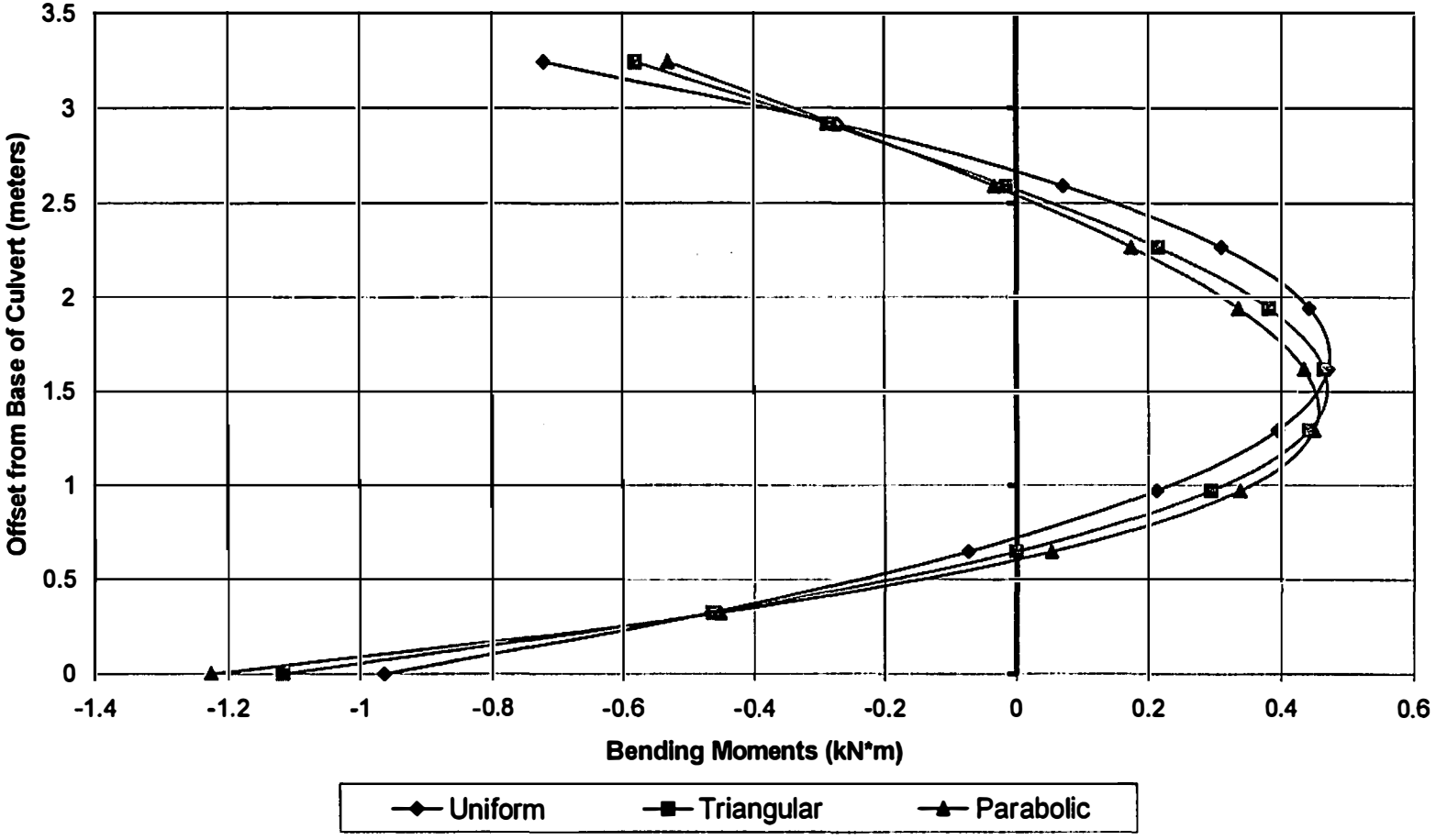


Figure 5-10. Wall Bending Moments with Varying load Distributions Rigid Support

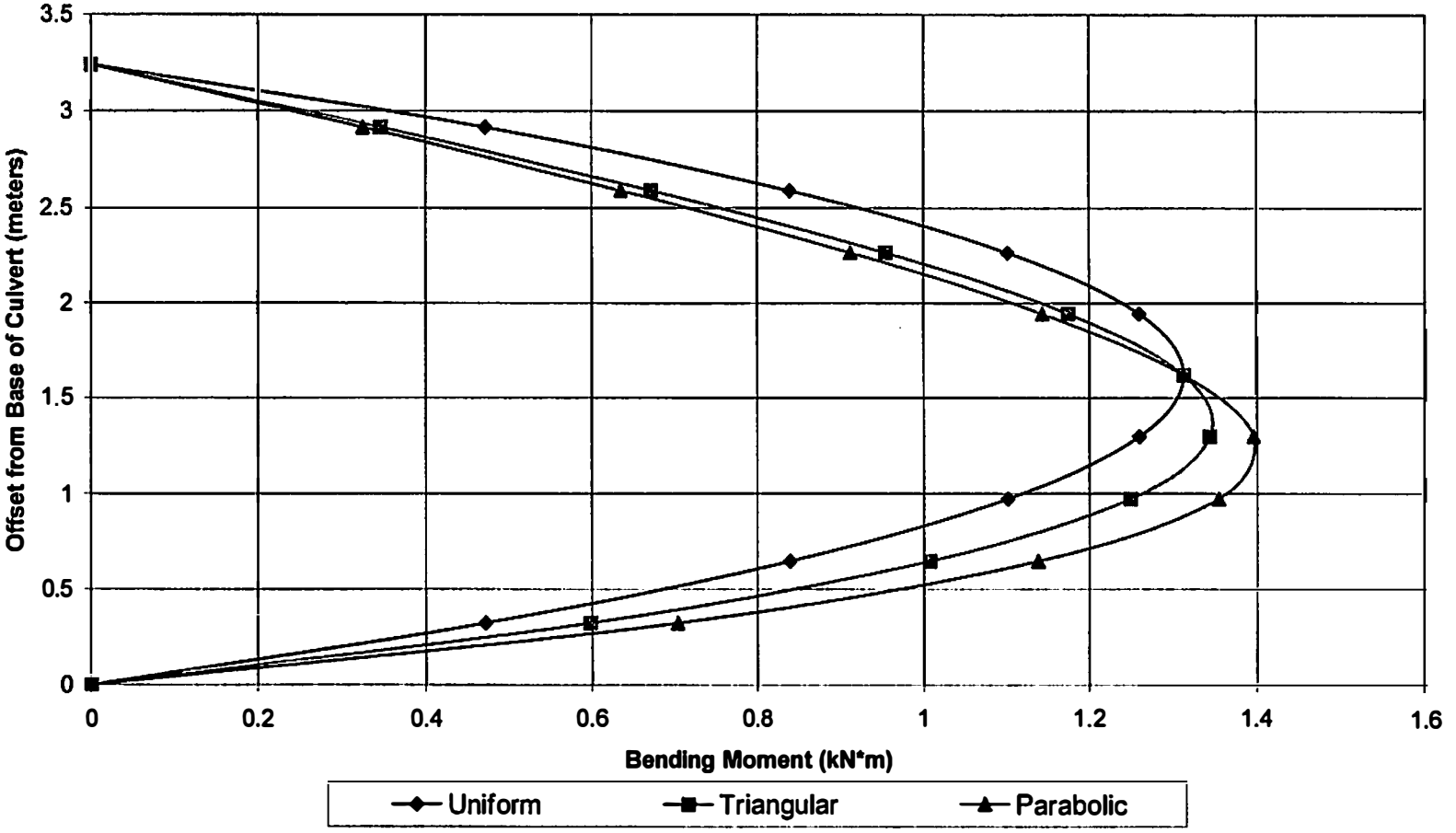


Figure 5-11. Bending Moments with Varying Pressure Distributions Simple Supported

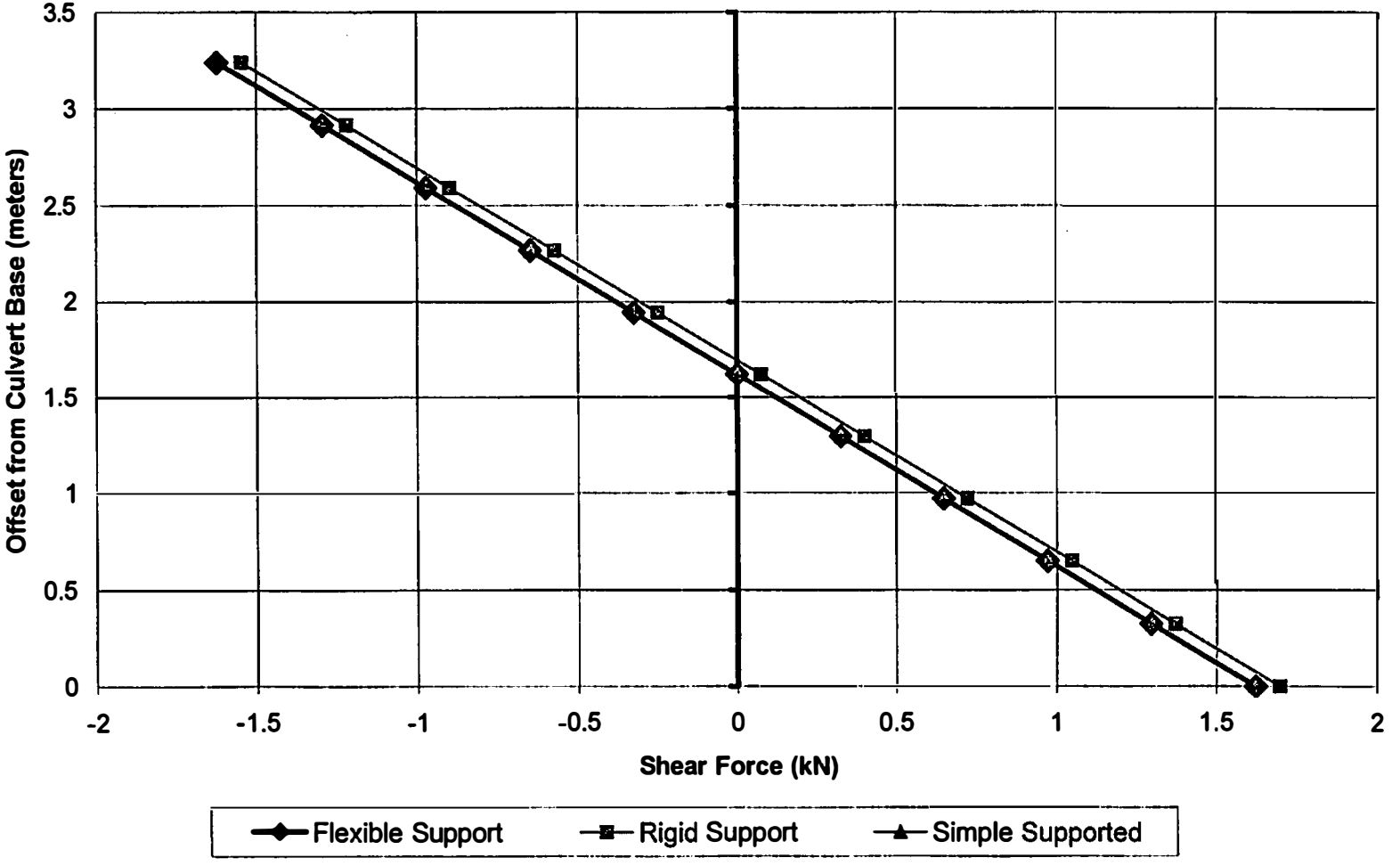


Figure 5-12. Wall Shear Forces with Uniform Load and Different Support Conditions

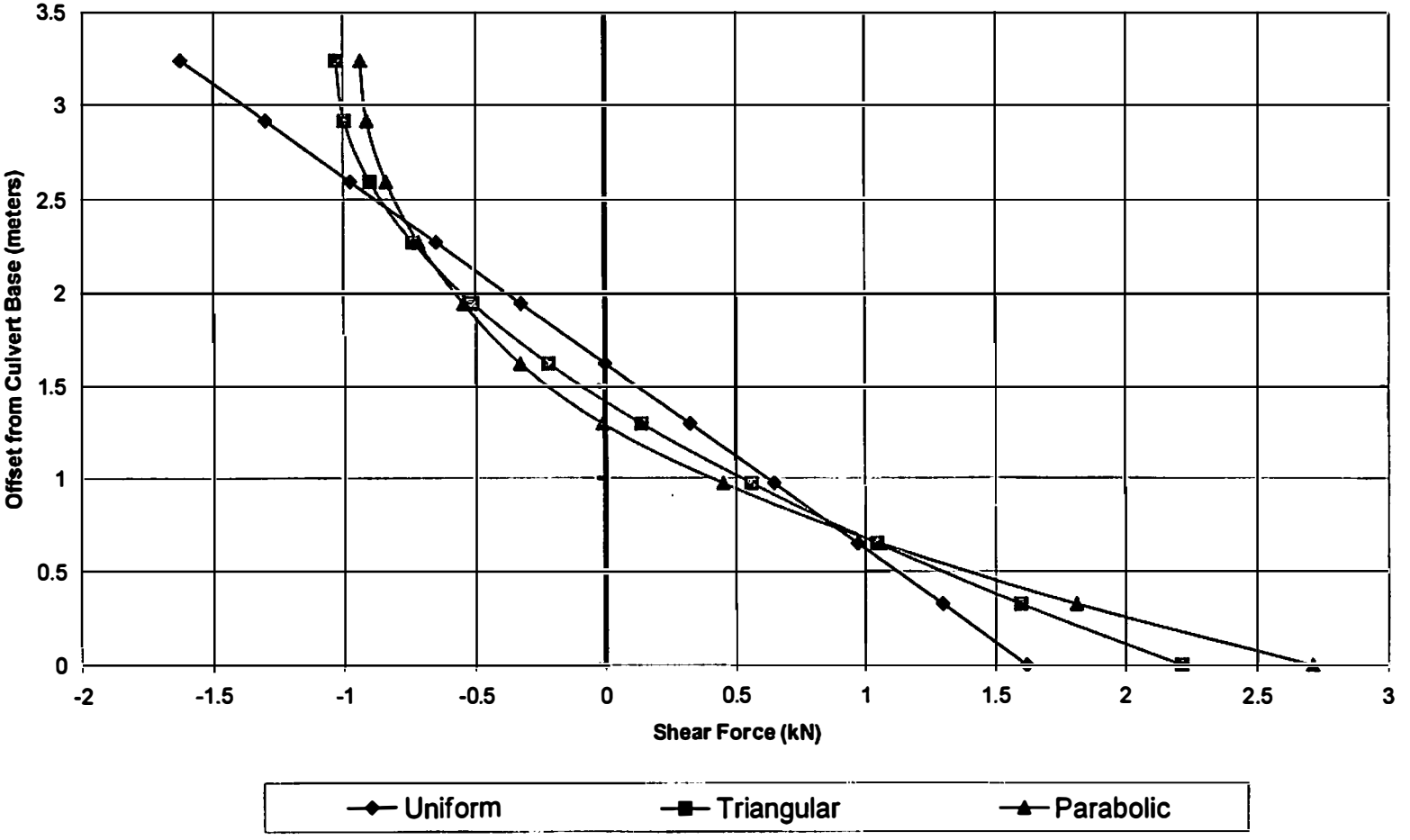


Figure 5-13. Wall Shear Forces with varying Load Distributions Flexible Support

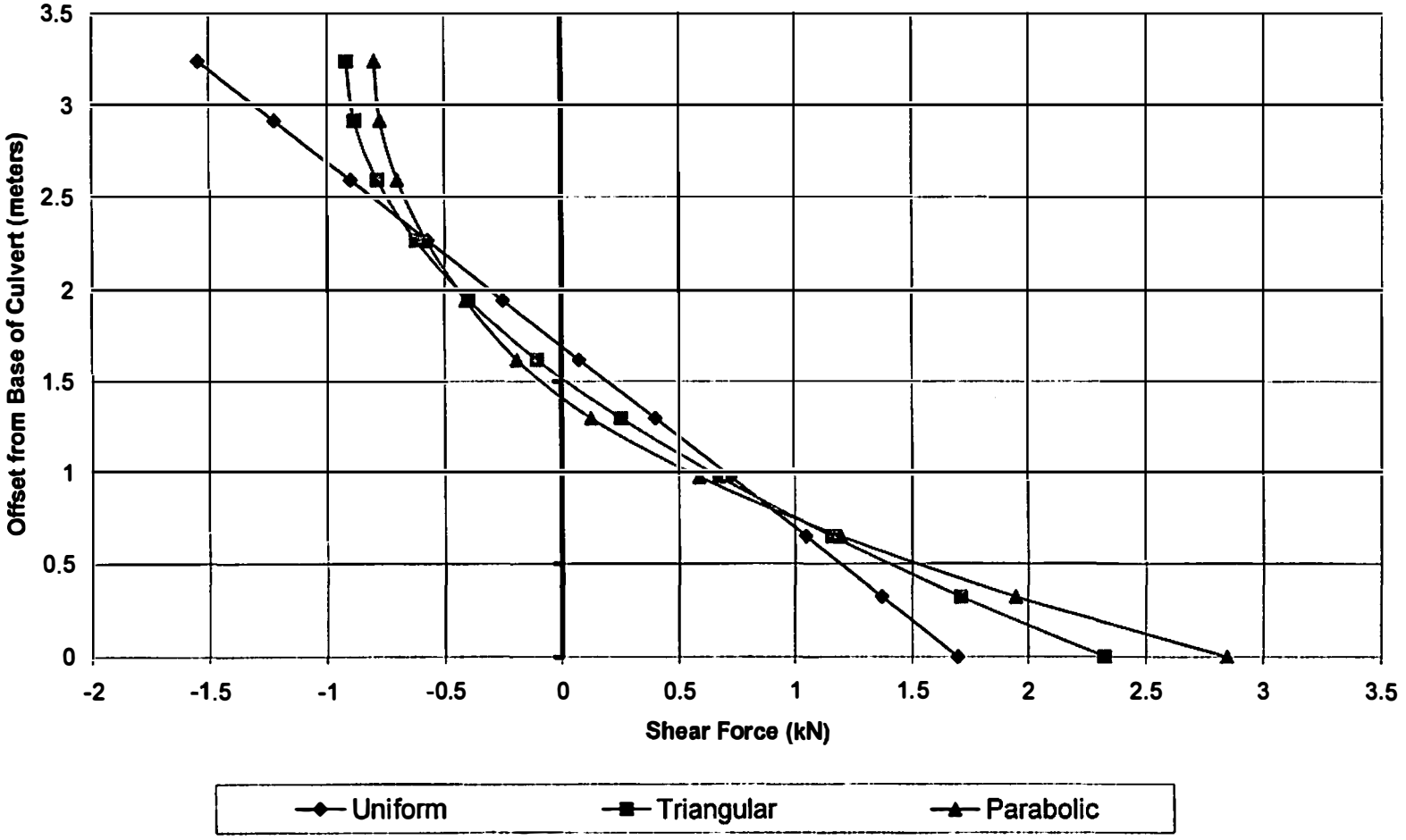


Figure 5-14. Wall Shear Forces with Varying load Distributions Rigid Support

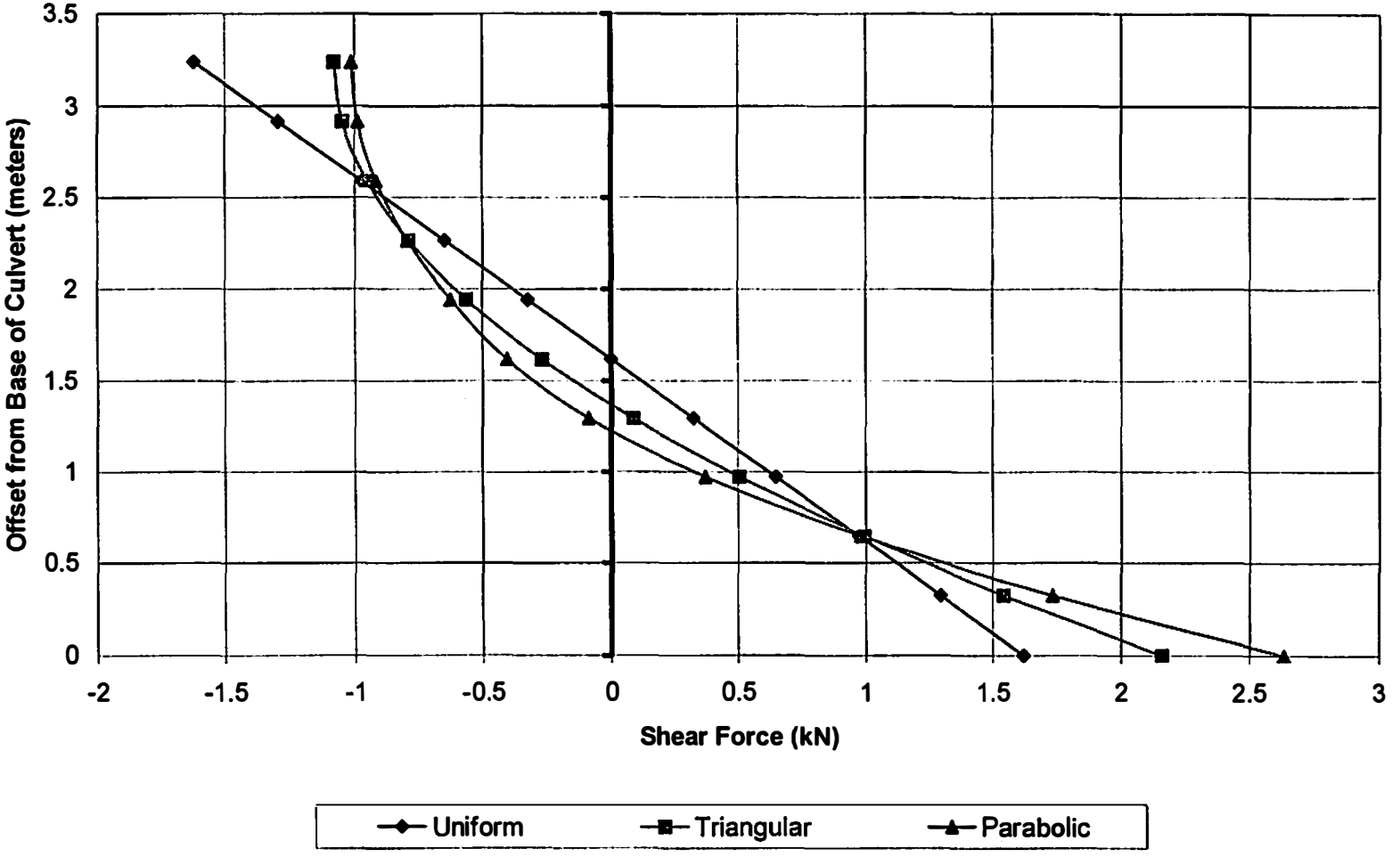


Figure 5-15. Shear Forceswith Varying Pressure Distributions Simple Supported

is about what AASHTO assumes for high embankments, gives the lowest value for shear at the base while using a triangular load distribution is about 36% higher and using a parabolic load distribution gives a 66% higher pressure at the base.

Different load distribution also has a large effect on the shear at the top of the culvert. Using the triangular load distribution gives the lowest shear at the top of the culvert while a parabolic distribution is only about 7% greater and a uniform pressure is approximately 60% greater.

5.3.3 Conclusions on Wall Forces

Load distributions have almost no effect on the bending moments in the culvert wall. Varying the support conditions does not have much of an effect between flexible and rigid but the bending moment is greatly increased when using a simple support.

Load distributions have a great affect on the shear forces on the wall of the culvert. Using a load distribution that has a higher load at the base gives a much higher shear at the base of the culvert while using a uniform load gives a much higher shear force at the top of the culvert. The support conditions did not have a significant affect on the shear force.

5.4 Roof Bending Moments with Varying Fill Height

An analysis was performed to study the effects of bending moment in the culvert roof with increase in fill height. Loads were applied to both the culvert roof, and walls in these analyses. Three pressure distributions were considered and were

then compared to the moments calculated from the strain gages. The first pressure distribution that was considered was the measured pressure from the pressure cells. The second and third pressure distributions were the pressure distributions from AASHTO, which gives a maximum and a minimum wall pressure. Three locations from each section were looked at and are located on the culvert roof next to the outside wall, half-way between the outside wall and the middle wall, and next to the middle wall, Figure 5-16 .

Figures 5-17 to 5-22 show the bending moments versus fill height for all the pressure distributions. The bending moments calculated from the strain gages and the slope of the measured bending moments from the strain gages are also included. The slope of the strain gage bending moments was found by fitting a best-fit trend line through the measured bending moments and then ignoring the y-intercept.

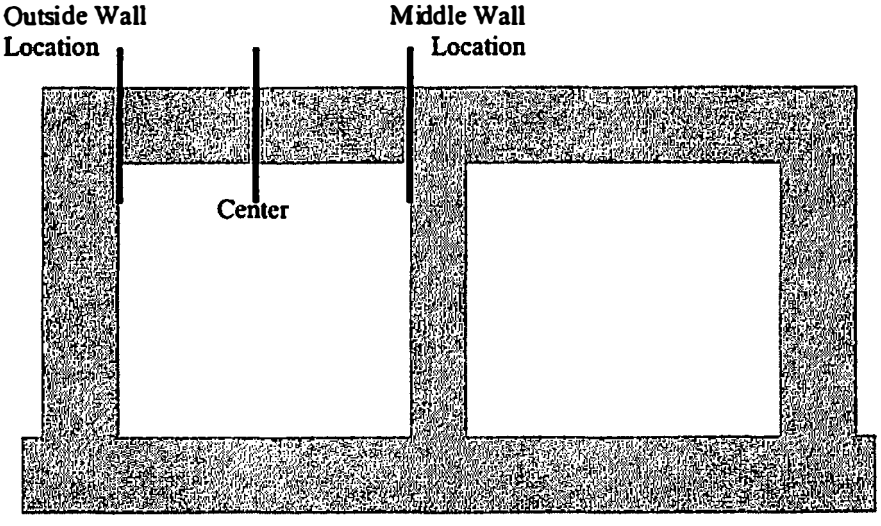


Figure 5-16. Location of Roof Bending Moments.

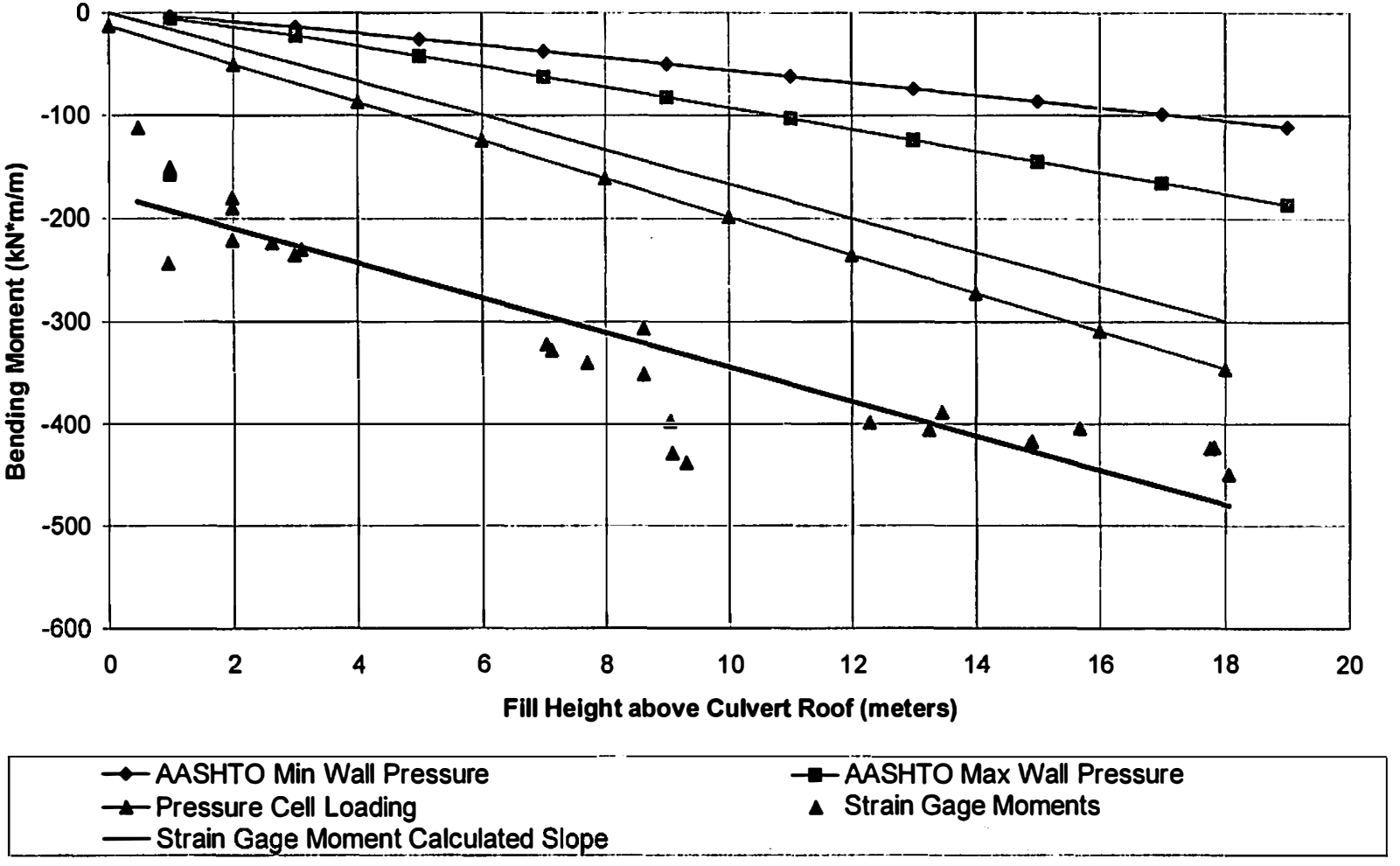


Figure 5-17. Section A Roof Bending Moments at Side Wall

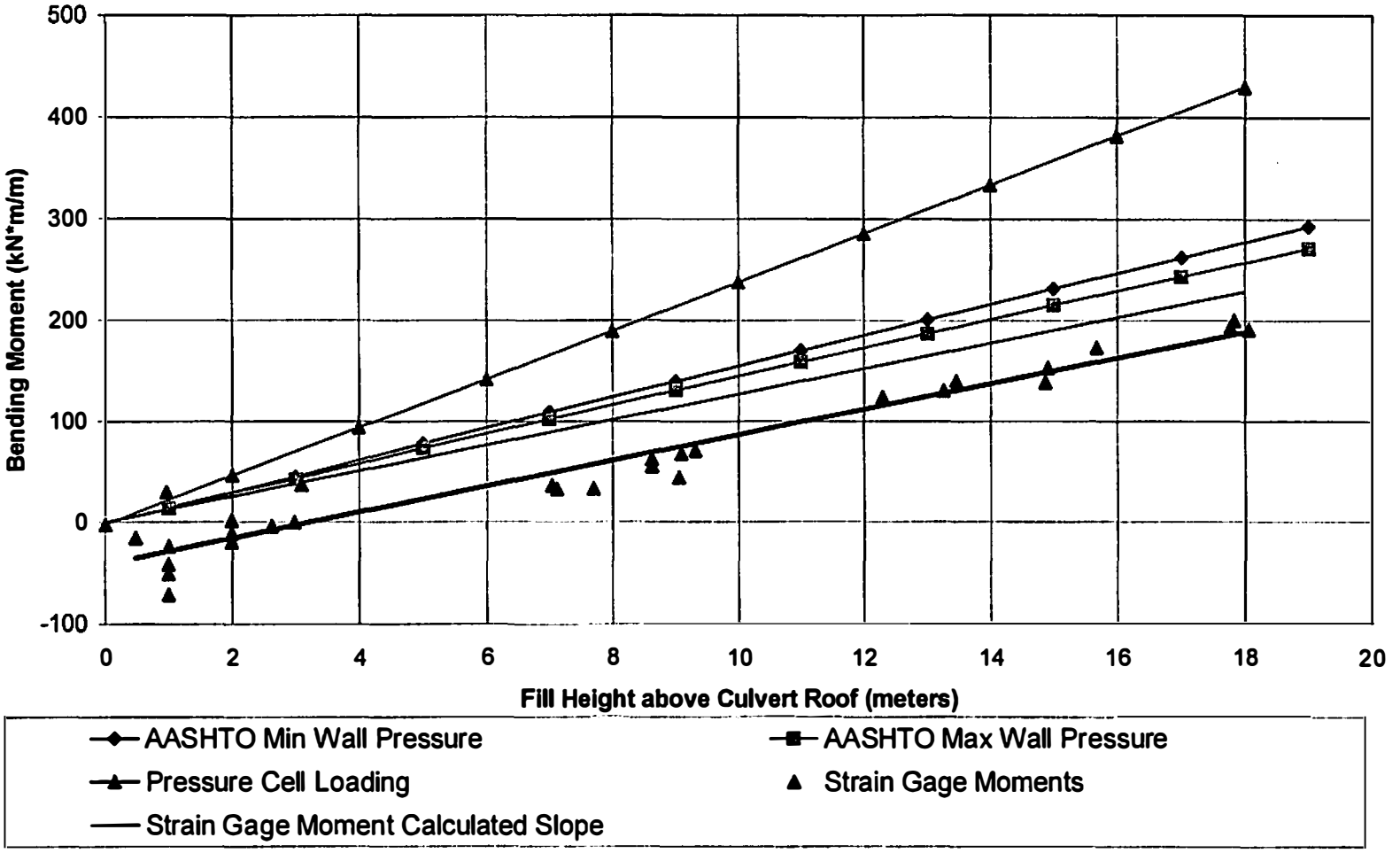


Figure 5-18
Section A Roof Bending Moments at Center

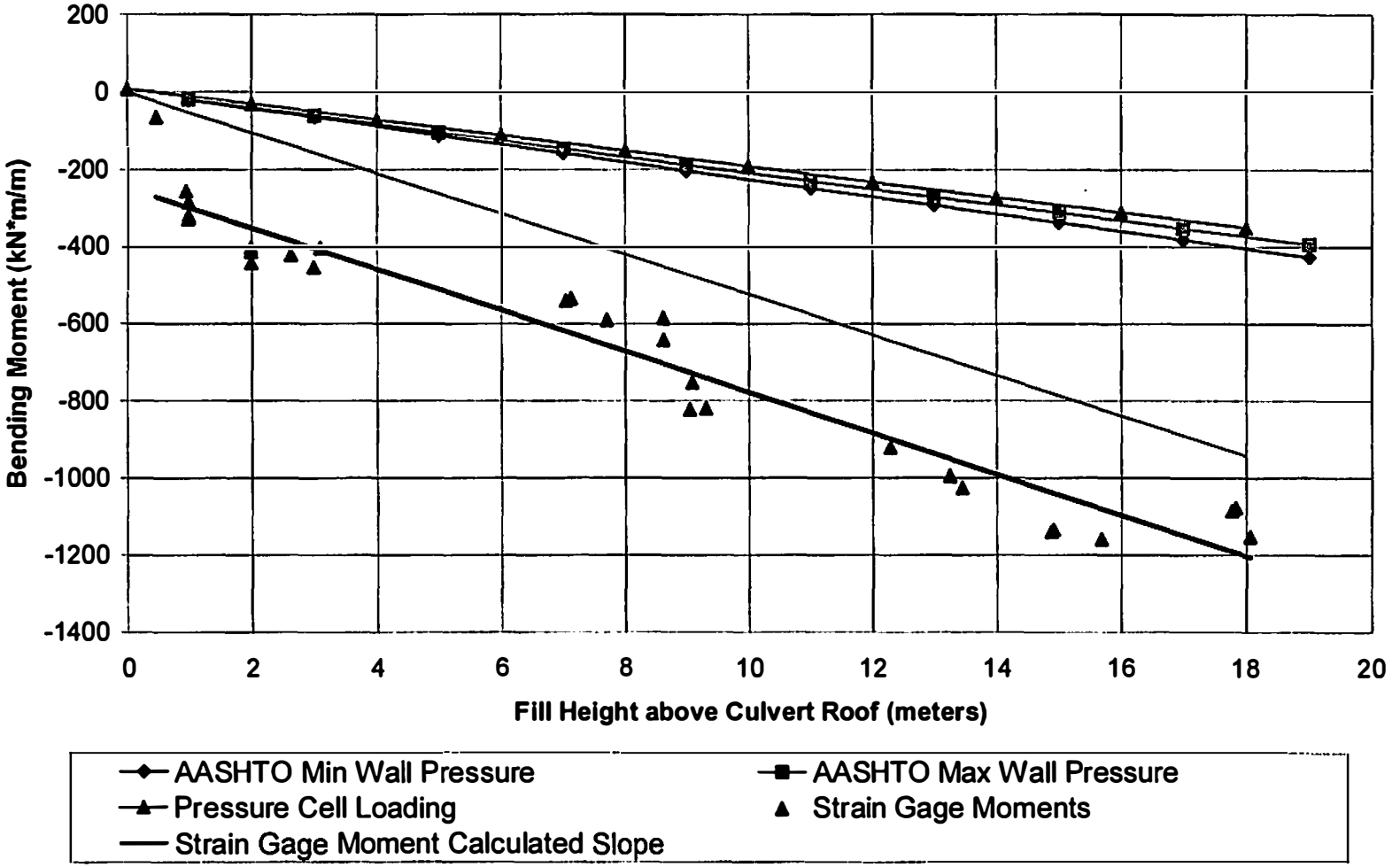


Figure 5-19
Section A Roof Bending Moments at Middle Wall

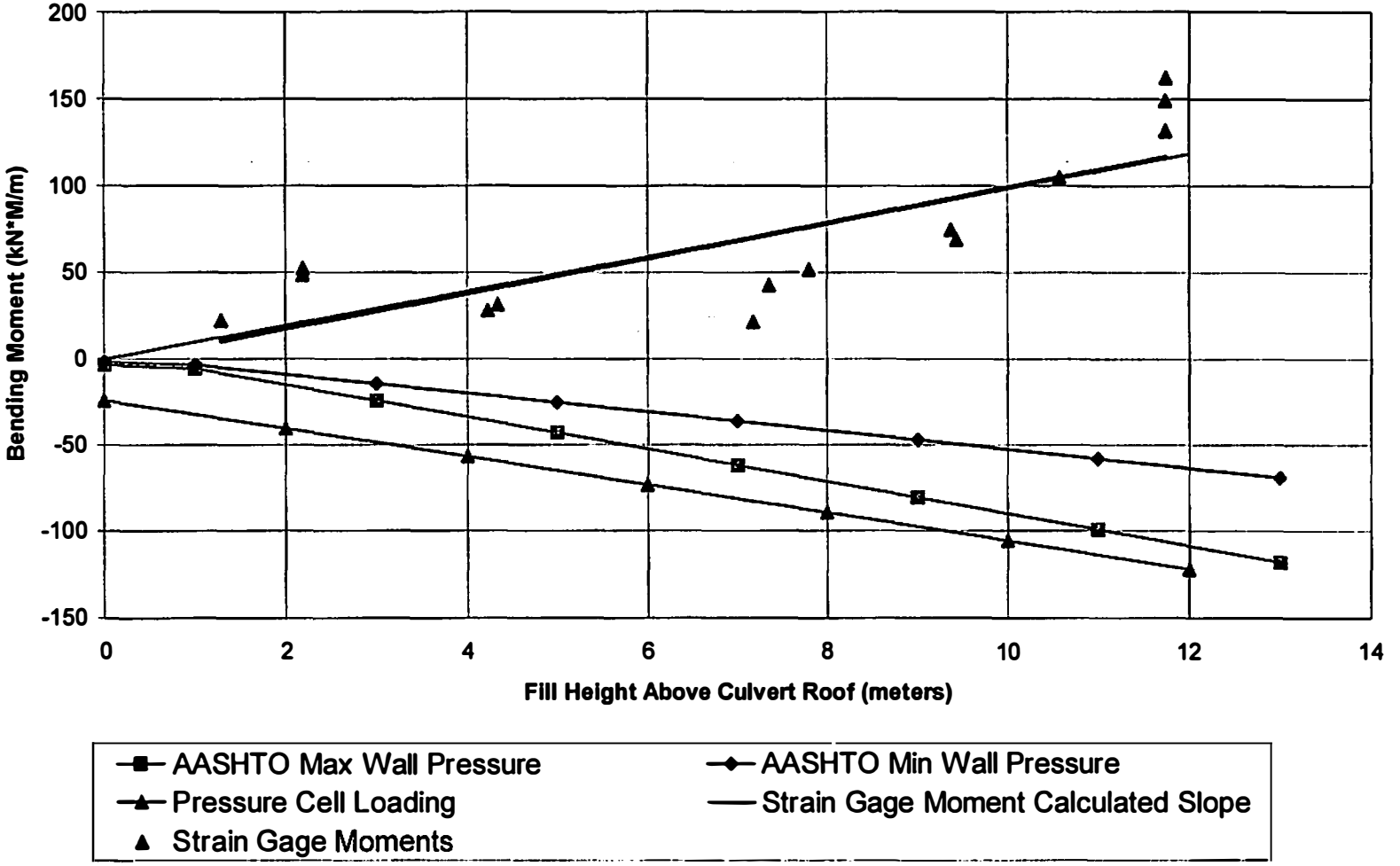


Figure 5-20
Section B Roof Bending Moments at Outside Wall

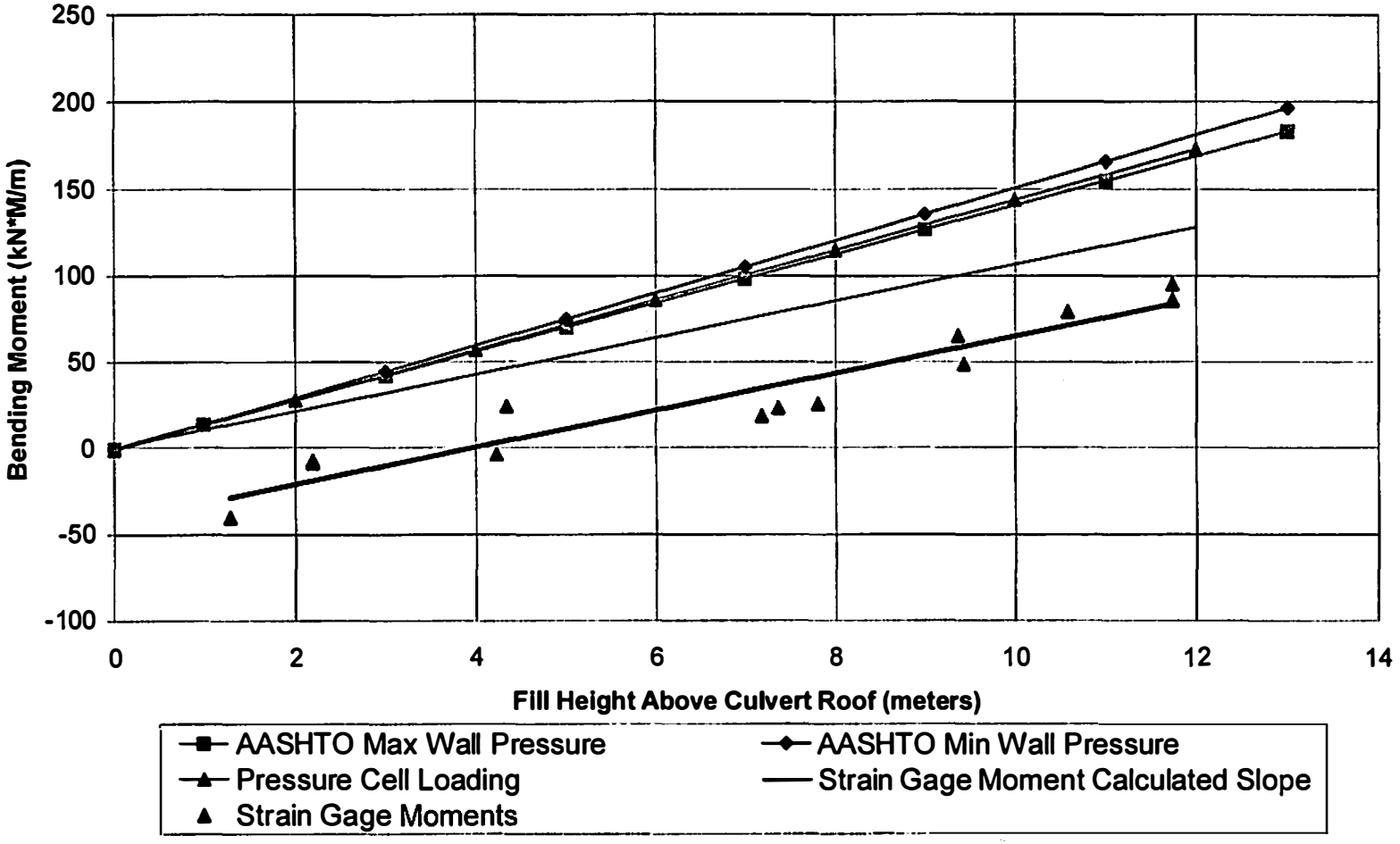


Figure 5-21. Section B Roof Bending Moments at Center

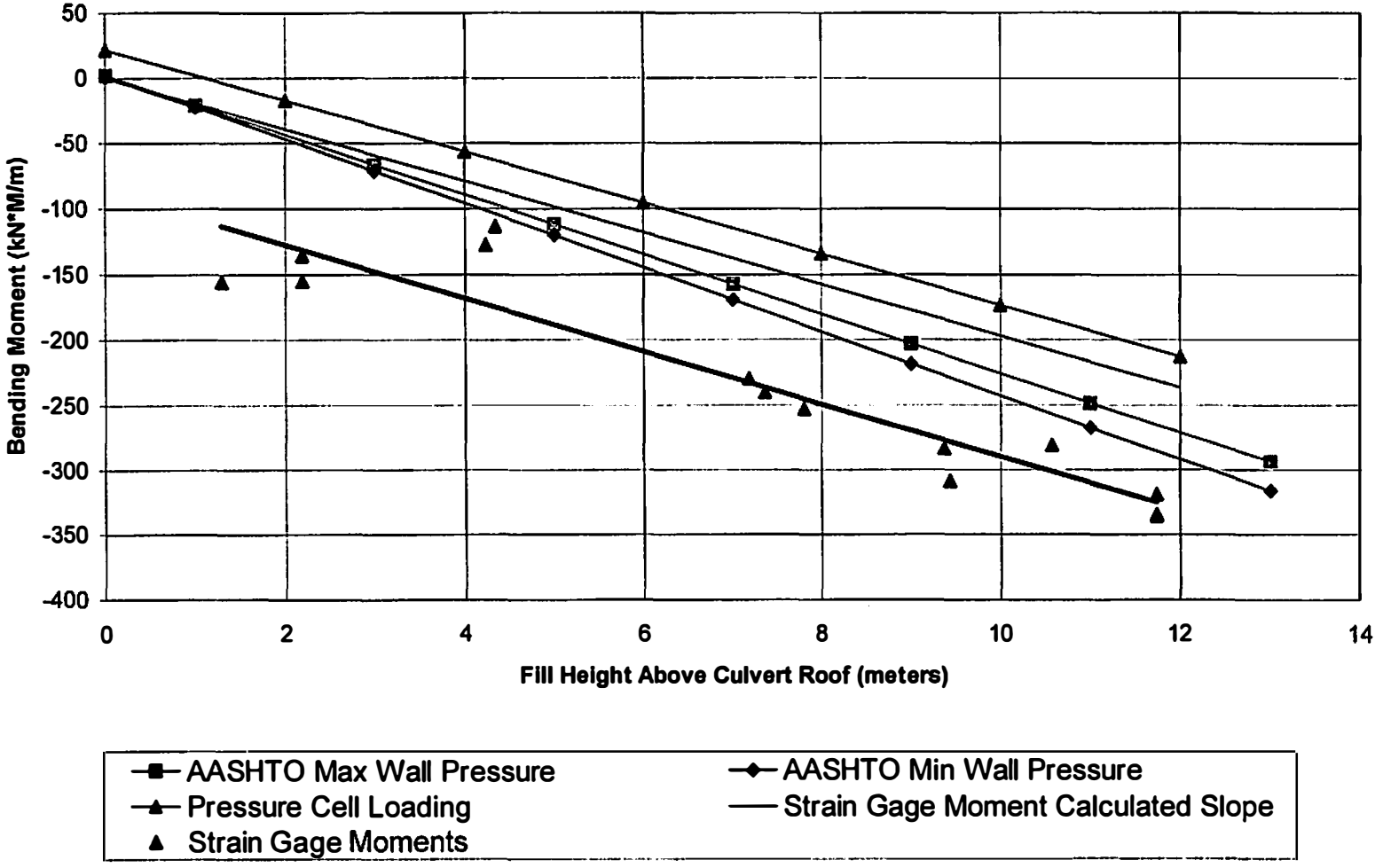


Figure 5-22. Section B Roof Bending Moments at Middle Wall

At section A, the pressure cell distribution gives a slightly higher bending moment next to the outside wall and at the center but shows a small decrease in the bending moment next to the middle wall when compared to the AASHTO pressure distribution. The strain gage moments show a slightly higher moment than AASHTO at the outside wall and the middle wall but are less at the center location.

At section B the pressure cell distribution gives a slightly higher moment at the outside wall when compared to AASHTO loadings, but at the center the bending moments are about the same as the AASHTO loadings. The bending moments calculated from the strain gages near the middle wall show a positive moment at this location unlike the AASHTO and pressure cell distribution which show a positive moment. This may be due to the high pressure that was applied to the wall.

Chapter 6
Comparison of Forces to Culvert Capacity

6.1 Introduction

The Greene county culvert is compared to allowable design criteria according to the American Association of State Highway and Transportation Officials (AASHTO) Standard Specifications for Highway Bridges. The capacity of the roof and wall is expressed in terms of an axial force-moment interaction diagram. The shear strength of the roof and walls is compared to the design criteria of AASHTO design guides.

6.2 Comparison of Axial Force and Moment to Culvert Capacity

6.2.1 Development of Capacity Interaction Diagrams

The interaction diagram was first constructed for the ultimate capacity of the culvert. Concrete was assumed to fail at a strain of 0.003, and an equivalent rectangular stress block was used for the concrete stress. The reinforcing steel was assumed to have an elastic-plastic stress-strain diagram neglecting strain hardening.

A factored interaction diagram was obtained by multiplying the ultimate capacity by the appropriate strength reduction factor. AASHTO specifications give a strength reduction factor of 0.75 for compression members with spiral reinforcement and 0.70 for members with tie reinforcement. Since the culvert roof and wall is not confined by reinforcement a strength reduction factor of 0.70 was used to create the interaction diagrams. When the axial load is less than $0.10f'_cA_g$, the strength reduction factor is increased linearly to 0.9, per AASHTO specifications.

A working stress interaction diagram was also constructed for the culvert. With working stress design, the concrete is assumed to behave linear elastic and the allowable concrete compressive stress is $0.40f'_c$. The allowable concrete compressive stress was taken as 11,000 kPa, and the allowable steel reinforcement stress was taken as 165 MPa.

6.2.2 Comparison of Axial Forces and Moments to Capacity

The axial forces and bending moments calculated from the strain gages at section A are plotted along with the interaction diagrams in figures 6-1 to 6-6. Generally, the applied forces should be within the working stress interaction range. Obviously, if the forces exceed the nominal capacity of the interaction diagram, the culvert has theoretically failed.

At all six locations in section A the applied axial force and bending moment is well within the ultimate capacity of the culvert. In fact, all sections are within the working stress diagram, with the exception of A1, which is only slightly outside the working stress range.

6.3 Shear Capacity

The typical cast-in-place box culvert does not have any shear reinforcement in the walls and roof. In general, there will also not be any prestressing, except in the case when precast panels are used to form the top slab. Neglecting the contribution of

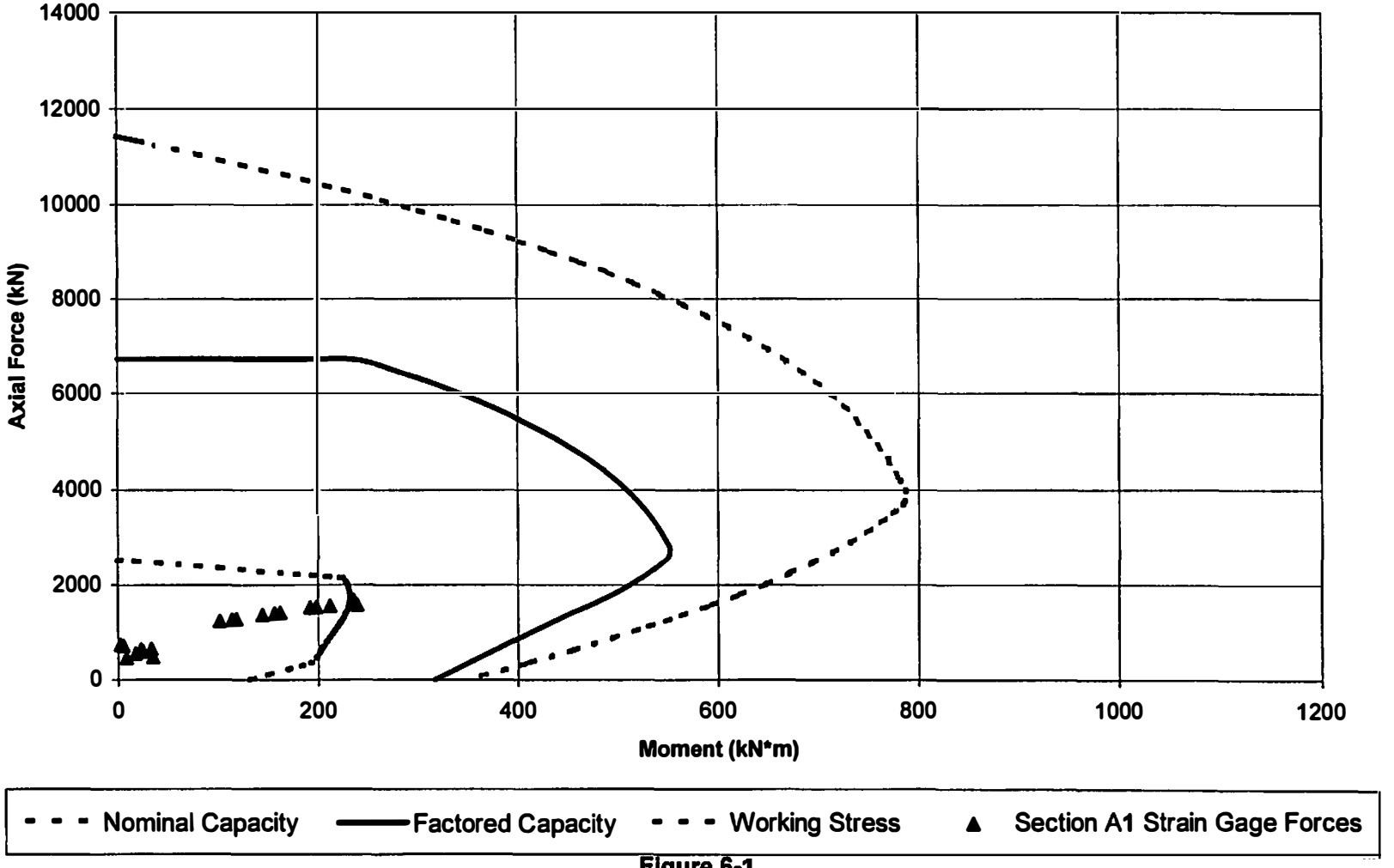


Figure 6-1.
Section A1- Moment Interaction Diagram for Culvert Wall

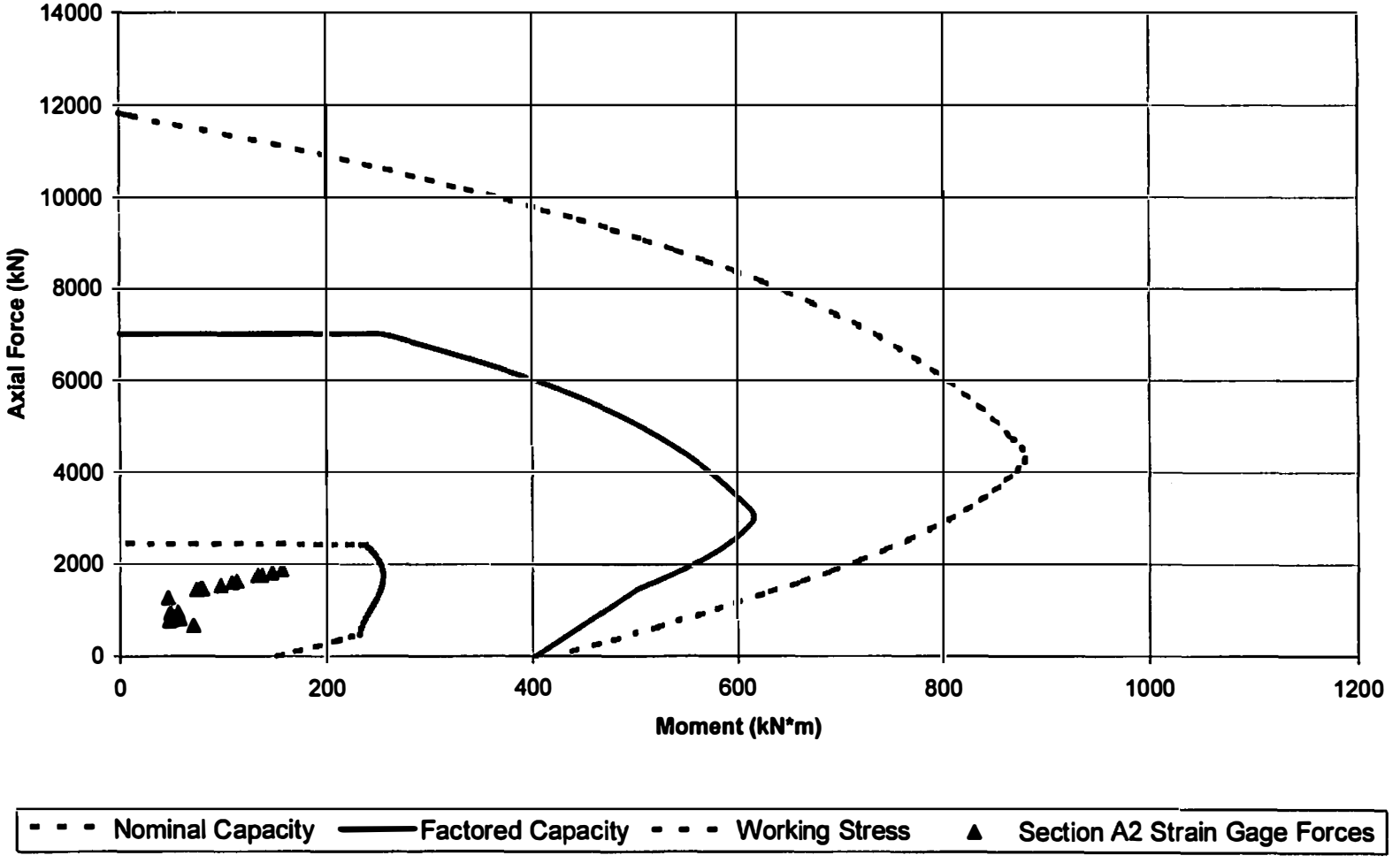


Figure 6-2.
Section A2- Moment Interaction Diagram for Culvert Wall

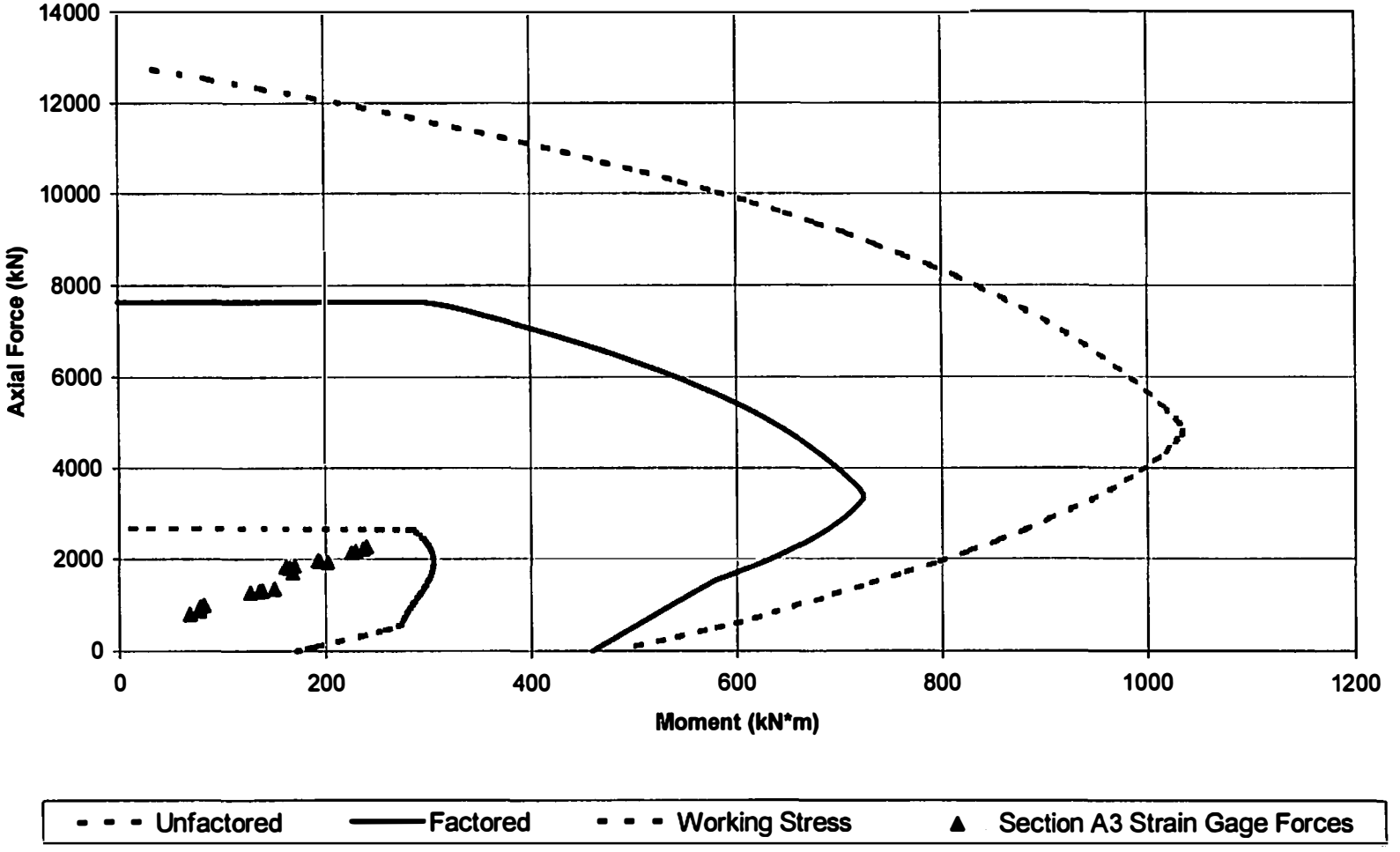


Figure 6-3.
Section A3- Moment Interaction Diagram for Culvert Wall

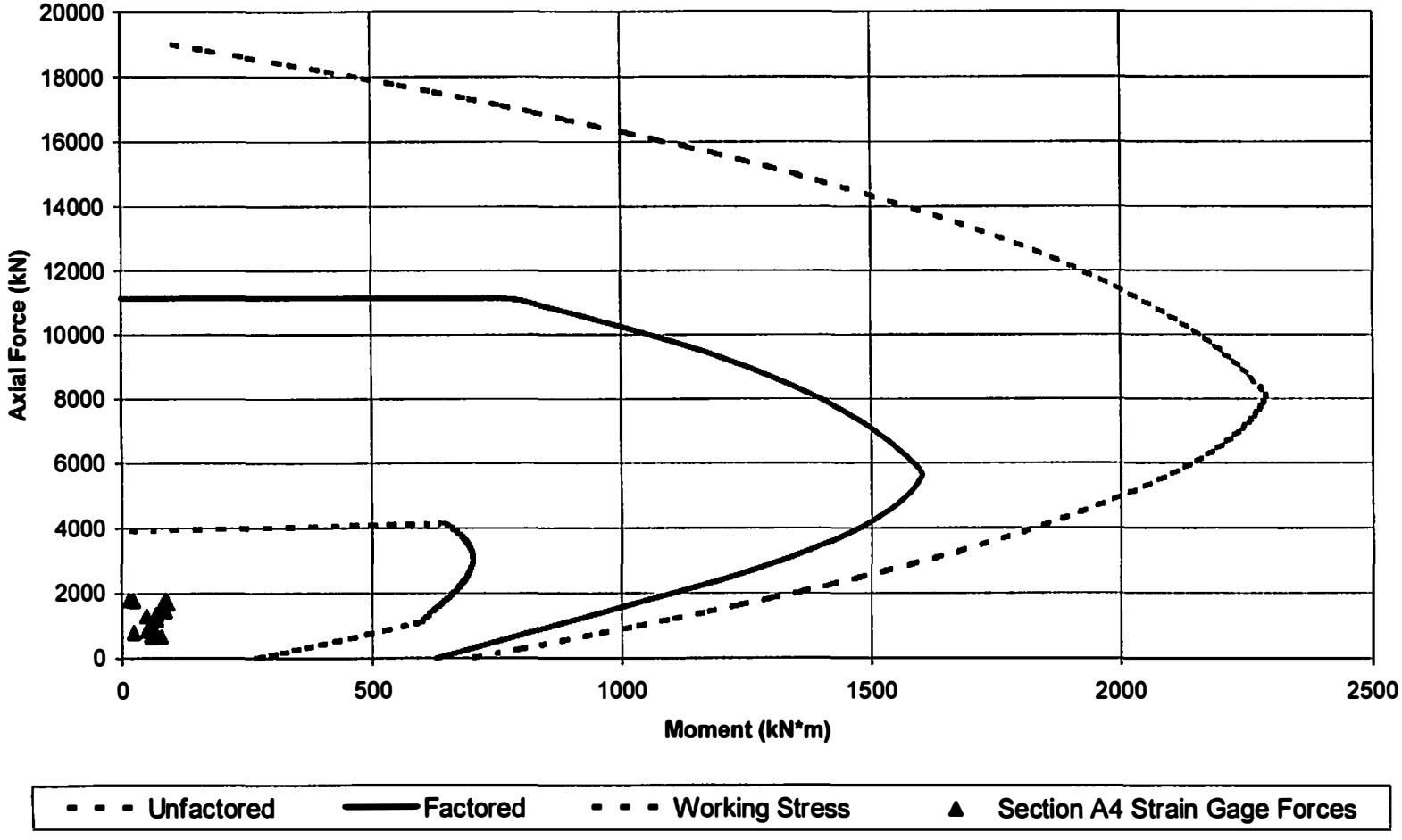


Figure 6-4.
Section A4- Moment Interaction Diagram for Culvert Wall

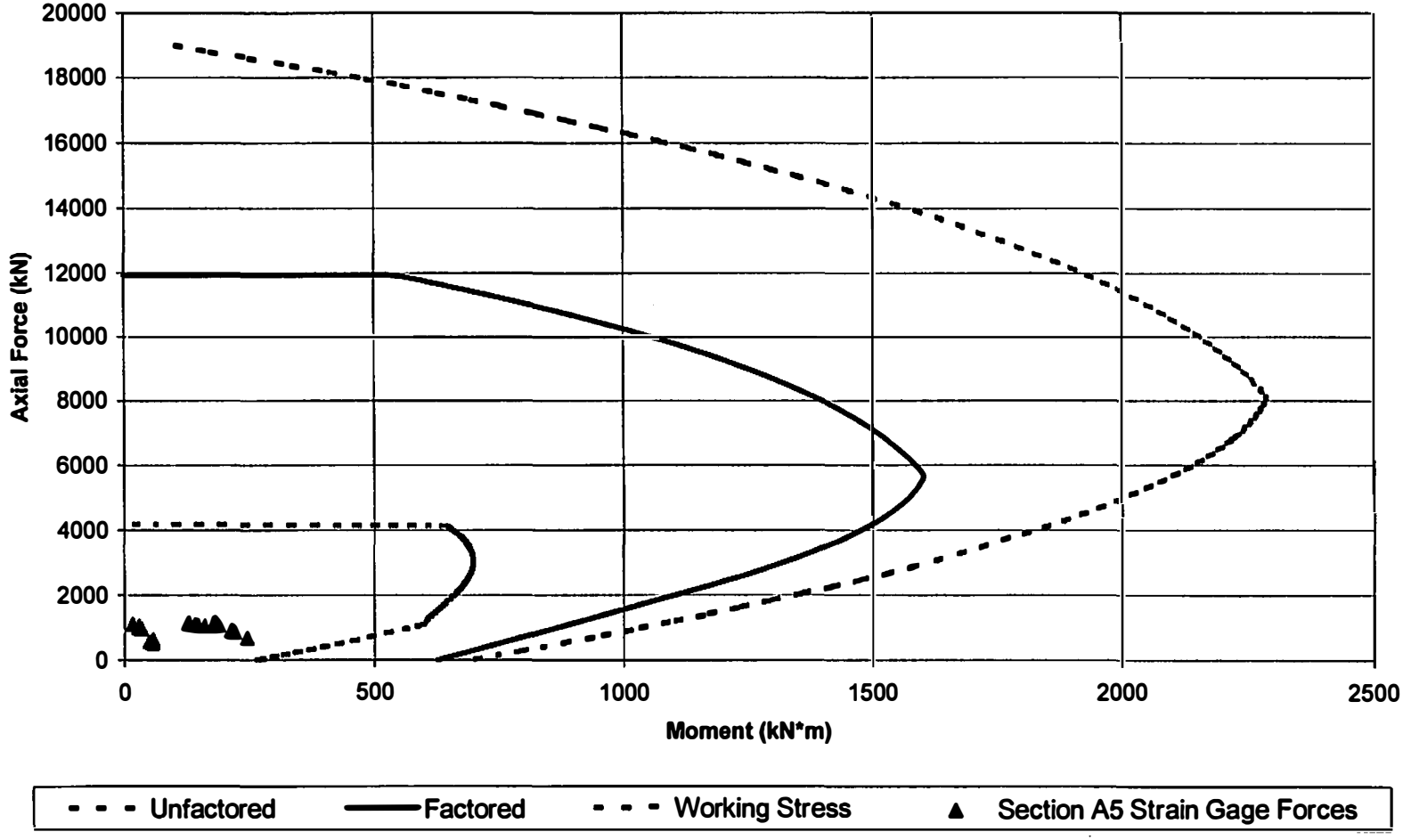


Figure 6-5.
Section A5- Moment Interaction Diagram for Culvert Wall

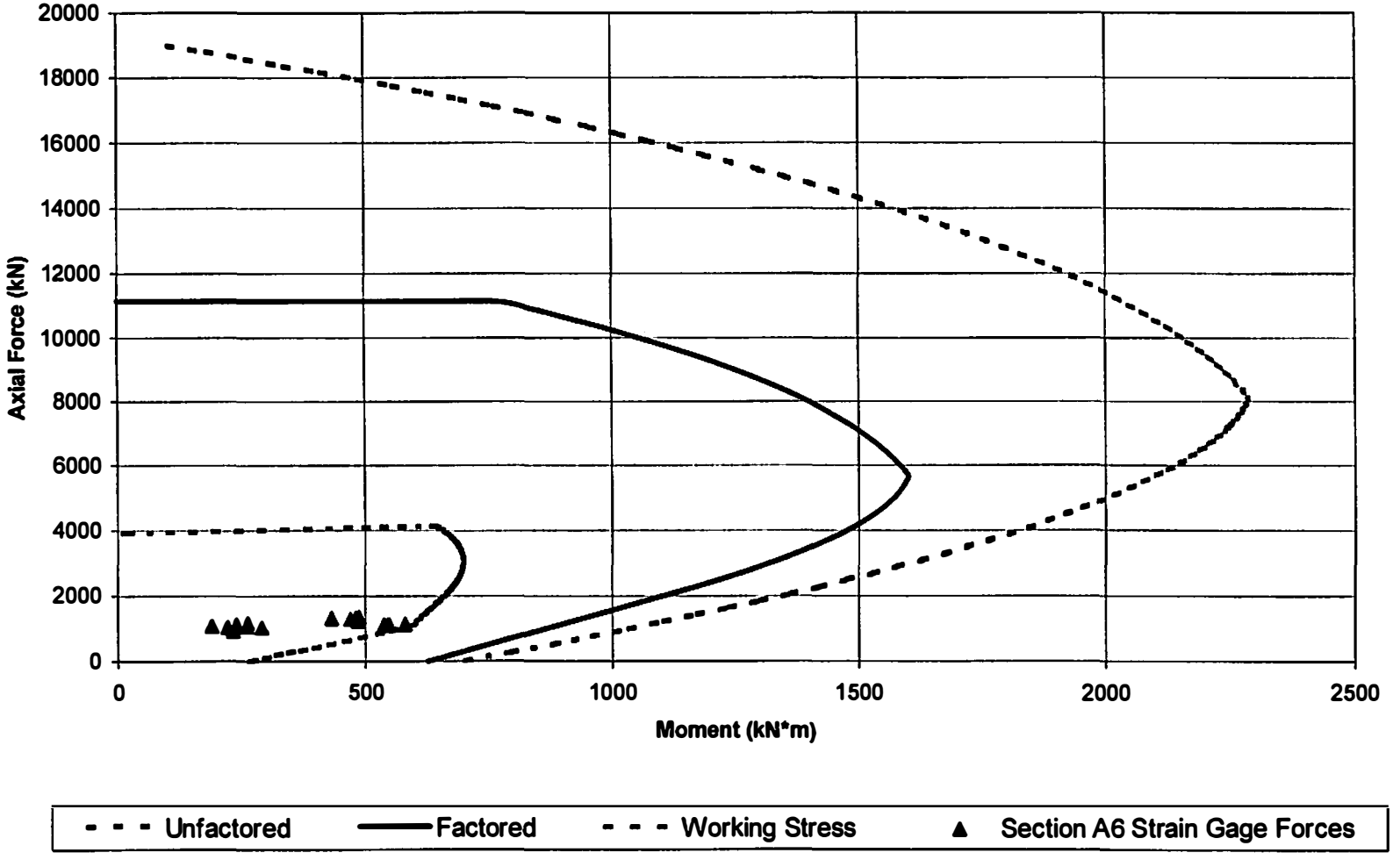


Figure 6-6.
Section A6- Moment Interaction Diagram for Culvert Wall

prestresses to the shear strength, AASHTO nominal shear stress for slabs of box culverts with 2 feet or more of fill is determined from the equation:

$$v_c = 2.14\sqrt{f'_c} + 4600\rho\left(\frac{Vd}{M}\right) \le 4\sqrt{f'_c} \qquad (6\text{-}1)$$

in which f'_c is the concrete compressive strength, ρ is the tension reinforcement ratio, V is the design shear force, d is the distance from the extreme compression fiber to the centroid of the tension reinforcement and M is the computed moment capacity. For a non-slab member the nominal shear stress may be taken as:

$$v_c = 1.9\sqrt{f'_c} + 2500\rho_w\left(\frac{Vd}{M}\right) \le 3.5\sqrt{f'_c} \qquad (6\text{-}2)$$

where ρ_w is a reinforcement ratio. Taking these two equations results in equation 6-1 giving slightly higher allowable shear capacity, as can be seen in figure 6-7. According the figure 6-7 it is shown that slab shear capacity can be taken as approximately 11% greater than wall shear. Due to the uncertainties in the bending moment in the culvert, the shear force is only compared to the axial force by the AASHTO equation:

$$v_c = 2\left(1 + \frac{N}{2000A_g}\right)\sqrt{f'_c} \qquad (6\text{-}3)$$

where N is the design axial force and A_g is the gross cross-sectional area. The quantity N/A_g shall be expressed in pounds per square inch. To get the factored capacity of the walls this equation is multiplied by 0.85.

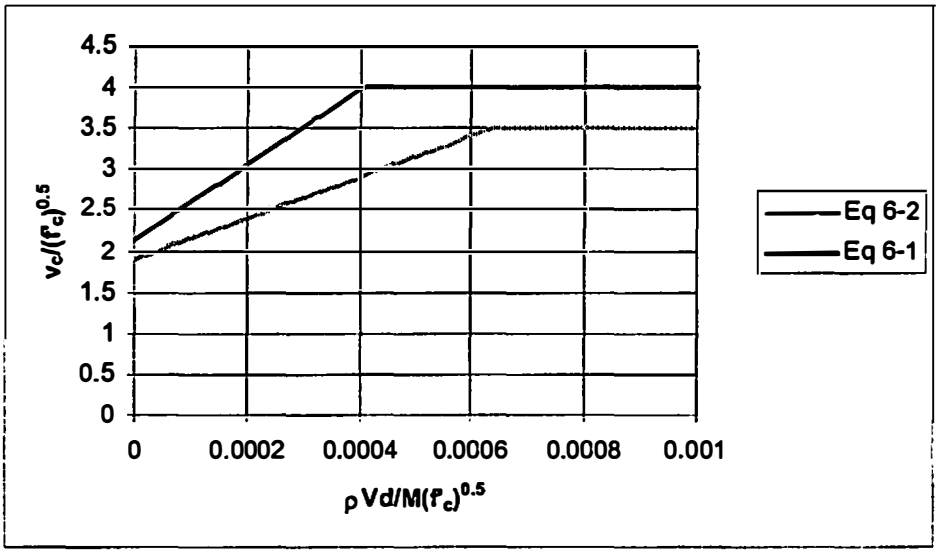


Figure 6-7. Comparison of AASHTO Shear Strength.

For the allowable shear stress of the culvert, the shear forces are compared to the equation in AASHTO for allowable shear stress for member in compression:

$$v_c = 0.9\left(1 + 0.0006\frac{N}{A_g}\right)\sqrt{f'_c} \qquad (6\text{-}4)$$

6.3.1 Comparison of Shear Forces and Capacity in the Culvert Wall

The shear force from the strain gages along with the shear capacity of the culvert wall is shown in figures 6-8 through 6-10. Three different load cases were examined for the wall of the culvert. These include a uniform load, a triangular load and a parabolic load with a high pressure at the base. According to AASHTO specifications the maximum shear force should be taken at a distance d from the face

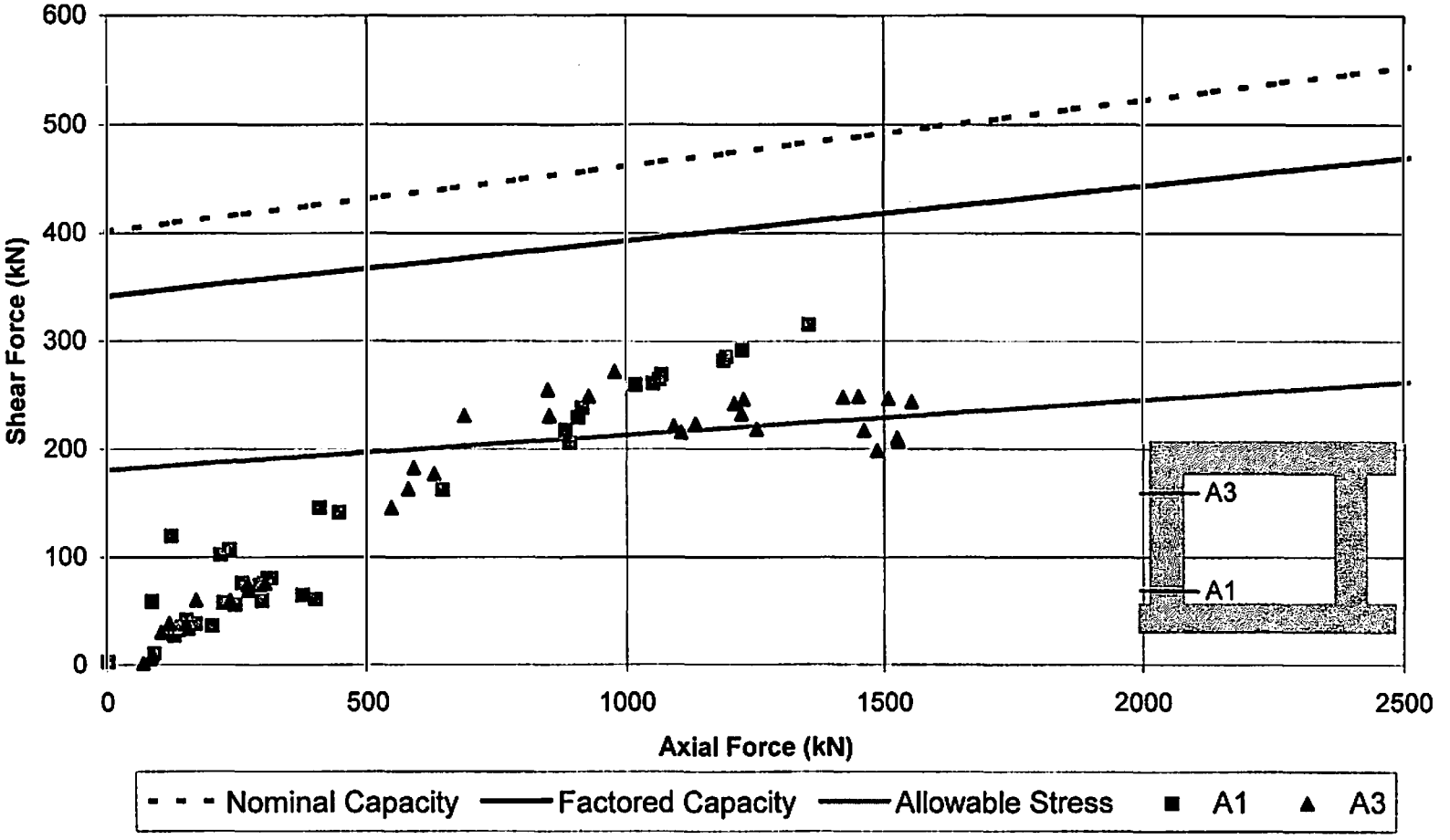


Figure 6-8.
Shear Force vs. Axial Force
Case 1 (Uniform Load)

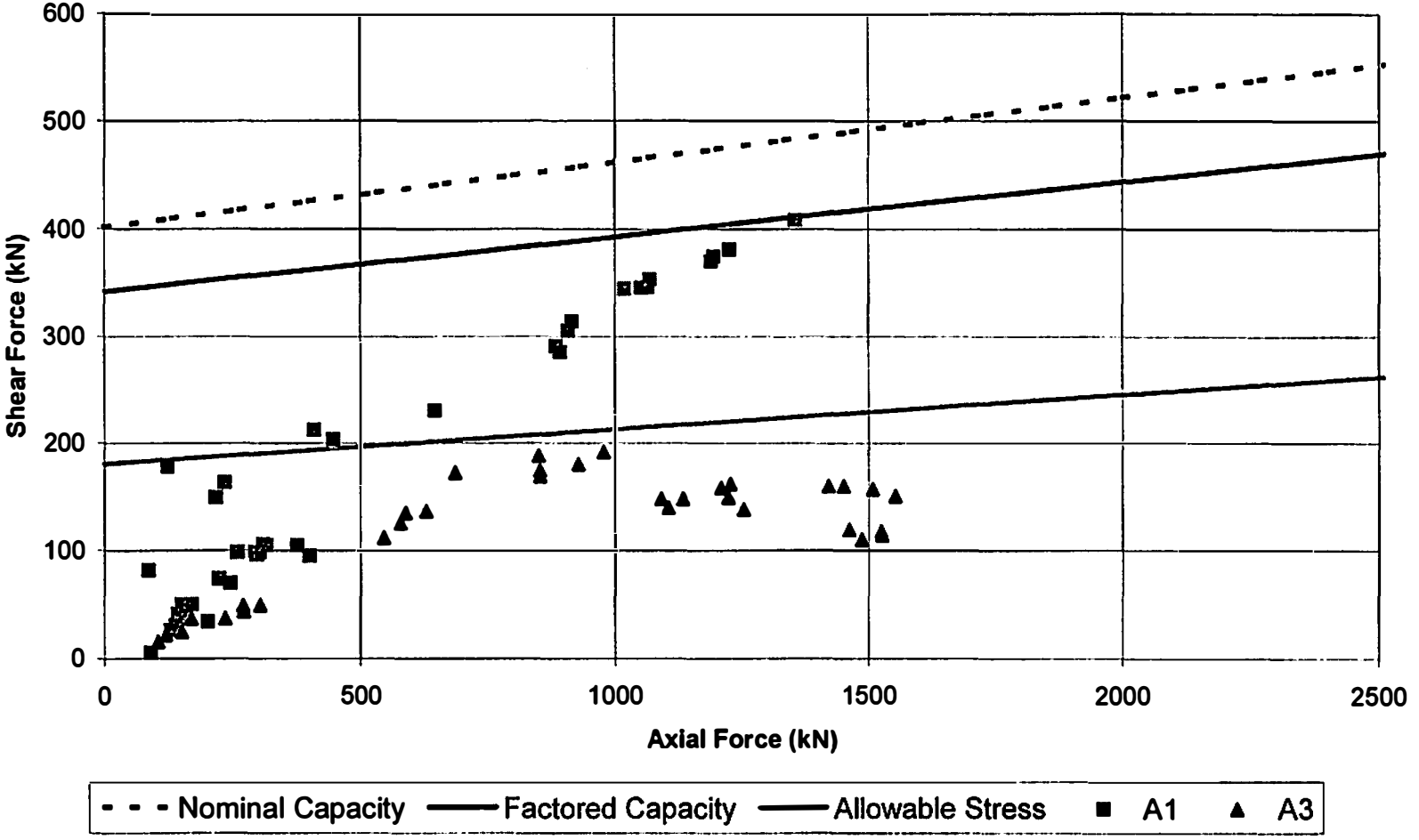


Figure 6-9.
Shear Force vs. Axial Force
Case 2 (Triangular Load)

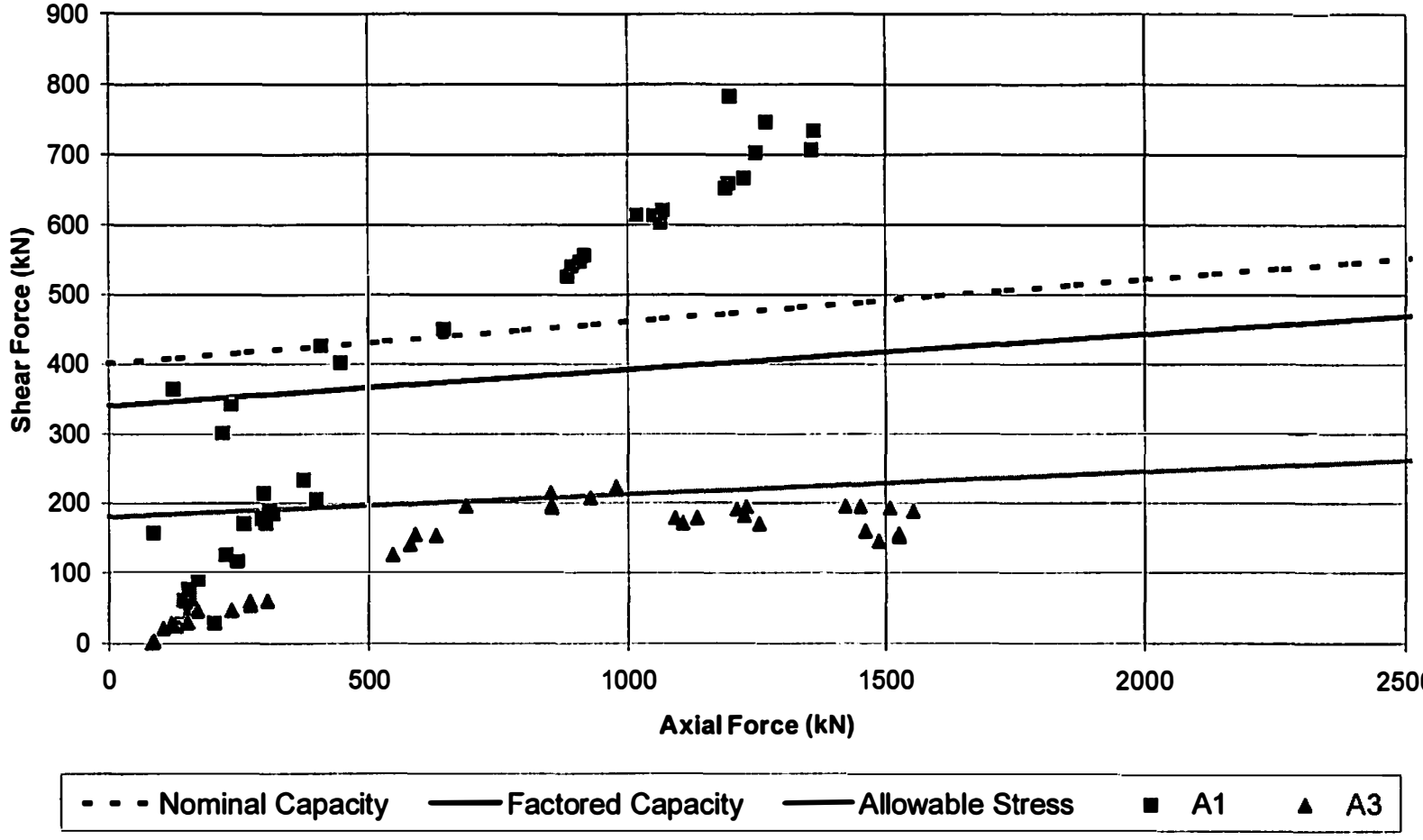


Figure 6-10.
Shear Force vs. Axial Force
Case 3 (High Pressure at Base)

of the support. Due to the complexity of finding the shear force at a distance d from the face of the support the maximum shear force was taken at the location of the strain gages, which are approximately 10 cm from shear stress at a distance d from the face of the support.

When an assumed uniform load distribution is applied to the wall of the culvert, all of the shear forces are below the factored shear capacity. When an assumed triangular distribution is applied to the wall, the shear forces near the bottom of the culvert are close to the factored shear capacity. Using an assumed parabolic load with a high pressure at the base results in shear forces at the bottom of the wall that exceeds the shear capacity of the section. When the shear forces are compared with the allowable shear stress, all three cases show shear forces that are above the allowable.

6.3.2 Comparison of Shear Forces and Capacity in the Culvert Roof

Figure 6-11 shows a comparison of the roof shear forces calculated from the strain gages along with the allowable shear capacity from AASHTO design criteria. An assumed uniform load distribution was used for the calculation of the shear forces. Due to the uncertainties in the applied axial force in the roof of the culvert, a different method was used to calculate the shear capacity of the roof that did not take account of the increase in shear strength due to axial compression. The maximum applied shear

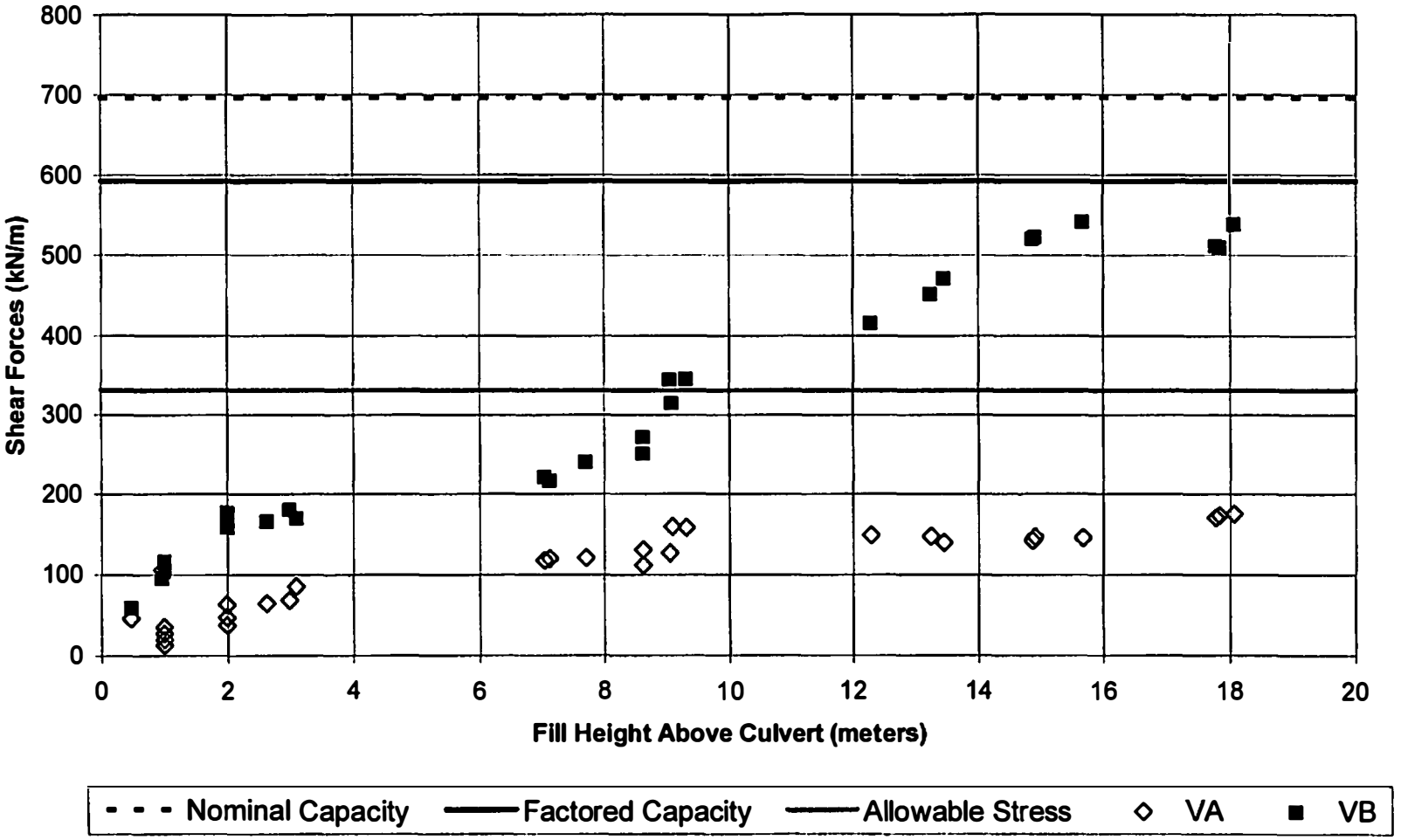


Figure 6-11.
Section A Roof Shear Strength

forces in the culvert roof are taken at a distance d from the face of the support. Roof shear forces and the shear capacity are plotted versus the fill height.

The calculated roof shear forces from the strain gages are all below the factored shear capacity of the roof section. The actual shear capacity of the roof may also be higher due to the prestressing panels that were used in the roof.

6.4 Conclusion on Culvert Capacity

The culvert has adequate capacity based on comparison of the applied loads from the strain gages to the moment-interaction diagram, and the applied loads are often within the allowable stress range. When the shear capacity of the culvert wall is compared to the applied wall shear forces, it can be seen that a change in the pressure distribution from uniform to a higher pressure at the base can result in shear forces that are higher than the shear capacities of the wall. The roof shear forces come close to the factored capacity of the roof, but due to the prestressing panel used the actual shear capacity may be slightly higher.

Chapter 7
Conclusion

7.1 Internal Forces

Based on the strain gage results, axial forces and bending moments in the box culvert are linearly related to the embankment height. The external pressures, measured from the pressure cells, gave results consistent with the strain gage calculations.

The roof pressures at section A gave results that were higher than the design pressures given in AASHTO, but section B gave results that near the design values. The roof pressures measured were not uniform, but this does not affect the internal forces.

Wall internal forces are affected by the load distribution applied to the wall. AASHTO assumes an almost uniform pressure for high embankment heights, but on this culvert a much higher pressure was measured at the base of the culvert. With the higher pressures applied at the base of the culvert, the shear force in the bottom of the wall increases greatly. Although the total horizontal design force on the wall of the culvert may be reasonable, a change in the load distribution significantly affects wall shears.

7.2 Capacity

The box culvert has adequate capacity according to the design equations from AASHTO. Most of the calculated pressures at section A were higher than the

recommended pressures from AASHTO, but almost all of the forces were within the working stress rage of the moment-interaction diagram. Shear forces on the roof are below the shear capacity of the culvert. When the load distribution is increased on the bottom of the wall, shear forces develop that exceed the capacity of the culvert.

The computer modeling of the culvert showed that the effects of boundary conditions give slightly different moments in the roof and wall. Load distributions on the roof show very little change in the bending moments and shears, but when the load distribution on the wall increases on the bottom, a significant increase in shear force is seen.

REFERENCES

References

1. Dasgupta, A. and Sengupta, B. (1991). "Large-Scale Model Test On Square Box Culvert Backfilled With Sand." *Journal of. Geotechenial Engineering. Div.*, ASCE, 117(1), 156-161.

2. *Design and Cnstruction of Reinforced Concrete Box Culverts* (1996), American Railway Engineering Association, Vol. 97, Bulletin 758, 625-639.

3. *Minimum Design Loads for Buildings and Other Structures,* (ANSI/ASCE 7-95, 1995). American Society of Civil Engineers, New York.

4. Sachs, L. (1984), *Applied Statistics a Handbook of Techniques*, 2nd Edition, Springler-Verlag, New York.

5. Spangler, M. G. and Handy, R. L. (1992). *Soil Engineering.* 4th edition, Harper & Row, New York.

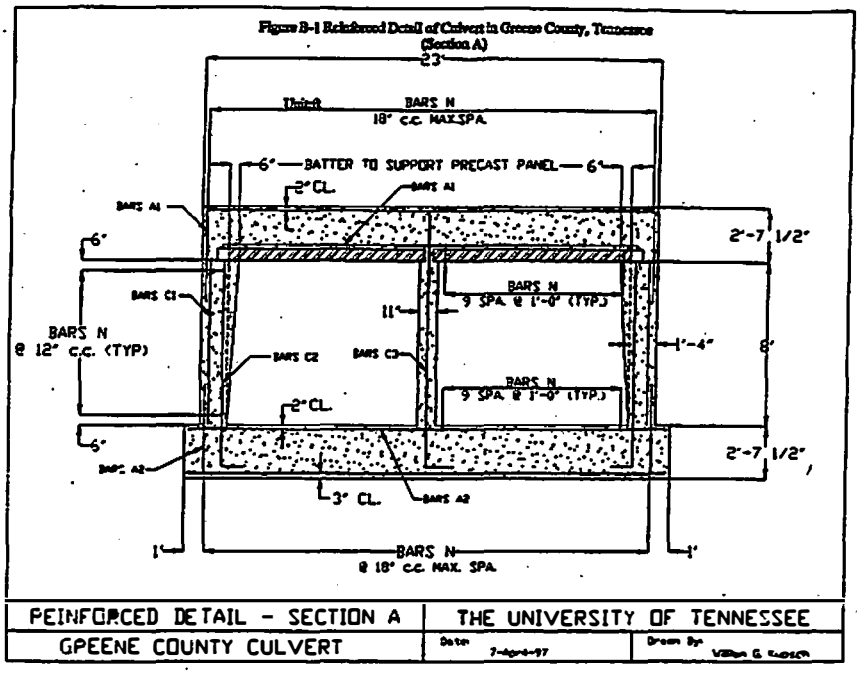
6. Standard Specifications for Highway Bridges. (1996). 16th Ed., The American Association of State Highway and Transportation Officials (AASHTO), Washington, D.C.

7. Tadros, M. K., Benak, J. V., Abdel-Karim, A. M. and Bexten, K. A. (1989). "Field Testing of a Concrete Box Culvert." *Transportation Research Record 1231*, 49 55.

8. Yang, M. Z. (2000). "Evaluation of Factors Affecting the Earth pressures on Buried Box Culverts." Disseration, University of Tennessee, Knoxville.

APPENDIXES

Appendix A
Greene County Culvert
Dimensions and Details



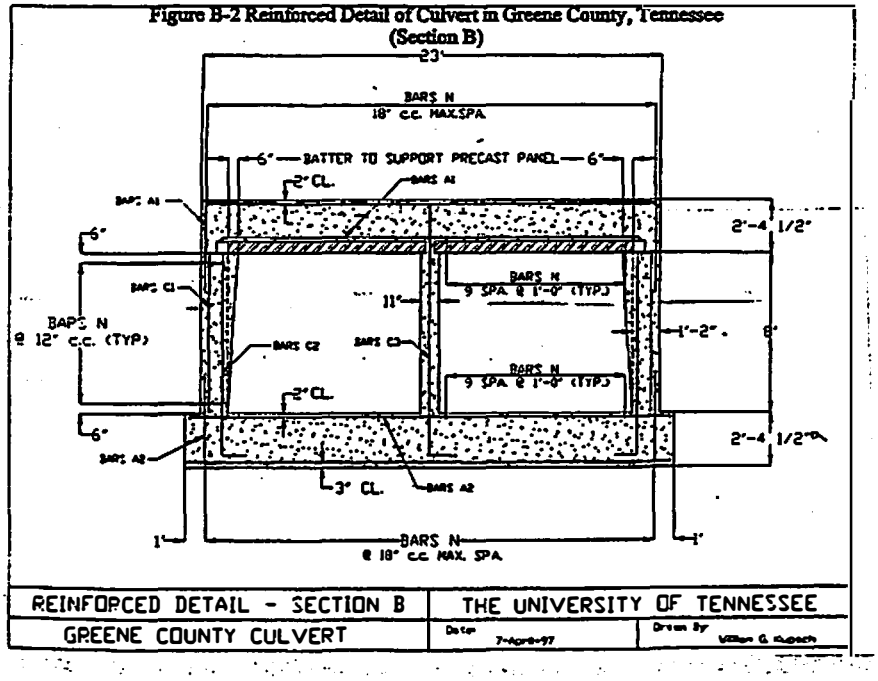
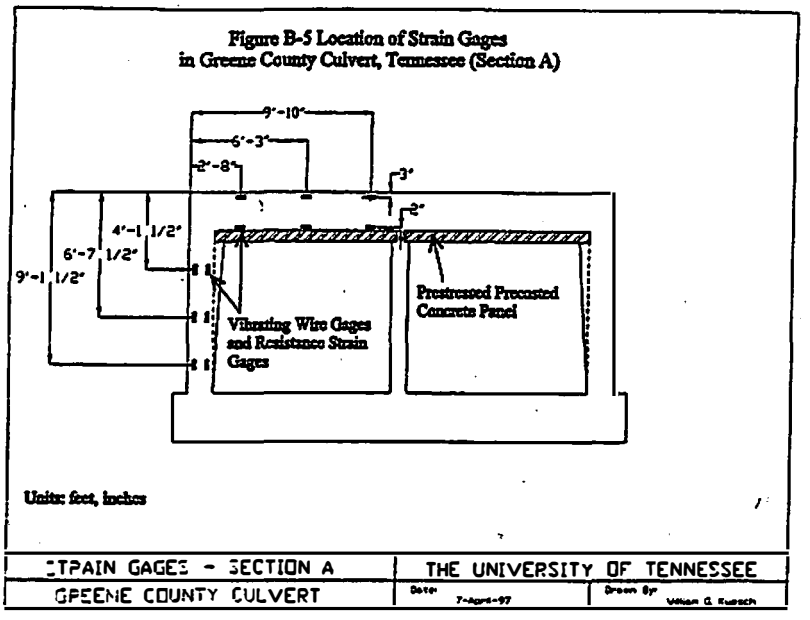


Figure A-1. Reinforcement Details.



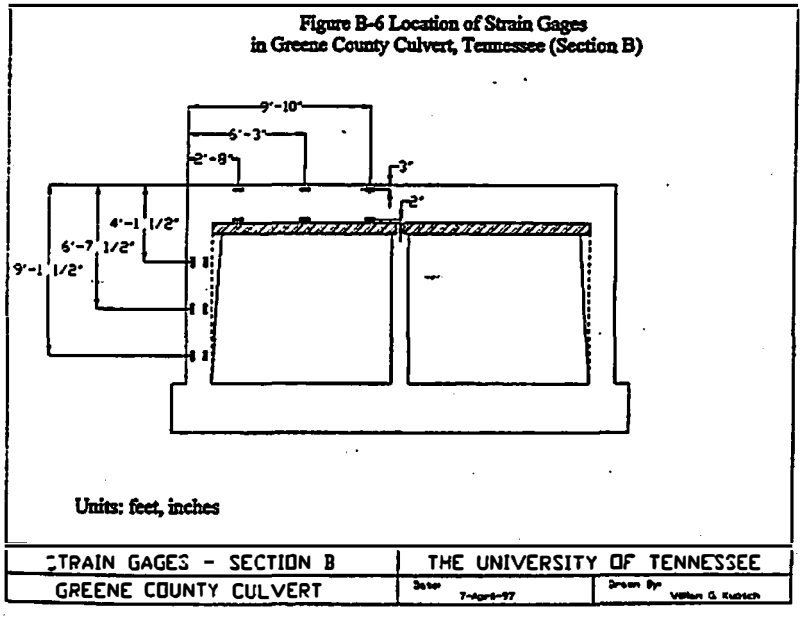


Figure A-2. Strain Gage Locations.

Appendix B
Section A Strain Gage Results

Figure B-1
Strain Readings Section A1

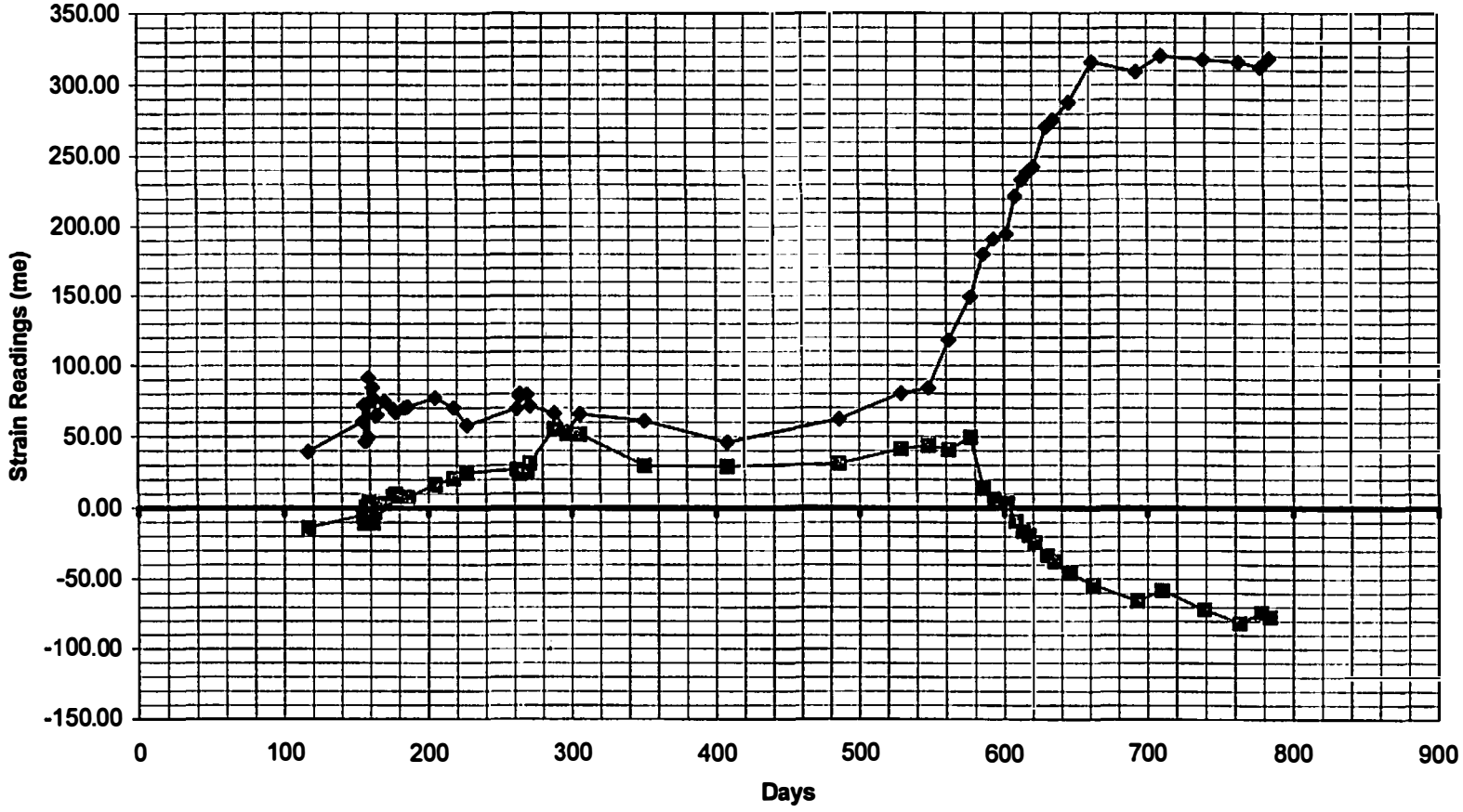


Figure B-2
Axial Force and Bending Moment Section A1

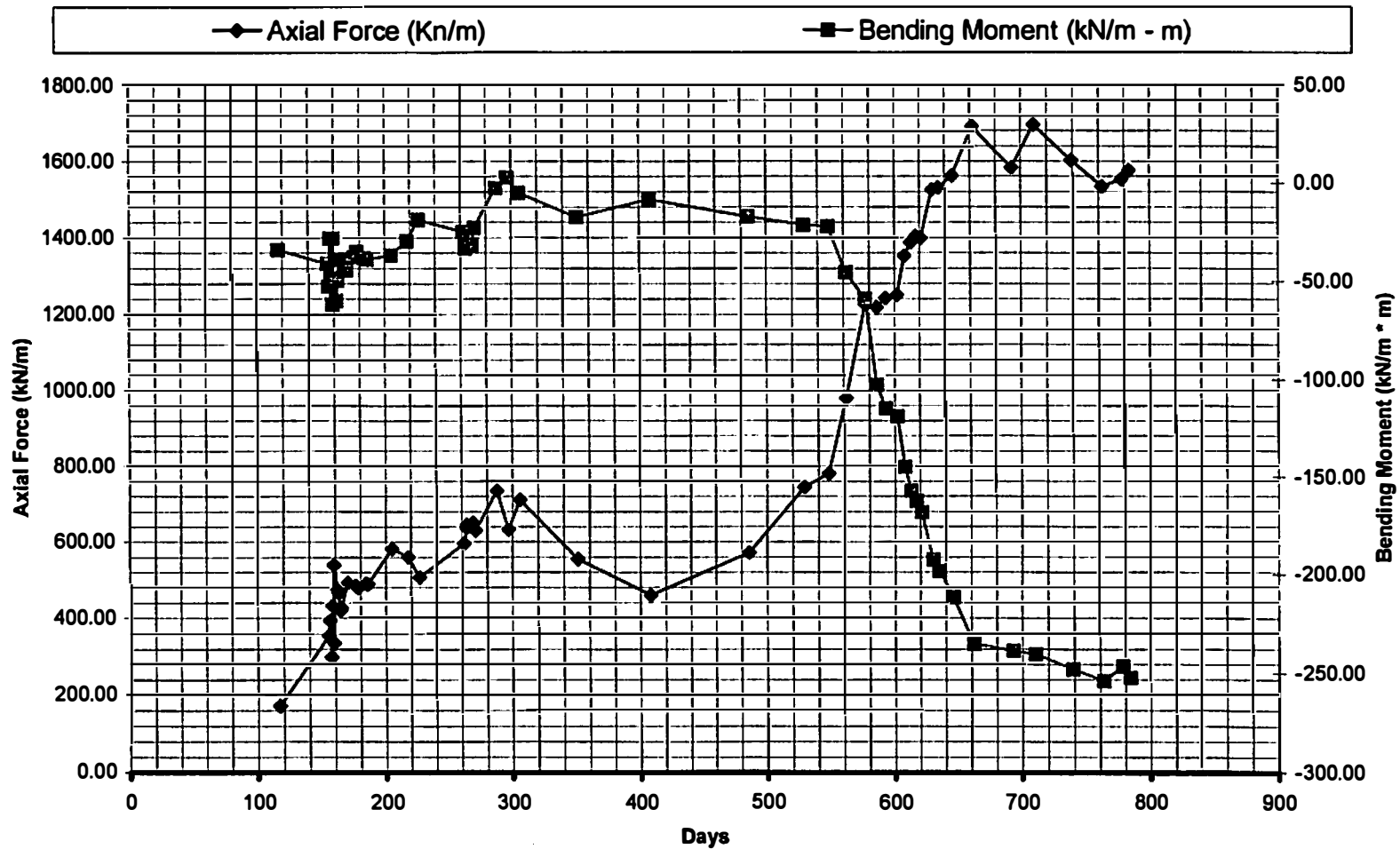


Figure B-3
Axial Force vs. Fill Height Section A1

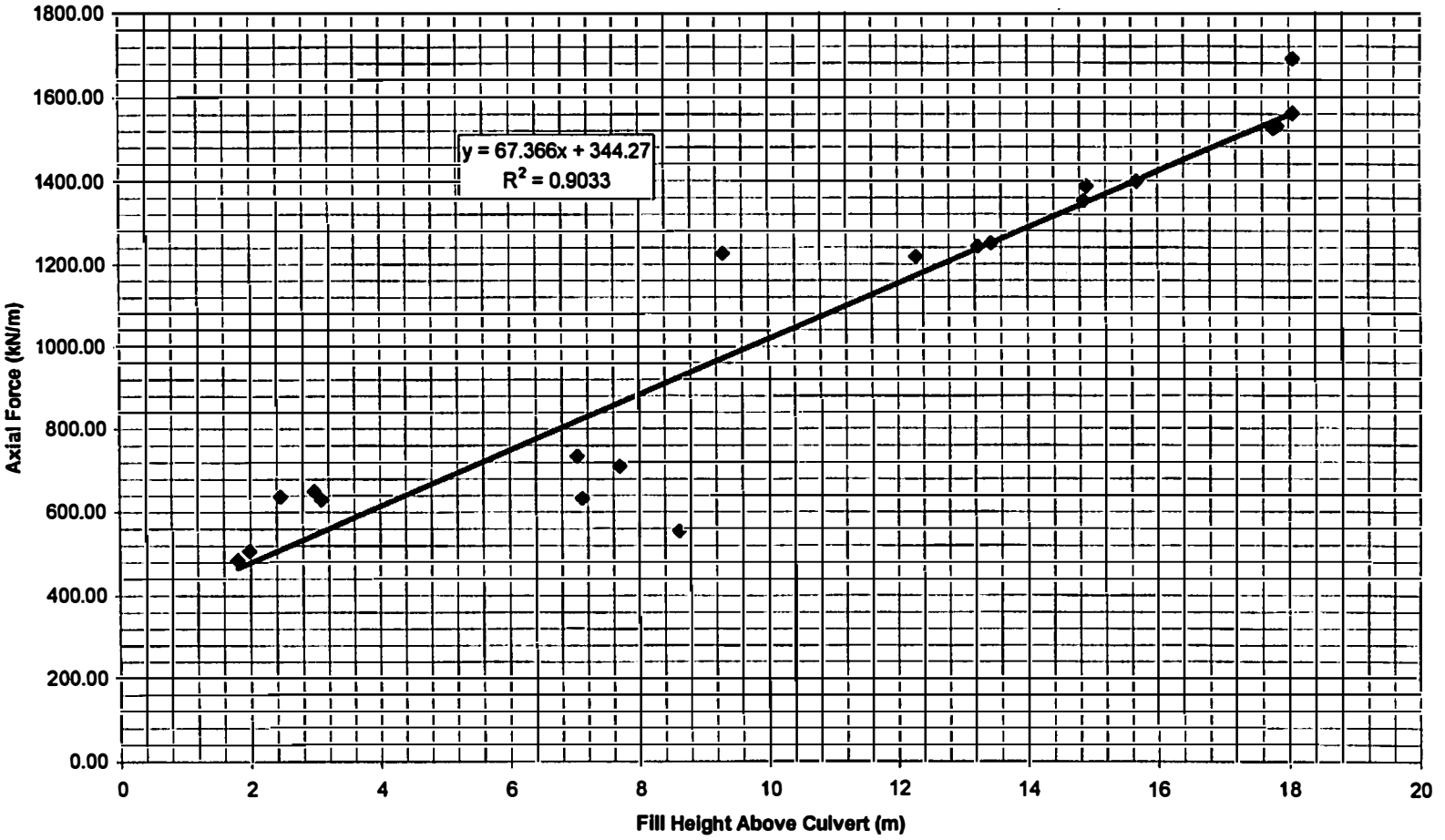
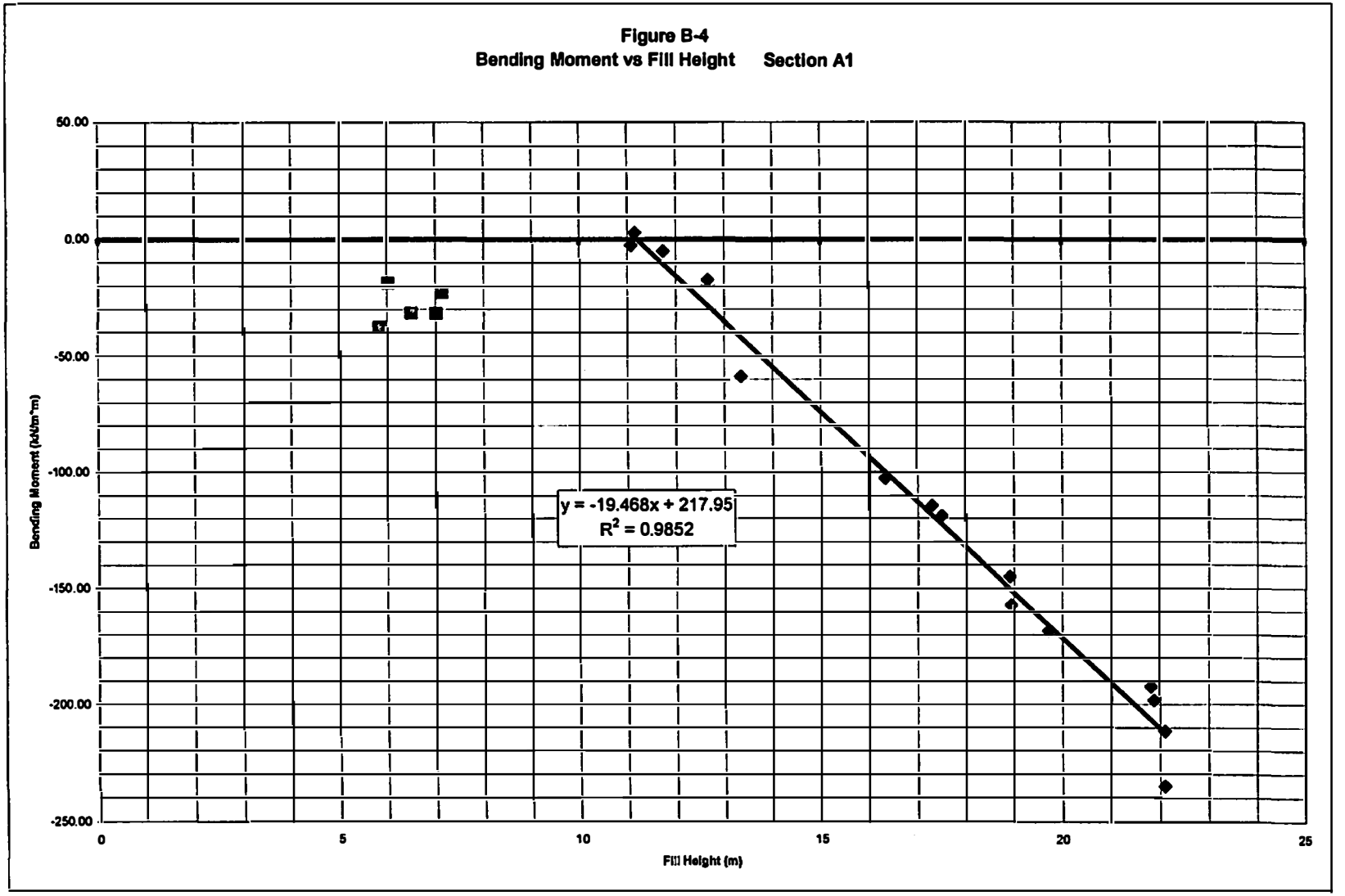


Figure B-4
Bending Moment vs Fill Height Section A1



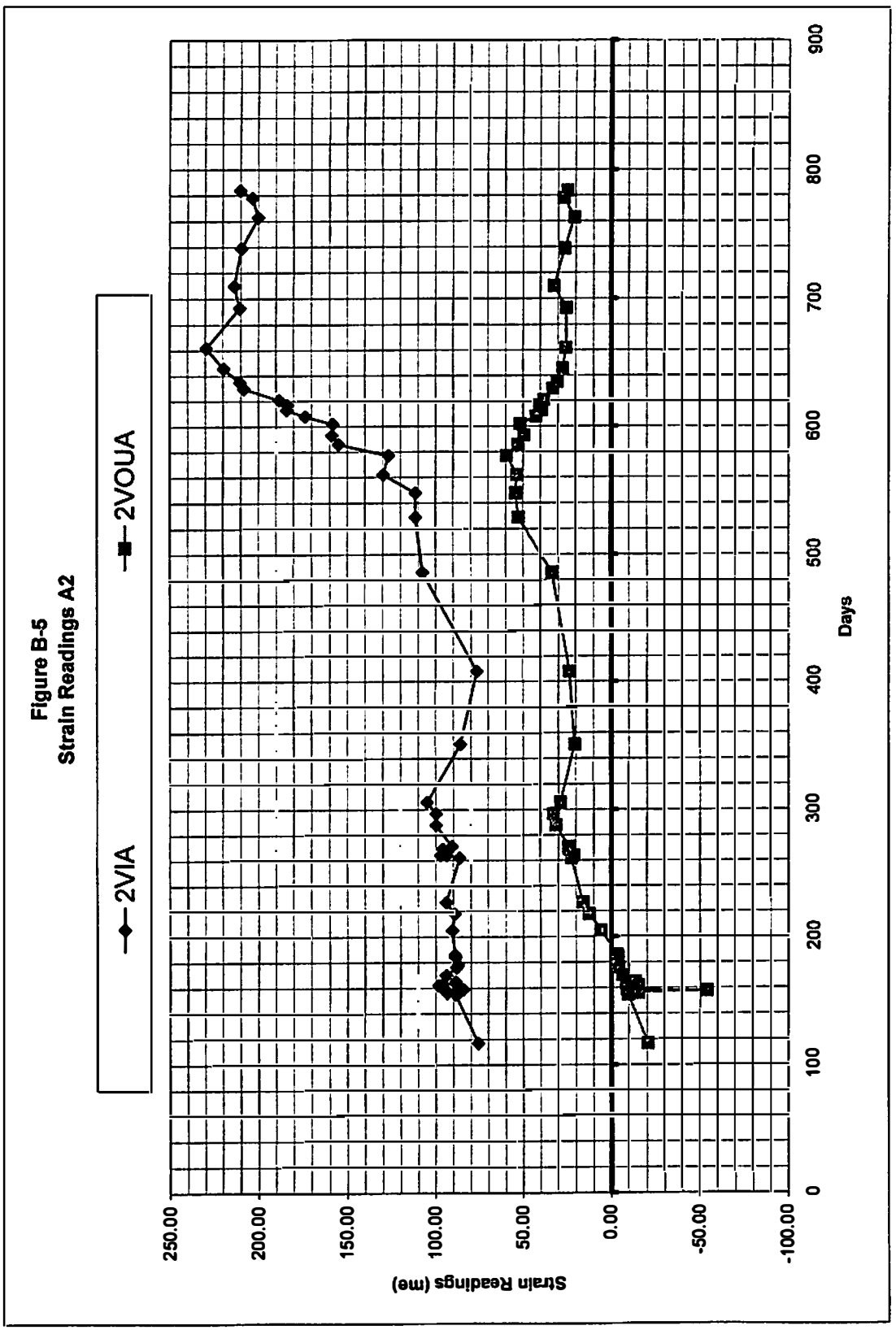

Figure B-5
Strain Readings A2
2VIA
2VOUA
Strain Readings (me)
250.00
200.00
150.00
100.00
50.00
0.00
-50.00
-100.00
0
100
200
300
400
500
600
700
800
900
Days

Figure B-6
Axial Force and Bending Moment Section A2

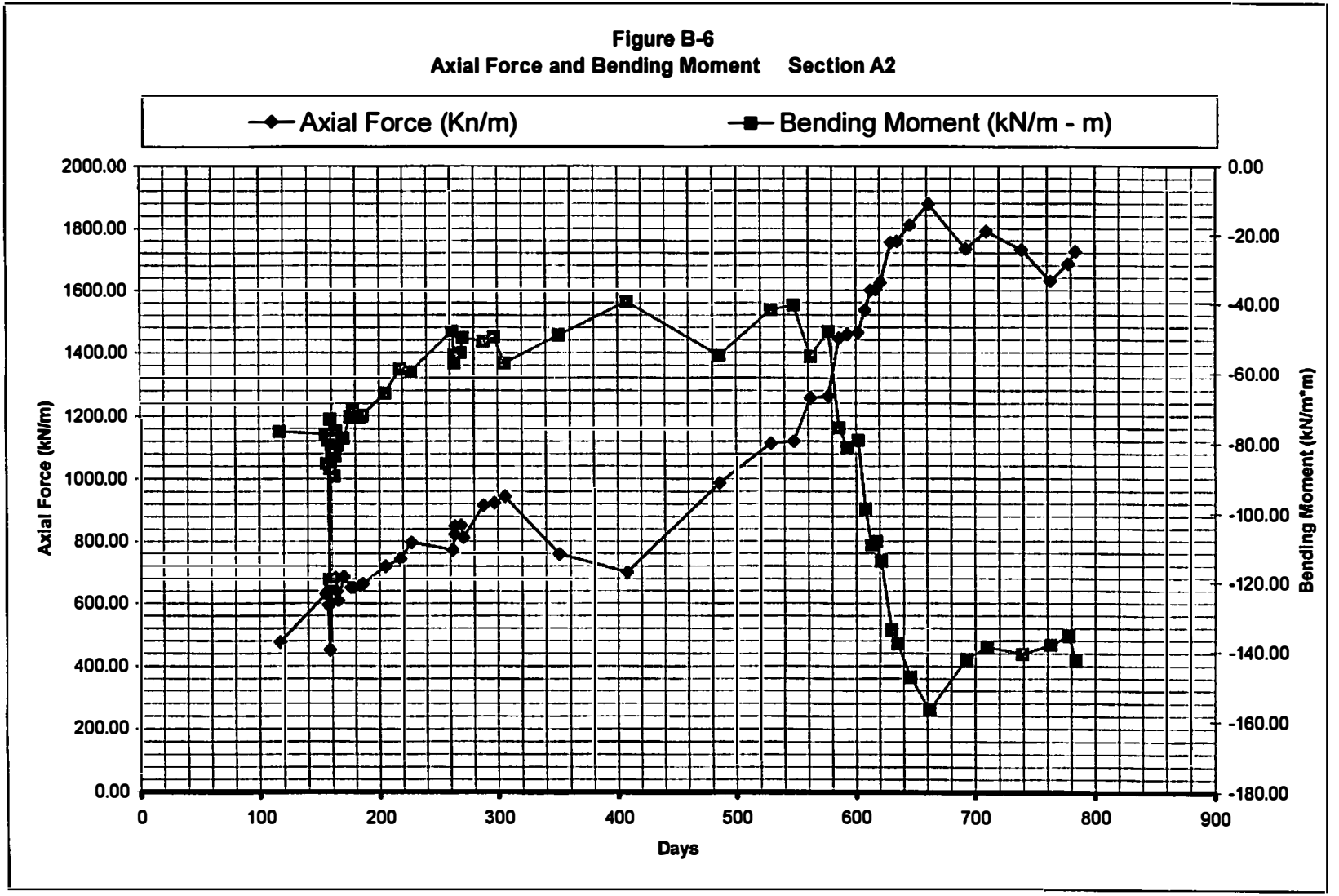


Figure B-7
Axial Force vs Fill Height Above Culvert Section A2

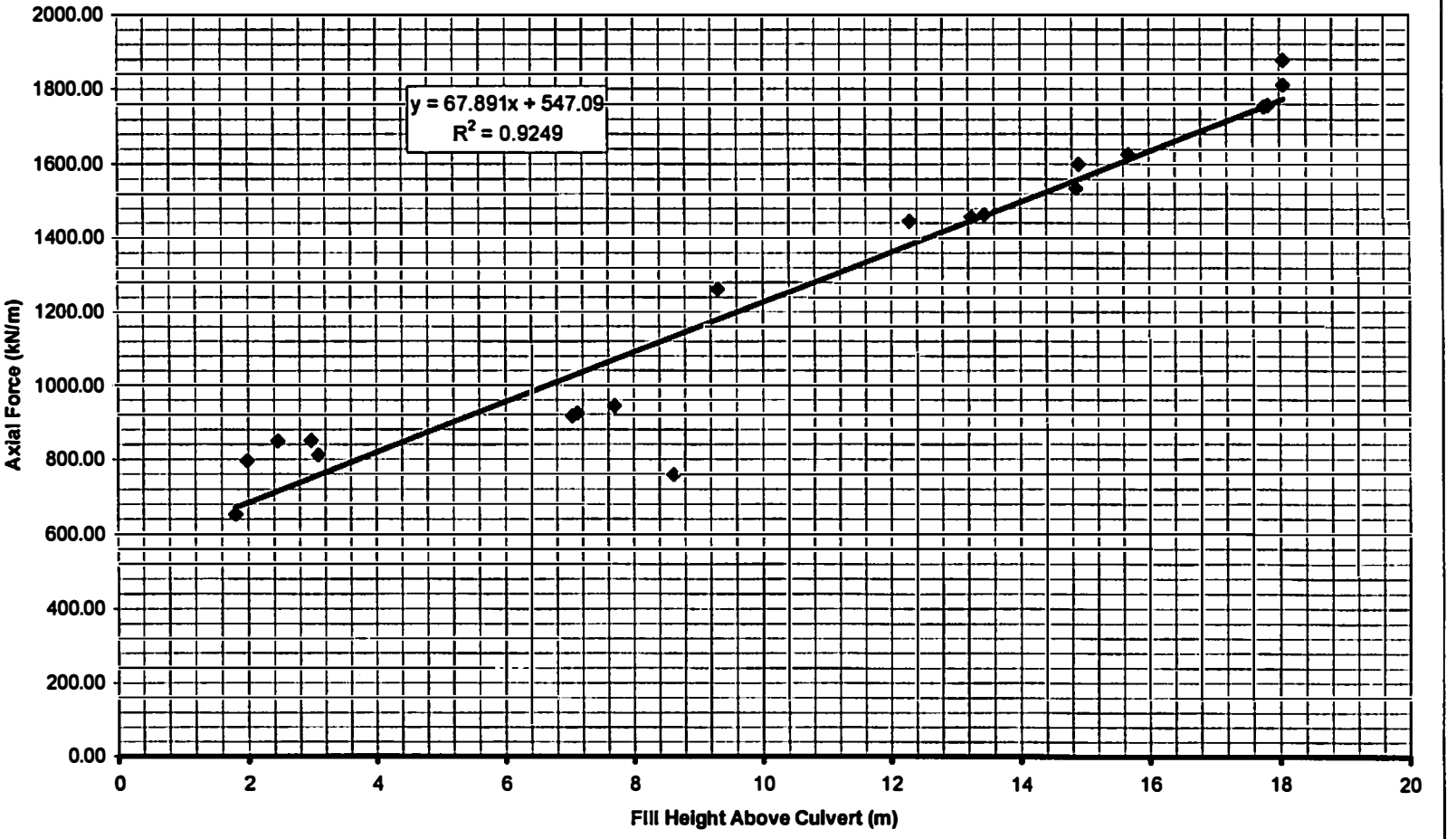
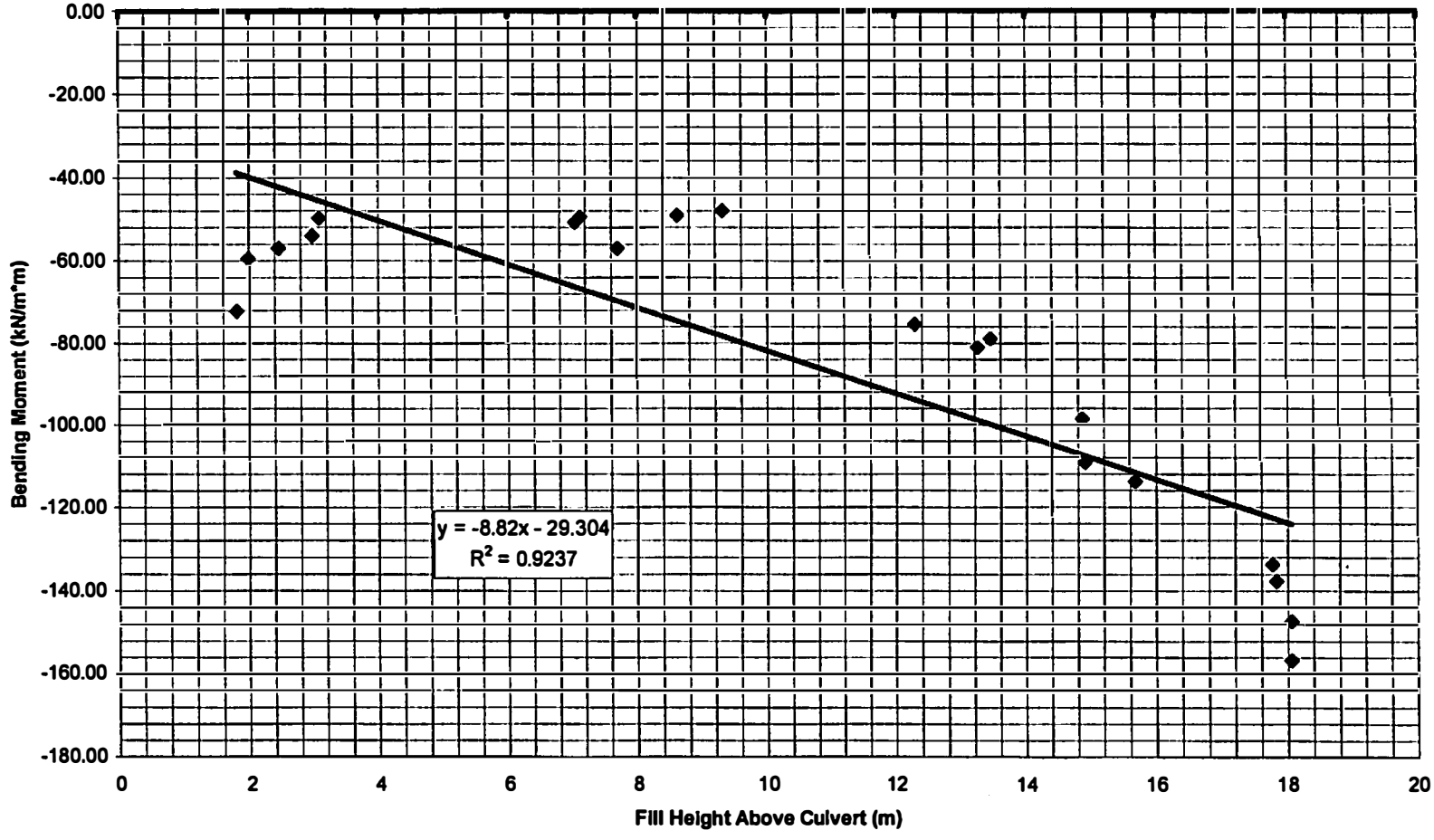
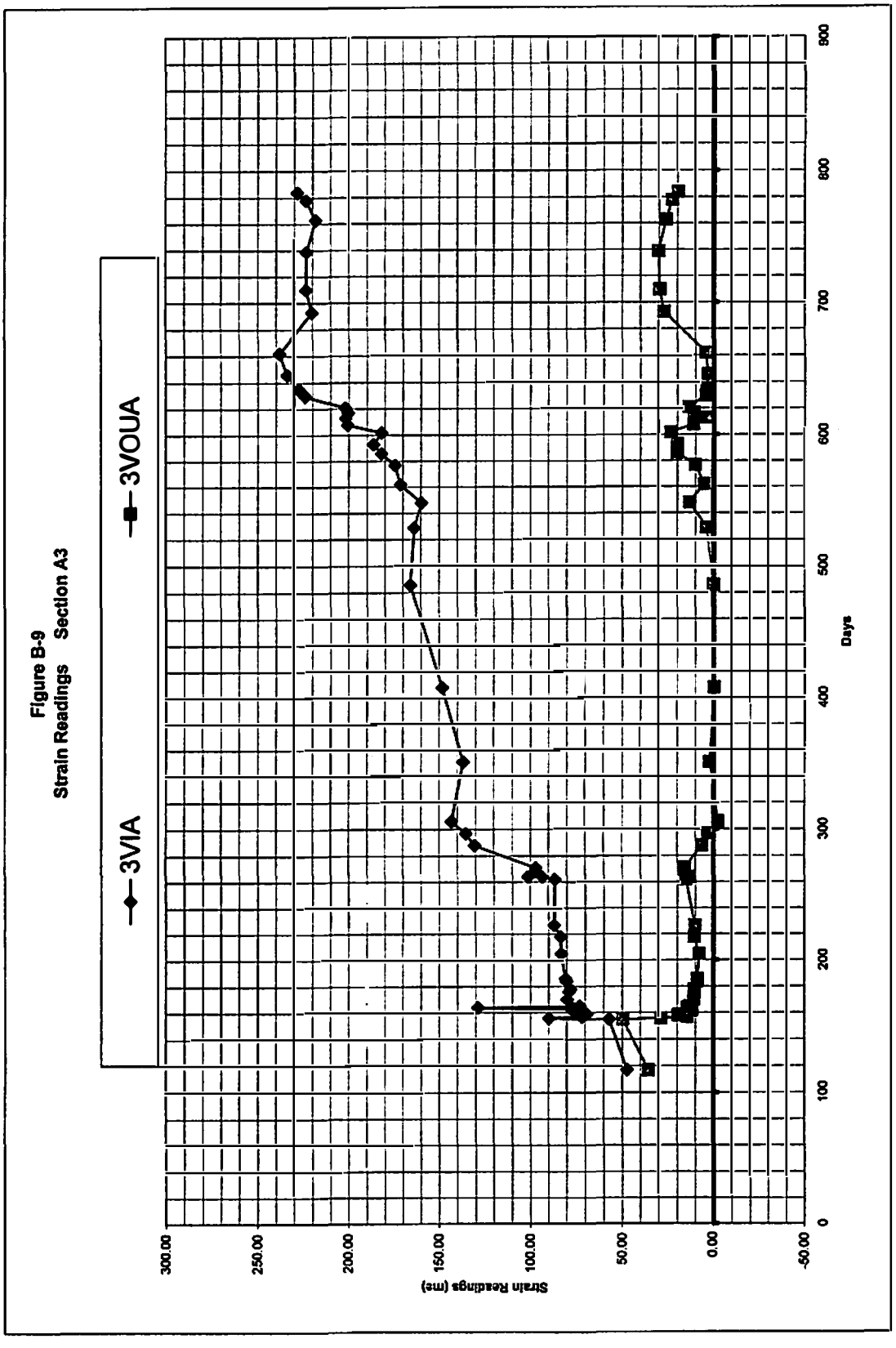


Figure B-8
Bending Moment vs Fill Height Above Culvert Section A2




Figure B-9
Strain Readings Section A3
3VIA
3VOUA
Strain Readings (me)
300.00
250.00
200.00
150.00
100.00
50.00
0.00
-50.00
0
100
200
300
400
500
600
700
800
900
Days

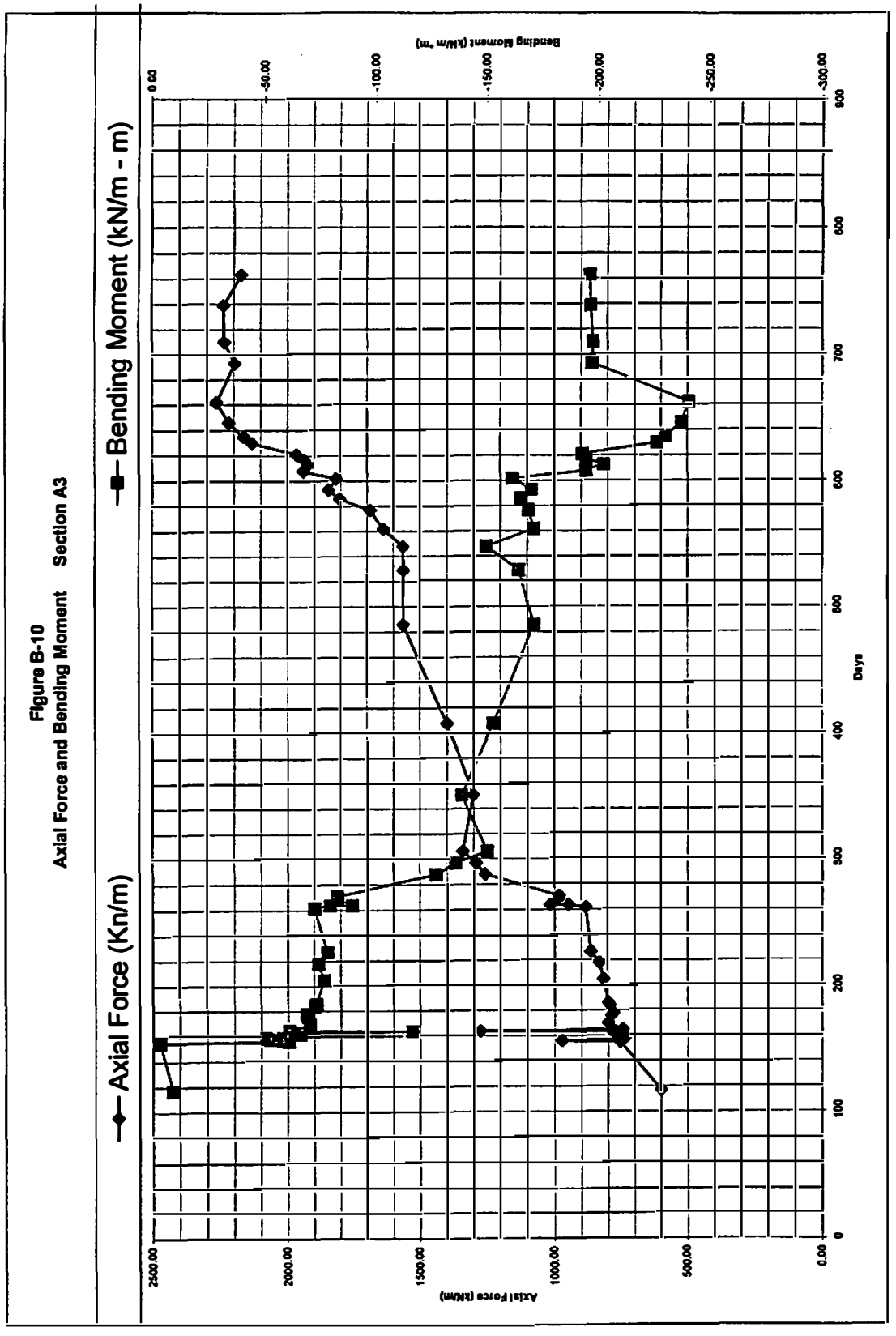


Figure B-10
Axial Force and Bending Moment Section A3

Figure B-11
Axial Force vs Fill Height at Section A3

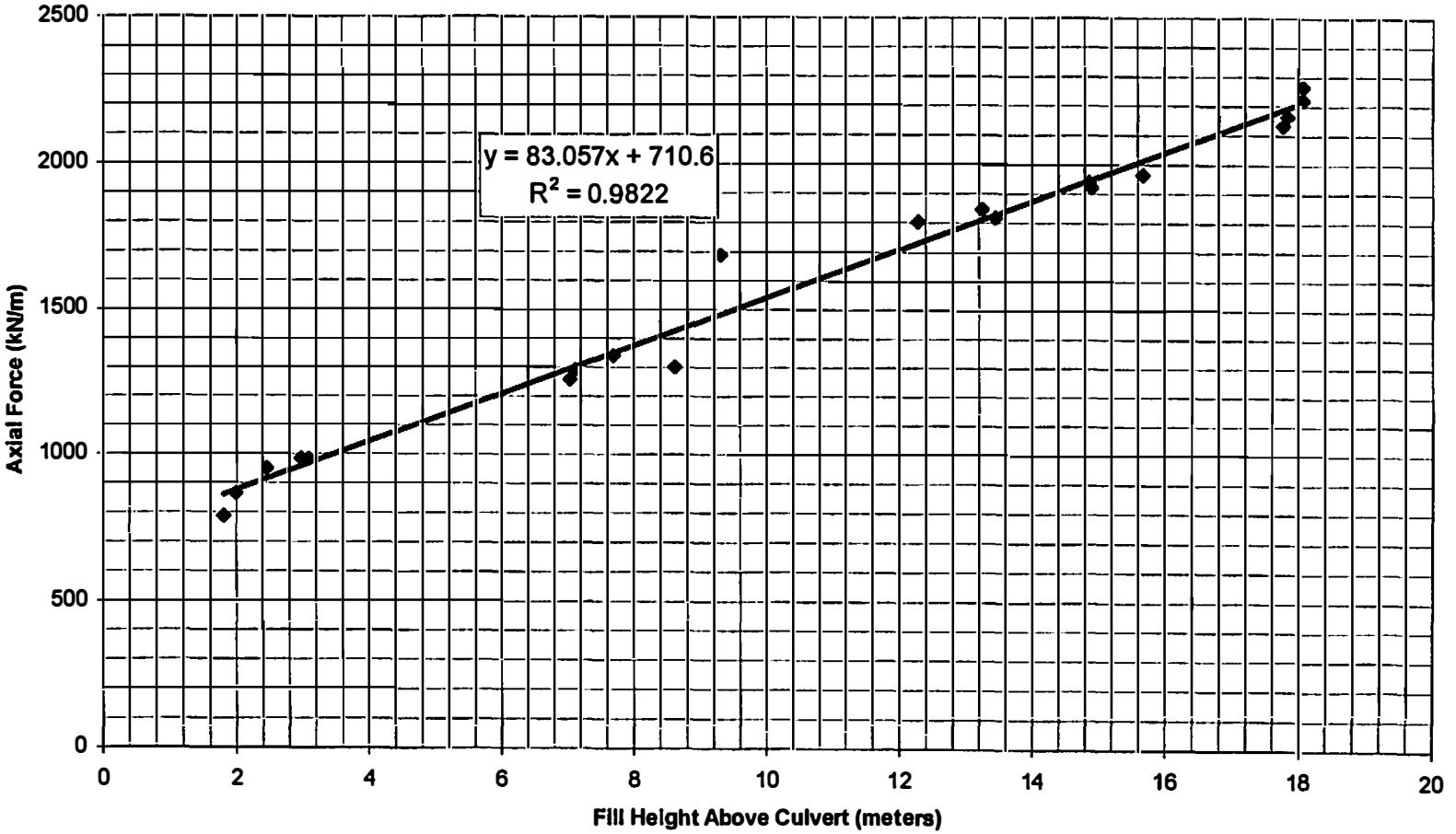
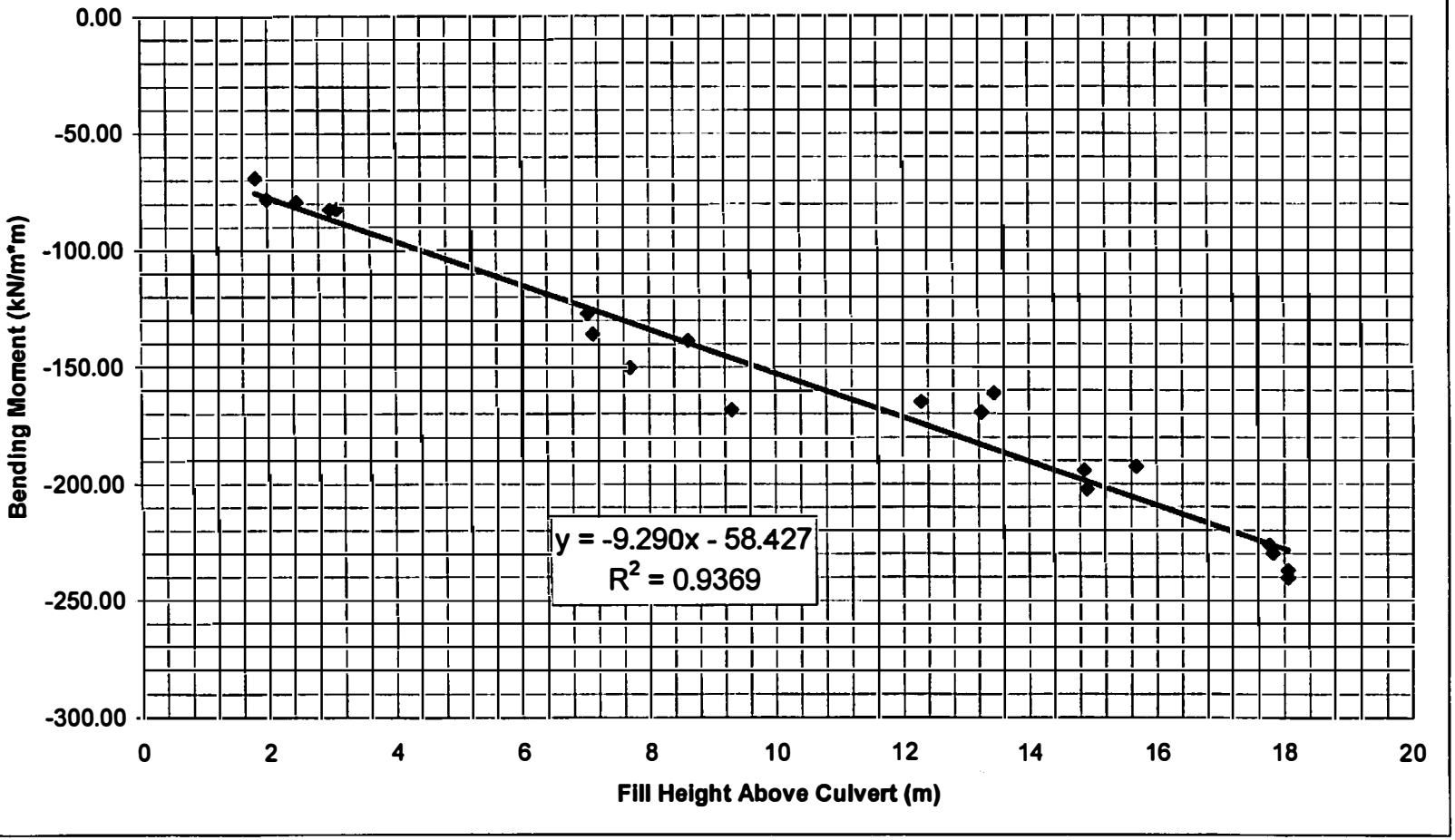


Figure B-12
Bending Moment vs Fill Height Section A3



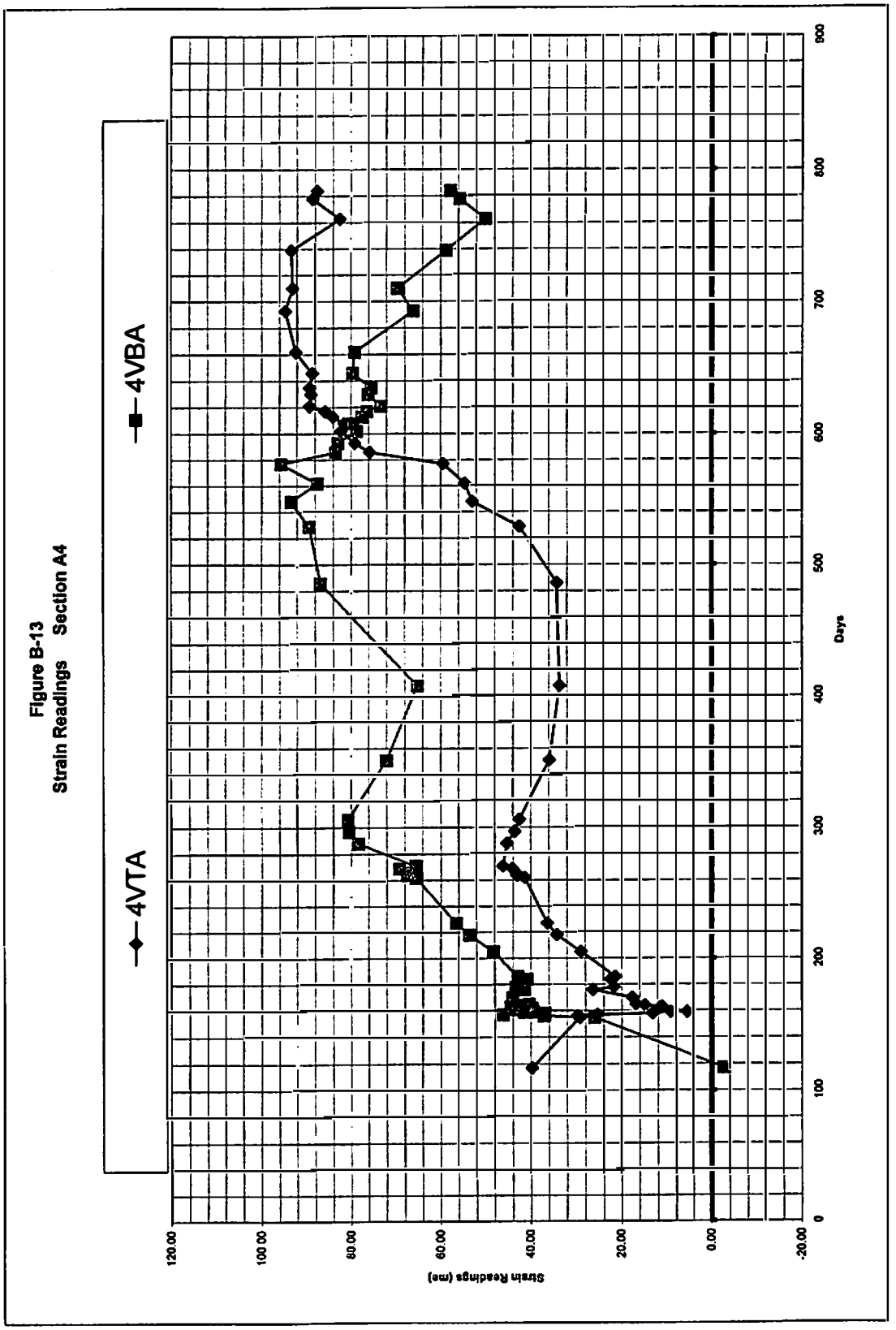


Figure B-13
Strain Readings Section A4

Figure B-14
Axial Force and Bending Moment Section A4

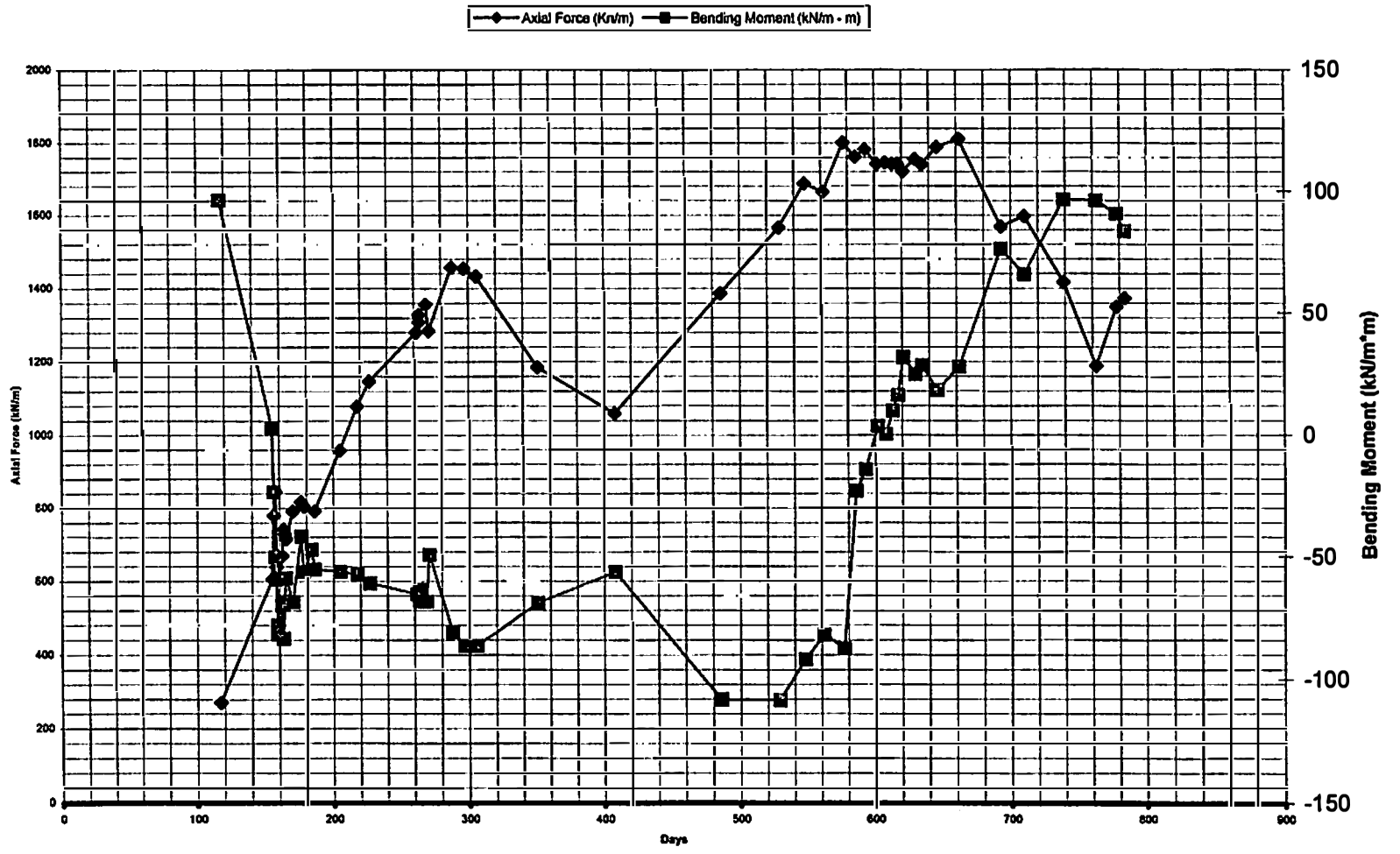


Figure B-15
Axial Force vs Fill Height Section A4

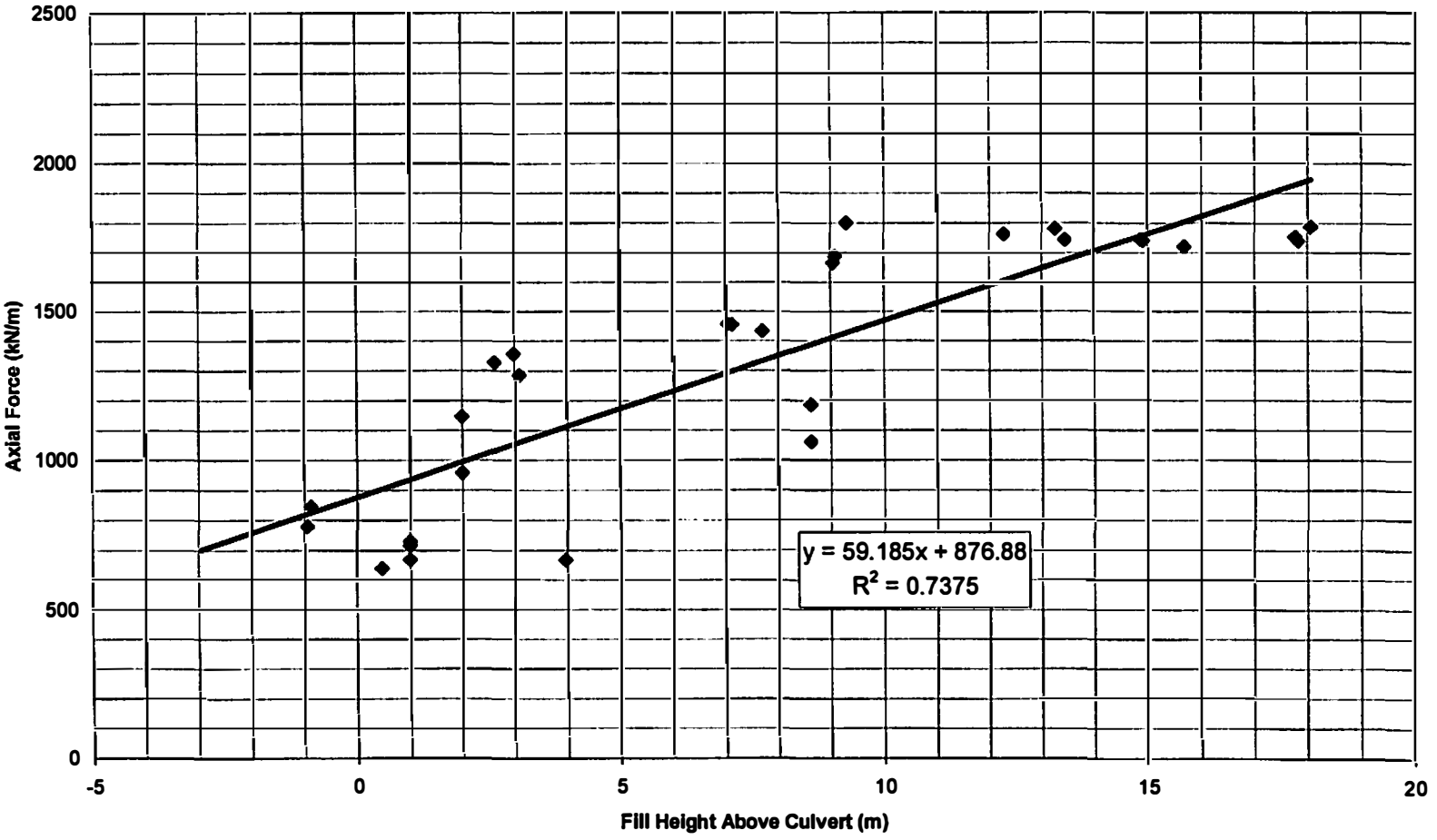
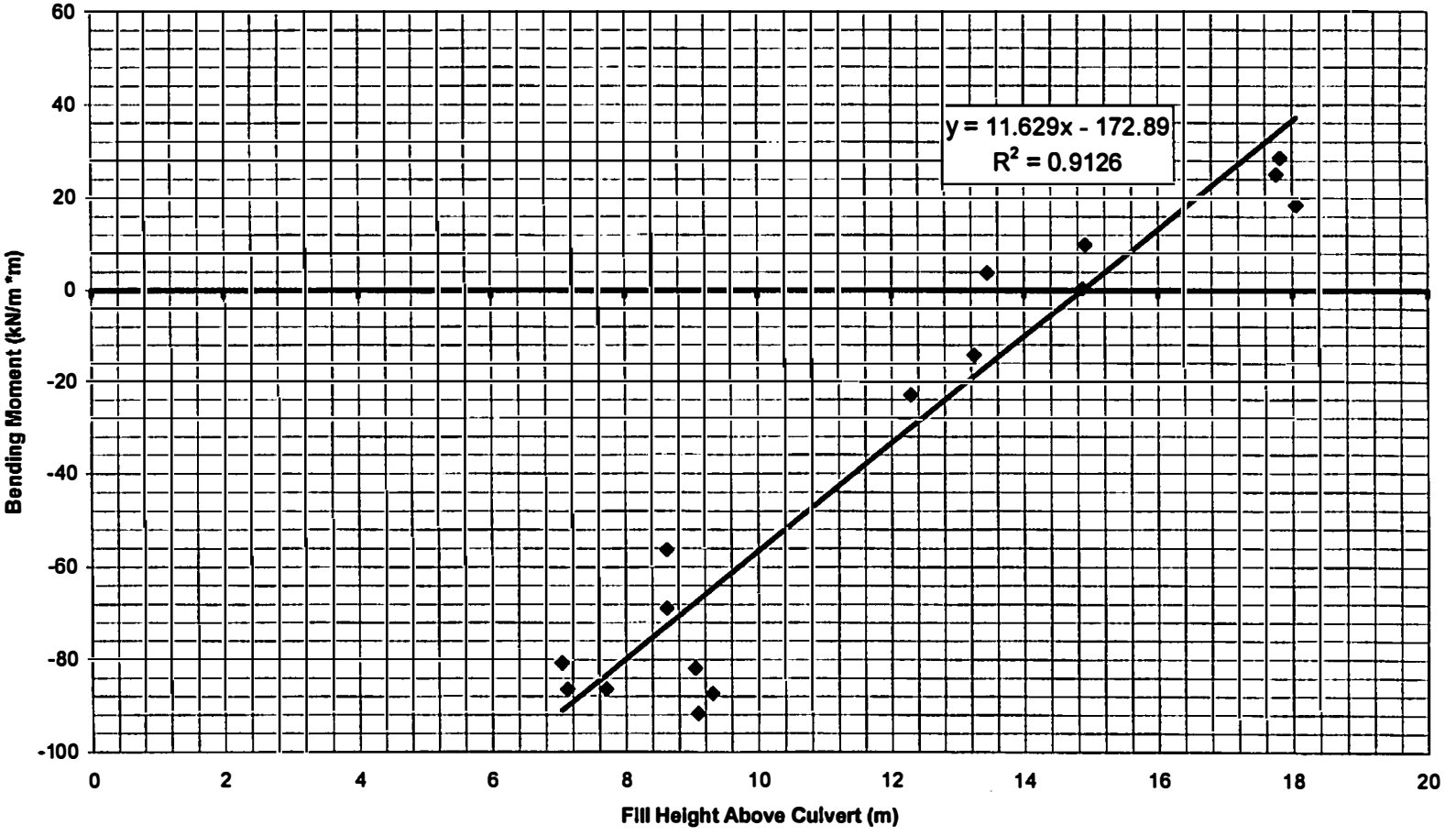


Figure B-16
Bending Moment vs. Fill Height Section A4



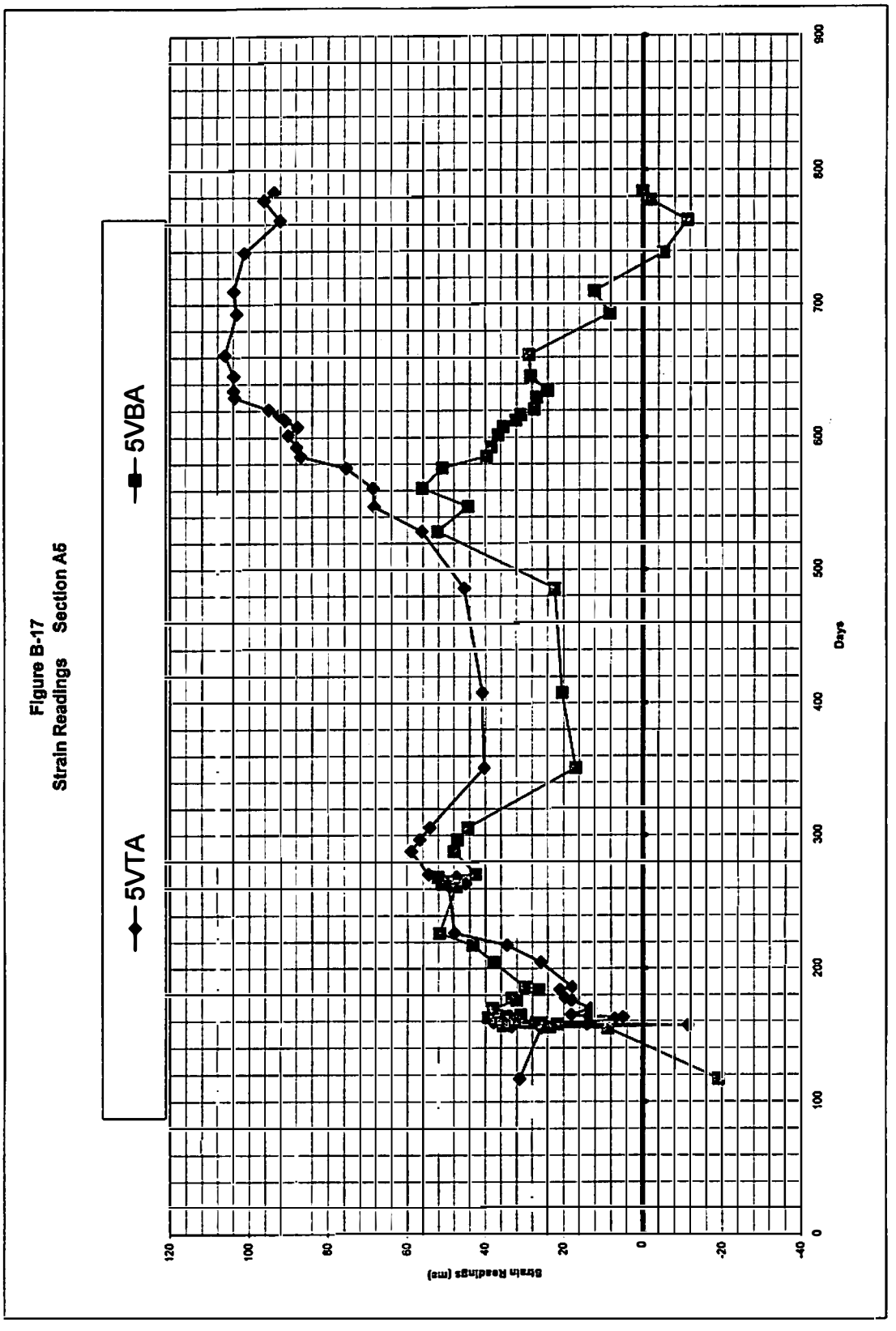


Figure B-17
Strain Readings Section A5

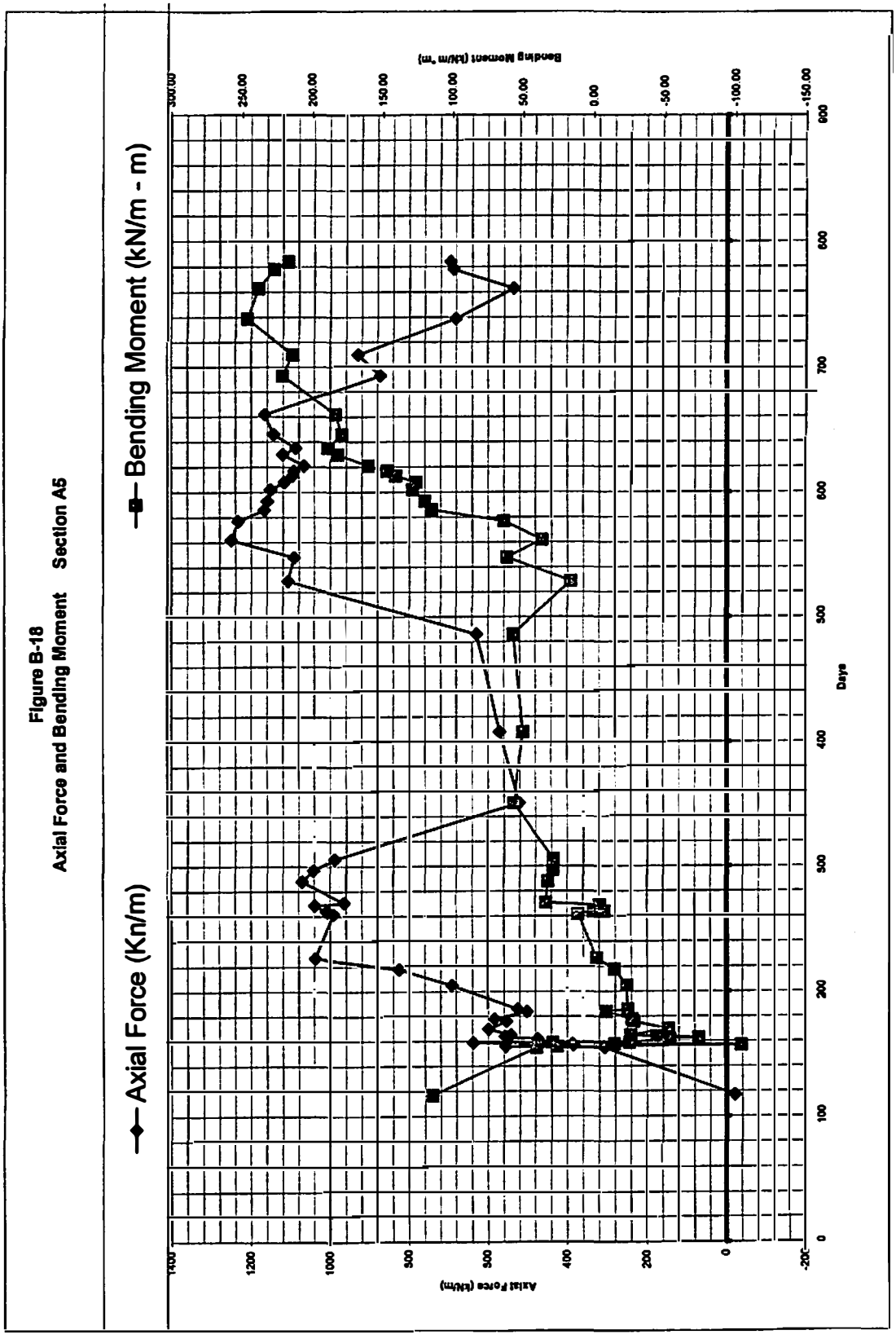


Figure B-18
Axial Force and Bending Moment Section A5

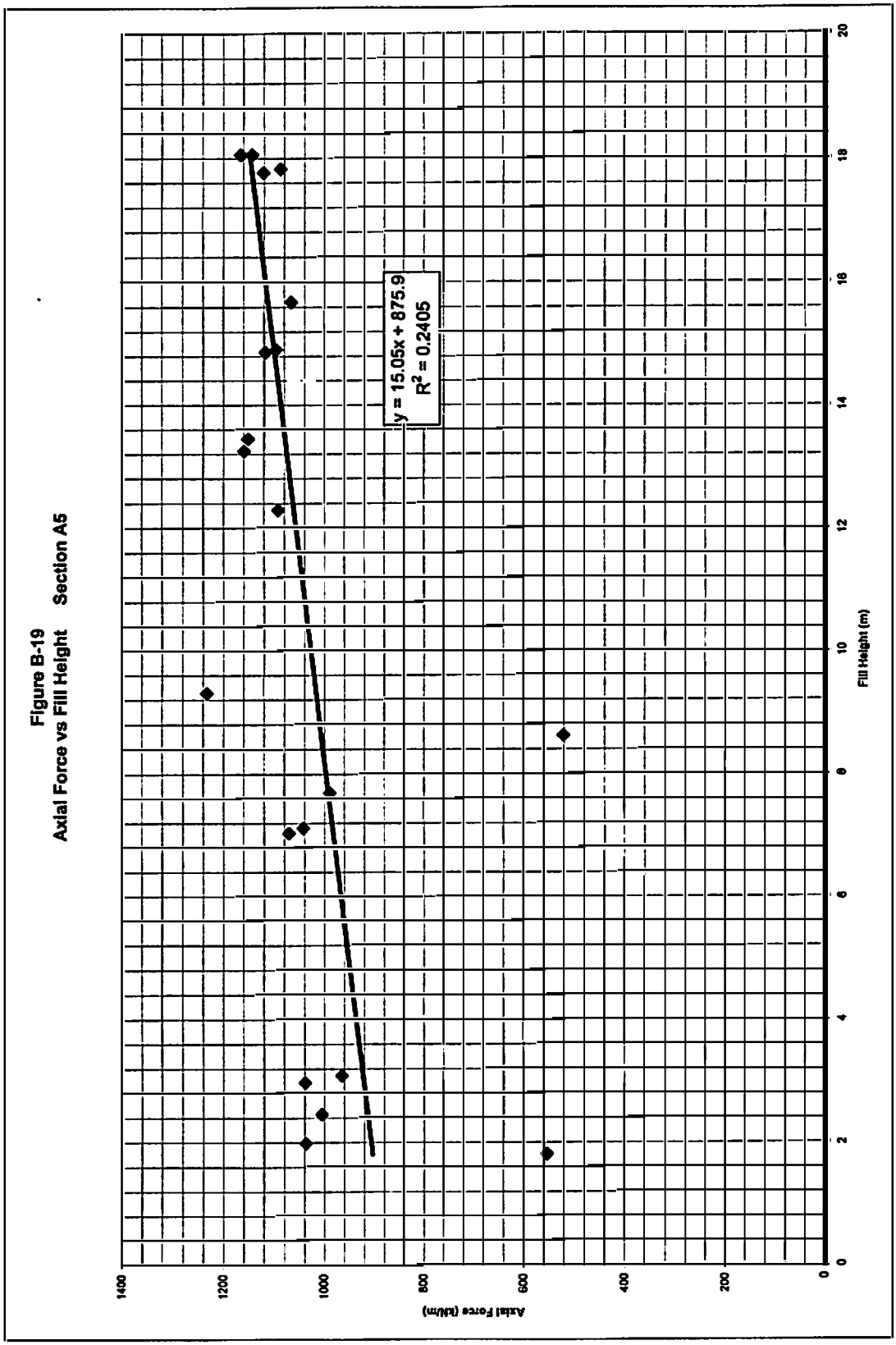
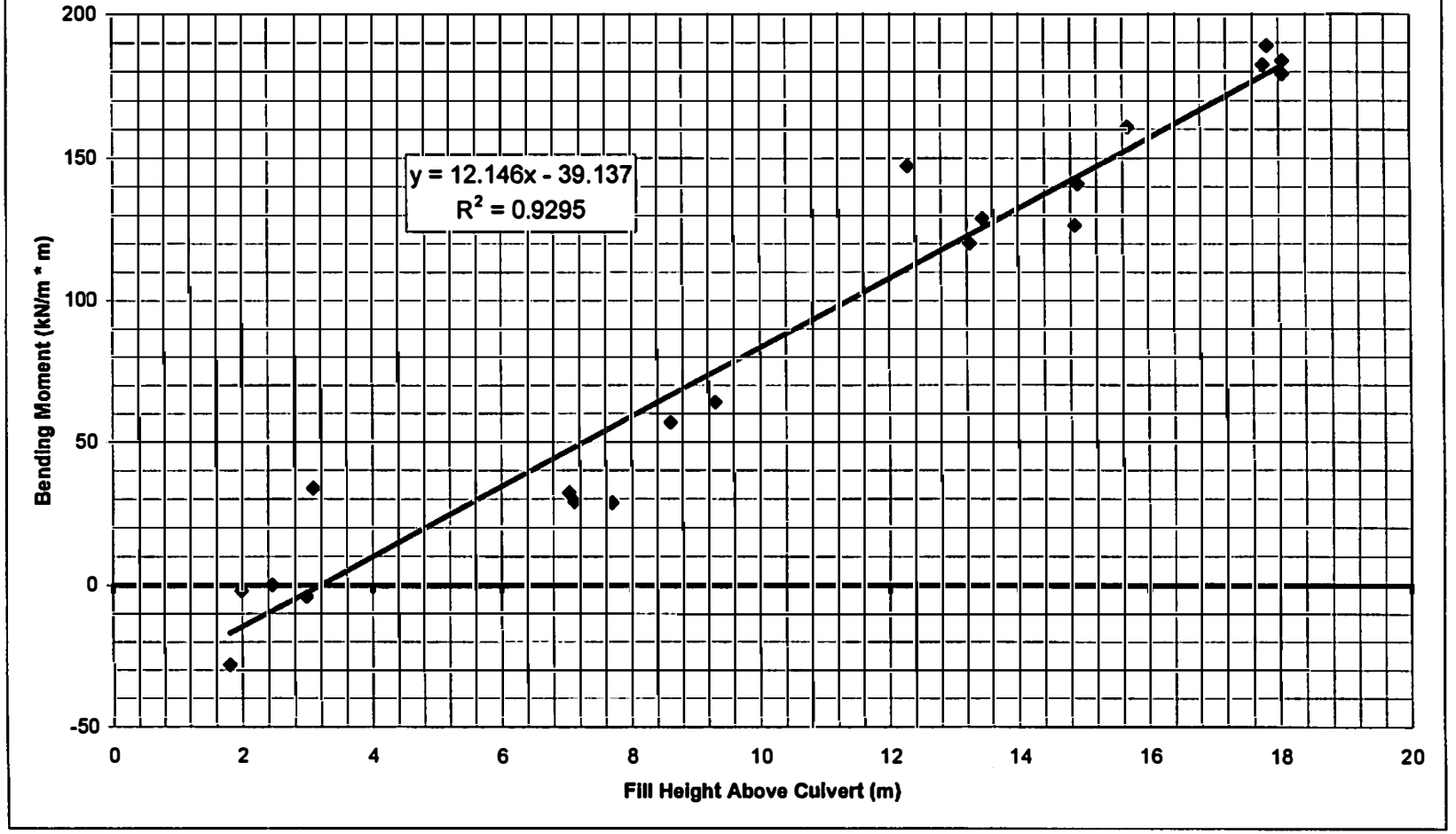


Figure B-19
Axial Force vs Fill Height Section A5

Figure B-20
Bending Moment vs Fill Height Section A5



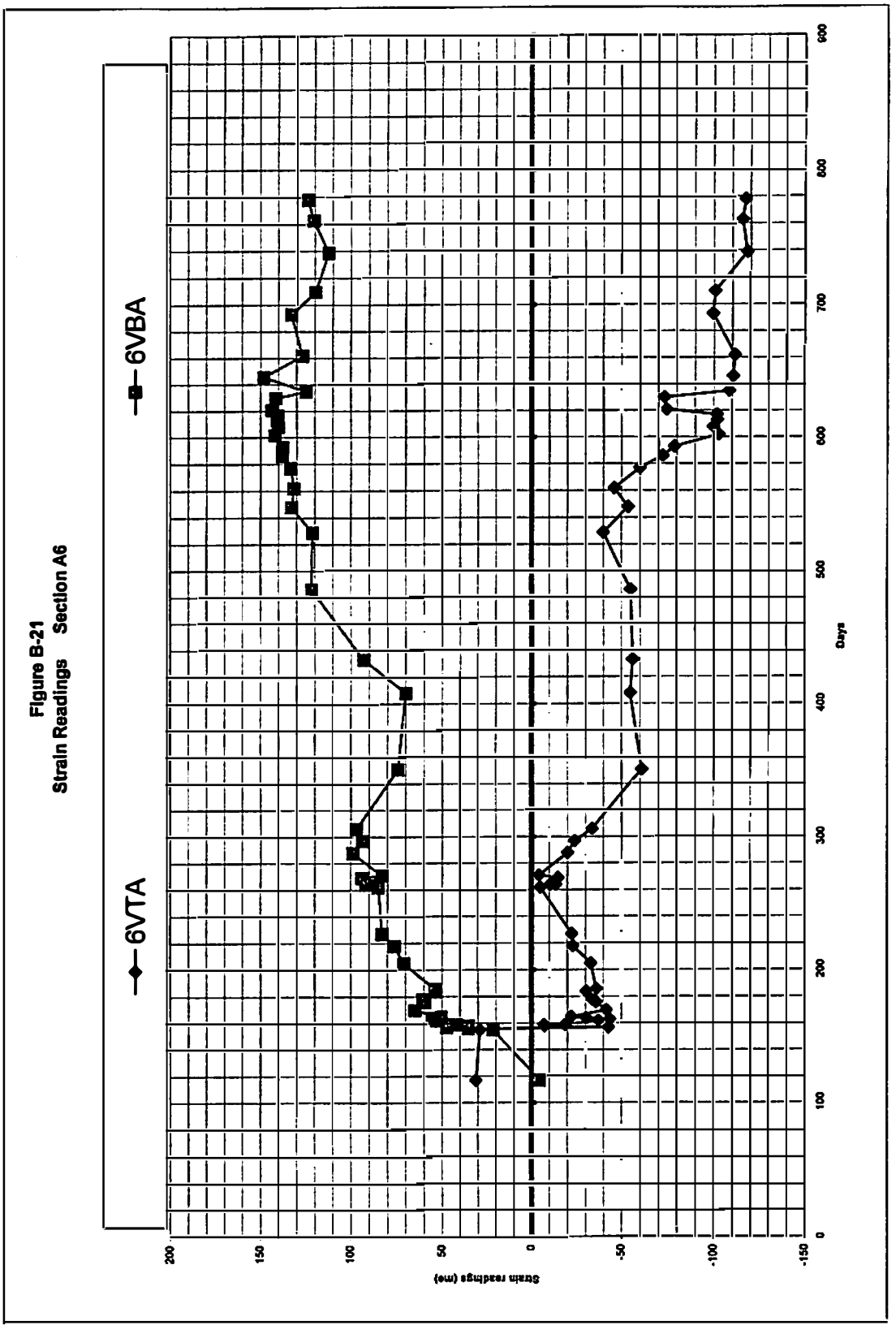


Figure B-21
Strain Readings Section A6

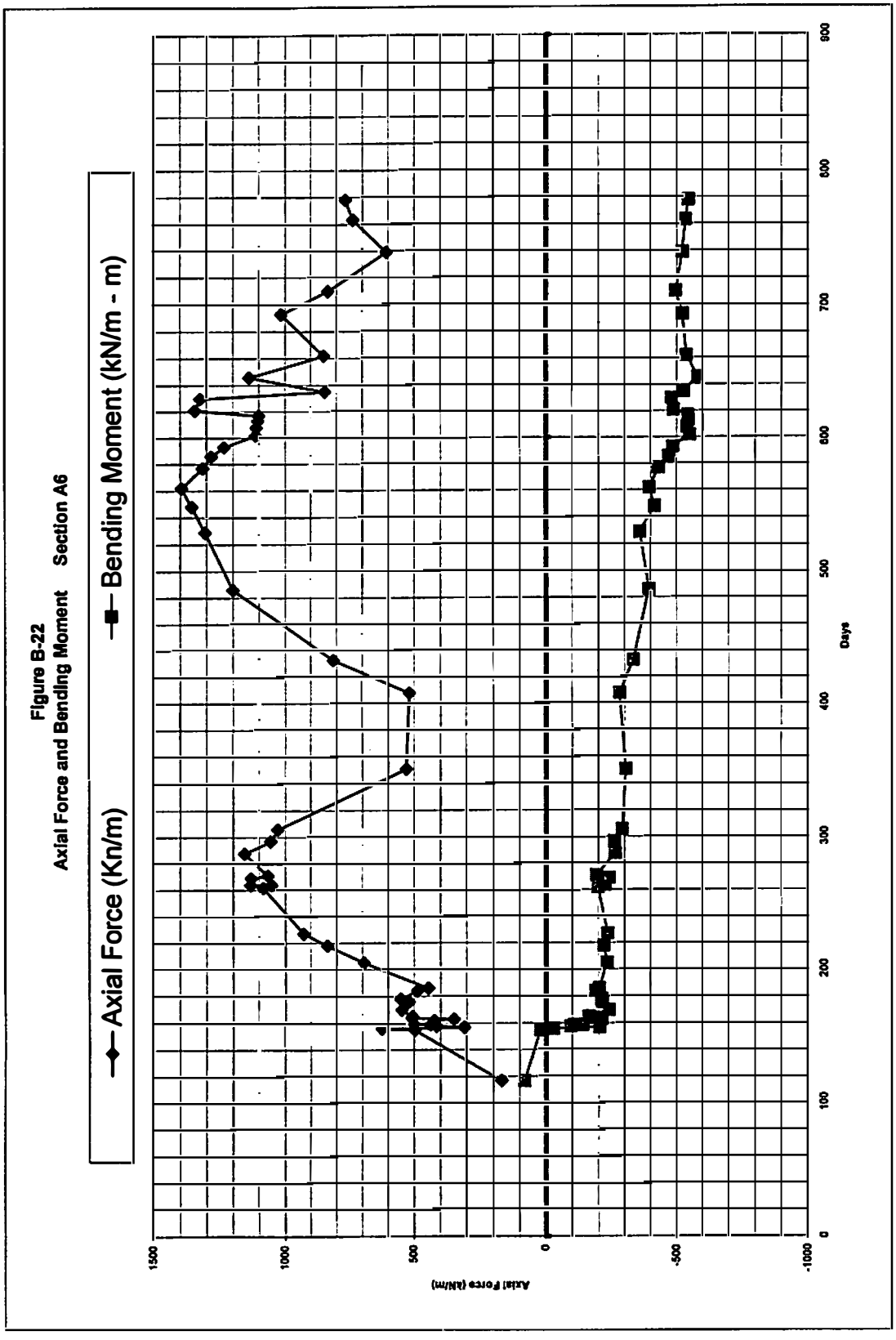


Figure B-22
Axial Force and Bending Moment Section A6

Figure B-23
Axial Force vs Fill Height Section A6

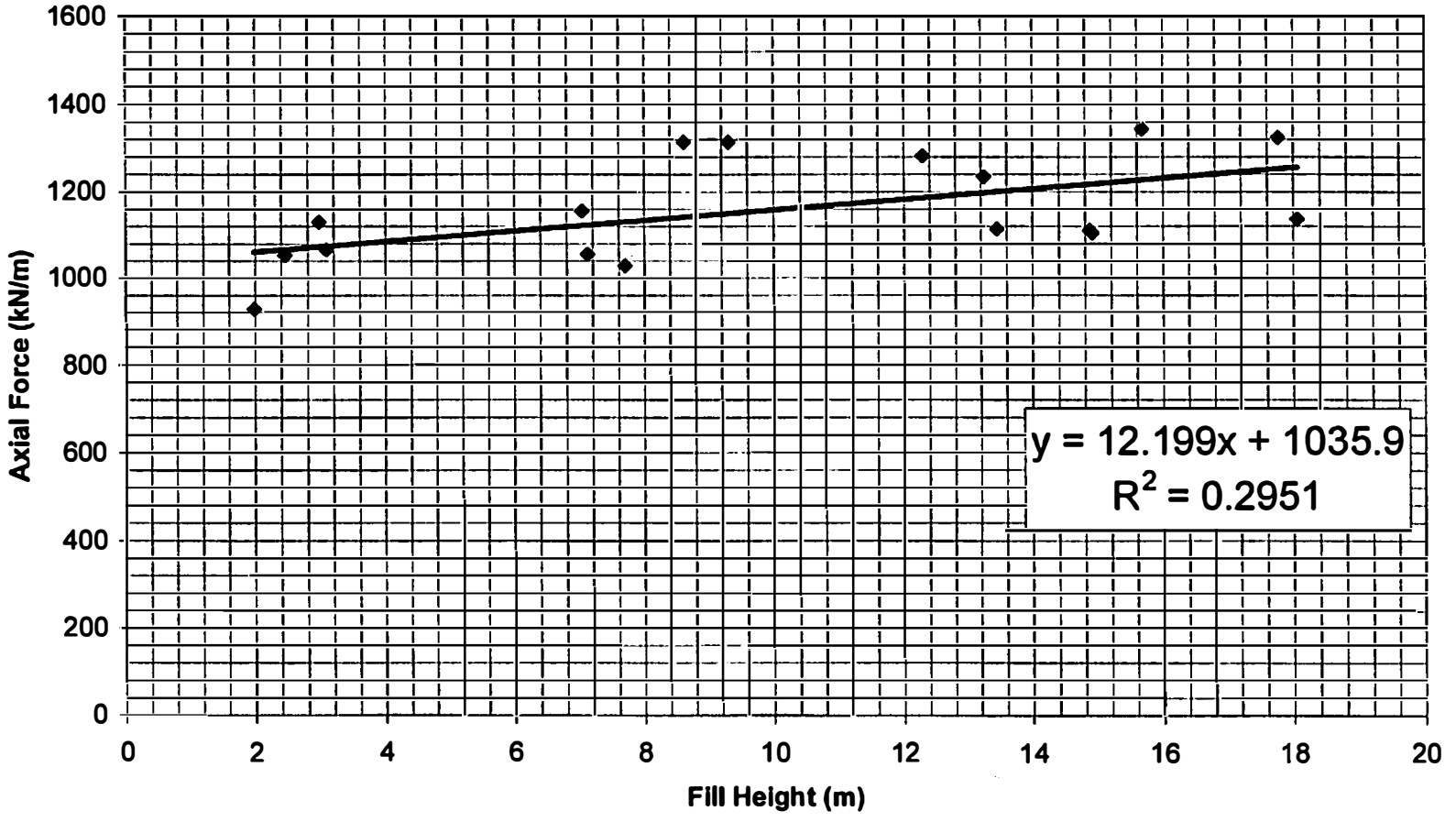
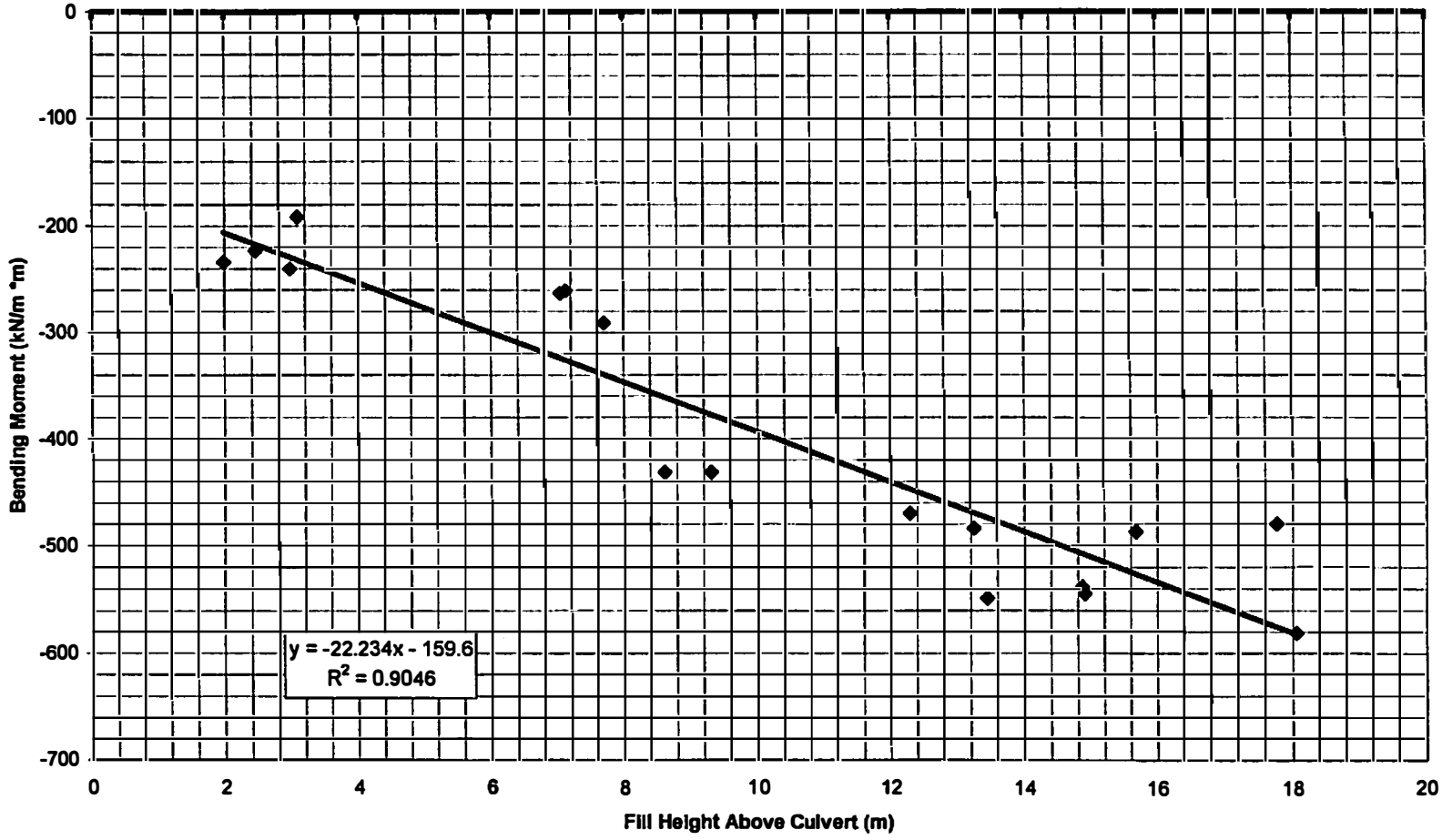


Figure B-24
Bending Moment vs Fill Height Section A6



Appendix C
Section B Strain Gage Results

Figure C-1
Strain Readings 1B

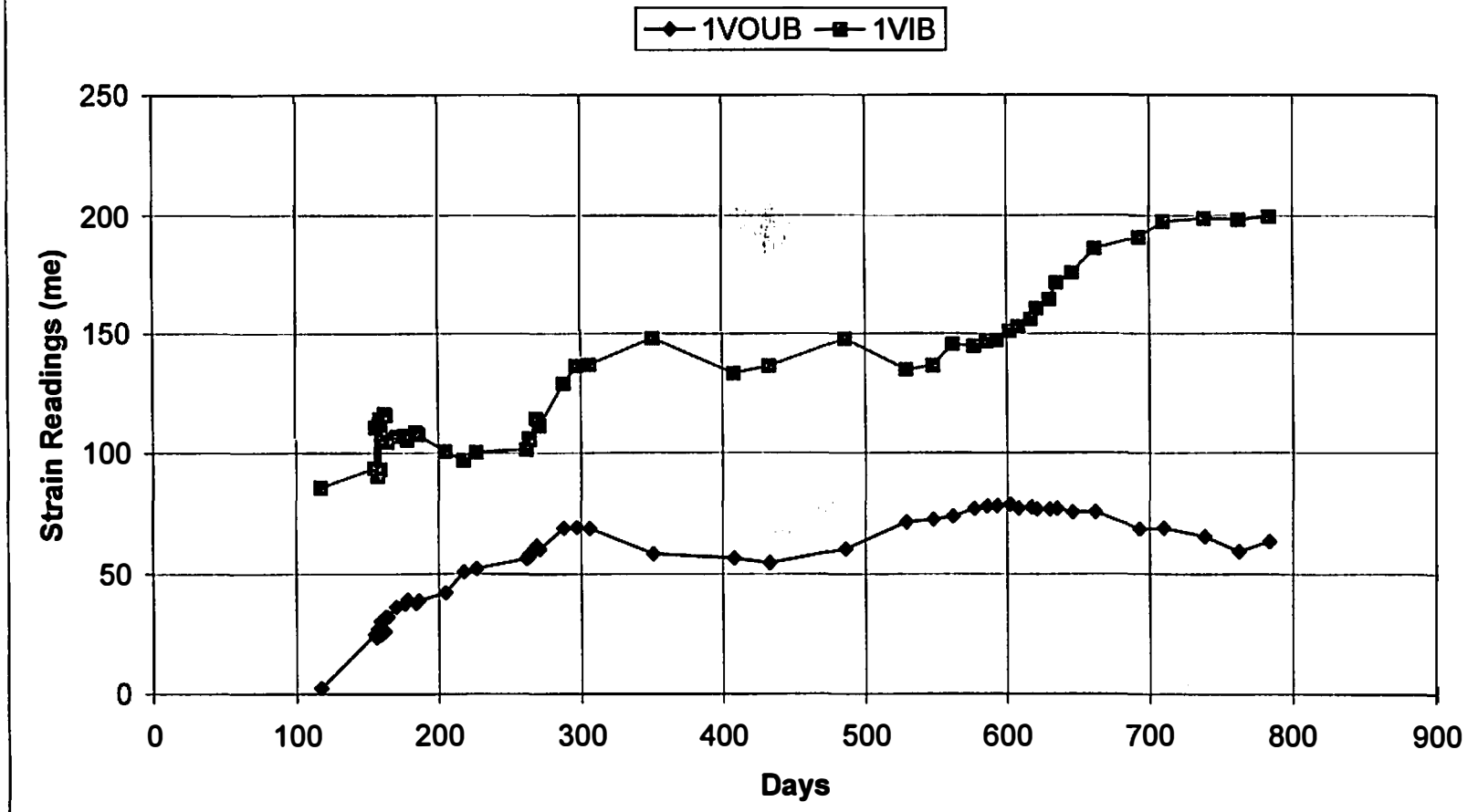


Figure C-2
Axial Force and Bending Moment Section B1

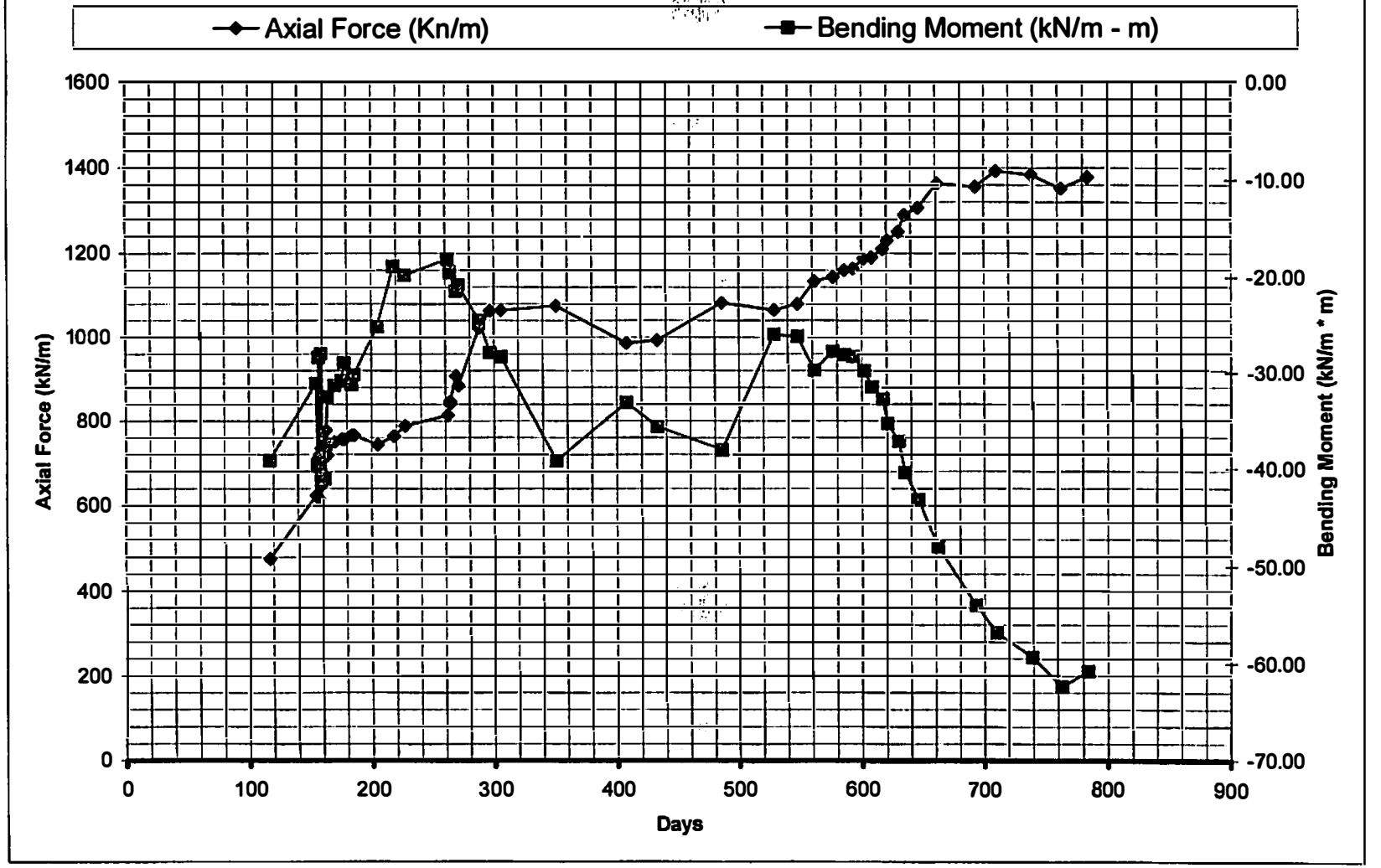


Figure C-3
Section B1 Axial Force vs Fill Height

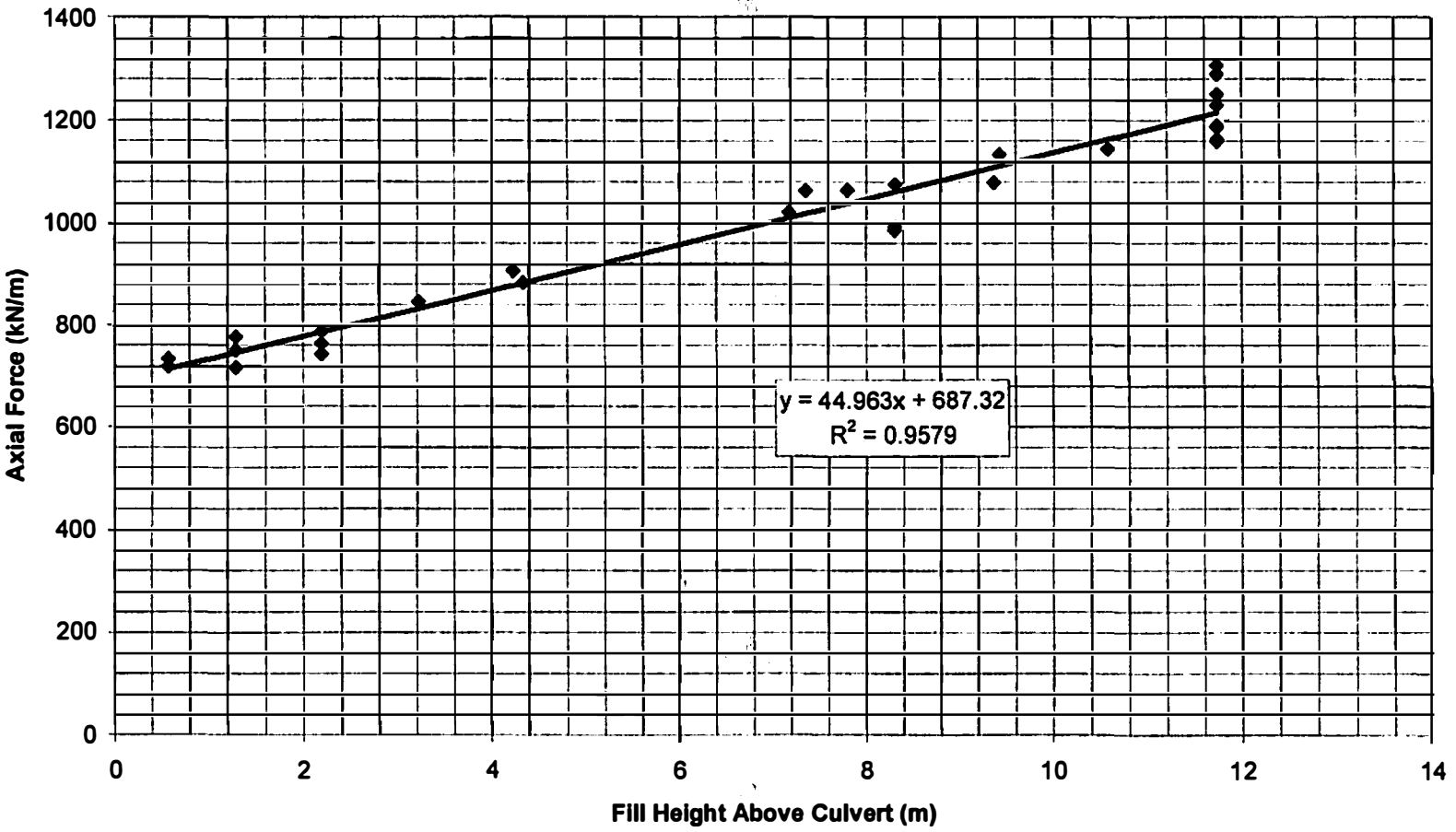


Figure C-4
Section B1 Bending Moment vs Fill Height

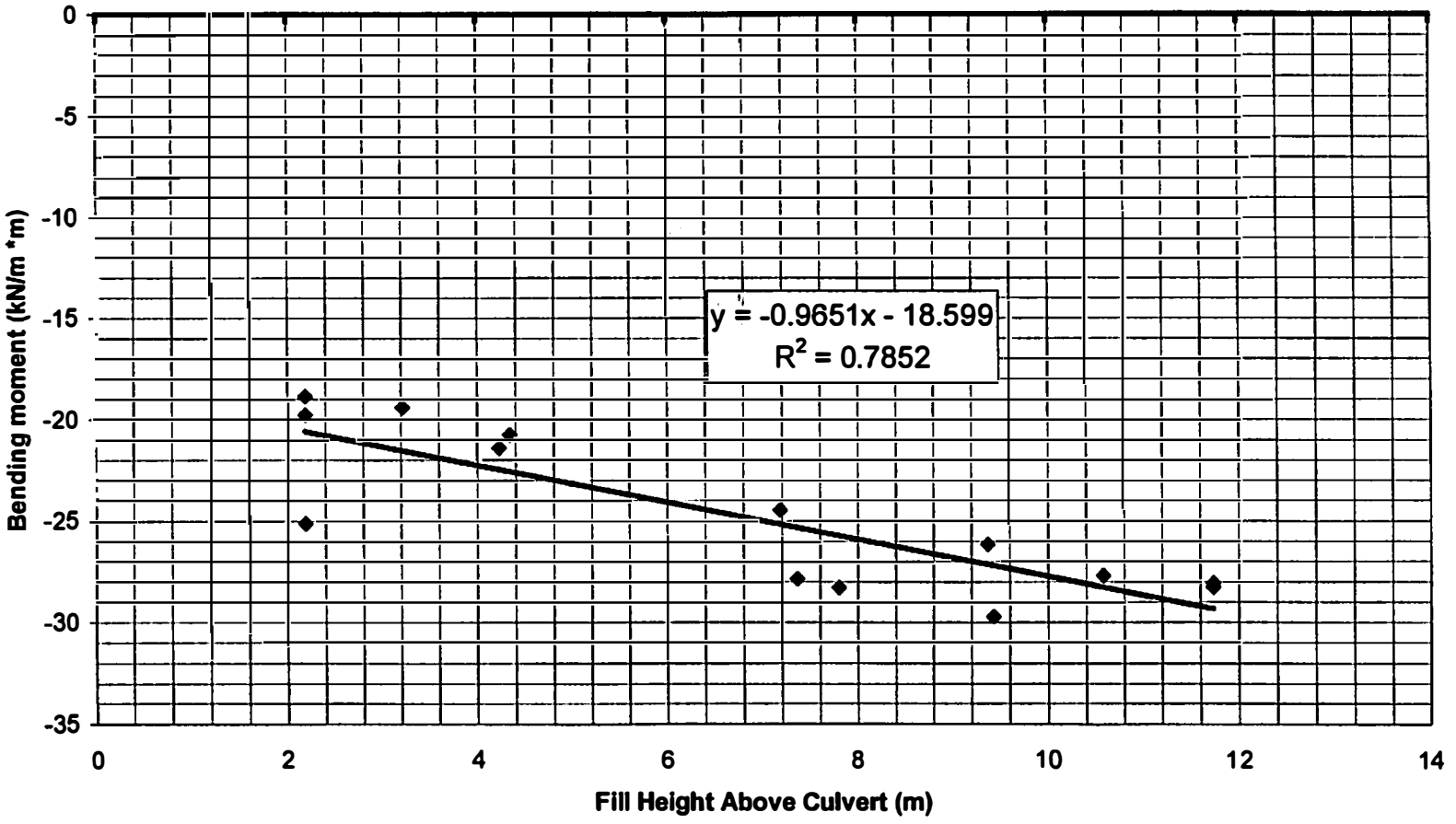


Figure C-5
Strain Readings 2B

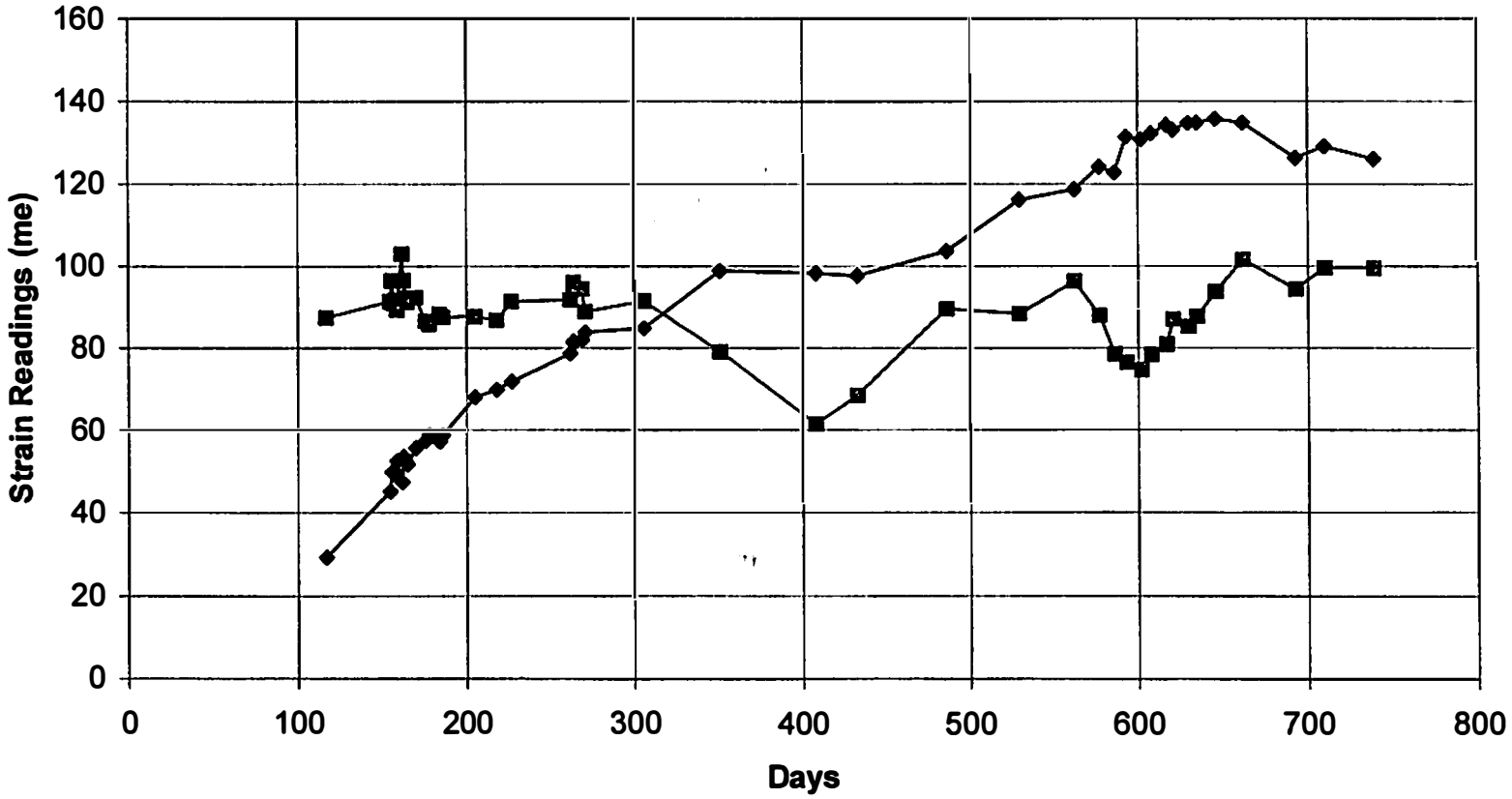


Figure C-6
Axial Force and Bending Moment Section B2

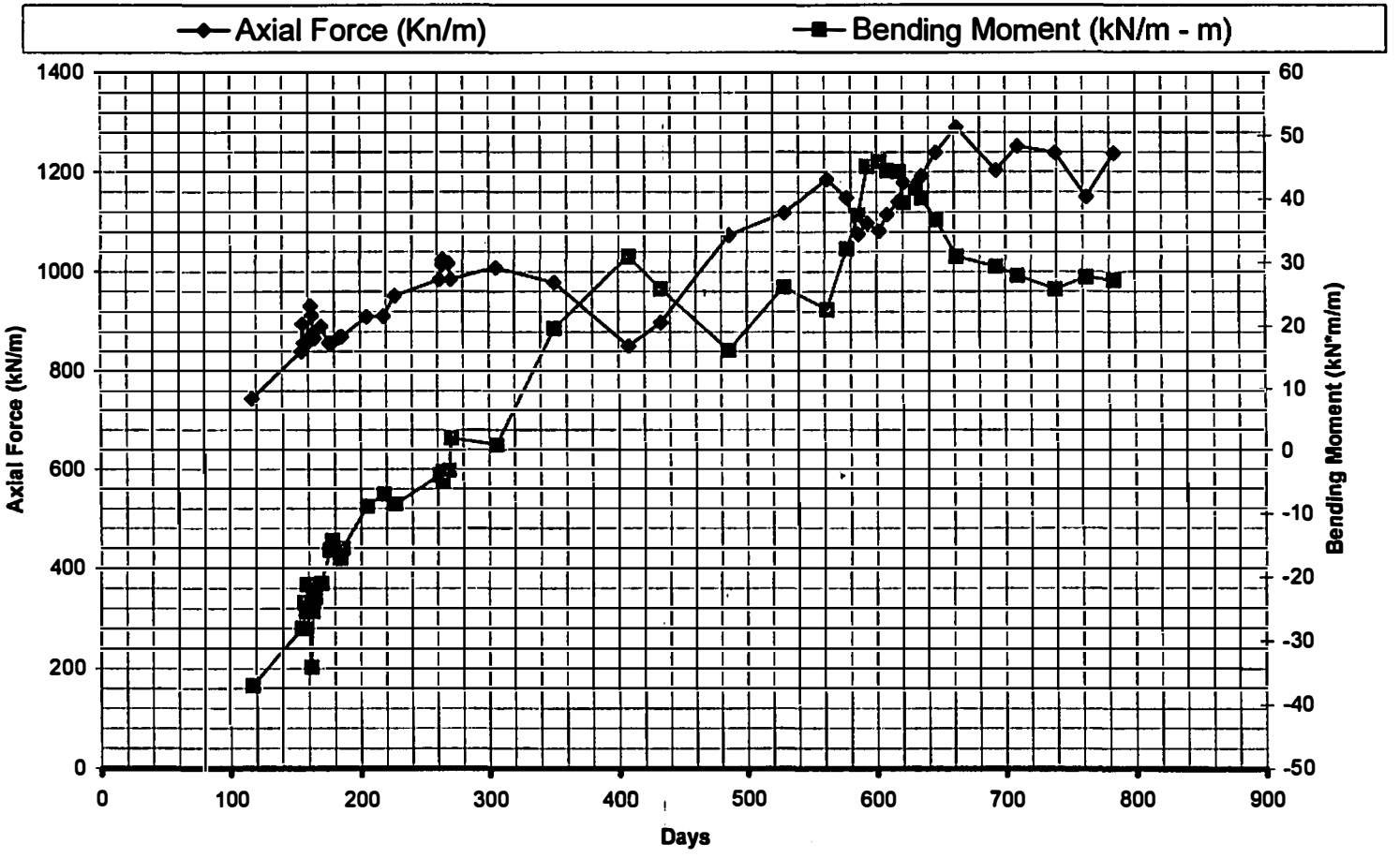


Figure C-7
Section B2 Axial Force vs Fill Height

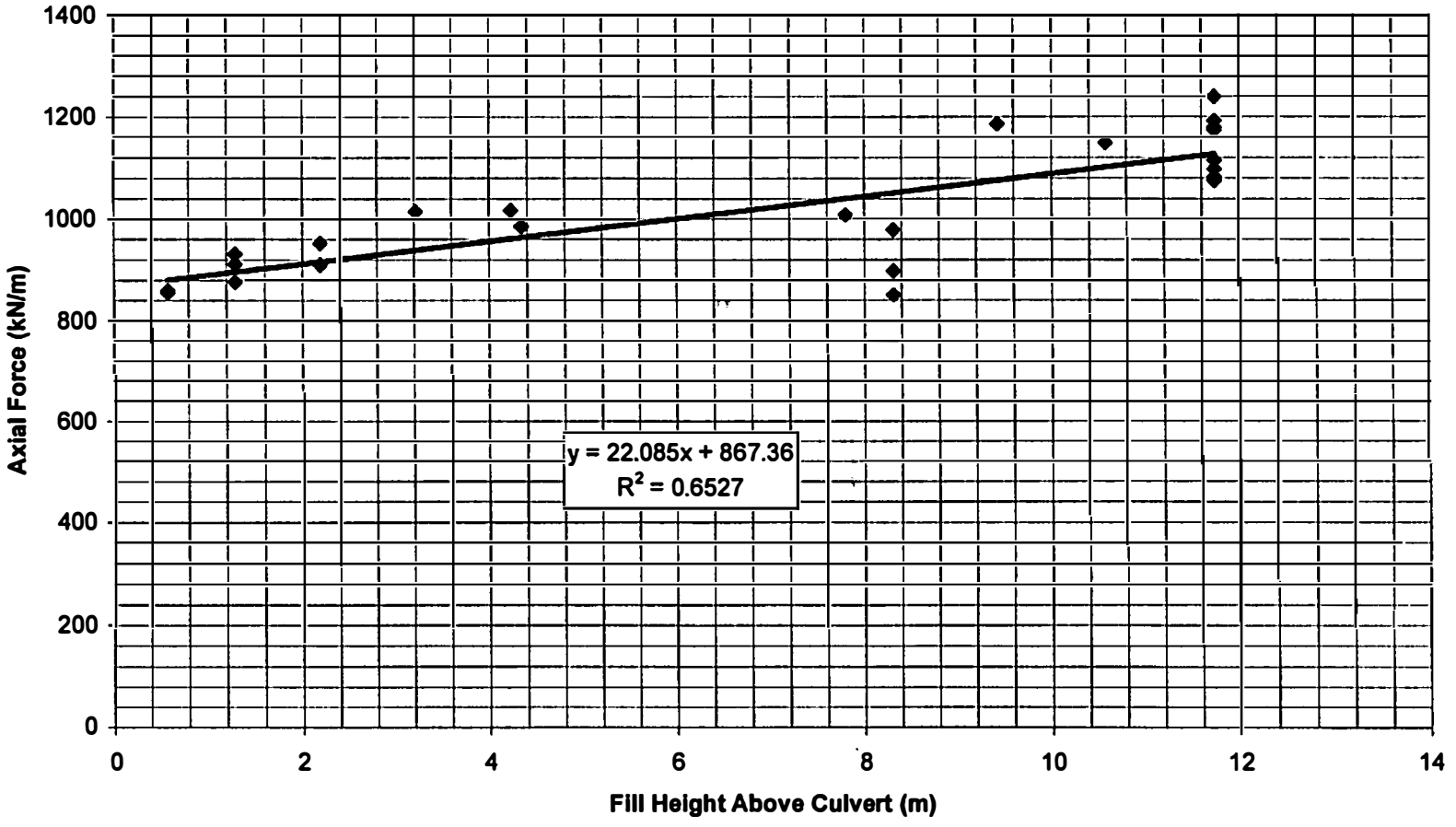


Figure C-8
Section B2 Bending Moment vs Fill Height

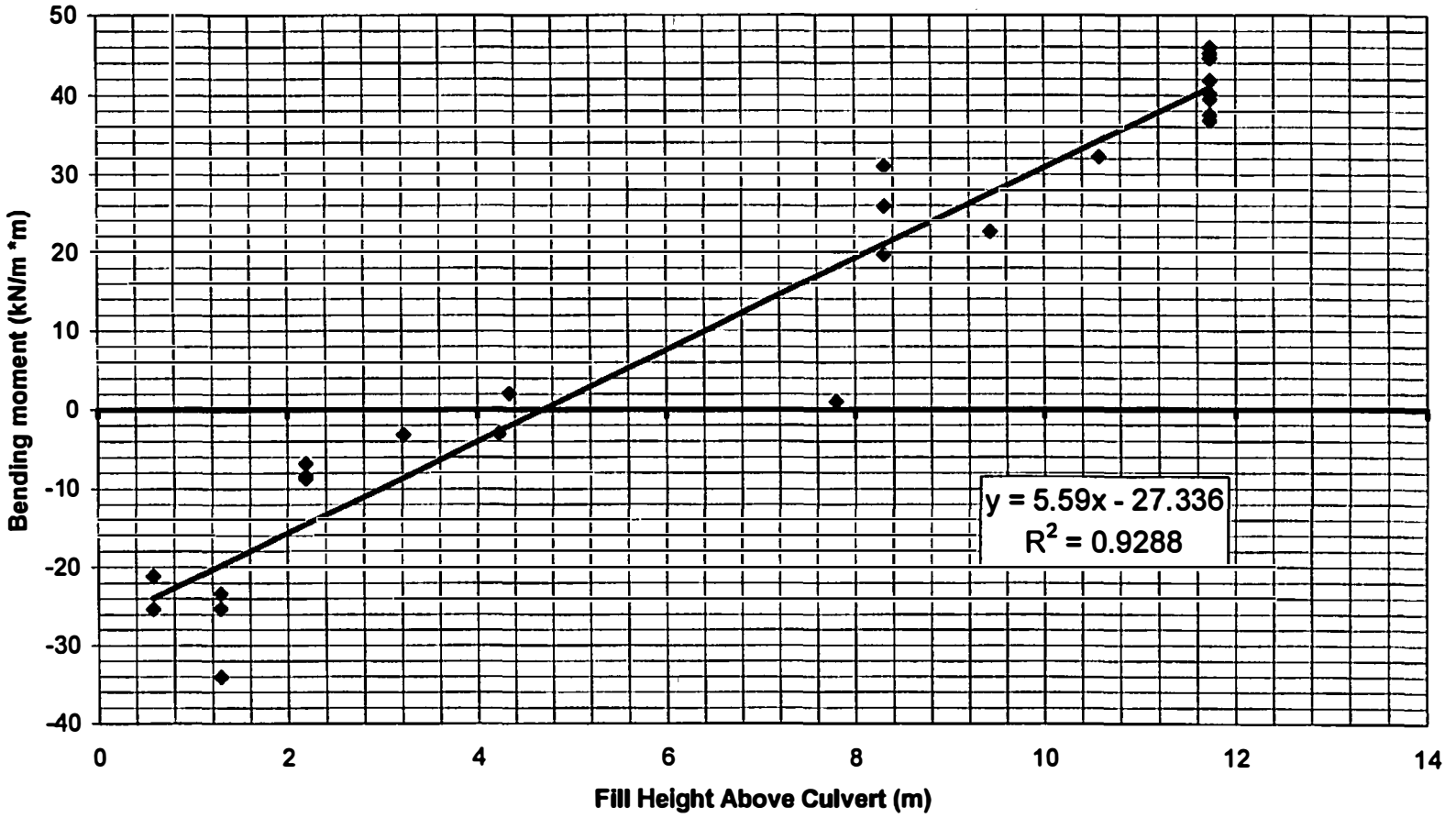


Figure C-9
Strain Readings 3B

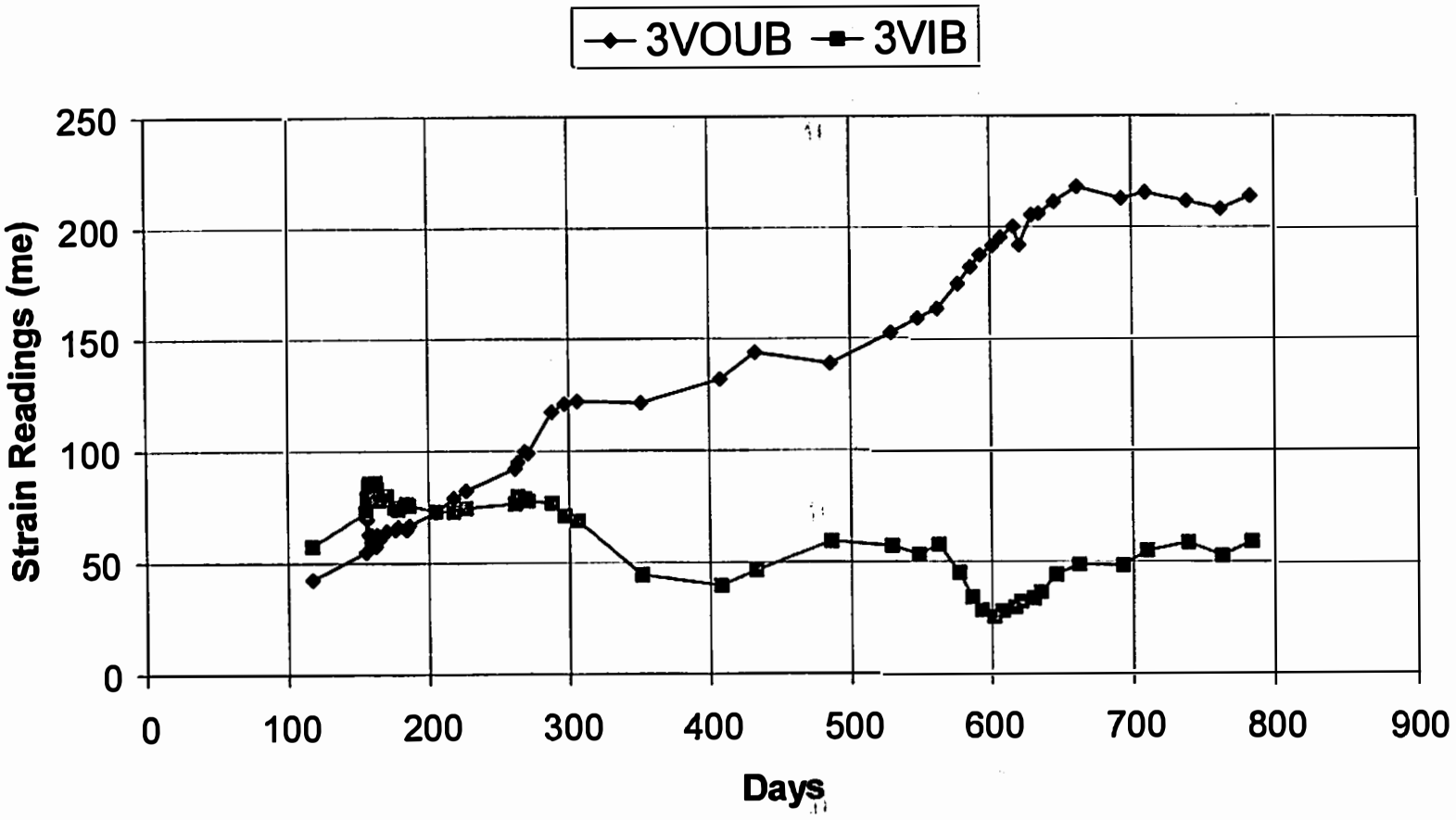


Figure C-10
Axial Force and Bending Moment Section 3B

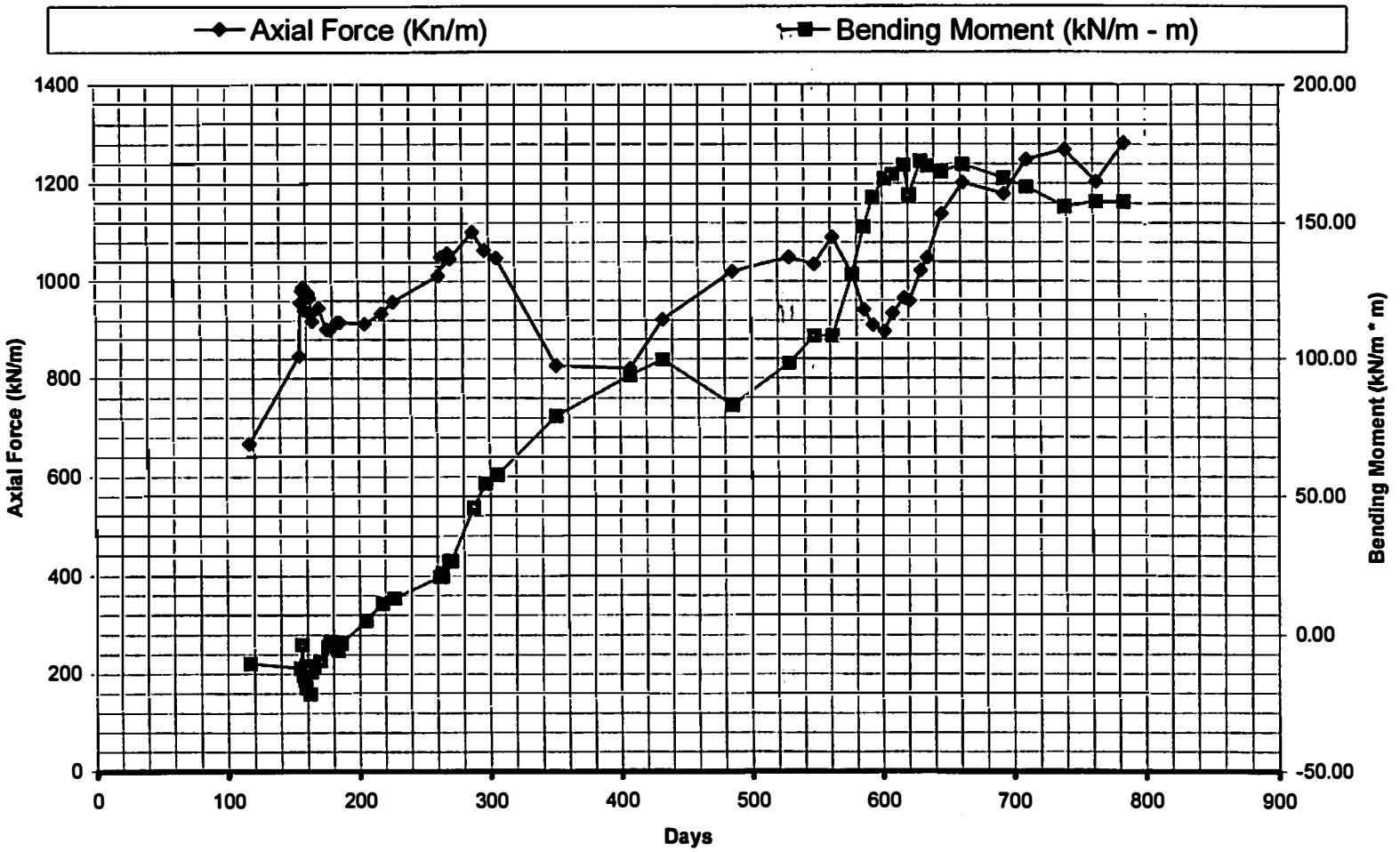


Figure C-11
Section B3 Axial Force vs Fill Height

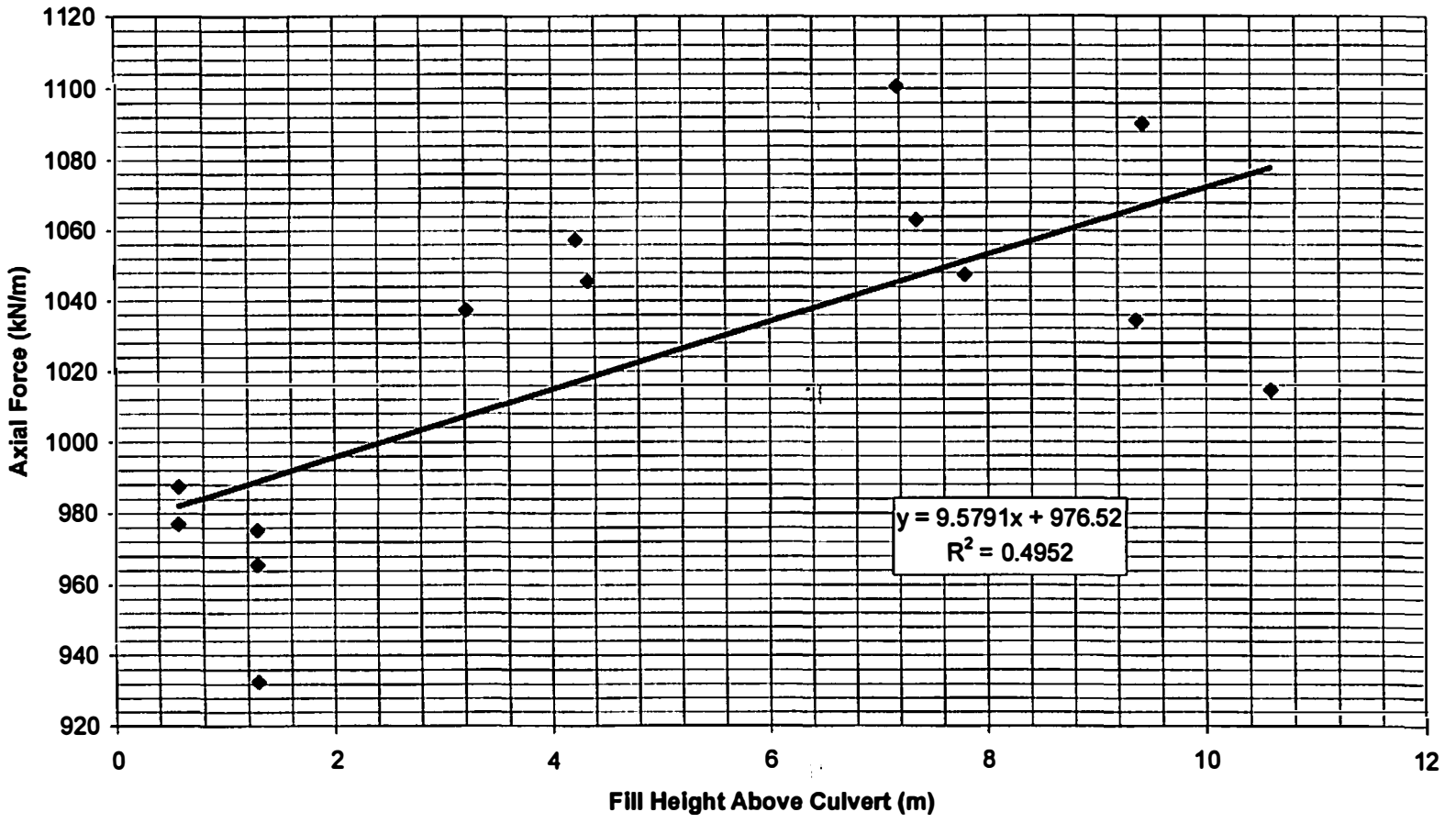


Figure C-12
Section B3 Bending Moment vs Fill Height

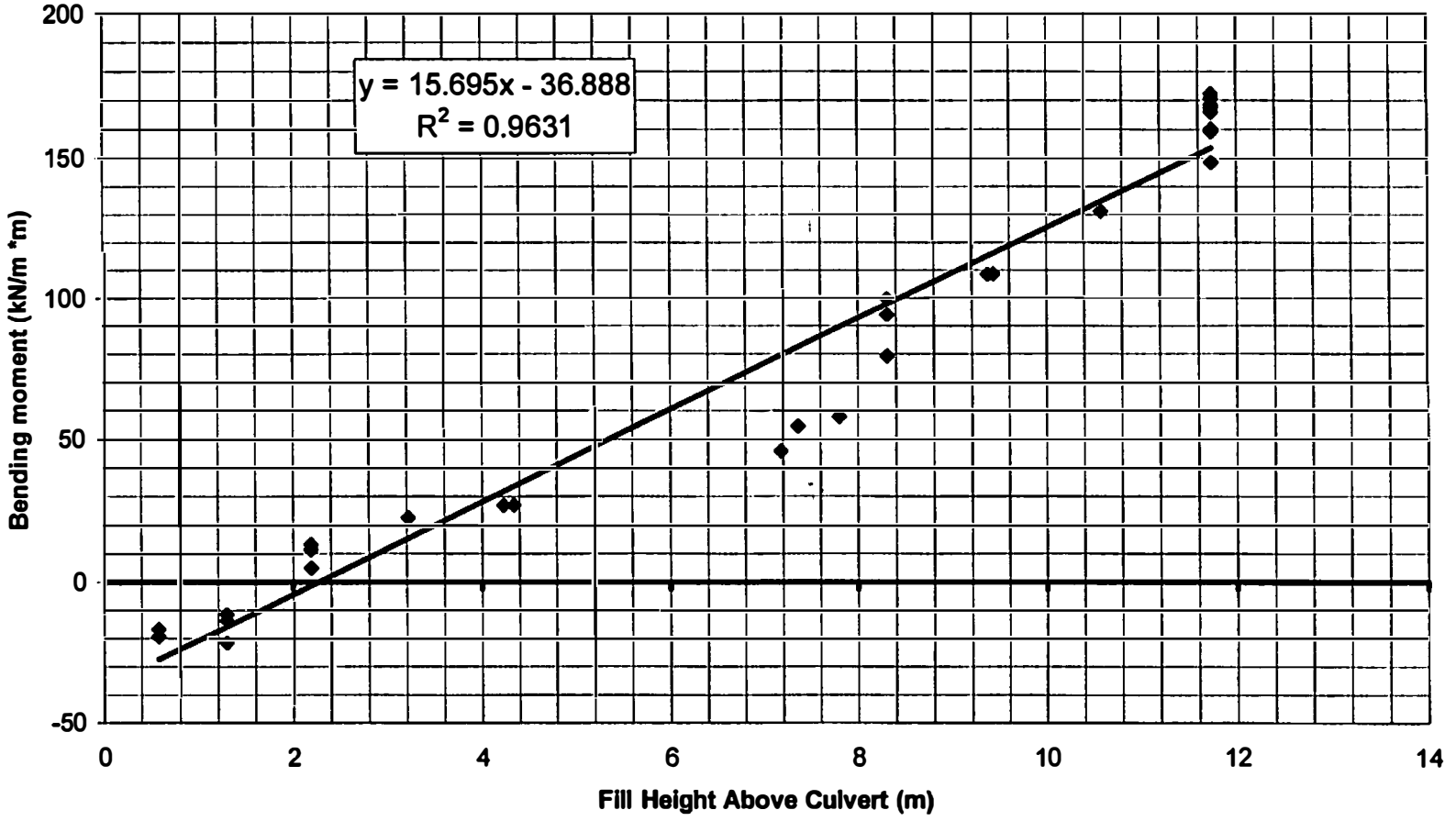


Figure C-13
Strain Readings B4

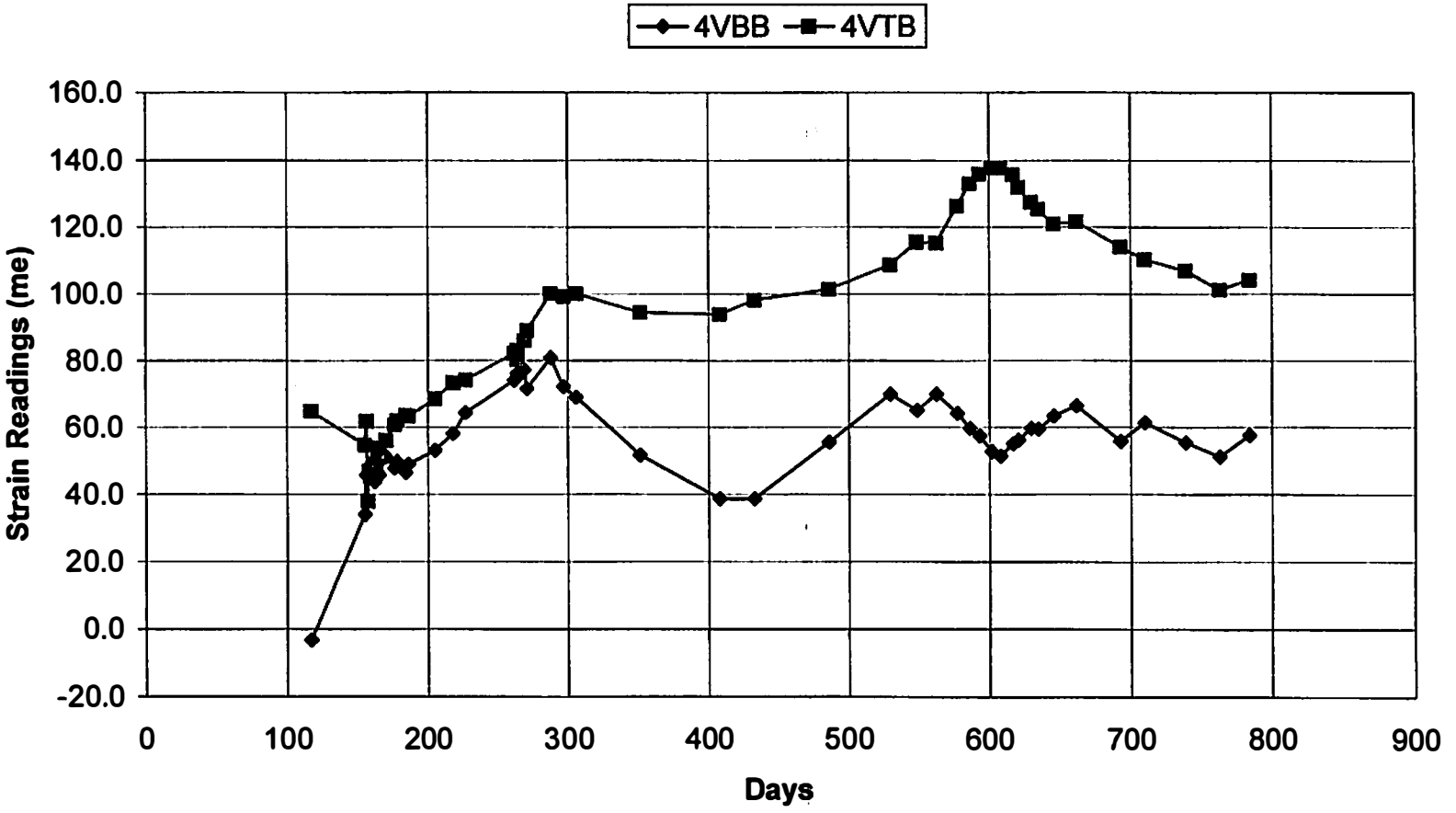


Figure C-14
Axial Force and Bending Moment Section B4

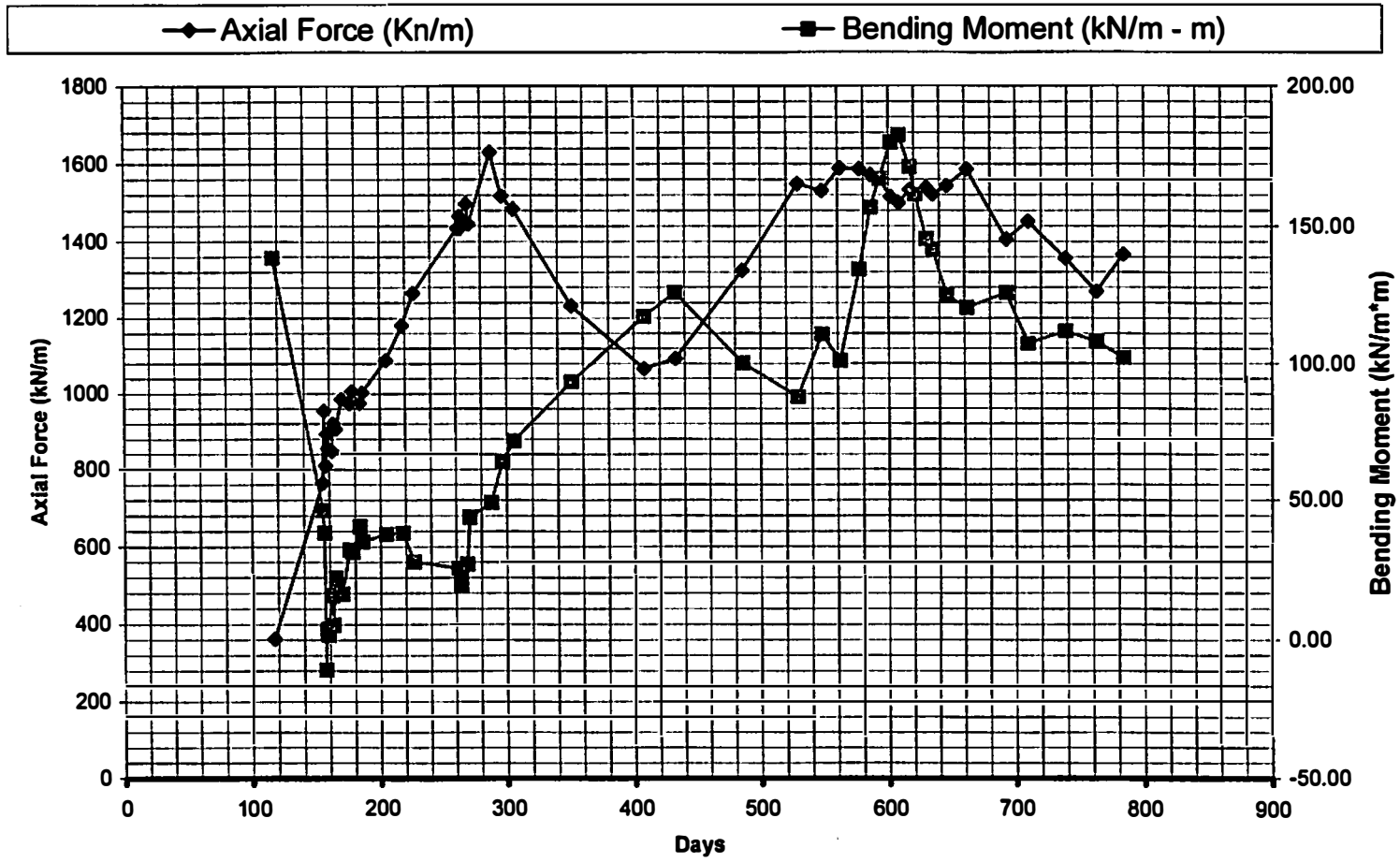


Figure C-15
Axial Force vs Fill Height Section B4

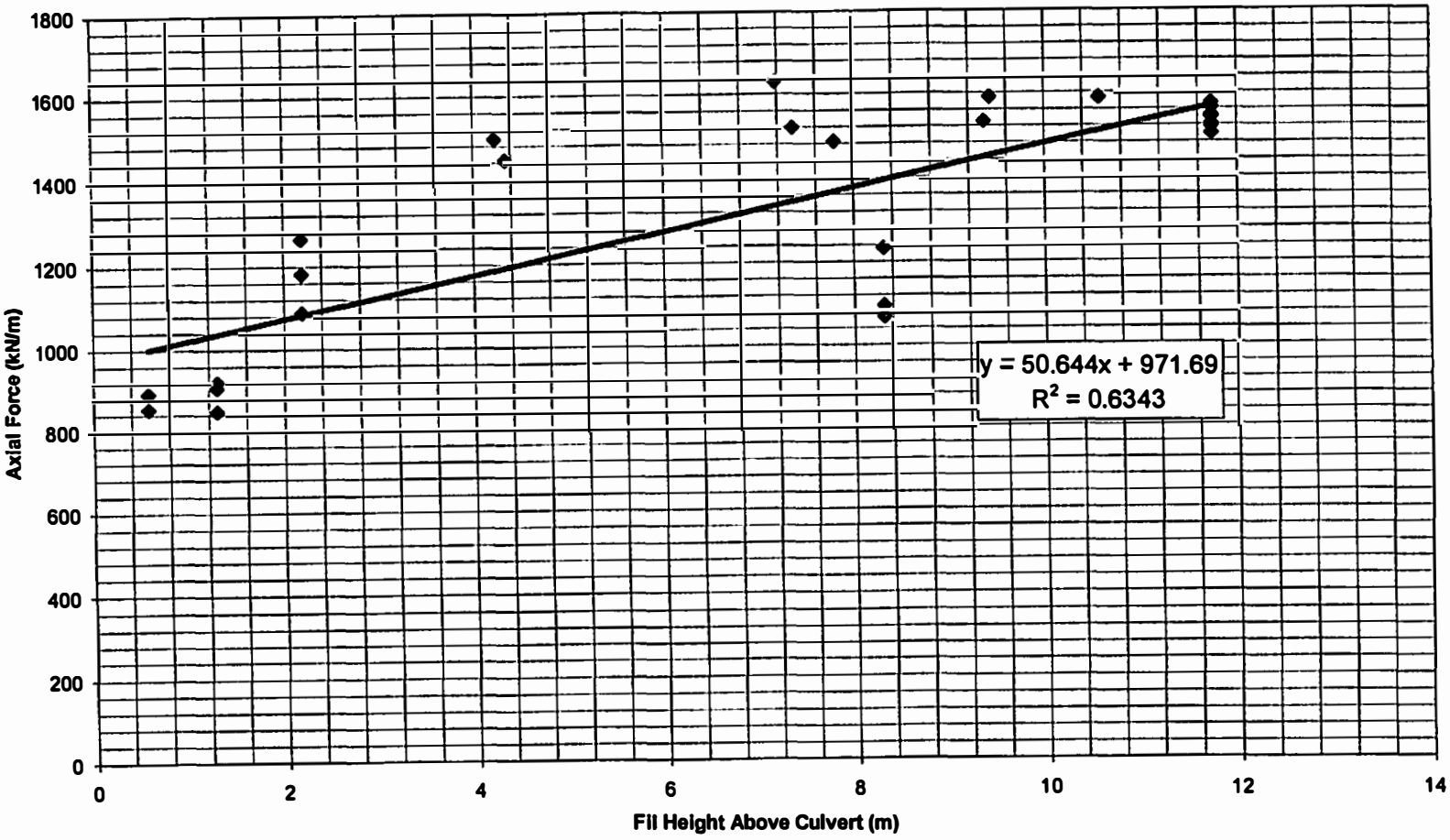


Figure C-16
Bending Moments vs Fill Height Section B4

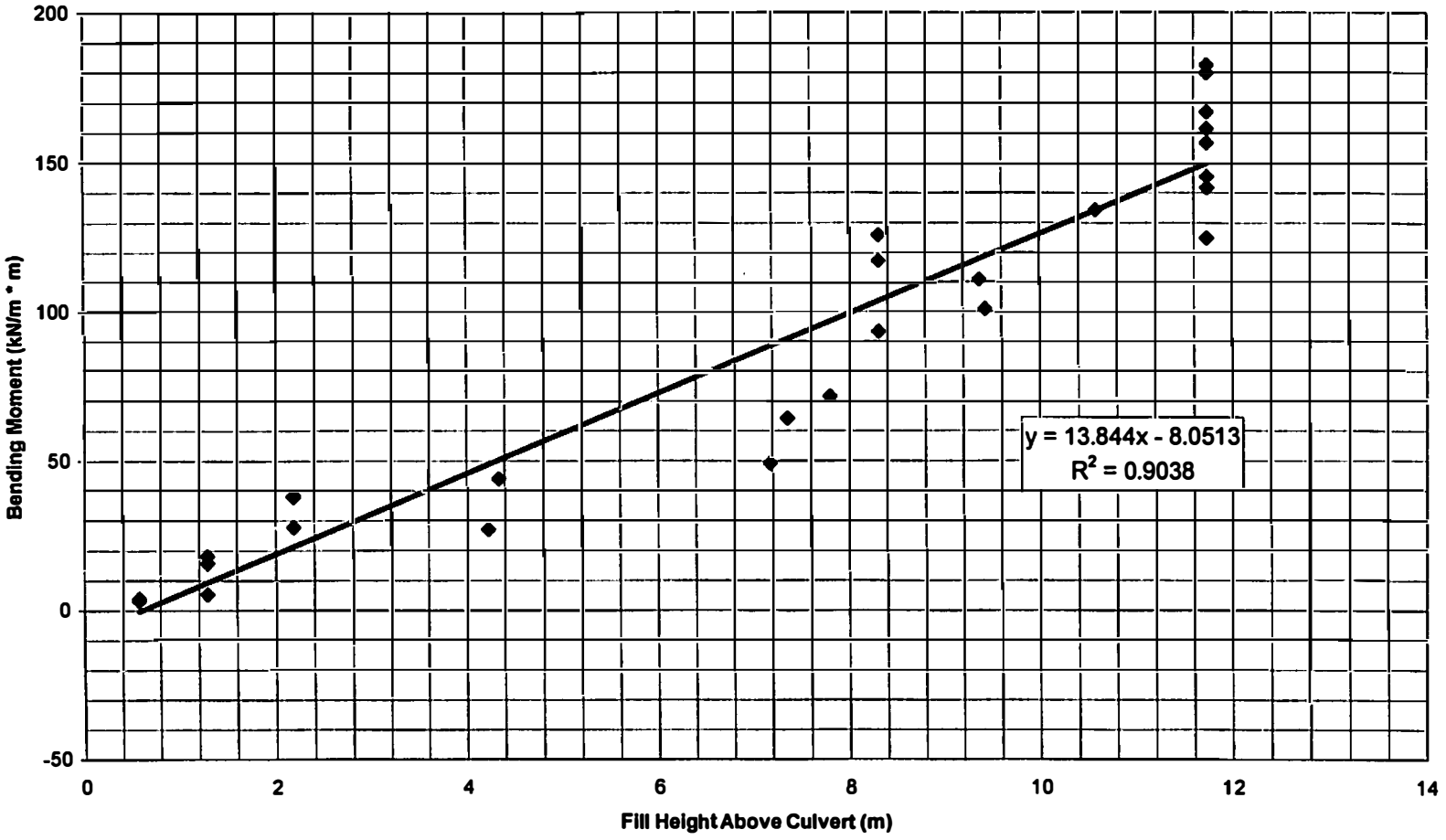


Figure C-17
Strain Readings B5

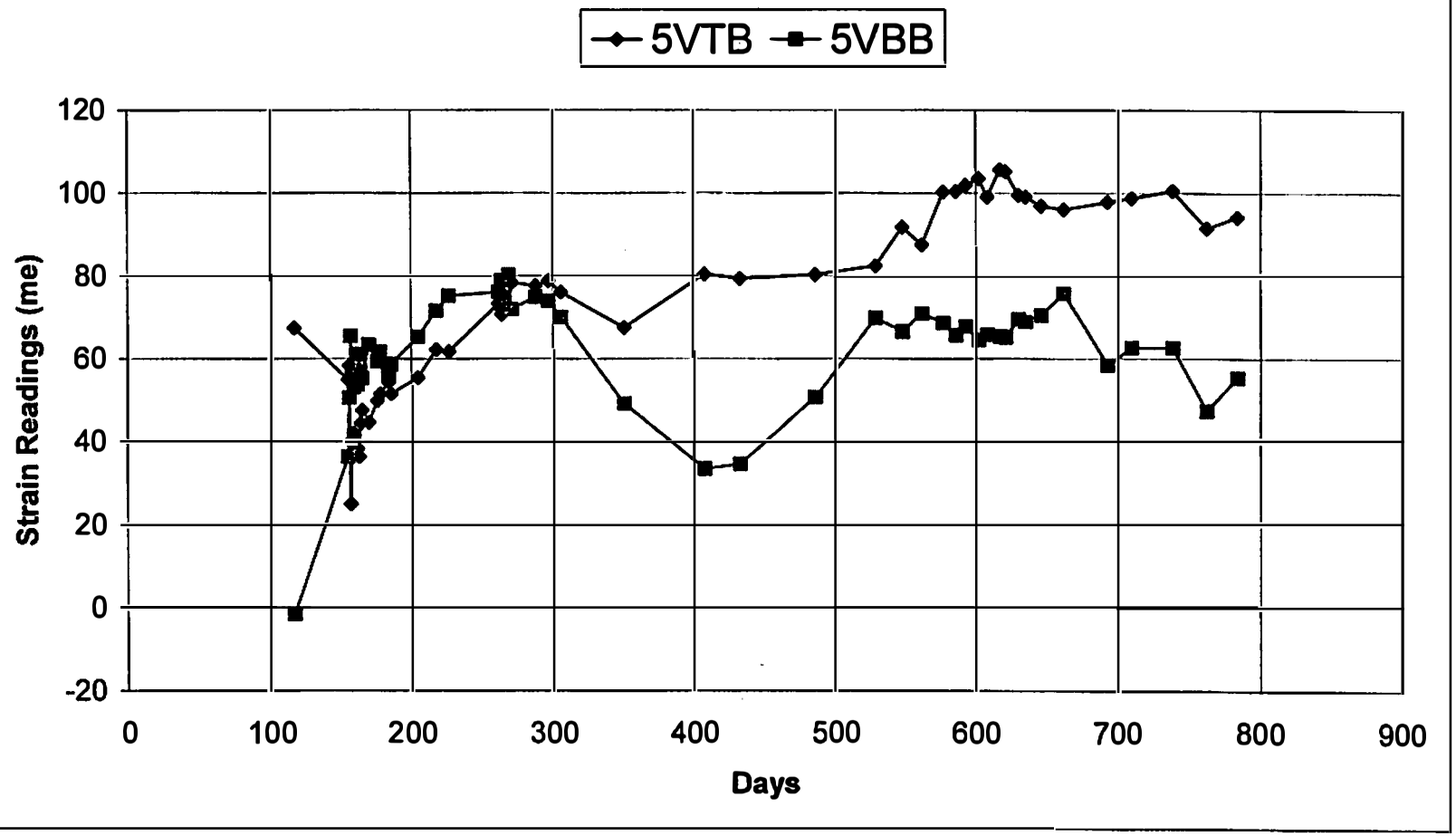


Figure C-18
Axial Force and Bending Moment Section B5

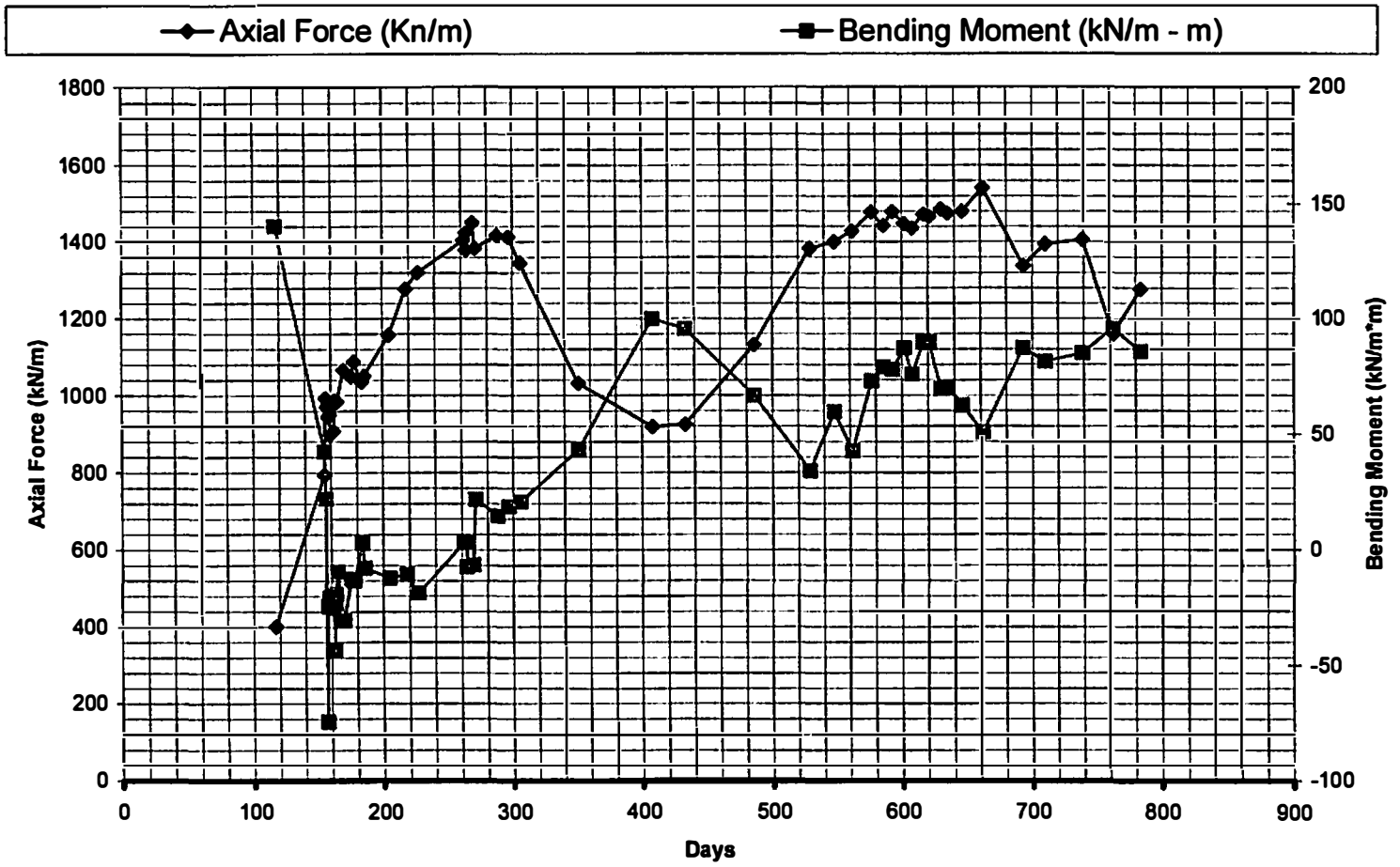


Figure C-19
Axial Force vs Fill Height Section B5

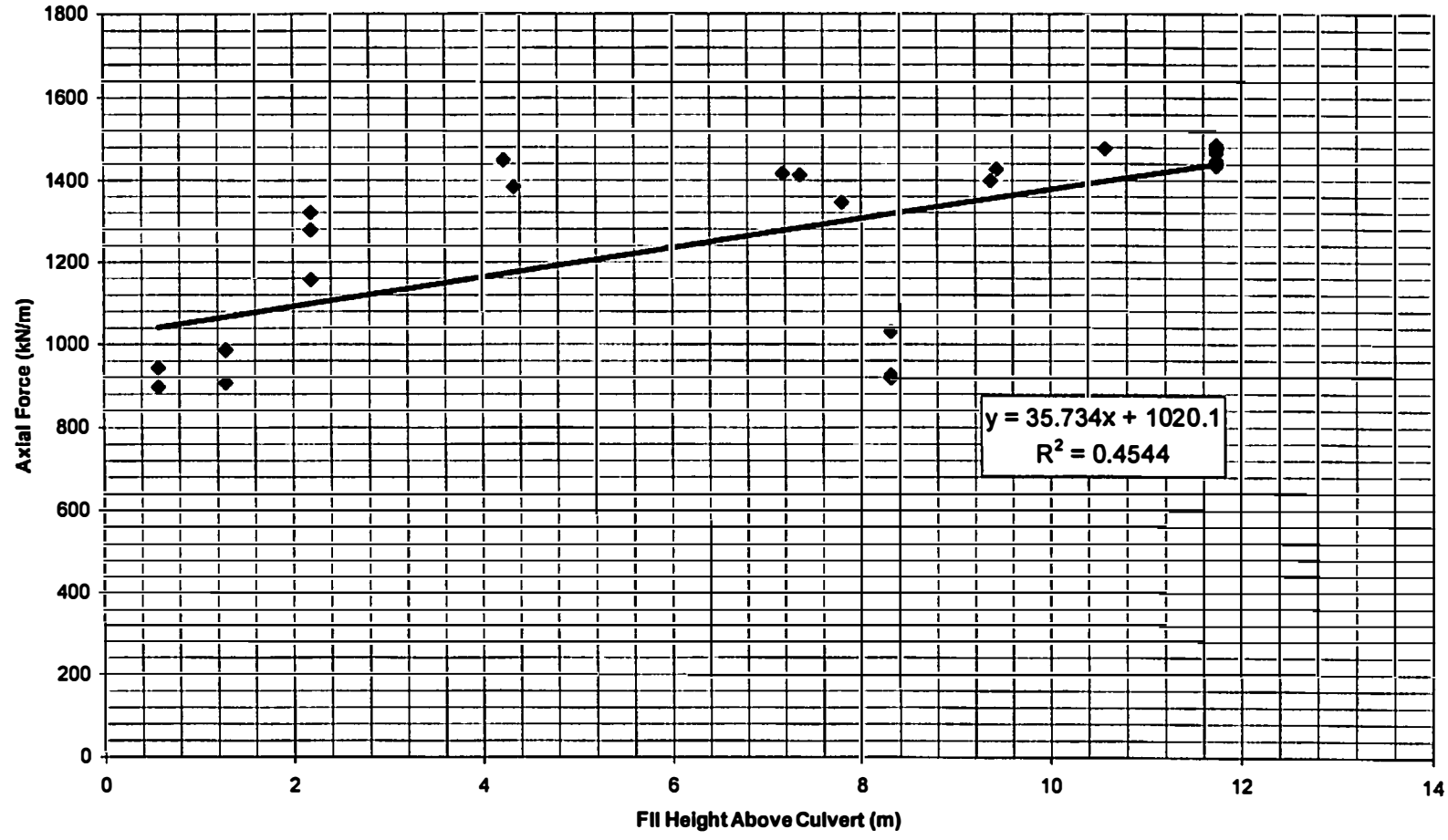


Figure C-20
Bending Moments vs Fill Height Section B5

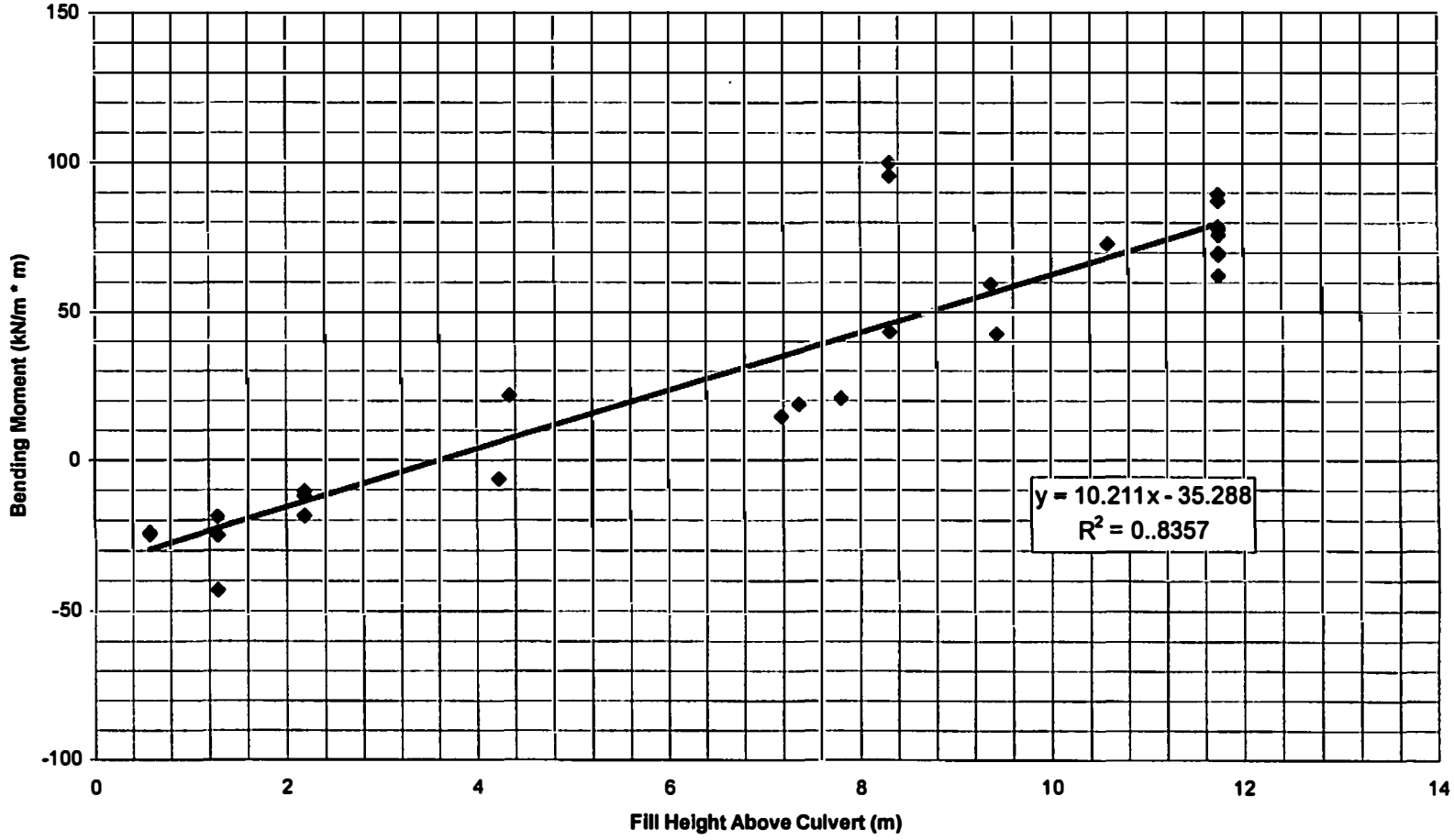


Figure C-21
Strain Readings B6

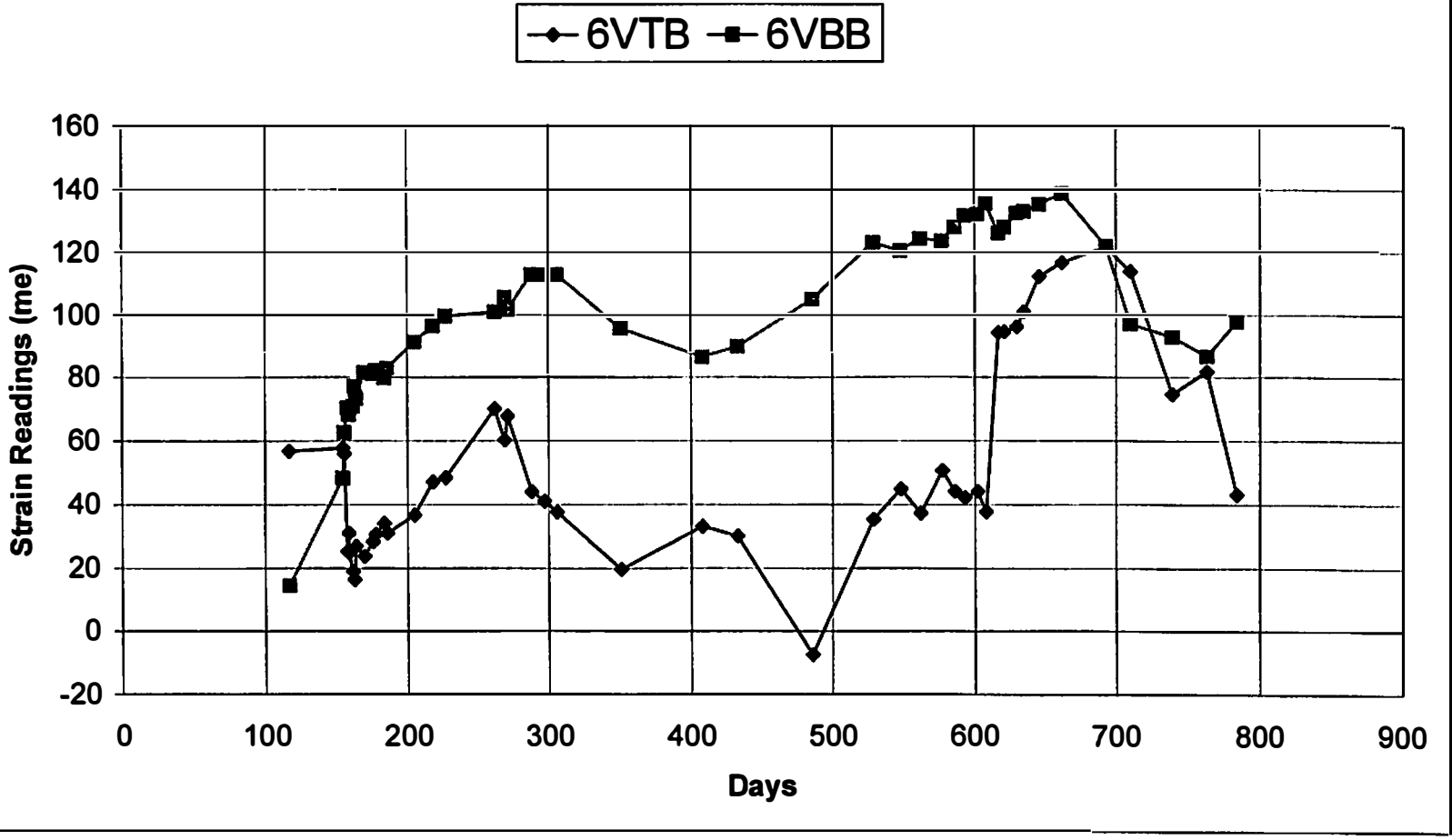


Figure C-22
Axial Force and Bending Moment Section B6

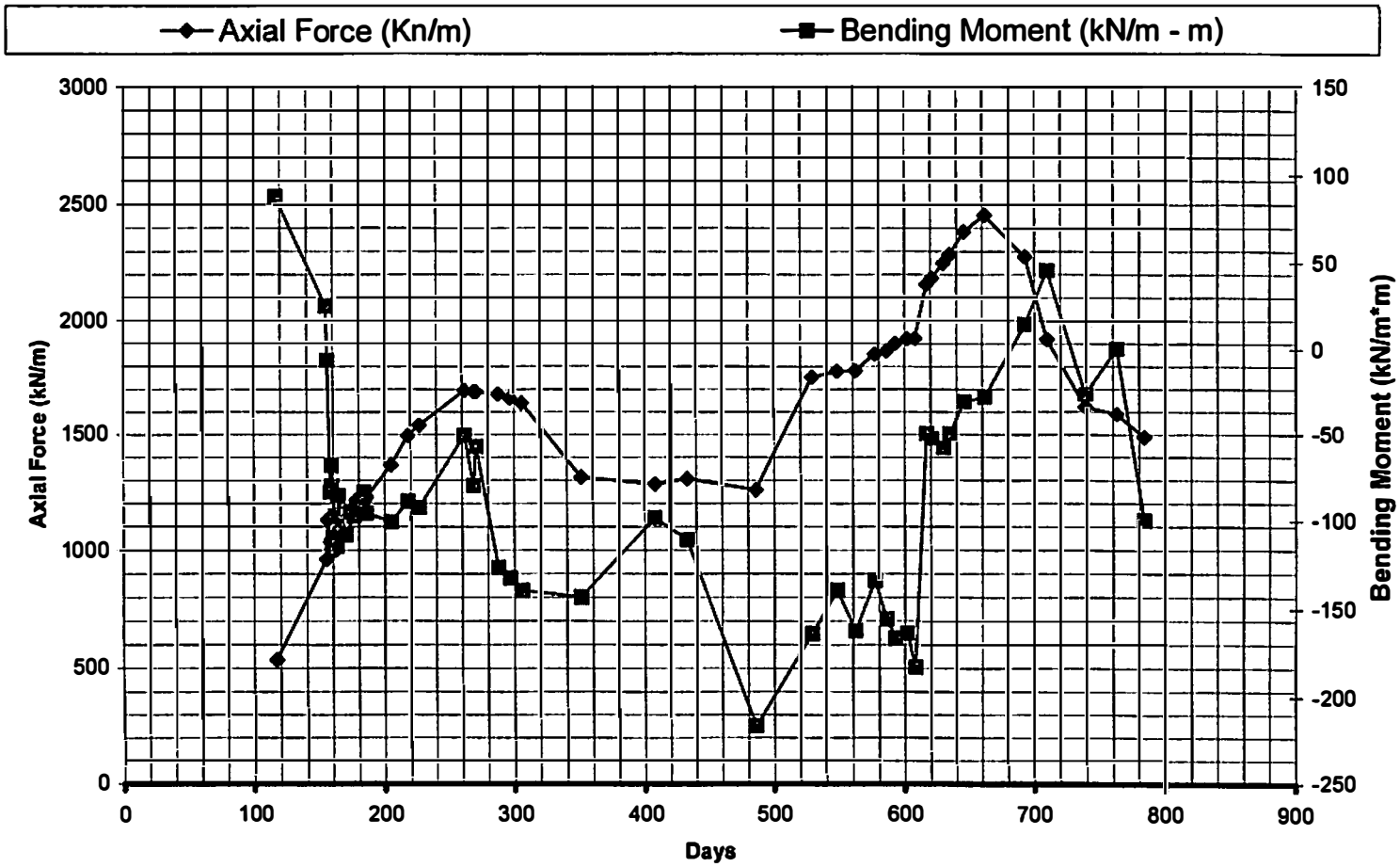


Figure C-23
Axial Force vs Fill Height Section B6

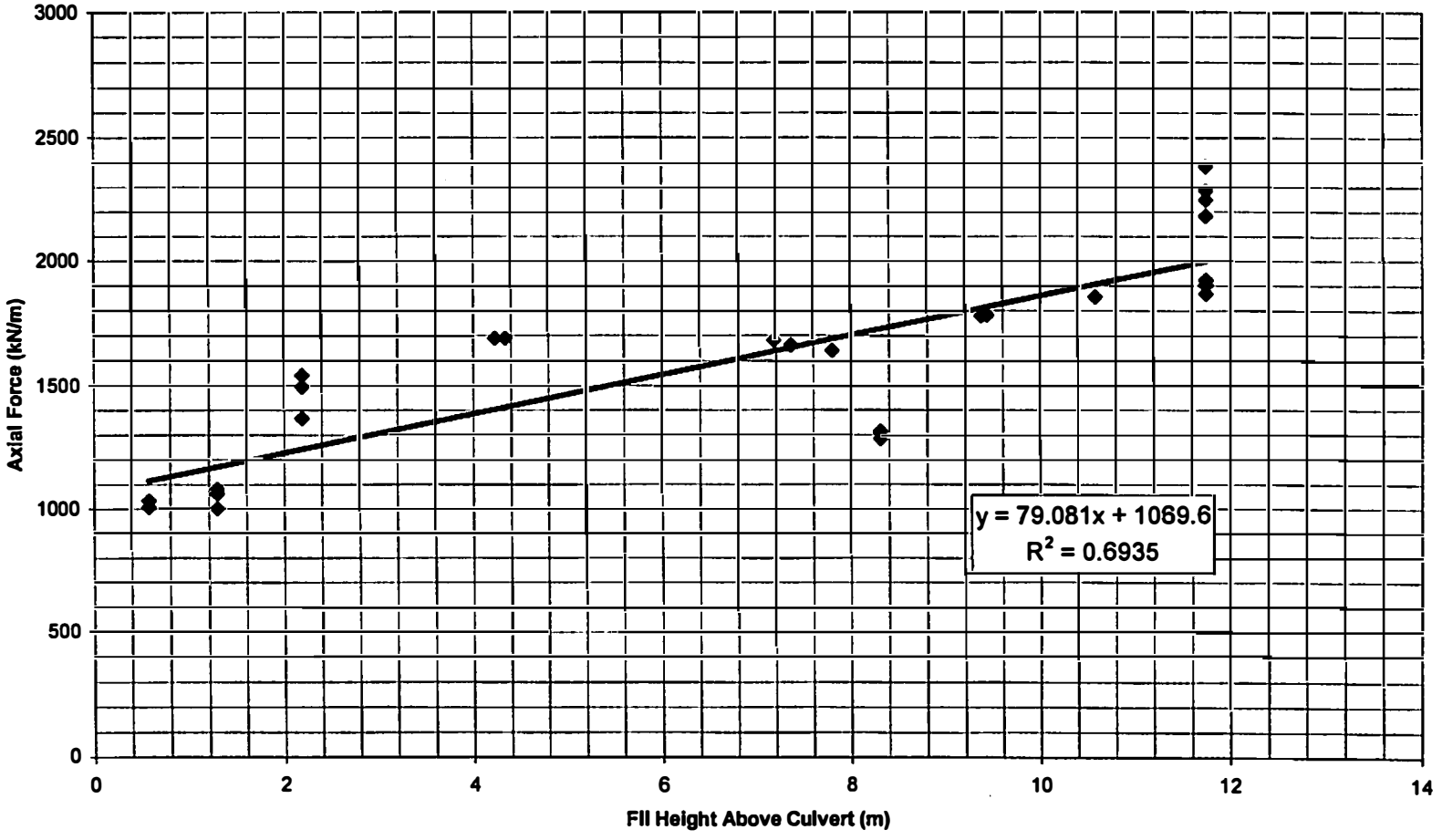
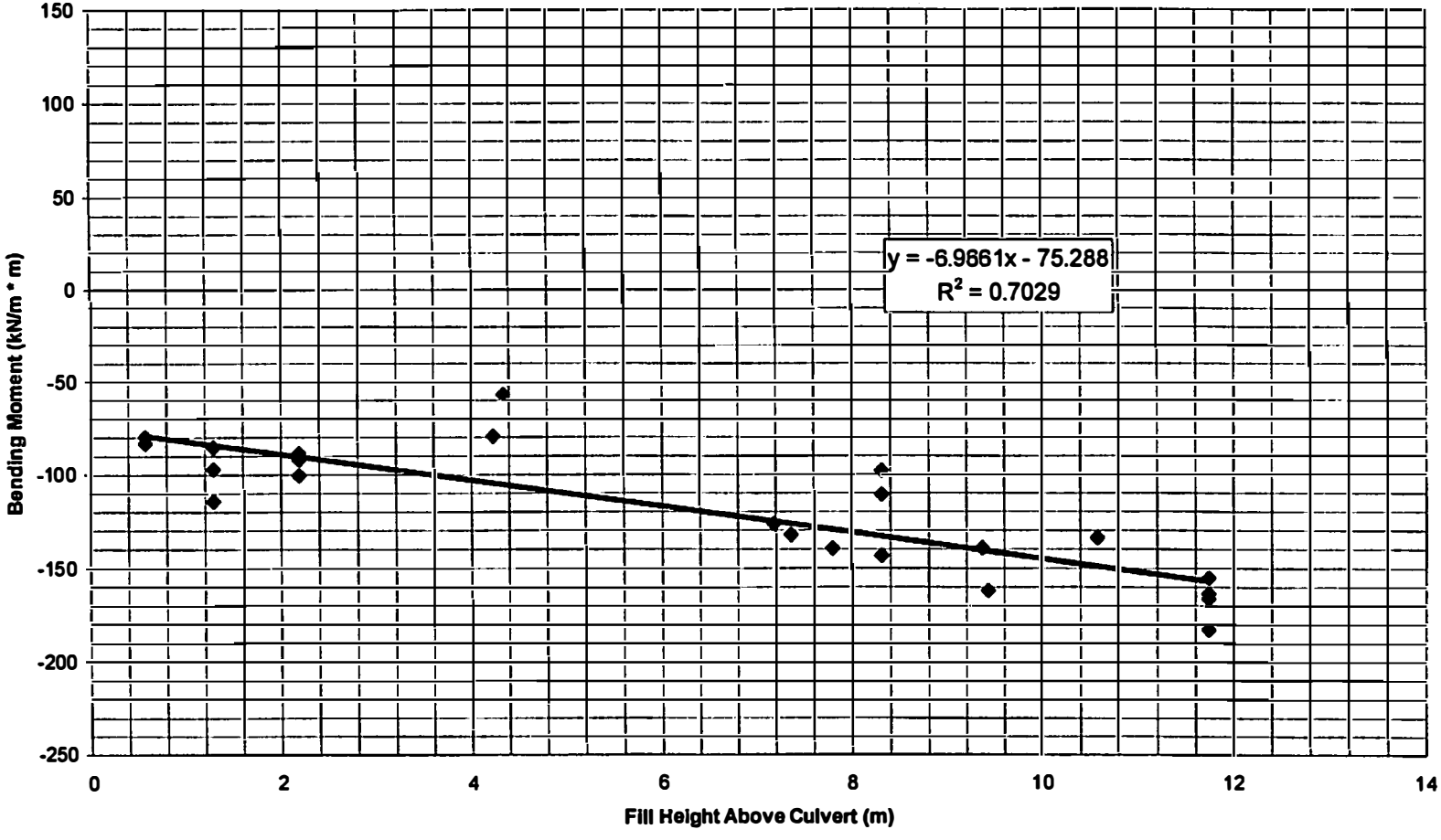


Figure C-24
Bending Moments vs Fill Height Section B6



Appendix D
Pressure and Shear Force Measurements

Figure D-1
Roof Pressure vs Days Section A

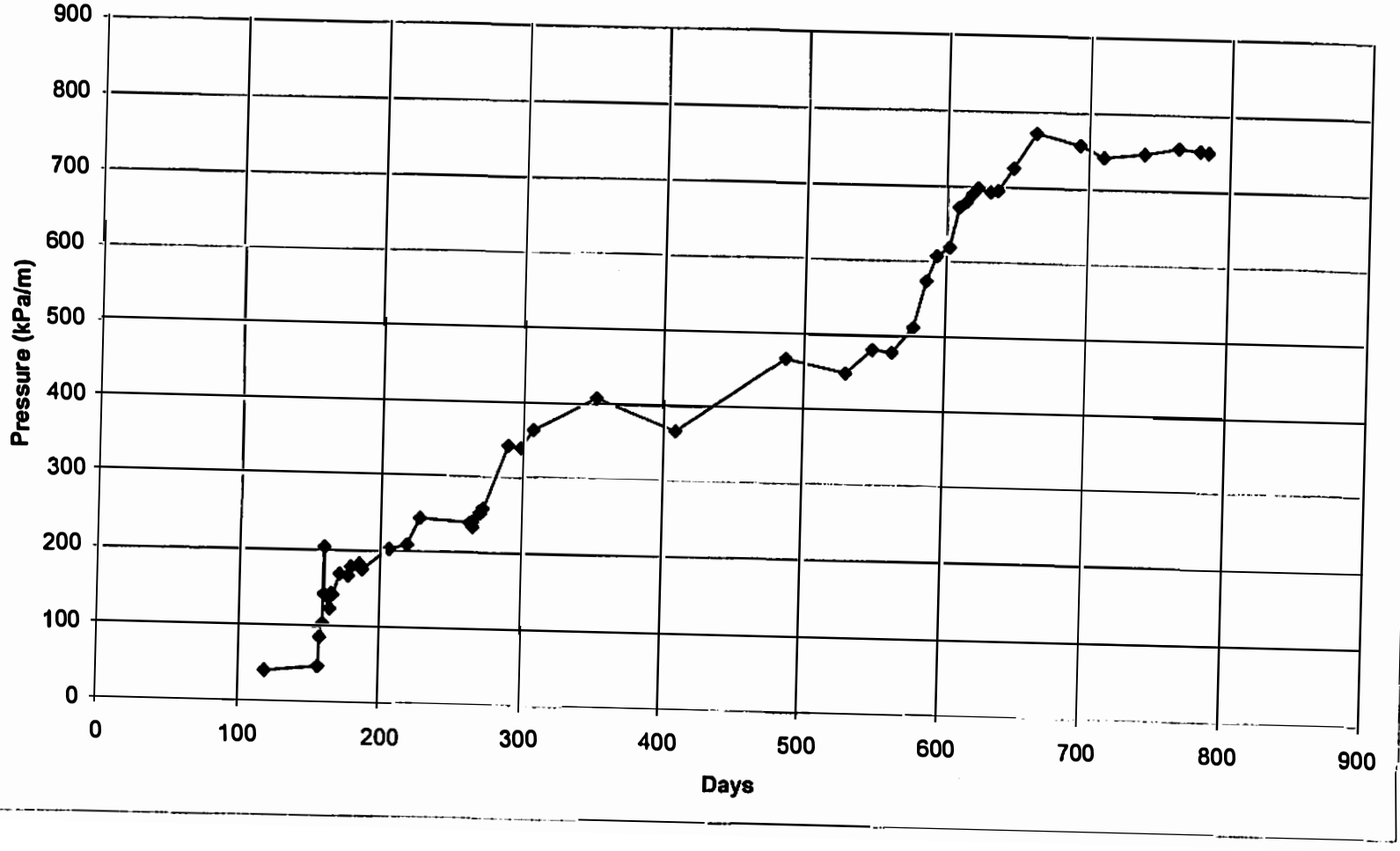
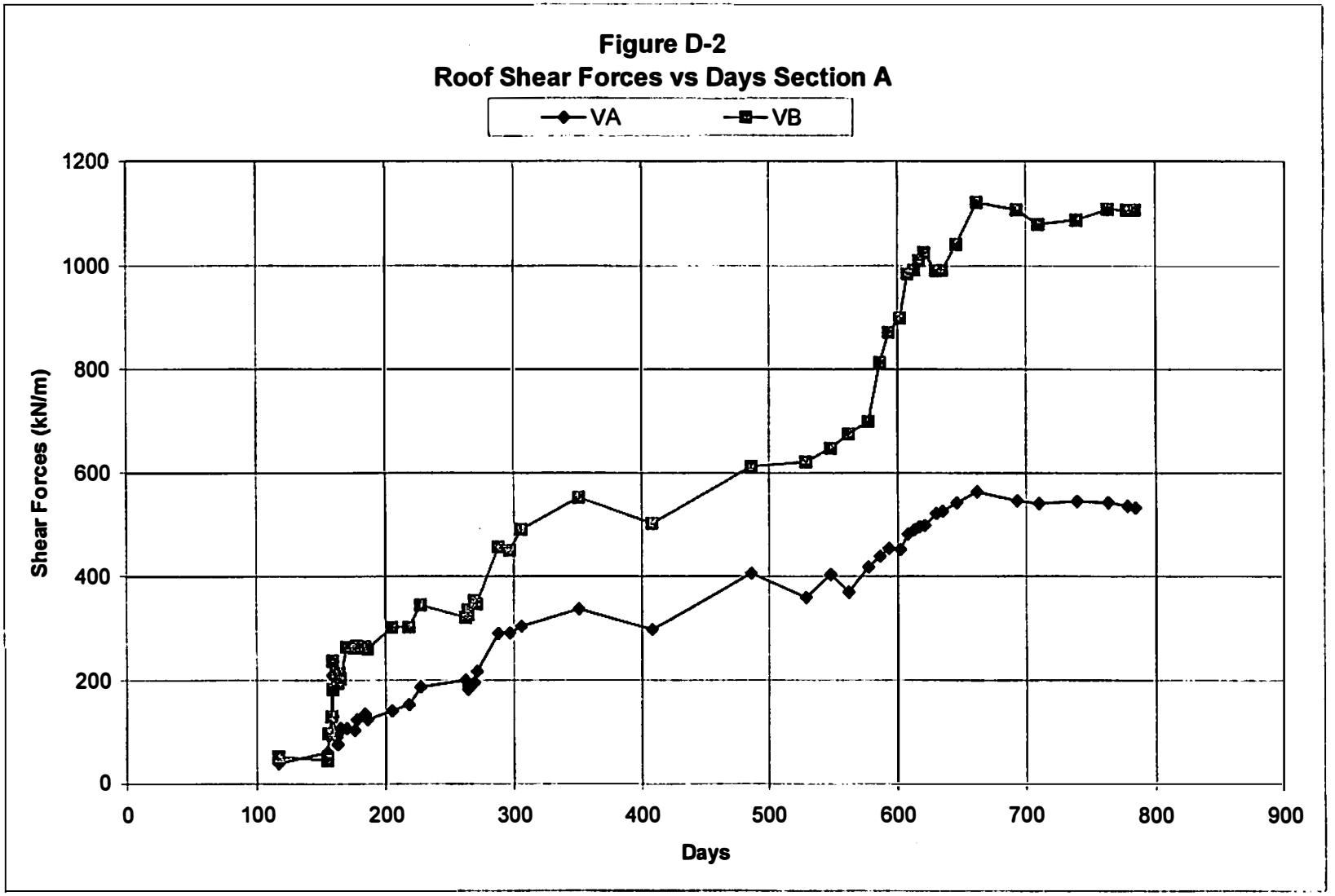


Figure D-2
Roof Shear Forces vs Days Section A



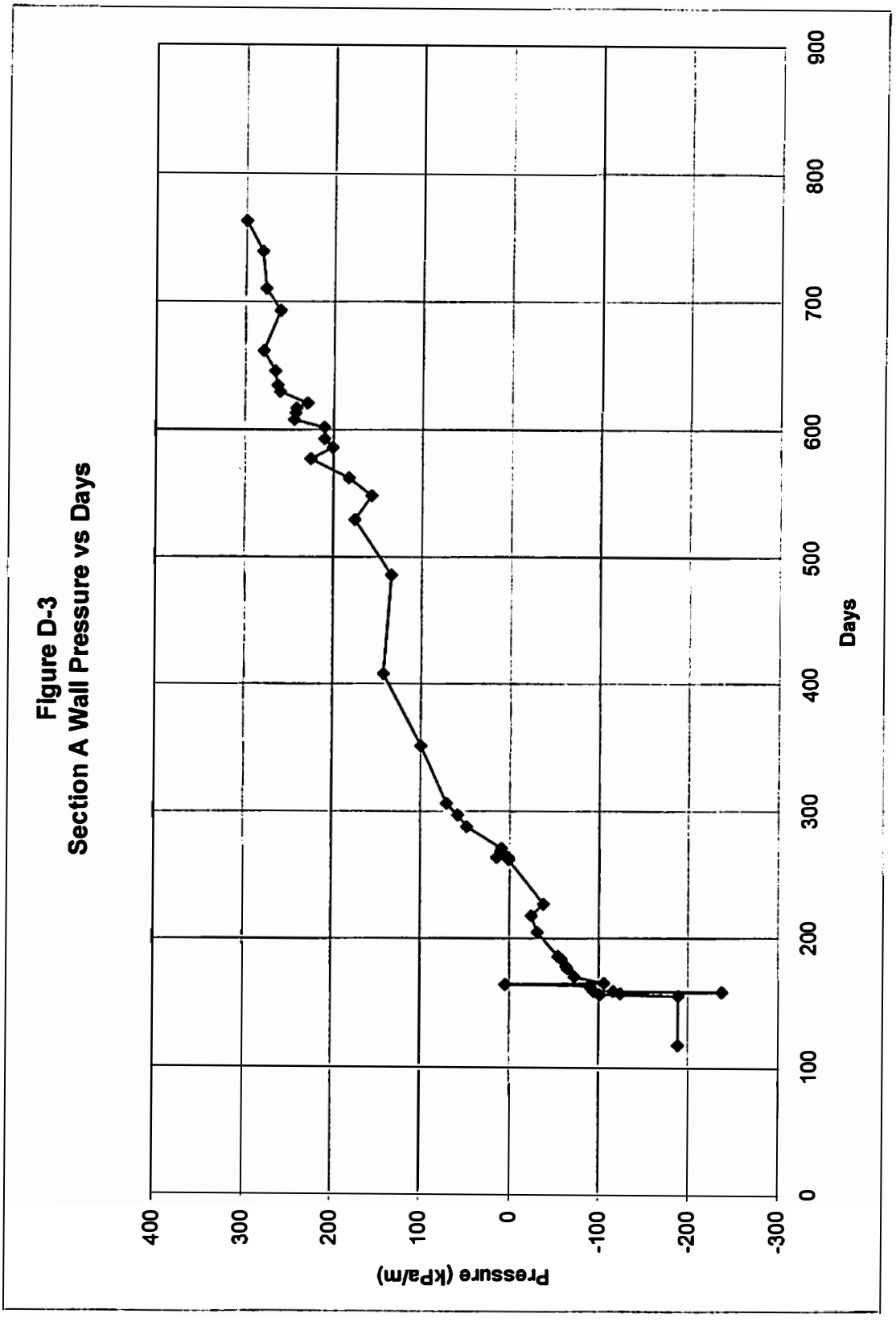

Figure D-3
Section A Wall Pressure vs Days
Pressure (kPa/m)
400
300
200
100
0
-100
-200
-300
0
100
200
300
400
500
600
700
800
900
Days

Figure D-4
Section A Wall Shear Forces vs Days

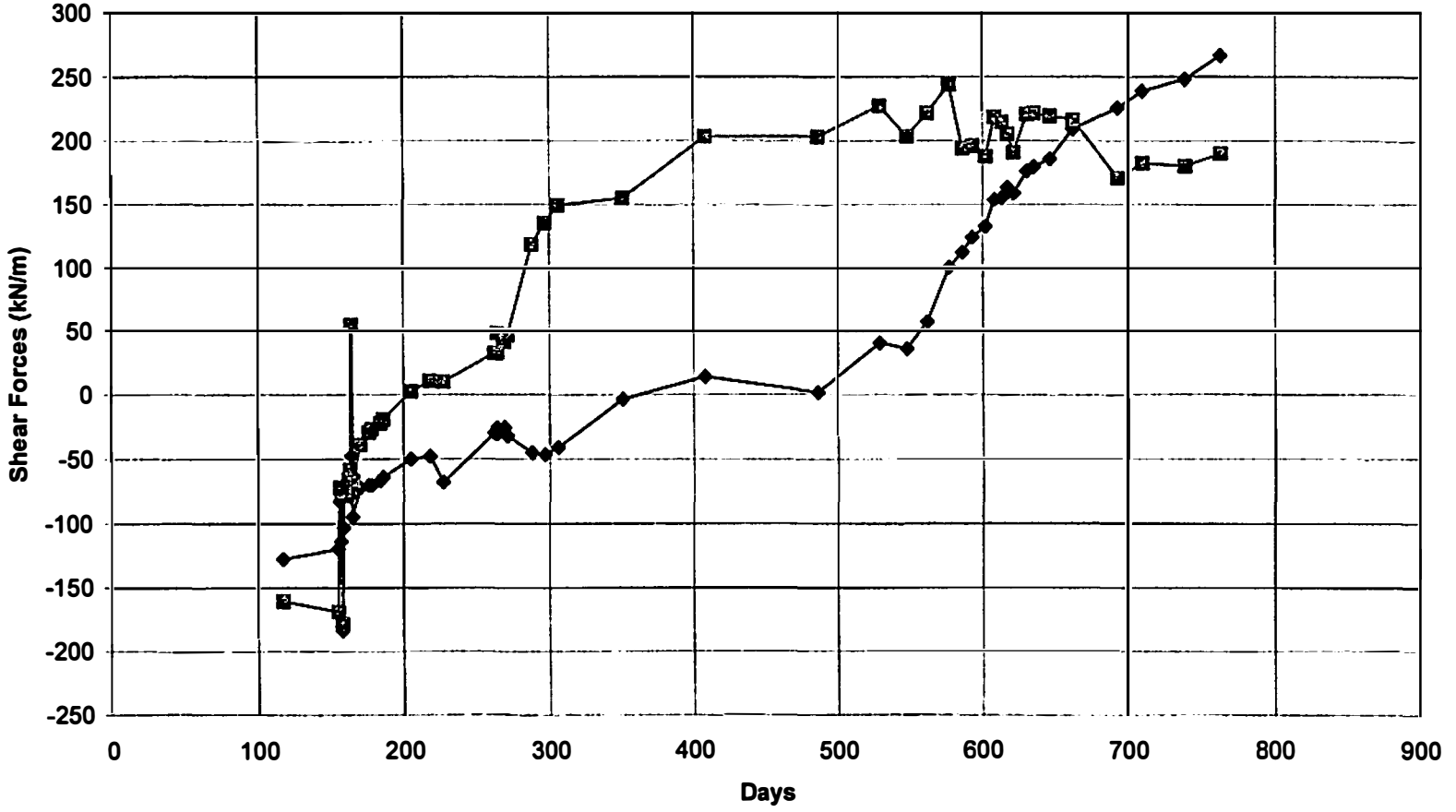


Figure D-5
Section B Roof Pressure vs Days

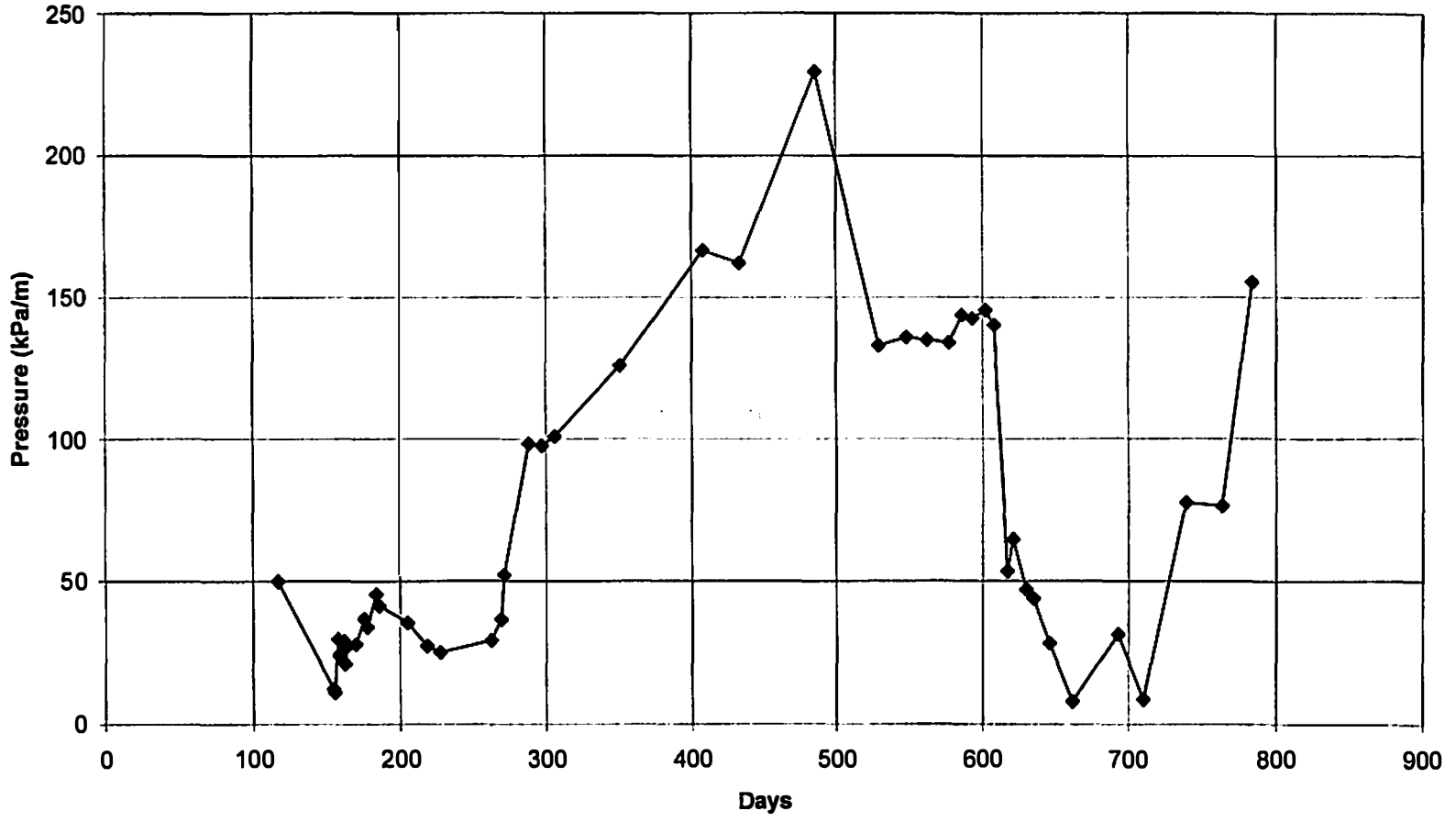
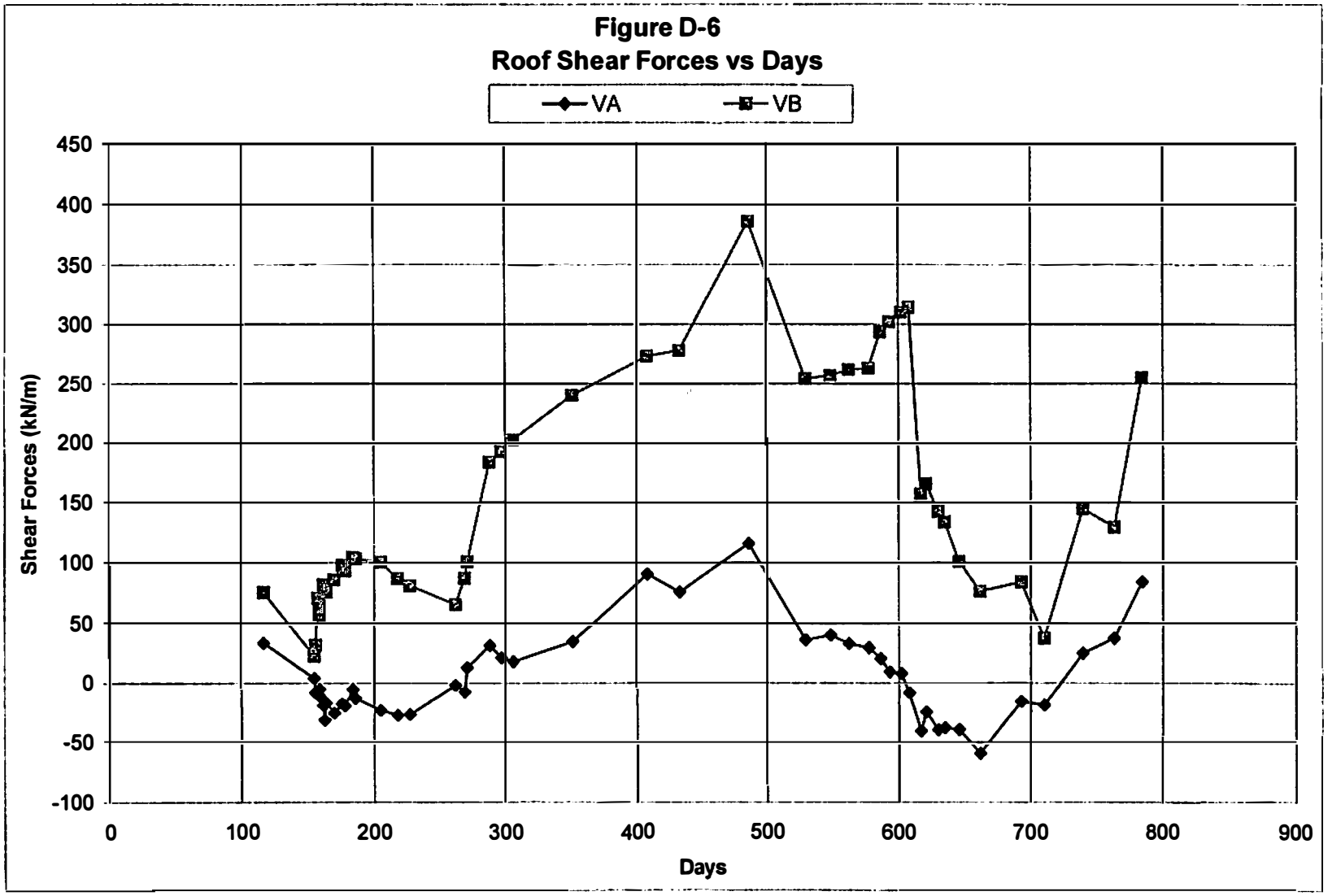


Figure D-6
Roof Shear Forces vs Days



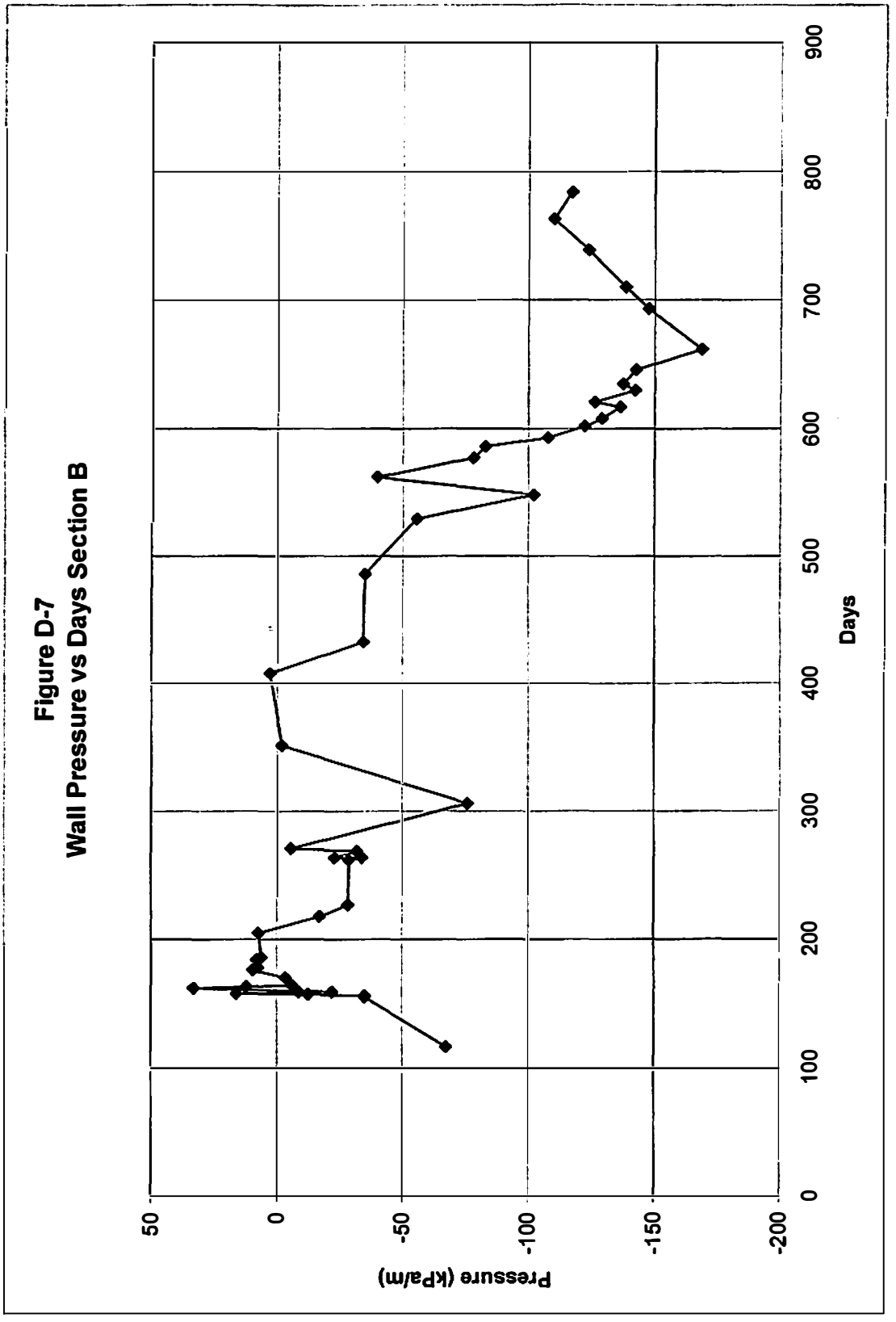
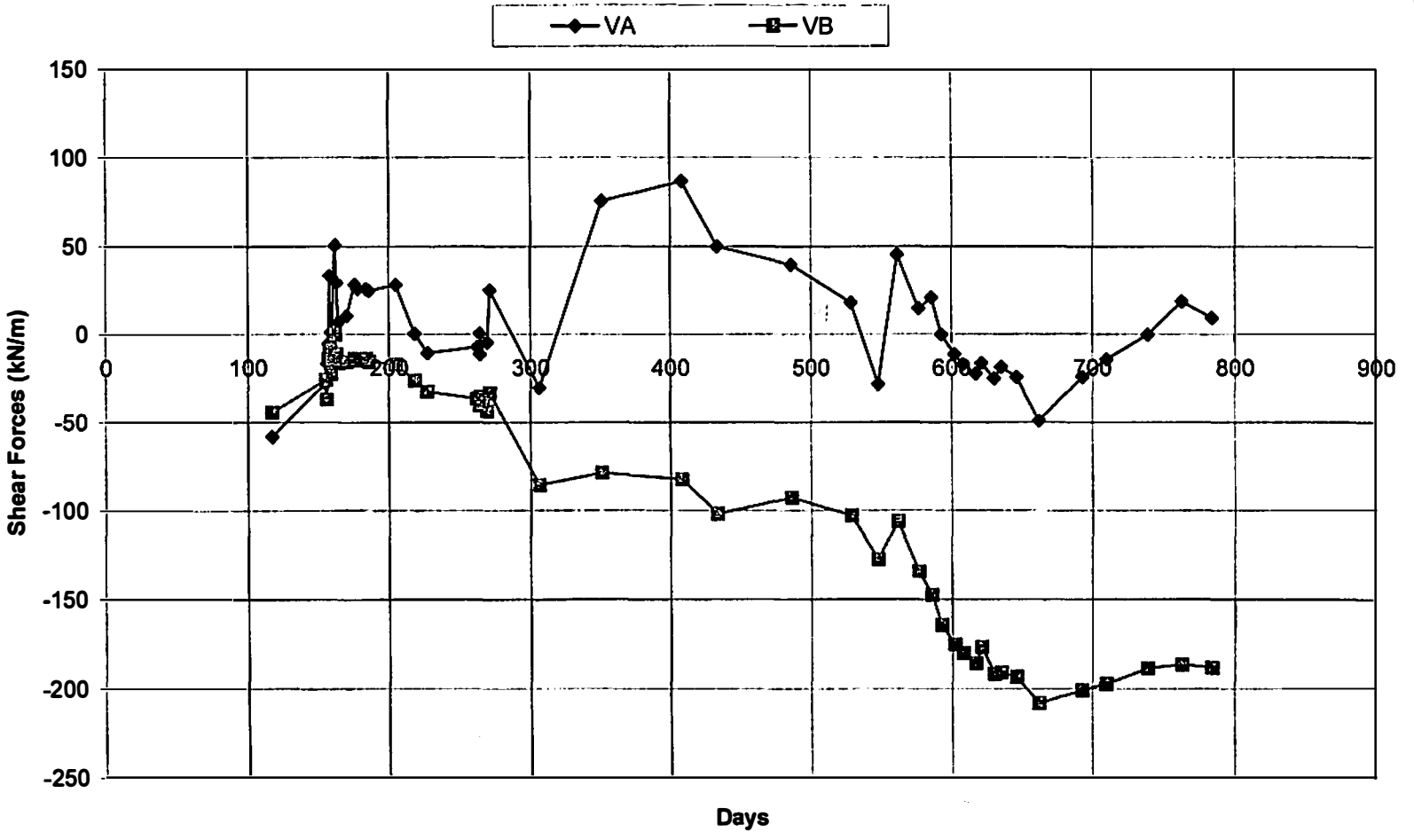

Figure D-7
Wall Pressure vs Days Section B
Pressure (kPa/m)
50
0
-50
-100
-150
-200
0
100
200
300
400
500
600
700
800
900
Days

Figure D-8
Wall Shear Forces vs Days Section B

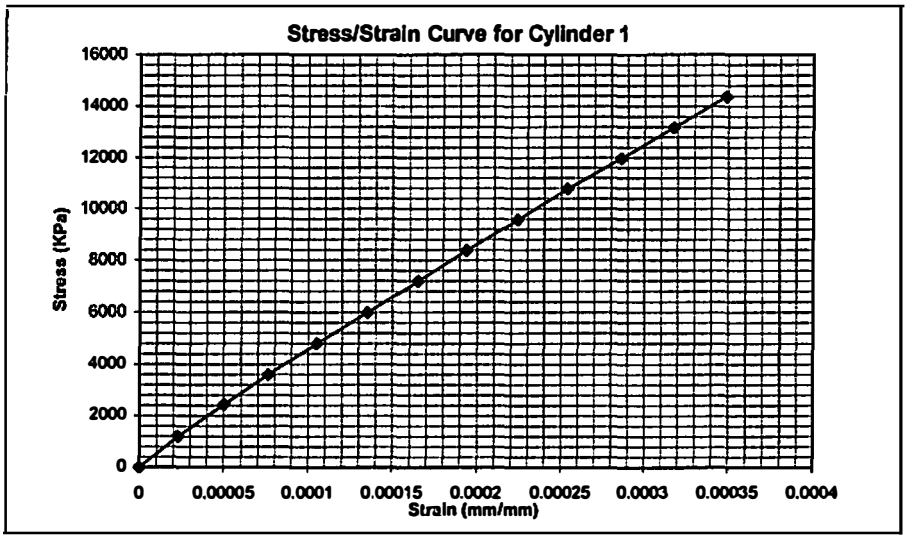


Appendix E
Greene County Culvert Concrete Test Data

GREENE CO. CULVERT CONCRETE TEST CYLINDERS

Cylinder 1 | Date Cast 9/25/96 | Test Date 6/26/97 | Dia.1(in.) 6.06 | Dia.2(in.) 6.05 | Ave.Dia. 6.055

Deformation(in.*0.00005)							
first run	second run	ave.	Load(lbs*10^3)		Stress(KPa)		Strain(mm/mm)
0	0	0	0		0		0
4.5	4.5	4.5	5		1197.321		0.0000225
10	10	10	10.1 / 10.3	10.2	2442.536		0.0000500
15.5	15	15.3	15		3591.964		0.0000763
21	21	21	20		4789.285		0.0001050
27	27	27	25		5986.607		0.0001350
33	33	33	30		7183.928		0.0001650
39	38.5	38.8	35		8381.249		0.0001938
45	44.5	44.8	40		9578.571		0.0002238
51	50.5	50.8	45		10775.89		0.0002538
57.5	57	57.3	50		11973.21		0.0002863
64	63	63.5	55		13170.53		0.0003175
70	69.5	69.8	60		14367.86		0.0003488
	Maximum Load=		131		31369.82		

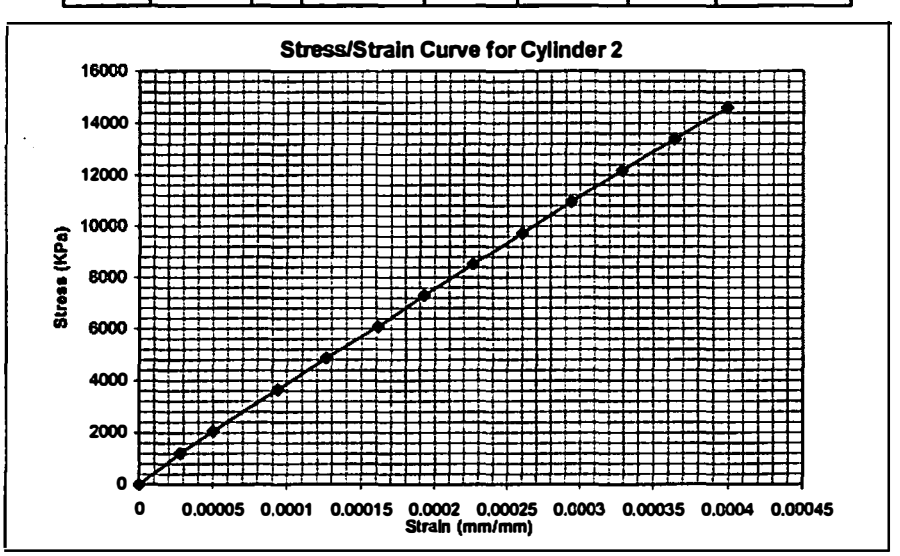


GREENE CO. CULVERT CONCRETE TEST CYLINDERS

Cylinder 2 | Date Cast 10/21/96 | Test Date 6/26/97

Dia.1(in.) 5.904
Dia.2(in.) 6.11
Ave.Dia. 6.007

Deformation(in.*0.00005) first run	second run	ave.	Load(lbs*10^4)		Stress(KPa)		Strain(mm/mm)
0	0	0	0		0		0
5.5	5.5	5.5	5		1216.533		0.0000275
10	10	10	8.6 / 8.4	8.5	2068.105		0.0000500
18.5	19	18.8	15		3649.598		0.0000938
25	25.5	25.3	20		4866.13		0.0001263
32	32.5	32.3	25		6082.663		0.0001613
38	39	38.5	30		7299.196		0.0001925
45	45.5	45.3	35		8515.728		0.0002263
52	52	52	40		9732.261		0.0002600
58.5	59	58.8	45		10948.79		0.0002938
66	65.5	65.8	50		12165.33		0.0003288
73	72.5	72.8	55		13381.86		0.0003638
60.5	79	79.8	60		14598.39		0.0003988
	Maximum Load		151.5		36860.94		

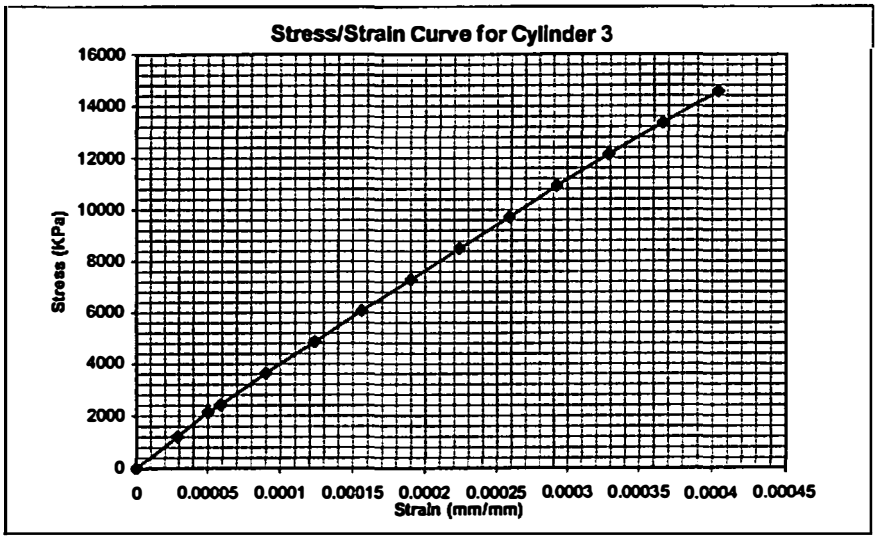


GREENE CO. CULVERT CONCRETE TEST CYLINDERS

Cylinder 3 | Date Cast 10/3/96 | Test Date 6/26/97 | wall section B

Dia.1(in.) 6.051
Dia.2(in.) 5.977
Ave.Dia. 6.014

Deformation(in.*0.00005)			Load(lbs*10³)		Stress(KPa)		Strain(mm/mm)
first run	second run	ave.					
0	0	0	0		0		0
6	5.5	5.75	5		1213.702		0.0000288
10	10	10	8.8/8.9	8.85	2148.253		0.0000500
11.5	12	11.8	10		2427.405		0.0000588
18	18	18	15		3641.107		0.0000900
24.5	25	24.8	20		4854.809		0.0001238
31	31.5	31.3	25		6068.511		0.0001563
38	38	38	30		7282.214		0.0001900
44.5	45	44.8	35		8495.916		0.0002238
51.5	52	51.8	40		9709.618		0.0002588
58.5	58.5	58.5	45		10923.32		0.0002925
66	65.5	65.8	50		12137.02		0.0003288
73.5	73	73.3	55		13350.73		0.0003663
81.5	80	80.8	60		14564.43		0.0004038
	Maximum Load=		128		31070.78		

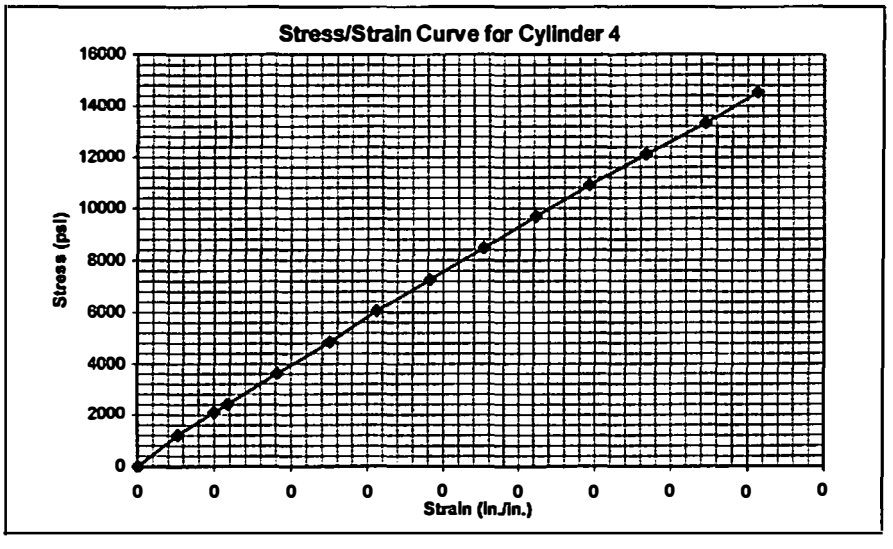


GREENE CO. CULVERT CONCRETE TEST CYLINDERS

Cylinder 4 | Date Cast 10/3/96 | Test Date 6/26/97 | wall section B

Dia.1(in.) 5.99
Dia.2(in.) 6.051
Ave.Dia. 6.0205

Deformation(in.*0.00005)							
first run	second run	ave.	Load(lbs*10^3)		Stress(KPa)		Strain(mm/mm)
0	0	0	0		0		0
5	5.5	5.25	5		1211.083		0.0000263
10	10	10	8.7/8.7	8.7	2107.284		0.0000500
12	11.5	11.8	10		2422.166		0.0000588
18	18.5	18.3	15		3633.249		0.0000913
25	25	25	20		4844.332		0.0001250
31	31.5	31.3	25		6055.415		0.0001563
38	38.5	38.3	30		7266.498		0.0001913
45	45.5	45.3	35		8477.581		0.0002263
52	52.5	52.3	40		9688.664		0.0002613
58.5	60	59.3	45		10899.75		0.0002963
66.5	67	66.8	50		12110.83		0.0003338
74	75	74.5	55		13321.91		0.0003725
81	81.5	81.3	60		14533		0.0004063
	Maximum Load		127		30761.51		

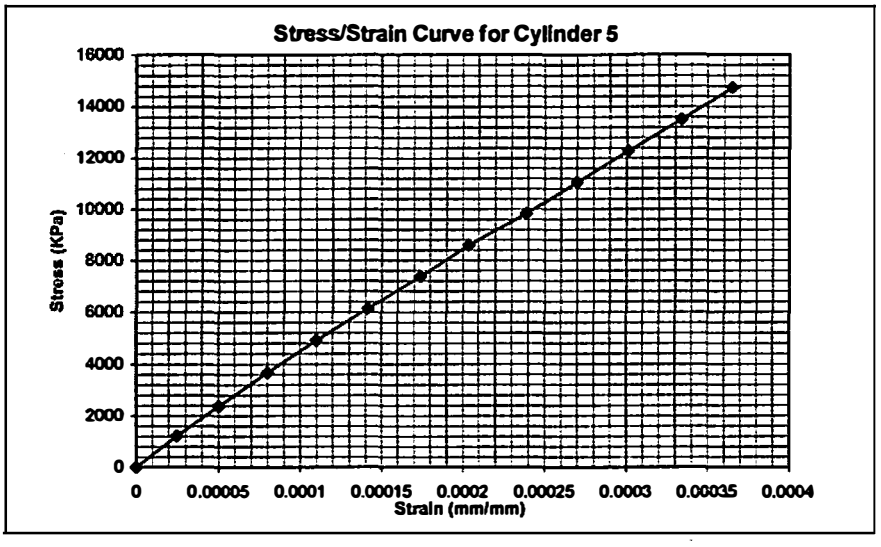


GREENE CO. CULVERT CONCRETE TEST CYLINDERS

Cylinder 5 | Date Cast 9/25/96 | Test Date 6/26/97

Dia.1(in.) 6.007
Dia.2(in.) 5.95
Ave.Dia. 5.9785

Deformation(in.*0.00005) first run	second run	ave.	Load(lbs*10³)		Stress(KPa)		Strain(mm/mm)
0	0	0	0		0		0
5	5	5	5		1228.159		0.0000250
10	10	10	9.8 / 9.6	9.7	2382.628		0.0000500
16	16	16	15		3684.477		0.0000800
22	22	22	20		4912.636		0.0001100
28	28.5	28.3	25		6140.794		0.0001413
34.5	35	34.8	30		7368.953		0.0001738
40.5	41	40.8	35		8597.112		0.0002038
47.5	48	47.8	40		9825.271		0.0002388
54	54	54	45		11053.43		0.0002700
60	60.5	60.3	50		12281.59		0.0003013
68.5	67	66.8	55		13509.75		0.0003338
73	73	73	60		14737.91		0.0003650
	Maximum Load		144.5		35493.79		



VITA

Scott Mitchell Wood was born and raised in Memphis, TN on February 22, 1975. He attended public schools in Memphis and graduated from Wooddale High in June 1993. He began his college career at the University of Tennessee at Martin for two years then transferred to the University of Tennessee at Knoxville, where he obtained his bachelors degree in civil engineering in summer 1998, and his master of science degree in spring 2000. Currently he is working as a structural engineer in Knoxville, TN.